DISCONTINUOUS DYNAMICS WITH GRAZING POINTS

A THESIS SUBMITTED TO
THE GRADUATE SCHOOL OF NATURAL AND APPLIED SCIENCES
OF
MIDDLE EAST TECHNICAL UNIVERSITY

BY

AYŞEGÜL KIVILCIM

IN PARTIAL FULFILLMENT OF THE REQUIREMENTS
FOR
THE DEGREE OF DOCTOR OF PHILOSOPHY
IN
MATHEMATICS

JULY, 2016

Approval of the thesis:

DISCONTINUOUS DYNAMICS WITH GRAZING POINTS

submitted by **AYŞEGÜL KIVILCIM** in partial fulfillment of the requirements for the degree of **Doctor of Philosophy in Mathematics Department, Middle East Technical University** by,

Prof. Dr. Gülbin Dural Ünver _____
Dean, Graduate School of **Natural and Applied Sciences**

Prof. Dr. Mustafa Korkmaz _____
Head of Department, **Mathematics**

Prof. Dr. Marat Akhmet _____
Supervisor, **Mathematics Department, METU**

Examining Committee Members:

Prof. Dr. Hasan Taşeli
Mathematics Department, METU _____

Prof. Dr. Marat Akhmet
Mathematics Department, METU _____

Prof. Dr. Serkan Dağ
Mechanical Engineering Department, METU _____

Assist. Prof. Dr. Hüseyin Altundağ
Mathematics Department, Hitit University _____

Assoc. Prof. Dr. Mehmet Onur Fen
Basic Sciences Unit, TED University _____

Date: _____

I hereby declare that all information in this document has been obtained and presented in accordance with academic rules and ethical conduct. I also declare that, as required by these rules and conduct, I have fully cited and referenced all material and results that are not original to this work.

Name, Last Name: AYŞEGÜL KIVILCIM

Signature :

ABSTRACT

DISCONTINUOUS DYNAMICS WITH GRAZING POINTS

Kıvılcım, Ayşegül
Ph.D., Department of Mathematics
Supervisor : Prof. Dr. Marat Akhmet

July, 2016, 222 pages

The scope of this thesis is to investigate the periodic solutions of impulsive systems with grazing and modeling through differential equations with impulses. By means of differential equations with impacts, the system which is modeled through two distinct differential equations is taken into account and such models are named as models with impact deformations. The surfaces as well as the coefficient of restitution are determined to be dependent on the impact velocity. The simulations are obtained for the relation of the displacement and the restitution with the impact velocity. Analytical formulas are also determined for them. The periodic solutions and their stability are examined analytically for the impulsive systems with the deformable surfaces and the velocity dependent coefficient of restitution and the results are actualized through simulations. The chattering, which was known infinitely many impact occurring in a finite time, is suppressed in the systems by utilizing deformable surfaces and velocity dependent coefficient of restitution. An appropriate definition for the grazing phenomenon is presented. Discontinuous dynamical systems with graziness are obtained. The differentiability and other properties of discontinuous dynamical system are widely investigated. The orbital stability of the periodic solutions are proved. Applying small parameter analysis, the bifurcation of periodic solutions is observed in specific examples. The non-autonomous grazing phenomenon is considered and some sufficient conditions are obtained for the differentiability with respect to initial values. The perturbations around the periodic solutions of those systems are consid-

ered and the theoretical results are visualized by simulations.

Keywords: Grazing solutions, Discontinuous dynamical Systems, Chattering, Impact deformations, Coefficient of restitution, Deformable surfaces, Grazing cycles of non-autonomous systems, Regular perturbations around the grazing cycles, Van der Pol's oscillators, Vertical and horizontal grazing

ÖZ

SIYIRIP GEÇEN NOKTALARA SAHİP SÜREKSİZ DİNAMİKLER

Kıvılcım, Ayşegül
Doktora, Matematik Bölümü
Tez Yöneticisi : Prof. Dr. Marat Akhmet

2016 , 222 sayfa

Bu tezin amacı sıyırıp geçen çözümlere sahip impalsif diferansiyel denklemleri araştırmak ve impalsif diferansiyel denklemler kullanarak modellemektir. Vuruşlu diferansiyel denklemler kullanarak farklı iki diferansiyel denklemlerle modellenen sistemleri tek bir diferansiyel denklem kullanarak modellenebilir. Bu modeller için restütasyon katsayısı ve yüzeylerin vuruş hızına bağlı olarak değişiklik gösterebileceği belirlenmiştir. Analitik formüller kullanılarak ve simülasyon yapılarak restitüsyon katsayısı ve yer değişiminin vuruş hızına bağlı değişimi elde edilmiştir. Deforme olabilen yüzeylere ve hıza bağlı restütasyon katsayısına sahip vuruşlu diferansiyel denlemlerin periyodik çözümleri ve onların kararlılığı incelenmiştir. Sınırlı zamanda sınırsız vuruş olarak tanımlanan tıkırdama deforme olabilen ve çarpma hızına bağlı restütasyon katsayısı kullanılarak sistemlerde baskılanmıştır. Sıyırıp geçen durumlar için uygun tanımlamalar verilmiştir. Sıyırıp geçen çözümler içeren süreksiz dinamik sistemler elde edilmiştir. Türevlenebilme ve diğer sistem özellikleri genişçe incelenmiştir. Bu sistemlerin periyodik çözümlerinin yörüngesel kararlılığı ispatlanmıştır. Küçük parametre yöntemi kullanılarak, periyodik çözümlerin dallanması belirli örnekler üzerinde elde edilmiştir. Otonom olmayan sıyırıp geçme durumlarına sahip sistemlerde türevlenebilme için gerekli koşullar elde edilmiştir. Bu sistemlerin periyodik çözümleri etrafında pertürbasyon yapılmıştır ve teorik sonuçlar simülasyon kullanılarak görselleştirilmiştir.

Anahtar Kelimeler: Sıyırıp geçen çözümler, Süreksiz dinamik sistemler, Sonlu zamanda sonsuz çarpma, Vuruş deformasyonları, Restütasyon katsayısı ve deforme olan yüzeyler, Otonom olmayan sistemlerin sıyırıp geçen periyodik çözümleri, Sıyırıp geçen periyodik çözümler etrafındaki düzenli pertürbasyonlar, Dikey ve yatay sıyırıp geçme

To my family

ACKNOWLEDGMENTS

Primarily, I would like to express my deepest gratitude to my supervisor Prof. Dr. Marat Akhmet, for preparing me to the academic life. I also would like to thank to him not only for his valuable guidance and constant support throughout the preparation of this thesis, but also for everything that he taught me.

I present my sincere thanks to the members of the examining committee for their valuable comments and suggestions. I extend my gratitude to all members of the Mathematics Department of Middle East Technical University for their continuous help during this long process.

I would not have succeeded in my studies without the patience and constant support of my family. I want to also thank my my parents for their confidence and support during the whole of my education life. Especially, I want to present my heartfelt thanks to my brother Zafer Savaş Kıvılcım who directed me to the Mathematics department in METU and supported and encouraged me during my academic research. He is more than a brother for me.

I want to present also my sincere gratitude to my friends that I worked with and it was a great pleasure for me to make fruitful discussions with them. Firstly, I would like to thank especially Mehmet Turan for his constant support and encouragement. I also want to thank Meltem Alişen Karacaören, Mehmet Onur Fen, Sabahattin Cağ, Ardak Kaskynbayev for their fruitful discussions.

I want to thank my beloved friends F. Sidre Oğlakkaya, Ersin Kızgut, Murat Uzunca and Sibel Doğru Akgöl for their constant support during my academic life and the preparation of this thesis.

This is last but not least, Tuğba Aktan, Nijat Aliyev and Adalet Çengel became heroes of my Phd journey and my life. It will be to hard for me to accomplish all these studies without their constant encouragement and support. I want to present my deepest thanks to them for their unbounded patience during my lifetime and preparation of this thesis.

TABLE OF CONTENTS

LIST OF TABLES

TABLES

LIST OF FIGURES

FIGURES

CHAPTER 1

INTRODUCTION

Ordinary differential equations serve as mathematical model for many exciting real world problems not only in science and technology but also in such diverse areas as economics, psychology, defense and demography. Rapid growth in the theory of differential equations and in its applications to almost every branch of knowledge have resulted in a continued interest in its study by students in many disciplines. This has given ordinary differential equations a distinct place in mathematics curricula all over the world.

In early stages, mathematicians were engaged in formulating differential equations and solving them tacitly assuming that a solution always existed. The rigorous proof of existence and uniqueness of first order initial value problem was first presented by Cauchy in his lectures in 1820-1830. He also extended his process to system of such initial value problems. In 1976, Lipschitz improved Cauchy's technique with a view making it more practical.

In 1893, Picard presented an existence theory based on a different method of successive approximations, which is considered more constructive than that of Cauchy-Lipschitz. The Pioneering works of Picard, Cauchy and Lipschitz are united in the analysis of a qualitative nature of ordinary differential equations. Instead of finding solutions explicitly, it provides sufficient conditions on the known quantities which ensure the existence of solution. Besides existence and uniqueness additional sufficient conditions to analyze the properties of solutions, asymptotic behaviour, oscillator, behaviour, stability, so on, carefully examined. Moreover, R. Bellman, I. Bendixon, H. Poincare and B. Van der Pol are some of the mathematicians who han-

dle with qualitative theory of differential equations.

Dynamical systems are mathematical objects used to model physical phenomena whose state (or instantaneous description) changes over time. If one needs to describe real world problems adequately discontinuity and continuity should be considered together. The discontinuity property of the motion is as old as the motion itself. The dynamical system theory takes us away from the idea of discontinuities because of the continuous nature of the dynamics. However, the applications in engineering, electronics, biology, medicine and social sciences requires the implementation of either sudden changes of an elsewhere continuous process or in the form of discrete time settings. Discrete time settings (Difference equations) can be considered as an instrument in the analysis of continuous motions such as Poincare maps. Moreover, such maps can be applied in the investigation of Impulsive differential equations where continuous alterations are mixed with impact type changes in equal portion. Such differential equations may admit discontinuity either at the fixed moments or at the moments when the integral curves reaches the curves in the extended phase space (t, x) as both time increases or decreases. For such system, there exists no general formula for the impact times in general. For this reason, such system of differential equations are called differential equations with variable moments of impulses. The interest in systems with discontinuous trajectories have grown in recent years because of the needs of modern technology. Still the theory of these systems seems very far being complete and there is still much to do make the application of the theory more effective. It is natural to assume short term perturbations act instantaneously that is in the form of impulses. It is known that many biological phenomena such as thresholds, bursting rhythm models in medicine and biology, optimal control models in economics, pharmakinetics and frequency modulated systems do exhibit impulsive effects. For this reason the theory of impulsive differential equations are far much richer than the corresponding theory of differential equations without impulses. These types of dynamical systems were considered at the beginning of the development of nonlinear mechanics and attracted the attention of physics. Because they give possibility to adequately describe processes in non-linear oscillating systems. A well-known example of such a problem is the model of a clock.

Because of the complexity in the analysis of differential equations with variable mo-

ments of impulses, the differential equations with fixed moments of impulses are widely investigated. However, modeling systems with fixed moment of impulse reduce the reality of the models. For this reason, to introduce the systems with variable moments of impulses is urgent. In this thesis, we mainly used the differential equations with variable moments of impulses and a method which was introduced by Akhmet [5] is used for the analysis of such systems. The method which reduce the systems with variable to fixed moments of impulses by preserving its dynamical properties is called a $B-$equivalent method.

1.1 Characteristics of Differential Equations with Impulses

In this thesis, $\mathbb{R}$, $\mathbb{N}$ and $\mathbb{Z}$ stand for real numbers, natural numbers and integers, respectively. Set by $\|\cdot\|$ the Euclidean norm and $\langle , \rangle$ inner product for the vectors in $\mathbb{R}^n$.

For some system of differential equations, there may exist some short term perturbations whose duration is negligible comparing with the whole system. These perturbations may cause change in the state of the motion. To illustrate the processes with impulse, let us take into account the bouncing ball model which impact against the horizontal flat surface. The velocity of the ball changes when it hits the surface. This type of model is important for the improvement of the theory of differential equations with impulses [3, 4, 5, 8, 109]. There are two different types of impulsive differential equation system. They are: system of differential equations with fixed moments of impulses and those with variable moments of impulses. Let us start with a system with fixed moment of impulses:

$$\begin{aligned} x' &= f(t,x), \\ \Delta x|_{t=\theta_i} &= I_i(x), \end{aligned} \tag{1.1}$$

where $'$ denotes the derivative of state variable $x \in \mathbb{R}^n$ with respect to time, $\{\theta_i\}_{i\in\mathbb{Z}}$ denotes the moments of the impulses and the index i belong to a finite or infinite index set. The function $f(t,x)$ in (1.1) is rate of continuous change of state variable and $I_i(x)$ is instantaneous change of phase variable x. Additionally second equation

in (1.1) can be interpreted as $\Delta x|_{t=\theta_i} = x(\theta_i+) - x(\theta_i)$, where $x(\theta_i+)$ is the position of the solution after impulse and $x(\theta_i)$ is the position of the solution before impulse. Moreover, in this thesis all solutions of the impulsive systems are considered as left continuous. To illustrate the behavior of any solution of (1.1), we will consider the following process. The solution of (1.1) behaves as a solution of $x' = f(t, x)$ until the impulse moment $t = \theta_i$. At the moment $t = \theta_i$, the solution admits jump. That is second equation in (1.1) will be used. Then, the solution will continue as a solution of $x' = f(t, x)$ with initial value $(\theta_i, x(\theta_i+))$, this process continue until the maximal interval of existence of solutions [5]. Moreover, we can conclude that the solution of (1.1) has discontinuities of the first kind.

In systems with variable impulse actions, the impulses occurs whenever solution meets the one of the surfaces of discontinuity in phase space. Comparing with the differential equations with fixed moments of impulses. However, modeling the real world problems with the system of differential equations with variable moments of impulses are far more adequate than those with fixed moments of impulses. An impulsive system with variable moments of impulses can be of the form,

$$\begin{aligned} x' &= f(t, x), \\ \Delta x|_{t=\tau_i(x)} &= I_i(x), \end{aligned} \tag{1.2}$$

where x, Δx $f(t, x)$ and $I_i(x)$ is described before. For each $i \in \mathbb{Z}$, $\tau_i(x)$ is the surface of discontinuity. It is easy to observe from the second equation in (1.2) that the impulse moments depend on the solution. Thus, each solution has its own impulse moments. For this reason, the analysis of these system are more complex than those with fixed moments of impulses. Moreover, it is easy to see that both (1.1) and (1.2) are non-autonomous differential equations with impulses. There is a class of differential equations with impulses which is autonomous. Such systems can be expressed as

$$\begin{aligned} x' &= f(x), \\ \Delta x|_{x\in\Gamma} &= I(x), \end{aligned} \tag{1.3}$$

where Γ is the surface of discontinuity. In order to introduce the solution of (1.3), take into account one of the trajectory of $f(x)$, the state point of this trajectory moves

until it coincides with the set Γ. Assume it meets with Γ at the moment ζ_i. After it meets, the point $x(\zeta_i)$ is mapped to $x(\zeta_i) + I(x(\zeta_i))$. Then, the state point moves along again as a trajectory of (1.3) with initial value $x(\zeta_i) + I(x(\zeta_i))$ until the next coincidence with the surface of discontinuity Γ and so on. If the vector field $f(t, x)$ in (1.1) is $f(x)$, then we will call such systems autonomous differential equations with fixed moments of impulses. Under certain conditions, such autonomous differential equations with both fixed and variable moments of impulses, form a discontinuous dynamical system. In book [5], some sufficient conditions for the discontinuous dynamical system are presented.

There exists also some interesting features in the models with contact. It is easy to say that the contact can be instantaneous or last for a while. We will call the system with impact if the duration of contact is negligible or instantaneous In an idealized world, there may exist some models where there occur infinitely many impacts in finite time. As we mentioned, such cases cannot been observed in real world applications. For those reason, to make the systems with chattering more realistic surface is considered as deformable and the coefficient of restitution is considered as variable. To model such systems, we considered a system of differential equation with variable moments of impulses.

There are some models where we can analyze them through two differential equation. For such models, to investigate the procedure the stitching method is used in literature, in this procedure the solutions of two different differential equations are glued one by one consecutively. It is appearant that to consider the dynamical properties of these models through stitching method is not efficient because the only way to overcome any problem is to find the exact solutions of differential equations. To solve the dynamical problems and to find the dynamical properties of system, we proposed a model which consists of differential equations with variable moments of impulses called models with impact deformations. Such models save the framework of the solutions of the model with two different differential equation.

1.2 Discontinuous Dynamical Systems

Because of the complex nature of real world, the modeling with continuous dynamical system is much more realistic because of its accuracy and reality of predictions of discontinuity in engineering. Dynamical systems consist of piecewise continuous trajectories. To investigate the behavior of the trajectories of discontinuous dynamical system, the properties of vector field should be considered with maps. The discontinuous trajectories can not be reduced to flows or cascades. But because of the fact that time is continuous for discontinuous trajectories, flows are much more similar to discontinuous flows in time sense. T. Pavlidis [103] is formulated the conditions for autonomous equations with discontinuities to be a dynamical system. Some other papers [3, 5, 8], also include some practical and theoretical ideas about discontinuous flows. There is a chapter in the book of M. Akhmet [5] which covers the provided conditions for the existence of a discontinuous flow and a differentiable discontinuous flow. In the same book also some sufficient conditions are presented for an autonomous impulsive system to be a $B-$ - flow and $B-$ smooth discontinuous flow. The $B-$ continuity and [109], some properties of discontinuous dynamical systems are provided and they are supported through examples. In these books [5, 109], the definitions, theorems and lemmas for discontinuous dynamical system are only considered for those whose trajectories intersects the surfaces of discontinuity transversal. There is no specific condition for discontinuous dynamical systems whose trajectories intersects the surfaces of discontinuity tangentially at least one point. We will call these type of trajectories grazing trajectories and the points where the tangential intersection occurs as grazing points.

1.3 A coincise review on grazing phenomenon

Grazing phenomenon is a special case which can be observed in impacting systems. There can be found two different approaches in the literature for the definition of grazing. One of them is that the grazing occurs whenever the trajectory meets with zero velocity to the surface of discontinuity [98],[99],[106]. Another one is that the trajectory meets with the surface tangentially [23, 27, 31, 46]. In the light of these

papers, we focused on the analytical expression of the tangency at the grazing point to define the horizontal grazing and vertical grazing.

In literature grazing phenomena is considered generally for systems where whose vector fields are non autonomous and the impulse functions and surfaces of discontinuities are only functions of space variable. Nordmark [97]-[100] in his seminal paper investigated the existence of grazing periodic and aperiodic solutions by utilizing a special map called Nordmark map. Budd is also considered the grazing as a bifurcation phenomena which can be interpreted as transition from the continuous trajectory to discontinuous under parameter variation. To handle with this problem, Budd defined a map which is called zero time discontinuity map. Feigin [39, 40] is also considered the the existence of periodic solutions and period doubling solutions in his papers. Ivanov found some sufficient conditions for systems with graziness which undergoes a bifurcation under a parameter chance.

There are wide ranges of studies about grazing phenomenon [23, 31, 27, 46, 98, 106]. All existing studies are conducted on autonomous systems [106, 53], the systems with discontinuous right hand side [19, 33] and non-autonomous system with autonomous surfaces of discontinuity [99]. In [46], a criterion for horizontal grazing motions in a dry friction oscillator is determined by means of the local theory of non-smooth dynamical systems on the connectible and accessible domains. In the study [99], the creation of periodic orbits associated with grazing bifurcations in the models of impacting systems and some sufficient conditions are obtained for the existence of a family of periodic solutions. In [42], two distinct types of grazing bifurcations are taken into account. One is that the stable motion disappears and system stabilized onto an already existing attracting solution and the other in which there is an immediate jump to chaos as part of an orbit grazes at a stop. In the paper [98], the stable periodic orbits and chaotic motions are determined analytically by utilizing the limit mapping. In [99], some sufficient conditions are obtained to determine the existence of a family of periodic orbits whose creation is caused by ramification from the grazing bifurcation point. The smallest appropriate parameter alteration for the horizontal grazing in a hybrid system is determined by applying numerical methods [36]. A general method is presented for the construction of suitable local maps near a horizontal grazing point for n-dimensional PWS systems in [33]. In our paper [6], we have taken

into account the grazing properties of discontinuous dynamical systems and we prove the orbital stability theorem for them.

In [76], some information about the strange attractor fragmentation which is caused by grazing in non-smooth dynamical systems is given. The sufficient and necessary conditions for grazing bifurcation in non-smooth dynamical system are considered. The initial sets of grazing mapping with the corresponding initial grazing manifolds are introduced and taken into account. The fragmentation of strange attractors of chaotic motions which is induced by grazing are presented. In the paper [98], the nonlinear dynamics of vibro-impact system is investigated utilizing the Poincarè map, which has piecewise property and singularity in it. Because two masses have the grazing contact with each other, the singularity is generated in the map and it gives rise to the instability of periodic motions.

The paper [97], the motion of single degree of freedom periodically forced oscillator subjected to a rigid amplitude constraint is taken into account. By analytical methods, the singularities caused by grazing impact are investigated. It is shown that as a stable periodic orbit comes to a grazing impact under control of single parameter a special type of bifurcation occurs. It is observed that the motion after the bifurcation may be non-periodic and a criterion for this based on orientation and eigenvalues are given.

Shaw and Holmes [111] studied the details of grazing bifurcation in a single degree of freedom one sided impact oscillator. It is explored that a grazing bifurcation take places when a point on the orbit of the Poincare map intersects the line of the stop with zero velocity. Some mathematical and numerical analysis have been done on single degree and multi-degree of freedom impacting harmonic oscillators. It is observed that they reveal variety of complex behaviour such as grazing bifurcation, chattering and trapping.

In the study [23], a new form of bifurcation called the grazing bifurcation is identified and exemplified that it leads to complex dynamics including chaotic behavior interspersed with period adding windows of periodic behaviour. The normal form for the grazing bifurcation is constructed to classify the dynamics around it. It is demonstrated that complex dynamic behaviour can be found at a grazing bifurcation.

It has been shown in [25] that new types of bifurcations exist if a system evolves from a nonimpacting to an impacting state as a system parameter varies smoothly. They named these type of bifurcations as grazing bifurcations. In the paper, different types of grazing bifurcation are observed in a simple sinusoidally forced oscillator system in the presence of friction and hard wall where impacts happen. In [44], it is observed that grazing or zero velocity impacts cause non-differentiability in Poincarè map. It has importance for the bifurcation when a stable impacting motion change to impacting motion. The grazing bifurcation is defined as a bifurcation where a zero velocity impact is involved. In the paper, they studied how the grazing bifurcation of a simple periodic motion can be analyzed in a class of periodically driven vibro-impact systems. By using local analytical methods an expression for the local Poincarè mapping is obtained. The rising and grazing touch which occur in sticking solutions of a two degree of freedom plastic impact oscillator are taken into account. Dynamics of vibro-impact system is described by a three dimensional map which has piecewise property and singularity. In [57], a linear oscillator undergoing impact with a secondary elastic support is considered experimentally and semi-analytically for near grazing conditions. In the study [99], the creation of periodic orbits associated with grazing bifurcations are taken into account and the existence of a family of orbits are given. A numerical example for an impacting system with one degree of freedom is presented.

In the papers [58, 59], the bifurcation around the grazing solution of the system with a parameter is examined. The bifurcations scenarios have been obtained for such system under variation of the parameter. The parameter variation is observed only in the vector-field of an impacting system. Some sufficient conditions for the stability of a grazing periodic solution is presented. In the paper [58], it is asserted that the grazing impact which is known to be a discontinuous bifurcation can be regularized with appropriate impact rule which differs in many aspects from the existing ones. In [59], considering the non-zero impact duration, the bifurcations which are related with grazing contacts are analyzed. To find the resulting motion, some algebraic conditions are derived. The theoretical results are exemplified by taking into account a mechanical system which consists of a disc with an offset center of gravity bouncing on an oscillating surface.

These all papers are united in the following sense, vector-field is the function of both time and space variables and the surfaces of discontinuity and the jump operator of it are defined only through the space variables, then it is easy to call the system a half-autonomous impulsive system. However, there exist some systems where both the vectorfield and the surface of discontinuity consist of space variables, then they are called autonomous impulsive system [21]. Finally, there are papers about mechanical systems where vectorfield as well as surface of discontinuity consist of both time and space variables. Then it is easy to see that such systems are non-autonomous impulsive systems [5].

1.4 Organization of Thesis

The organization of this thesis is of the following form. In Chapter 2, a large class of viscoelastic mechanisms with impact deformations such that colliding parts are deformable and the Newton's coefficient of restitution is variable is taken into account. It is shown that the Kelvin-Voigt viscoleastic model is displaced by the system with variable moments of impacts in analysis of mechanisms with contacts. The suggested impact deformations are compared with the experimental data. By applying deformable surfaces and the variable coefficient of restitution in the models with impacts, we suppress the chattering. By making use of the qualitative theory for the systems with variable moments of impulses, we have investigated the existence of periodic solutions and their stability. To actualize the theoretical results, extended examples with simulations are presented. In Chapter 3, discontinuous dynamical systems with grazing solutions are taken into account. The group property, continuity and smoothness of motions and continuation of solutions, are widely analyzed. A variational system around a grazing solution which depends on near solutions is constructed. Orbital stability of grazing cycles is examined by linearization. The method of small parameter is widen for investigation of neighborhoods of grazing orbits, and grazing bifurcation of cycles is demonstrated in an example. Linearization around a grazing equilibrium point is discussed. The mathematical aspect of the work depends on the theory of discontinuous dynamical systems [5]. Our approach is analogous to that one of the continuous dynamics analysis and the results of this section can be

widened for functional and partial differential equations and others. Some illustrations with grazing limit cycles and bifurcations are picture to actualize the theoretical results. As an example for those systems, we have taken into account a coupled Van der Pol oscillators and the orbital stability of it is considered by applying our results which we have presented before as well as in the paper [6]. In Chapter 4, the grazing phenomenon is considered in two different types of non-autonomous systems. First one is of the form where the vector field is defined by the time and space variables and the surfaces of discontinuity and impact function are defined by only space variables. For those systems, we have considered the sufficient conditions for the asymptotical stability and the regular perturbations around the asymptotically stable grazing solutions. Some examples are provided to show the applicability of our results. The other type is defined by the time dependent vector field as well as the surfaces of discontinuity which is of the form $t = \tau_i(x)$, $i \in \mathbb{Z}$. For this systems, the grazing is defined, the differentiability of solutions with respect to initial values and the regular perturbations around the grazing periodic solution is considered. Additionally, appropriate definitions for the vertical and horizontal grazing are given for non-autonomous systems. For those, the periodic grazing solutions and their stability is considered by applying special linearization technique. In Chapter 5, the discussion about the existing results in this thesis is considered and the future works which can be done in the light of this thesis are summarized.

CHAPTER 2

MODELING

Vibro-impact system [16, 20] is the term used to present a system which is driven in some way and which also exhibits an intermittent or continuous sequence of contacts with limiting constraints of the motion. Vibro-impact systems involve multiple impact interactions in the form of jumps in the state space. The dynamics and properties of vibro-impact systems and specifications of nonlinear phenomena with discontinuity have been investigated in the literature for decades [17, 52, 83, 107]. Compared with a single impact, the non-linear dynamics of vibro-impact systems are more complicated. The trajectories of such systems have discontinuities, which are caused by the impacts, in phase space. Although the presence of non-linearity and discontinuity complicates the dynamic analysis of such systems, they can be described theoretically and numerically with discontinuities in good agreement with reality. Such systems with impacts appear in a wide variety of engineering applications. The operation of vibration hammers, impact dampers, inertial shakers, pile drivers, milling and forming machines, and other vibro-impact systems is based on the impact action for moving bodies [24, 63, 80]. Machines with clearances, heat exchangers, steam generator tubes, fuel rods in nuclear power plants, rolling railway wheel-set, piping systems, granular gases, gear transmissions, and other such systems perform impacts.

An overwhelming number of investigations on vibro-impact mechanisms consider models with rigid flat surfaces of impact [13, 37, 41, 62, 104, 124]. It is natural that some materials behave more elastically on impact than others. Any material body deforms under external forces. A deformation is called elastic if it is reversible and time independent. That is, the deformation vanishes instantaneously as soon as

forces are removed. A viscoelastic deformation is reversible but it is a time dependent deformation. It increases with time after application of the load, and it decreases slowly after the load is removed. A plastic deformation is irreversible, in other words, it is a permanent deformation. A mechanical model for plastic deformation is drawn in Fig. 2.5.

The primary contributions of the present study are summarized below:

- The contact model with the Kelvin-Voigt viscoelastic motion [35, 64, 123] is replaced by contact model with impact deformations in analysis of mechanisms with contacts. By comparing with the Kelvin-Voigt model, the surfaces of discontinuity and coefficient of restitution are determined analytically and numerically.

- The model with impact deformations is compared with the experimental data [15, 43, 45, 49]. It is shown that our equations, derived for the coefficient of restitution and displacement, are in accordance with the experimental data in the literature.

- Chattering, which can only be observed in an idealized model of an impact system [22, 66, 55], is suppressed by using impact deformations. The acquired models are compared with the existing ones with chattering in the literature.

- Systems with impact deformations are exemplified through several mechanical models. Stability and periodicity for these systems are demonstrated by simulations. Using the differentiability properties of the impulsive system, the stability of these systems are also verified analytically.

- Granular materials, comprised of many single solid particles regardless of particle size, are presented for possible applications of impact deformations. The investigations, done on the mechanical systems, can be also conducted on granular gases [61, 90, 102]. Granular materials are supposed to have chattering phenomena. To give a more realistic model for these materials, the chattering should be suppressed. By utilizing our results, the engineering problems can be investigated extensively.

2.1 Rigid flat surfaces and the constant coefficient of restitution

The main mathematical model of impact is generally characterized by the coefficient of restitution, R, defined as $v_f = -Rv_i$, where v_i is the relative normal velocity before collision, and v_f is the relative normal velocity after collision [86]. Additionally, the coefficient of restitution varies between 0 and 1.

A system with rigid flat surfaces of impact and the constant coefficient of restitution can be modeled by the differential equations with variable moments of impulses [1, 5, 69, 73, 109] One can observe that such systems can be modeled as follows

$$y'' + ky' + my = f(t, y, y'), \quad y \neq 0, \tag{2.1a}$$

$$\Delta y'|_{y=0} = -(1 + R)y' \tag{2.1b}$$

where R is the coefficient of restitution , $R \in [0, 1]$, k is the damping constant, m is the spring's stiffness, and $f(t, y, y')$ is the force which is applied from outside to the system. The equality $\Delta y'(\theta) = y'(\theta^+) - y'(\theta^-)$ denotes the jump operator in which $t = \theta$ is the time when a mass reaches the rigid obstacle which is at position $y = 0$. Also, $y'(\theta^-)$ is the pre-impact velocity, which is the velocity before impact (which is the left limit of the velocity) and $y'(\theta^+)$ is the post-impact velocity, i.e., the velocity after impact (which is the right limit of the velocity). In mechanical models, the solutions are assumed to be left continuous [5]. Thus, the velocity is assumed as left continuous, i.e., $y'(\theta^-) = y'(\theta)$. System (2.1) is extensively used in applications such as mechanics and electronics [5, 13, 119]. It is called a model with the Newton's law of impact.

There can be found some applications of mechanisms with a constant coefficient of restitution in biology. For example, the mechanical base of impact resistance in a biological armor is investigated. By using the coefficient of restitution, an informative analysis of a biological system have been conducted [117].

There is no system in the real world which is as idealized as the system with rigid flat surfaces and the constant coefficient of restitution. By introducing new conditions

on colliding bodies, we aim to develop a model for the vibro-impact systems, which includes the framework of equation (2.1). A detailed illustrations of such a model can be found in the remaining part of the study.

2.1.1 The Kelvin-Voigt model and the mechanisms with contacts

Consider a vibro-impact model, at some time intervals the bodies interact with each other and at other time intervals, they move separately. In general, the investigations on motions of such systems are comprised of two phases, i.e., Free Flight Motion (FFM) and Contact Motion (CM). FFM is observed when the parts of the mechanisms are not in contact. A motion which has the period of time when the colliding bodies are in contact with each other, is called CM. The interaction between bodies can be of different types. For example, one body penetrates another body or strikes another body, *being in contact*. An impact action can last several seconds or can be instantaneous. In the literature, different types of differential equations are utilized to analyze CM, such as the Kelvin-Voigt viscoelastic motion (KVM) [35, 64, 123] and the Maxwell viscoelastic model [35, 64]. In the case of a non-elastic impact, the model with Newton's law of impact is also considered as a contact model [41, 62, 86, 119]. If we diminish the contact time zero, then one may consider contact motions as impact ones. In the last several decades, mechanisms with impacts are considered through differential equations with impulse. Thus, in our study, we consider two types of contact motion. One is considered by KVM and other one is impulse motion. More precisely, we consider impulse motion in the form of Newton restitution law with constant and variable coefficients of restitution.

KVM is investigated as an illustration for CM. Many original applications of the model can be found in robotics [86] and biology [12, 128]. For example, Argatov [12] have examined some experimental outcomes with a non-linear viscoelastic impact model. The main properties of the articular impact have been qualitatively predicted using the linear viscoelastic theory. For the main parameters of the Kelvin-Voigt and Maxwell models, exact analytical solutions have been attained.

KVM consists of a damper in parallel with a spring and they are linked with a table. The mechanism illustrating the Kelvin-Voigt model is depicted in Fig. 2.1, and the

mathematical formulation of the model can be given as follows:

$$my'' + ny' + cy = -mg, \;\; y < 0 \tag{2.2}$$

where m is the mass of the bead, n is a damping coefficient, and c is a linear spring constant.

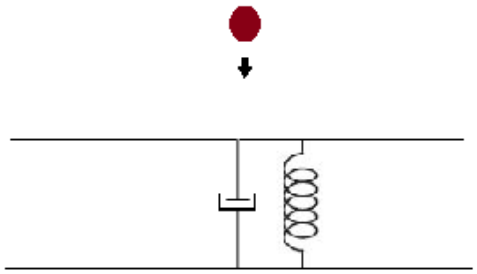

Figure 2.1: The Kelvin-Voigt Model with a spring and a damper.

In a mass-spring-damper system, the main energy dissipation is caused by a damper. Energy in a vibrating system is either dissipated into heat or radiated away. A vibrating system may encounter many different types of damping forces from internal molecular friction to sliding friction and fluid resistance.

For $n = 0$ and $c \neq 0$, there is no damper attached to the system. In such system, the bead reaches the table with velocity v_0 and squeezes the table and leaves the table with the same velocity v_0, only the direction of the velocity changes after the termination of the contact. When $n \neq 0$ and $c \neq 0$, the system consists of a damper and a spring such system may dissipate or produce energy during motion. When $n > 0$, the system dissipates energy during motion. Some kinetic energy is transformed into the deformation of the material, heat, sound and other forms of energy [95]. The bead reaches the table with the velocity v_0 at the level $y = 0$ and compresses the table. After the maximum displacement is attained, the bead moves up and reaches the level $y = 0$ with the velocity less than v_0. This motion proceeds until the bead stops. On the other hand, when $n < 0$, the system produces energy during motion [10]. This type of systems are applicable in mechanical and electrical models [10].

Let us consider the following model. The bead has a free fall in a uniform gravitational field without air resistance from a height y_0 with an initial velocity $v_0 = 0$ to the table which lies at the position $y = 0$. After the bead meets with the table, it exerts pressure on the table and it squeezes the table. Additionally, the Kelvin-Voigt viscoelastic model is *only* valid when the bead and the table act in unison.

A contact motion can be distinguished by two phases, i.e., a loading phase and an unloading phase. The loading phase, starts with the contact, continues up to the maximum displacement. The maximum displacement is attained whenever the velocity of the bead becomes zero. The unloading phase, begins with the maximum displacement, lasts until the bodies are separated from each other. In both the loading and the unloading phases, the model is governed by equation (2.2). During loading phase kinetic energy of the motion is transformed into the internal energy of the deformation by the contact force.

Let us consider the solution of equation (2.2) with the conditions $y(t^*) = 0$ and $y'(t^*) = v$, where t^* is the first time the bead reaches the table (the position $y = 0$). The solution of the equation (2.2) with a damped oscillatory process can be given as follows

$$y(t) = -\frac{mg}{c} + \frac{mg}{c}\exp(-\frac{n}{2m}(t-t^*))\Big[\cos(\frac{\sqrt{4mc-n^2}}{2m}(t-t^*)) + \frac{2cv+ng}{g\sqrt{4mc-n^2}}\sin(\frac{\sqrt{4mc-n^2}}{2m}(t-t^*))\Big]. \tag{2.3}$$

The conditional period, the logarithmic decrement, the conditional amplitude, and the phase angle are quantities which characterize a mechanism with a damped oscillatory process. By utilizing the features of the system, we can determine the conditional period and the logarithmic decrement. However, the initial conditions are needed to determine the amplitude and the phase for an oscillatory mechanism [10].

It is known that the model with the Newton's law of impact and the model with the Kelvin-Voigt viscoelastic motion are autonomous systems. Thus we can consider the meeting moment with the table in the motion with the Kelvin-Voigt viscoelastic model as an initial moment of the motion. That is, we can take an initial condition as $y(0) = 0$ and $y'(0) = v$.

The classical approach of analyzing vibro-impact problems is stitching [14, 74, 118], i.e., integrating motion between impacts and using impact conditions to switch between time intervals of solution. It has been observed that the researchers have analyzed the processes with elastic impact by combining the solutions of two different differential equations. One can understand the process through the following example. Consider a mechanical model whose motion is comprised of FFM and KVM. At first, we suppose that it performs FFM, we can denote the equation of FFM as $x(t, t_0, x_0)$, where x_0 is the initial position of the body and t_0 is the initial moment of the motion. When two bodies collide at time t_1, the solution can be analyzed through the equation of KVM. The equation is investigated as a solution of the differential equation which governs the impact process, i.e., $y(t, t_1, x(t_1, t_0, x_0))$. After KVM, the body continues again its motion as an equation of FFM, which is $x(t, t_2, y(t_2, t_1, x(t_1, t_0, x_0)))$, where t_2 is the time when details are separated. Then it continues its motion as an equation of KVM and so on. This process continues until the bead stops.

Consider a mechanical model with the Kelvin-Voigt viscoelastic motion. The motion of the model is comprised of two phases, FFM which is governed by equation $x'' = -g$ and CM, which is governed by KVM, equation (2.2). Thus, we have introduced Contact Model with Kelvin-Voigt viscoelastic Motion (CMKVM). A diagram for CMKVM is depicted in Fig. 2.2. Now, we will describe the motion as follows. First, the bead starts its motion from the height y_0 with initial velocity $v_0 = 0$ in a uniform gravitational field without air resistance. The first time when the bead meets with the table is $t^* = \sqrt{2y_0/g}$. It is the moment when the bead is in the position $y = 0$. After meeting with the table, the bead applies a force, which is stemming from the weight and the velocity of the bead, on the table. As a consequence, the table is compressed by these forces (loading phase). To calculate how deep the bead travel, we must find the minimum value of the function (2.3). In order to verify it, we need to check the time when the derivative of the position function is zero, i.e. the first root of the function (2.3) gives the moment when the maximum displacement is taken and it is apparent that the velocity of the bead is zero at this time. The following equation (2.4), which also corresponds to the velocity of the bead, is the derivative of the function (2.3)

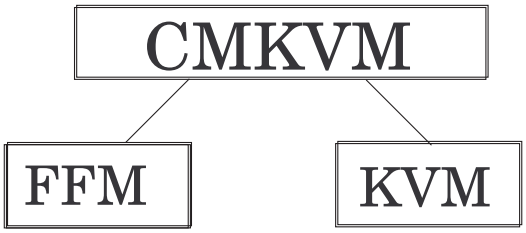

Figure 2.2: The diagram of the Contact Model with the Kelvin-Voigt Viscoleastic Motion.

$$y'(t) = \exp\Big(-\frac{n}{2m}(t-t^*)\Big)\Big[v\cos(\frac{\sqrt{4mc-n^2}}{2m}(t-t^*)) \\ -\frac{nv+2mg}{\sqrt{4mc-n^2}}\sin(\frac{\sqrt{4mc-n^2}}{2m}(t-t^*))\Big], \tag{2.4}$$

and ξ is the time when the bead reaches the maximum displacement after the motion starts. It can be evaluated as follows

$$\xi = \frac{2m}{\sqrt{4mc-n^2}}\arctan\Big(\frac{v\sqrt{4mc-n^2}}{nv+2mg}\Big) + \sqrt{\frac{2y_0}{g}}. \tag{2.5}$$

Additionally, one can evaluate the level of the bead when it attains the maximum displacement as

$$\phi(v) = -\frac{mg}{c} + \frac{mg}{c}\exp\Big(-\frac{n}{\sqrt{4mc-n^2}}\arctan\Big(\frac{v\sqrt{4mc-n^2}}{nv+2mg}\Big)\Big) \\ \times\frac{nvg+mg^2+cv^2}{g\sqrt{mcv^2+mnvg+m^2g^2}}. \tag{2.6}$$

However, the stitching method is not appropriate to investigate the dynamical properties of the vibro-impact systems. If the duration in contact motion is considered small with respect to the duration of FFM, then the model can be called contact model with impact deformations.

2.1.2 Impact deformations

The first stage of impact system studies based on the hypothesis of hard impact with a constant coefficient of restitution [107]. The second level is characterized

by introducing concept of soft impact described by the linear characteristics of force-deformation or/and force-velocity relations during contact. That is, the surfaces are not rigid flat, and the coefficient of restitution is variable. There are some mechanisms with elastic and deformable parts, the coefficient of restitution of which cannot be assumed as constant. Modeling of such mechanisms is more complicated than that of those with rigid flat surfaces and the constant coefficient of restitution. In some papers [32, 89, 124], the coefficient of restitution is considered variable, and a detailed mechanical analysis of the coefficient of restitution is presented. A general impacting hybrid system is considered, where the coefficient of restitution is assumed to be variable in [32]. However, many other papers and books [37, 41, 62], the coefficient of restitution is taken as constant if one considers a concrete mechanical model. The interesting problem of bifurcation and chaos is investigated in a system with deformable surfaces [72] and the constant coefficient of restitution in [81]. Additionally, it is the first time that the surface of discontinuity is considered as perturbed nonlinearly and the detailed analysis of existence of discontinuous limit cycle for the Van der Pol equation with impacts has been given in [8].

It is recognized that the evaluation of the coefficients is still unclear for any particular system and we need to know a detailed nature of elastic waves [32] to calculate it. It has been shown that [86] at low impact velocities and for most materials with linear elastic range, the coefficient of restitution can be approximated by the equation

$$R(v) = 1 - \alpha v,$$

where v is the velocity before collision. In [89], by means of the simulations and experiments, it is demonstrated that the coefficient of restitution is a function of impact velocity if the particle undegoes both the viscoelastic and the plastic deformations at low and high velocities. Additionally, two different analytical expressions are demonstrated for the impact velocity dependent coefficient of restitution in [29, 60]. Both are compatible with the nature of the impact velocity dependent coefficient of restitution, i.e., the coefficient of restitution is varied form zero to unity, and inverse proportional to the absolute value of the impact velocity.

Force characteristics are used to describe the contact interaction of two bodies during impact. Two approaches are considered to analyze force characteristics for the

interaction between solids [14]. One is proposed by Stearmann which consists of two elastic bodies that deform under compression by a force. The force can be interpreted as follows

$$F = c_1 u_0^{\frac{3}{2}}, \tag{2.7}$$

where u_0 is the distance between the centers of masses of the objects in the meeting time and c_1 is the proportionality constant determined via experiments. When the plastic deformation is taken account this model is not appropriate. Thus, Pöschl proposed another formula for the force characteristics

$$F = c_1 u_0^{\frac{3}{2}} \pm b_1 (\frac{du_0}{dt})^2, \tag{2.8}$$

where the positive and negative signs correspond to the loading and unloading phases of collision, respectively.

Indeed, Babitsky [14] stated more general formula to analyze the force characteristics, i.e.,

$$F = \Phi(u_0, \frac{du_0}{dt}). \tag{2.9}$$

From equation (2.9), one can understand that the force characteristics depend on both the impact velocity and the surface position.

Utilizing the implicit function theorem, we can propose that equation (2.9) have a solution of the form $u_0 = \phi(\frac{du_0}{dt})$. *It means that the displacement depends on the impact velocity. We can denote* $\frac{du_0}{dt} \approx x'$*, then the displacement can be presented as*

$$x = \phi(x'). \tag{2.10}$$

In [127], it was shown experimentally that $\phi(x')$ changes linearly with the pre-impact velocity. Additionally, the relation with the pre-impact velocity and the variable coefficient of restitution can be found in [14, 86]. So, we can propose that the graphs $\Phi(x')$ and $\psi(x')$ can be pictured in Figs 2.3 and 2.4, respectively[14, 86].

In systems with impact deformations, the interacting bodies apply some forces to each others. Depending on these forces and the material properties of the bodies, some are deformed under these forces. These deformations can be in a various type such as plastic, elastic and viscoelastic. During these deformations, the displacement changes. As mentioned before, in such systems, where deformation occurs, the coefficient of restitution can not be assumed as constant. Thus, the deformable surfaces and the variable coefficient of restitution are the direct consequences of impact deformations. Let us consider a mechanical system with an impacting object and a surface of discontinuity. When the object meets with the surface, it apply some force on the surface. Due to this force, if the impacting object is rigid, only the surface of discontinuity is deformed. Depending on the velocity of the object at the impact time, a displacement occurs on the surface of discontinuity. It can be observed that the displacement is proportional to the impact velocity, that is, if the impact velocity is higher, the displacement is deeper.

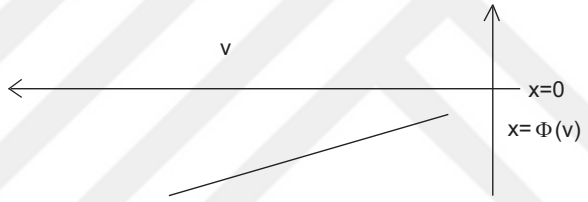

Figure 2.3: The graph of the displacement versus the pre-impact velocity.

In Fig. 2.3, the graph of the displacement of the bead versus the pre-impact velocity has been depicted. It can be observed that the displacement increases whenever the pre-impact velocity of the bead increases in absolute value. We only forecast how the displacement changes with the pre-impact velocity in Fig. 2.3 . Additionally, the forecast will be supported by simulation results in the next section.

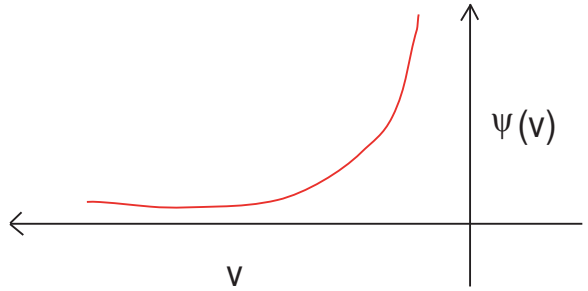

Figure 2.4: The graph of the coefficient of restitution versus pre-impact velocity.

The relation between the coefficient of restitution and the pre-impact velocity is pictured in Fig. 2.4. It is observed that the coefficient of restitution is inverse proportional to the pre-impact velocity [37, 55, 60, 66, 86, 90, 91, 117].

2.1.3 Granular materials

Granular material is composed of many single solid particles regardless of particle size. In numerical simulations of rapid granular flows, particles collide with each other. As a consequence of these collisions, energy is dissipated and the dissipation is *characterized by the coefficient of restitution*. In contrast to elastic interaction of particles in molecular gases, the collision of macroscopic granules are generally inelastic. There is a huge literature about the inelastic collision of granular gases [61, 90, 91, 102]. The important difference between granular media and ordinary gases or liquids is that interactions between granules are naturally inelastic. It is crucial to remember that any apparently fluid-like behavior of a granular material is a completely dynamic phenomenon. To illustrate, the surface waves do not emerge as a linear response to external energy input but are the consequence of a highly nonlinear hystretic transition out of the solidlike state [61]. As a consequence, in each collision some energy is dissipated away. The interactions in a granular gas can be modeled by utilizing a standard approach based on the assumption of instantaneous collisions among granules with energy dissipation characterized by a constant coefficient of restitution [102]. The consequences of recent molecular dynamic simulations of a two dimensional granular medium is presented in [91]. It is assumed that a gas of inelastic discs in which the interactions occur only through collisions.

For the granules, it is possible to collide infinitely often in a finite time which is called an inelastic collapse [61, 91]. For mechanical systems, the inelastic collapse is called chattering [61, 102]. The detailed literature about the chattering behavior will be given in the next section. The important difference between an ordinary gas molecules and a gas of granules is that the interactions are dissipative, pairwise collisions of granules preserve momentum but they do not preserve kinetic energy [102]. The steady removal of kinetic energy in the granules due to dissipative collisions whenever it is compared with common molecular gases. In [89], the properties of granular gases

has been investigated and the particles are assumed to be colliding viscoelastically . As a consequence of the viscoelastic collision, it is observed that the restitution coefficient is a function of the pre-impact velocity. Thus, the investigations, done on the impact mechanisms, can be also performed on granular gases.

2.1.4 Chattering

Chattering is one of the most interesting features of an impacting system which is characterized by *an infinite number of impacts* occurring in *a finite time* [22, 66]. The chattering behavior can be observed in the vibro-impact systems with rigid flat surfaces and the constant coefficient of restitution. It can be only seen in an idealized model of an impacting system, only a large but a finite number of impacts occurs in a more realistic model. In the book of Ibrahim [55], chattering is understood as special type of oscillation characterized by very small amplitudes that are decreasing with time. Some analytical results, which demonstrate chattering, are exhibited. An asymptotic estimate of the chattering time with respect to a small parameter proportional to the excitation amplitude is demonstrated for a linear model of inverted pendulum impacting between lateral walls [29]. Lenci, Demeio and Petrini [66] have presented a method to compute the time length of chattering in a model for an impacting linear inverted pendulum between two lateral walls. This method also serves information about suppression of chattering as the excitation amplitude is increased. Chattering oscillations are depicted for different excitation values in [66] Fig. 10. In a cooling gas of rigid particles interacting with a constant coefficient of restitution, groups of particles within the gas may experience chattering. It is demonstrated through molecular dynamic simulations that a two dimensional gas of inelastic disks collide infinitely often in a finite time along their joint line of centers [91]. In [90], the dynamics of a one dimensional gas of inelastic point particles are investigated. It has been shown through simulations that three particle perform an infinite number of impacts in a finite time [90]. A detailed analysis of chattering for impact oscillators can be found in the paper of Budd and Dux [22]. In the study [22], chattering is not only investigated for autonomous systems, but it is also considered for non-autonomous systems. A systematic study of chattering behavior is provided for a periodically forced, single degree of freedom impact oscillator with a restitution law

at each impact. The relation between the chattering behavior and the certain types of chaotic behavior is also observed. Guisepponi, Marchesoni and Borromeo have proposed [48] that chattering resembles with the inelastic collapse. In the process, inelastic balls dissipate their energy through an infinite number of collisions in a finite amount of time. It is also checked numerically [48] that the bouncing ball chattering is suppressed in the limit when the coefficient of restitution is approaching unity. Chattering trajectories in the impact space for the model of the bouncing bead with a vibrating platform is depicted, one can see in Fig. 7 in paper [48]. In the work of Wagg and S. Bishop [125], chatter and sticking, which are the nonsmooth phenomena of the impacting systems, has been extensively investigated for a two-degree of freedom impact oscillator. Luck and Metha [68] have carried out the dynamic analysis of a bouncing ball on a vibrating platform. An infinite number of smaller and smaller bounces in a finite time is defined as a complete chattering for the system. It is also demonstrated that generic trajectories result in a complete chattering, or locking. In other words, the ball bounces infinitely many times in an absorbing region without arriving the transmitting region, since there exists an exponential decay in the bouncing amplitudes. Luo and Connor [79] investigated the dynamic mechanisms of the impacting chatter with stick by using the local singularity theory of discontinuous dynamical system and in the study [78], they examined the motion mechanism of impacting chatter with stick exploiting the theory of discontinuous dynamical system.

It has been demonstrated through above studies that chattering is one of the important phenomena in mechanics and media. As a consequence, one either produces mathematical methods to discover and investigate chattering or constructs models such that chattering will not be possible as a motion for the system. There is no wide amount of work about chattering phenomena which serves detailed mathematical analysis. Except possibly the eminent paper of Budd and Dux [22], where chattering is observed through exact solutions of models. Additionally, the book of Nagaev [94] contains a huge computational work on the investigation of chattering in concrete models. Due to the scarcity of the mathematical theory of chattering, it is crucial to consider models with chattering, and substitute them convenient perturbations in order to suppress any chattering in the acquired models. This study is especially devoted to this problem. The *suppression* of chattering can be comprehended as *a modification of a model with*

chattering to the model whose solutions may admit only finite number of discontinuities on a finite time interval of existence. It is essential to assert that chattering can be suppressed not only in mechanical systems but also in granular media [91, 102] by our results.

In Section 2.4, the suppression of chattering is attained through perturbations in the coefficient of restitution and the surfaces of discontinuity. Thus, we bring theoretical dynamics, which can be understood as the dynamics of the idealized model, closer to reality by using perturbations.

The outline of the remaining part of this study is as follows. In Section 2, a model for a vibro-impact system with viscoelastic parts is obtained and illustrated. In the third section, three concrete mechanical examples are presented for the systems with impact deformations. The existence and stability of the periodic solutions for such models are analyzed by using Poincaré map and the differentiability with respect to the initial condition for differential equations with variable moments of impulses. In the fourth one, chattering has been suppressed on two different mechanical systems by introducing impact deformations. The fifth section covers the discussions about this study.

2.2 The modeling

2.2.1 Models with impact deformations

In the following discussion, the bead is not considered as a point in the coordinate system, i.e., it admits nonzero radius. Its lowest point should be considered to determine the meeting moment with the surface of impact. The bottom point of the bead is denoted as P. The meeting moment, θ, can be calculated from the equation $x(\theta) = \phi(x'(\theta))$, where $x(\theta)$ is the position of P at time θ. If $z(\theta)$ is the position of the center, c, of the bead, then we have that $x(\theta) = z(\theta) - r_0$ and $z(\theta) = r_0 + \phi(x'(\theta))$, where r_0 is the radius of the bead. During the motion, the bead is assumed to be non deformable.

The position of the bead when it reaches the level $x = 0$ can be seen in Fig. 2.5 part

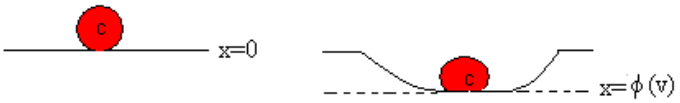

Figure 2.5: A model with a bead and a surface (a) The bead reaches the level $x = 0$ with a velocity v, and the deformation begins. (b) The plastic deformation occurs on both the bead and the surface. After deformation, the bead lies at the position $x = \phi(v)$.

(a). In Fig. 2.5 part (b), it can be observed that the plastic deformation occurs both on the bead and the surface. The deformation of the system can be understood as a combination of deformations that occur on the ball and the surfaces of discontinuity at the same time.

Let us start with a simple model which has been considered in the literature as a bouncing bead model. It is known that the bouncing bead model is the *origin* of the mechanical systems. In the model, there is a steel bead having a free fall from a height x_0 with an initial velocity $x'(0) = 0$ in the uniform gravitational field without air resistance. By utilizing differential equations with variable moments of impulses, we can give a mathematical model for the bouncing bead as follows:

$$\begin{aligned} x'' &= -g, \quad x \neq 0, \\ \Delta x'|_{x=0} &= -(1+R)x'. \end{aligned} \tag{2.11}$$

In this model, the bead is dropped from height x_0 with zero initial velocity on the surface which is at the level $x = 0$ and both are rigid flat. When $R = 1$, the collision is totally elastic, i.e., there is no energy dissipation during collision. When the coefficient of restitution is $R = 0$, we have a totally inelastic collision. In this collision, all of the energy is dissipated away and the bead stops abruptly.

In this study, we consider the model where the level of the strike as well as the coefficient of collision (the Newton's coefficient of restitution) are variable, i.e., both depend on the velocity of the bead at the moment of strike.

The idea of the variable coefficient of restitution is not new. Hertz stated that the coef-

ficient of restitution varies with the pre-impact velocity [37]. The displacement of the bead also depends on the pre-impact velocity when the surfaces are not rigid. That is, in various impact velocities the displacements of the bead are different. Additionally, there are some papers [37, 81] which affirm that the displacement of the bead, $\phi(x')$, is linear.

Now, it is reasonable to change system (2.11) into the following one

$$\begin{aligned} x'' &= -g, \quad x \neq \Phi(x'), \\ \Delta x'|_{x=\Phi(x')} &= -(1+\psi(x'))x'. \end{aligned} \tag{2.12}$$

In this model, the bead has a free fall until it reaches the level $x = \Phi(x')$, and the motion of the bead is governed by differential equation $x'' = -g$. When the bead reaches the level $x = \Phi(\tilde{v})$, the impact occurs and the velocity changes with $\tilde{v}^+ = -(\psi(\tilde{v}))\tilde{v}$, where $\tilde{v} = x'^-$ and $\tilde{v}^+ = x'^+$. It moves up as a solution of the differential equation $x'' = -g$ with the initial condition $x(0) = \Phi(\tilde{v})$ and $x'(0) = -(\psi(\tilde{v}))\tilde{v}$. This motion continues until the velocity of the bead becomes zero when it reach the level $x = 0$, or the velocity of the bead becomes zero somewhere between $x = \Phi(\tilde{v})$ and $x = 0$.

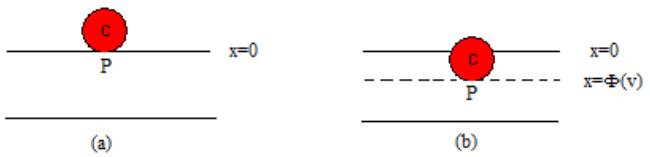

Figure 2.6: (a) A model consisting of a bead and a ground, where the bead is at the level $x = 0$. At that level, the elastic deformation begins. (b) A model consisting of a bead and a ground, where the bead is at the level $x = \Phi(v)$, maximum deformation occurs.

In Fig. 2.6 part (a), it is depicted that after performing a free fall, the bead meets with the ground which lies at the level $x = 0$. After meeting, the deformation occurs on the ground but no deformation occurs on the bead. The shape of the bead does not change and the material of the bead is not lost after collision. The displacement is considered to be depending on the velocity, v. It is the velocity when the bead meets

with the surface which lies at the position $x = 0$.

2.2.2 Replacing the Kelvin-Voigt model with the impulse model and analysis of mechanisms with impacts

In this part of our study, we replace the Kelvin-Voigt model with the impulse model, where the all dynamical properties of the Kelvin-Voigt model is preserved. By comparing KVM and IM, we derive proper analytical expression for the functions $\Phi(x')$ and $\psi(x')$.

We calculate the displacement as $y(\xi) = \phi(y'(0))$ and at that level the velocity, which is the meeting velocity of the bead with the table, is calculated from the model with the Kelvin-Voigt viscoelastic motion. The maximum displacement is taken when the velocity of the bead becomes zero, i.e., $y'(\xi) = 0$, where ξ is considered as a moment when the maximum displacement is attained. In the motion with the Newton's law of impact, we will consider that the bead meets with the level $x = 0$ with velocity v. The beads meet the surface which lies at the level $x = 0$ with velocity v in both models. In our calculations, the time η corresponds the travel time of the bead, whose motion modeled by by using system (2.12), from the level $x = 0$ to the level where it attains maximum displacement. Additionally, we will suppose that the beads in both models reach the level $x = 0$ again with velocity $\bar{v}$ at a time T. The equations, needed to calculate the displacement and the coefficient of restitution, can be presented as follows:

$$x(t) = -\frac{1}{2}gt^2 + vt, \tag{2.13}$$

$$x(t) = -\frac{1}{2}g(T-t)^2 + \bar{v}(T-t). \tag{2.14}$$

Moreover by finding the first minimal positive root of the equation (2.3), we have calculated the time T and by substituting T to equation (2.4) we have evaluated the velocity, $\bar{v}$, numerically. By utilizing equations (2.13), (2.14), T and $\bar{v}$, we calculate the time η as follows:

$$\eta = \frac{2\bar{v}T - gT^2}{2v + 2gT + \bar{v}}. \tag{2.15}$$

Now, substituting (2.15) to equation (2.13), we evaluate the maximum displacement for the model (2.12) as follows:

$$x(\eta) = -\frac{1}{2}g(\frac{2\bar{v}T - gT^2}{2v + 2gT + \bar{v}})^2 + \frac{2\bar{v}Tv - gT^2v}{2v + 2gT + \bar{v}}. \tag{2.16}$$

To calculate the function $\psi(v)$ for system (2.12), we use the velocities v and $\bar{v}$, it is reasonable to consider v as the pre-impact velocity and $\bar{v}$ as the post-impact velocity [115]. Consequently, the coefficient of restitution can be calculated as

$$\psi(v) = -\frac{\bar{v}}{v}. \tag{2.17}$$

In previous section, we consider the vibro-impact system which is modeled by using two different differential equations for two different stages of the motion, i.e, FFM and Impulse Motion (IM). In this section, instead of analyzing FFM and IM separately, we have analyzed the Contact Model with Impact Deformations (CMID) as a combination of two stages of the motion. This can be understood through Fig. 2.7.

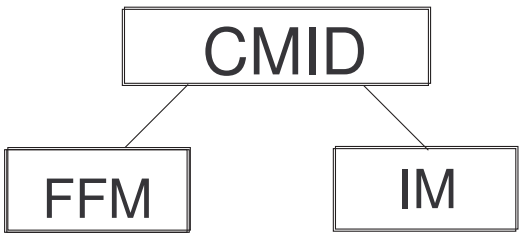

Figure 2.7: The diagram of the contact model with impact deformations.

As a consequence of the combination, we have presented a new model for CMID - a differential equation with variable moments of impulses for the motion. The idea of modeling with the impulsive differential equations is taken from the book [5] and the papers [7, 8]. Such models serve many dynamical properties. CMID is governed by

the following system

$$x'' + ax' + bx = f(t, x, x'), \quad x \neq \Phi(x'), \tag{2.18a}$$

$$\Delta x'|_{x=\Phi(x')} = -(1 + \psi(x'))x' \tag{2.18b}$$

where $x = \Phi(x')$ is the level of strike and $\psi(x')$ is the coefficient of restitution. In (2.18), during the FFM, which is governed by (2.18a), the system may gain or loss some energy depending on the mechanical properties of the system. For this reason, we introduce the constants a and b to the system (2.18). Our aim is to provide a model, described by (2.18), becomes mechanically and physically realistic. Since $y'(\theta^+) = -[R]y'(\theta^-)$ in (2.18) is replaced, now with $x'(\theta^+) = -[\psi(x'(\theta^-))]x'(\theta^-)$. Then it is reasonable to call CMID.

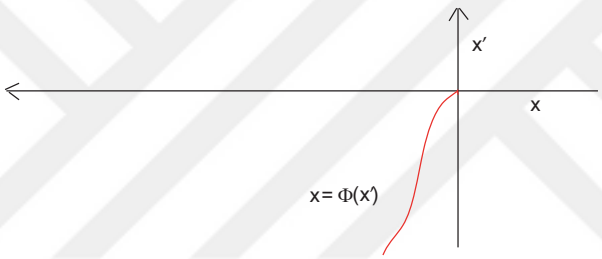

Figure 2.8: The graph of the displacement function for the contact model with impact deformations.

By using the equations (2.18a) and (2.2), we present the following system

$$y'' + ay' + by = f(t, y, y'), \quad y \geq 0, \tag{2.19}$$

$$my'' + ny' + cy = -mg, \quad y < 0. \tag{2.20}$$

Our aim in this study is to give appropriate model for the mechanisms with viscoelastic parts by using the impulsive differential equation (2.12). So, by utilizing the Kelvin-Voigt viscoelastic model, we find appropriate approximations for the function $\Phi(x')$ and $\psi(x')$. Now, in system (2.12), the function $\Phi(x')$ is replaced with the equation (2.16) and the function $\psi(x')$ is replaced with the equation (2.17), we assert

that the blue curve and the red curve in Fig. 2.10 overlap for $x, y \geq 0$. We can replace the system (2.19)+(2.20) with the system (2.18) in the analysis if the contact time for system (2.19)+(2.20) is small. In other words, if the contact motion time is small in CMKVM, we can replace CMKVM with CMID. Diagrams for CMKVM and CMID are depicted in Fig. 2.2 and Fig. 2.7, respectively. The analysis of CMKVM is done by using stitching method. Stitching method is not convenient in the dynamical analysis of such systems. CMID is a special type of differential equations with variable moments of impulses. The dynamical properties of this system can be analyzed easily by using the properties of differential equations with variable moments of impulses. As a consequence of these replacement, we can analyze the dynamical properties of CMKVM by using CMID under certain conditions. Thus, CMID does not only present a new modeling type for CMKVM but it also make the investigations easier.

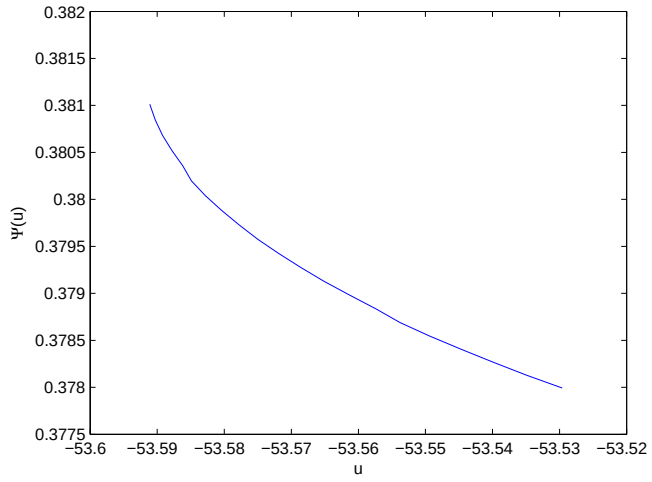

Figure 2.9: The coefficient of restitution versus the absolute value of the velocity at the level $x = 0$.

In Fig. 2.10, the red curve is the time series of the mechanical model with the Kelvin-Voigt viscoelastic motion and the blue curve is the time series of system (2.12). If the duration of time needed for contact motion in the model with the Kelvin-Voigt viscoelastic motion is taken as zero approximately then the blue curve and the red curve approach to each other, and if in equation (2.2) the linear spring constant, c, is larger, then the function $\phi(v)$ approaches to zero. The time, needed for the bead to travel from the level $x = 0$ to level $x = \phi(v)$ in the model with the Kelvin-Voigt viscoelastic motion, approaches to zero whenever the linear spring constant, c,

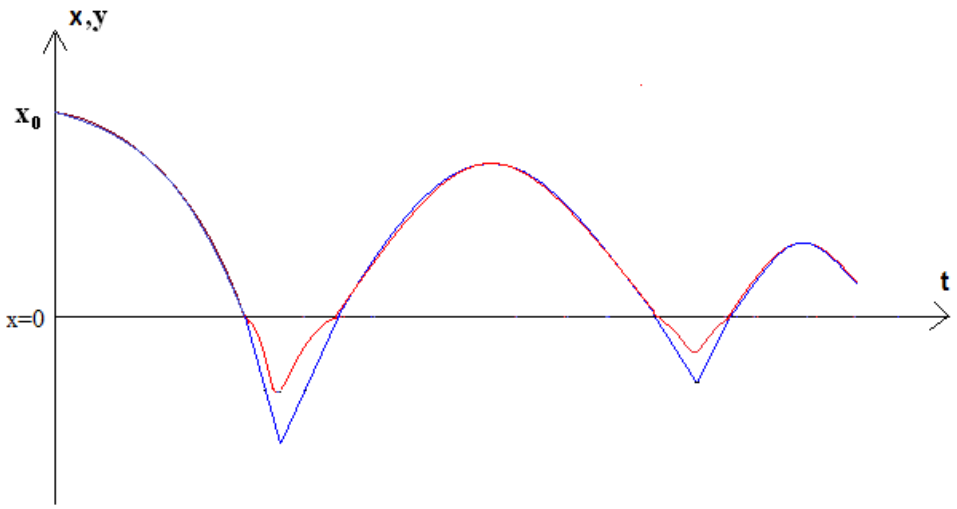

Figure 2.10: The red curve is the time series of CMKVM and the blue one is the time series of system (2.12) (CMID).

tends to infinity. If in equation (2.2), the mass m is small, then the acceleration is large and the velocity increases rapidly [10]. This rapid change in velocity leads to a formulation of condition of jump. We can assert that the function (2.6) increases to zero if the time ξ in formula (2.5) decreases. If the function (2.6) is zero, then the blue and red curves coincide. Accordingly, the implementation of the impulsive differential equation (2.12) to analyze the viscoelastic mechanisms is realistic.

2.2.3 Discussions on the surface of discontinuity and the coefficient of restitution

In this part of the work, we depicted in Figs 2.11 and 2.12 for an illustration of our analytical data and investigated the coherence of our analytical and numerical results with the existing ones in the literature.

In our simulations given in Figs 2.11 and 2.12, we take gravitational acceleration g as 9.8, the constants $m,\ n,\ c$ as $64,\ 16,\ 1601$, respectively, and the velocity v as -10. For model (2.12), we will denote the displacement as $x(\eta) = \Phi(v)$. By means of equation (2.16), we draw Fig. 2.11. It can be observed through Fig. 2.11 that the displacement increases whenever the absolute value of the meeting velocity increases.

Some studies are conducted on the penetration depth and the pre-impact velocity by using a single projectile fired into concrete in [49]. The graph of penetration depth which depends on pre-impact velocity has been illustrated in [49] Fig. 12. It can be observed from Fig. 12 in [49] that the penetration depth increases whenever the absolute value of the pre-impact velocity increases. Additionally, other experimental results about the penetration depth and pre-impact velocity can be found in [43]. The experiments are conducted on the depth of penetration into grout and concrete targets with ogive-nose steel projectiles. Through these experiments, it is observed that the penetration depth increased when the absolute value of the striking velocity increases until the nose erosion is excessive [43].

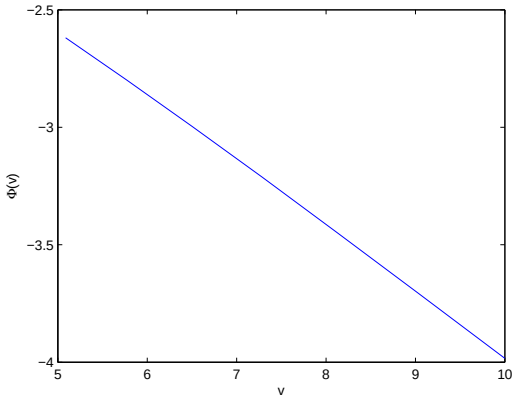

Figure 2.11: The displacement versus the absolute value of the velocity at the level $x = 0$.

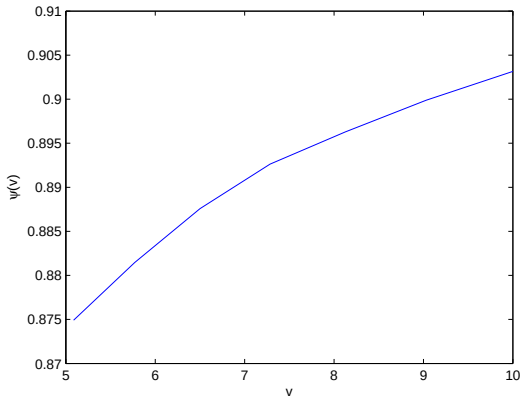

Figure 2.12: The coefficient of restitution versus the absolute value of the pre-impact velocity.

In Fig. 2.12, the coefficient of restitution versus the absolute value of the pre-impact velocity has been simulated. The pre-impact velocity is taken as the velocity when the interacting bodies meet with each other [115, 127]. It is reasonable to assume that the function $\psi(v)$ is a function of the pre-impact velocity. In real experiments for the ideal bouncing bead model, the restitution coefficient depends on the velocity of the ball before impact relative to the platform [60, 89, 116]. In Fig. 2.12, it can be observed that when the absolute value of the pre-impact velocity is higher the coefficient of restitution is higher. In collisions, the energy dissipation increases if the pre-impact velocity increases [37]. That is, the coefficient of restitution and the absolute value of the pre-impact velocity are inverse proportional to each other [37]. In [89], the simulations of vibrated granular medium present that the restitution coefficient depends on the velocity before impact. Fig. 1 in paper [89] illustrates the behavior of the coefficient of restitution with respect to the pre-impact velocity. The paper of Tabor [116] contains a detailed analysis of the restitution coefficient and it is observed that the coefficient of restitution depends on the pre-impact velocity. The relationship between the restitution coefficient and the velocity before impact is pictured in Fig. 6 in paper [116]. In the paper of Wu, Li and Thornton [127], an analytical expression for the restitution coefficient, which depends on the velocity before the impact, has been presented. The computer simulation, which represents the connection between the pre-impact velocity and the coefficient of restitution, is exhibited in Fig. 3 in paper [127]. In [60], the coefficient of restitution, which depends on the pre-impact velocity, is presented analytically. In paper [60] Fig. 5, the correlation between the coefficient of restitution and pre-impact velocity is pictured for two different models. Additionally, the comparison of several models to experimental results of aluminum oxide spheres impacting a aluminum flat and a steel flat are depicted in Figs 7 and 8, respectively [60]. One can compare Fig. 1 in paper [89], Figs 5, 7, 8 in paper [60], Fig. 3 in paper [127] and with the our simulation result which is illustrated in Fig. 2.12. It can be observed through mentioned simulations, and our simulation presented by Fig. 2.12 that the coefficient of restitution depends on the pre-impact velocity but in our simulation the coefficient of restitution is increases whenever the absolute value of the pre-impact velocity increases. On the other hand, in [45], the impact behavior of wet granules was investigated by measuring the coefficient of restitution. It is observed that the coefficient of restitution is increased with velocity, when the elastic

energy exceeds the associated with adhesion. Then, it is observed that the restitution decreases with velocity when the yield stress is exceeded. In paper [45] Fig. 6, it can be observed that the coefficient of restitution increases up to a maximum value with the increasing impact speed, then decreases with the impact speed after the maximum coefficient of restitution is attained. Our simulation result, which can be observed through Fig. 2.12 that the restitution increases with the velocity and varies between zero and one. Additionally, in Fig. 5 paper [15], the graph of the coefficient of restitution for millimetric water drops hitting a super-hydrophobic surface is drawn. In low velocities at the impact, it can be observed that the restitution increases with the increasing velocities. Our simulation, illustrated in Fig. 2.12, agrees with the results of the simulations given in papers [15, 45]. Our system is comprised of a spring and a damper, for this system there is no specific material properties like a steel or an aluminum. The graph of the coefficient of restitution given in Fig. 2.12 does not agree with the graphs presented in papers [60, 89, 116]. Because they consider the dynamics of the contact motion as less elastically. That is, they use hard materials such as steel and aluminum in their experiments. We propose that the materials with small elasticity has to be investigated in a different way in a contact motion.

There are some mechanisms [14] with rigid flat surfaces and a constant coefficient of restitution which have a periodic solution under certain conditions. It is significant to investigate the existence and stability of the limit cycles of the systems with a variable coefficient of restitution and deformable surfaces. Because there is no such system can be found in the real world as idealized as the system with the constant coefficient of restitution and rigid flat surfaces.

2.3 Periodic motions and stability in mechanisms with impact deformations

In order to demonstrate what kind of problems arise for the mechanisms with impact deformations, we consider the following examples. In the literature, many researches have been done on vibroimpact systems with the constant coefficient of restitution and rigid flat surfaces (impact deformations) [41, 54, 55, 62, 80, 81, 115, 119, 124]. Some works on the variable coefficient of restitution and deformable surfaces can be also found in the literature [32, 37, 60, 89]. In these works a mechanical model is given

but whenever the analytical computations are considered, the models are considered with rigid flat surfaces and the constant coefficient of restitution.

As a **first example**, let us consider a mass, which is hinged to the wall vertically with a spring and a damper parallel to each other [47]. When the mass is passing through the position $x_1 = \mu|x_2 - 1|, \quad x_2 > 0$, a bullet with an infinitesimal mass, fired with a constant velocity, sticks in the mass. Due to the action of the bullet, the mass is subdued to an impact which affects as a constant increase in the velocity. The increment in velocity can be comprehended as follows $x_2(\bar{\theta}^+) - x_2(\bar{\theta}^-) = I_1$, where $\bar{\theta}$ corresponds to the sticking moment of the mass and the bullet. After that time, the mass continues its motion and reaches maximum angular displacement. Then, it swings back and reaches the level $x_1 = 0, \quad x_2 \leq 0$. At that moment, the bullet with an infinitesimal mass, fired with a constant velocity, sticks in the mass, again. Then, the mass experiences a constant increase in the velocity, i.e., the equality $x_2(\tilde{\theta}^+) - x_2(\tilde{\theta}^-) = I_2$, is the difference between pre-impact and post-impact velocities and $\tilde{\theta}$ is the moment when the bullet sticks in the mass. The above process of the mass and the bullet lasts until the mass stops and at each moment when the mass passes through the levels $x_1 = \mu|x_2 - 1|, \quad x_2 > 0$ and $x_1 = 0, \quad x_2 \leq 0$, the mass performs impacts. The motion of the system is described by

$$
\begin{aligned}
&x_1' = x_2, \\
&x_2' = -x_1 - x_2, \quad x_1 \neq \mu|x_2 - 1|, \\
&\Delta x_2|_{x_1 = \mu|x_2 - 1|} = I_1, \qquad\qquad x_2 > 0, \\
&x_1' = x_2, \\
&x_2' = -x_1 - x_2, \quad x_1 \neq 0, \\
&\Delta x_2|_{x_1 = 0} = I_2, \qquad\qquad x_2 < 0,
\end{aligned}
\tag{2.21}
$$

where $I_1 = 3$, $I_2 = 4\exp(-\frac{\pi}{\sqrt{3}}) - \exp(\frac{\pi}{\sqrt{3}})$ and $\mu = 0$, the non-perturbed system (2.21) has a periodic solution with the initial condition $(0, 1)$. The periodic solution can be presented as

$$
x(t) = 4\Big(\mathrm{e}^{-\frac{\mathrm{t}}{2}} \sin(\frac{\sqrt{3}\mathrm{t}}{2}), \mathrm{e}^{-\frac{\mathrm{t}}{2}} \cos(\frac{\sqrt{3}\mathrm{t}}{2})\Big), \ \mathrm{t} \in (0, \frac{2\pi}{\sqrt{3}}],
$$

$$x(t) = -\mathrm{e}^{-\frac{(\mathrm{t}-4\pi/\sqrt{3})}{2}}\Big(\sin(\frac{\sqrt{3}(\mathrm{t}-2\pi/\sqrt{3})}{2}), \cos(\frac{\sqrt{3}(\mathrm{t}-2\pi/\sqrt{3})}{2})\Big),$$
$$t \in (\frac{2\pi}{\sqrt{3}}, \frac{4\pi}{\sqrt{3}}].$$

There is a $4\pi/\sqrt{3}-$periodic solution for the non perturbed system (2.21). The graph of the periodic solution can be seen in Fig. 2.13.

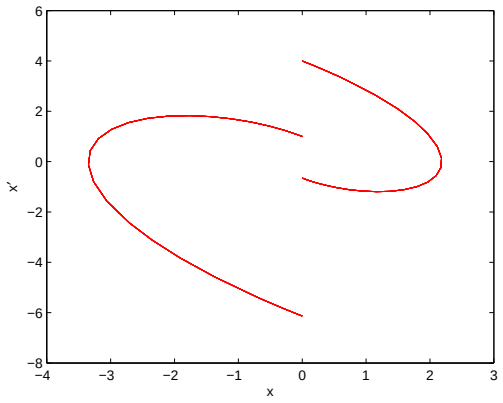

Figure 2.13: The periodic solution of the non perturbed-system (2.21) with the initial condition $x(0) = 0, \quad x'(0) = 1$.

It is observed that the system with the constant coefficient of restitution and rigid flat surfaces exhibits a periodic motion under some parameter values. It is important also verify the existence of a periodic solution whenever the surfaces are not rigid flat and the coefficient of restitution is not constant. Let us consider the perturbed system (2.21) with parameters $I_1 = 3$, $I_2 = 4\exp(-\pi\sqrt{3}) - \exp(\pi\sqrt{3})$, $\mu = 0.01$. Moreover, $x(t, 0, x^0, \mu)$ is the solution of the perturbed system with initial value $x^0 = (x_1^0, x_2^0)$. It is crucial to understand how the solution of the perturbed system behaves with respect to the initial condition as time increases whenever it is close to the initial condition of the periodic orbit. Denote by $F(x_2^0, \mu)$ the mapping of semi-line $x' \geq 0, \quad x = 0$ into itself given by $F : \mathbb{R}^+ \to \mathbb{R}^+$,

$$F(x_2^0, \mu) = x(\bar{T}(\mu), 0, x^0, \mu), \tag{2.22}$$

where $\bar{T}(\mu)$ is the time needed for the perturbed system to reach the semi line $x = 0, \quad x' > 0$, after two jumps. $\bar{T}(0) = 4\pi/\sqrt{3}$ is the period of the non-perturbed

system. The fixed points with $\kappa \geq 0$ of the mapping, $F(\kappa, \mu) = \kappa$, lead up to disconnected cycles of system (2.21), periodic motions along which are subject to two impulsive effect in the period. The stability of the disconnected limit cycle of system (2.21) is determined by the stability of fixed point of the mapping. To check the stability of the mapping, we calculate the derivative of the map at the initial moment, i.e.,$\frac{\partial F(x_2^0,\mu)}{\partial x_2^0} = \frac{\partial x(\bar{T}(\mu),0,x^0,\mu)}{\partial x_2^0}$. The partial derivative, $\frac{\partial x(t,0,x^0,\mu)}{\partial x_2^0}$, is a solution of the following variational equation

$$
\begin{aligned}
u_1' &= u_2, \\
u_2' &= -u_1 - u_2, \quad t \neq 0, \\
\begin{bmatrix} \Delta u_1(0) \\ \Delta u_2(0) \end{bmatrix} &= \begin{bmatrix} \frac{I_1}{x_2^0(1+\mu \mathrm{sgn}(x_2^0-1))} & \frac{-I_1\mu \mathrm{sgn}(x_2^0-1)}{x_2^0(1+\mu \mathrm{sgn}(x_2^0-1))} \\ \frac{I_1}{x_2^0(1+\mu \mathrm{sgn}(x_2^0-1))} & \frac{-I_1\mu \mathrm{sgn}(x_2^0-1)}{x_2^0(1+\mu \mathrm{sgn}(x_2^0-1))} \end{bmatrix} \begin{bmatrix} u_1(0) \\ u_2(0) \end{bmatrix}, \quad t \in [0, \frac{2\pi}{\sqrt{3}}) \\
u_1' &= u_2, \\
u_2' &= -u_1 - u_2, \quad t \neq \frac{2\pi}{\sqrt{3}}, \\
\begin{bmatrix} \Delta u_1(\frac{2\pi}{\sqrt{3}}) \\ \Delta u_2(\frac{2\pi}{\sqrt{3}}) \end{bmatrix} &= \begin{bmatrix} \frac{I_2}{\bar{x}(1+\mu \mathrm{sgn}(\bar{x}-1))} & 0 \\ \frac{I_2}{\bar{x}(1+\mu \mathrm{sgn}(\bar{x}-1))} & 0 \end{bmatrix} \begin{bmatrix} u_1(\frac{2\pi}{\sqrt{3}}) \\ u_2(\frac{2\pi}{\sqrt{3}}) \end{bmatrix}, \quad t \in [\frac{2\pi}{\sqrt{3}}, \frac{4\pi}{\sqrt{3}}),
\end{aligned}
\tag{2.23}
$$

where $\bar{x} = x_2(\frac{2\pi}{\sqrt{3}})$ and $u(0) = (0, 1)$. The system (2.23) is constructed by using the differentiability properties of solutions with respect to the initial condition for impulsive differential equations [5]. We have calculated the derivative of the map through the solution of system (2.23). That is,

$$
\begin{aligned}
\frac{\partial F(\kappa,\mu)}{\partial \kappa} = \sqrt{\Big(\frac{I_1\mu \mathrm{sgn}(\kappa-1)}{\kappa(1+\mu \mathrm{sgn}(\kappa-1))}\Big)^2 + \Big(1 - \frac{I_1\mu \mathrm{sgn}(\kappa-1)}{\kappa(1+\mu \mathrm{sgn}(\kappa-1)}\Big)^2} \\
\exp(-1/\sqrt{3}(2\pi - \arctan(\frac{-I_1\mu \mathrm{sgn}(\kappa-1)}{\kappa(1+\mu \mathrm{sgn}(\kappa-1)) - I_1\mu \mathrm{sgn}(\kappa-1)}))).
\end{aligned}
\tag{2.24}
$$

The fixed point of the map $F(\kappa, \mu)$ is $x^* = 1$. The fixed point corresponds to the discontinuous cycle of the perturbed system (2.21). To analyze stability of discontinuous limit cycle, we calculate the derivative (2.24) at the point x^*. It can be computed as $\frac{\partial F(\kappa,\mu)}{\partial \kappa}|_{\kappa=x^*} = \exp(-2\pi/\sqrt{3})$. By means of the correspondence with the fixed point of the map and discontinuous limit cycles of the system [50, 108], we can say that the

system has a stable discontinuous limit cycle [7, 8]. The stability of the discontinuous cycle can be observed in Fig. 2.14.

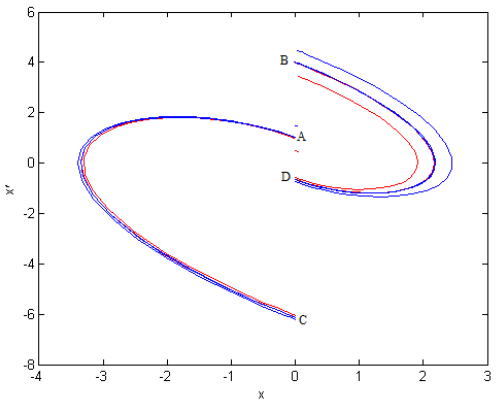

Figure 2.14: The red one is a solution of the perturbed-system (2.21) with the initial condition $x(0) = 0, \quad x'(0) = 0.8$, and the blue one is a solution of the perturbed-system (2.21) with the initial condition $x(0) = 0, \quad x'(0) = 1.2$.

In Fig. 2.14, one can observe that the inner solution of system (2.21) with the initial condition $(0, 0.8)$ is drawn in red curve and the outer solution of the system (2.21) with the initial point $(0, 1.2)$ is drawn in blue curve. As time increases, these two solutions approach to the limit cycle from inside and outside, respectively. In the light of the simulations, it can be understood that the system (2.21) has a stable periodic solution.

As a **second example**, we will give a model of an impacting system comprising a mass, a spring, and a damper. The spring and the damper are attached to the wall in parallel with each other and they are linked with a mass. They are placed on the ground horizontally. Additionally, in our example the damper has a negative resistance on the system , i.e., the energy of the system increases. In the book of Andronow and Chaikin [10], some mechanical and electrical models with negative resistance can be found. For example, the Froude pendulum is one of the popular model which has a negative resistance. In [120], a mathematical model is presented for an impact print hammer to describe the characteristic behavior and the velocity dependent coefficient of restitution is also introduced with the model. In our example, the obstacle is placed at the position $z_1 = \mu_1(z_2 - 1)^2$. When the mass meets with the obstacle, the impact occurs. During an impact, the velocity of the mass changes with

$z_2(\hat{\theta}^+) - z_2(\hat{\theta}^-) = -(1 + R - 0.03z_2(\hat{\theta}^-))z_2(\hat{\theta}^-)$, where $\hat{\theta}$ is the moment when the mass collides with the obstacle.

A linear oscillator, which is subdued to impacts, can be described by the following system

$$\begin{aligned} z_1' &= z_2, \\ z_2' &= -z_1 + z_2, \quad z_1 \neq \mu_1(z_2 - 1)^2, \\ \Delta z_2|_{z_1=\mu_1(z_2-1)^2} &= -(1 + R - 0.03z_2)z_2, \quad z_2 > 0, \end{aligned} \tag{2.25}$$

where $\mu_1 = 0.001$ and $R = \exp(-\frac{\pi}{\sqrt{3}}) + 0.03$.

Let us determine a $2\pi/\sqrt{3}$-periodic solution of the non-perturbed system (2.25). It can be presented as follows:

$$z(t) = \begin{cases} (0, 1), & \text{if } t = 0 \\ -\mathrm{e}^{-\frac{\pi}{\sqrt{3}}}(\mathrm{e}^{\frac{\mathrm{t}}{2}} \sin(\frac{\sqrt{3}}{2}\mathrm{t}), \mathrm{e}^{\frac{\mathrm{t}}{2}} \cos(\frac{\sqrt{3}}{2}\mathrm{t})), & \text{if } t \in (0, \frac{2\pi}{\sqrt{3}}]. \end{cases} \tag{2.26}$$

The phase portrait of the periodic solution for the non-perturbed system is depicted in Fig. 2.15.

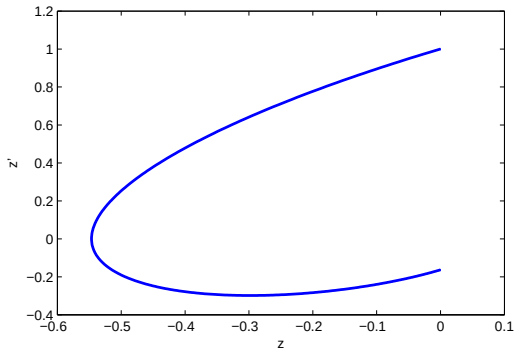

Figure 2.15: The periodic solution of the non perturbed system (2.25) with the initial condition $z(0) = 0, \quad z'(0) = 1$.

To prove the existence of the periodic solution for the perturbed system, we define the map $P(z_2^0, \mu_1) : \mathbb{R}_+ \to \mathbb{R}_+$ as follows:

$$P(z_2^0, \mu_1) = z(T(\mu_1), 0, z_0, \mu_1), \tag{2.27}$$

$z(T(\mu_1), 0, z_0, \mu_1)$ is the state position after a period $T(\mu_1)$ taken by $z(t, 0, z_0, \mu_1)$ which is a solution of the perturbed system (2.25) with $\mu_1 = 0.001$, $T(0) = 2\pi/\sqrt{3}$, and the initial condition $z_0 = (0, z_2^0)$. In order to determine the stability of the periodic solution, we need to check the derivative of the map (2.27) with respect to the second component of the initial value, z_2^0, at the fixed point of the map (2.27). The fixed point of the map is $z^* = 1$. It can be derived easily that the derivative $\frac{\partial z(t,0,z_0,\mu_1)}{\partial z_2^0}$ is a solution of the following system

$$\begin{aligned}
&v_1' = v_2,\\
&v_2' = -v_1 + v_2,\\
&\begin{bmatrix}\Delta v_1(0)\\ \Delta v_2(0)\end{bmatrix} = \begin{bmatrix}\frac{-1-R+0.03z_2^0}{1-2\mu_1(z_2^0-1)} & \frac{2\mu_1(z_2^0-1)(1+R-0.03z_2^0)}{1-2\mu_1(z_2^0-1)}\\ \frac{0.03z_2^0}{1-2\mu_1(z_2^0-1)} & \frac{2\mu_1(z_2^0-1)(1+R-0.03z_2^0)-1-R+0.06z_2^0}{1-2\mu_1(z_2^0-1)}\end{bmatrix}\begin{bmatrix}v_1(0)\\ v_2(0)\end{bmatrix}
\end{aligned} \tag{2.28}$$

with the initial condition $v(0) = (0, 1)$. Above system can be obtained by using the theory of the differentiability of solutions with respect to the initial condition for impulsive differential equations [5].

Using the solution of (2.28), the derivative of the map (2.27), $\frac{\partial P(\zeta,\mu_1)}{\partial \zeta}$, can be found as follows:

$$\begin{aligned}
\frac{\partial P(\zeta, \mu_1)}{\partial \zeta} &= \Big(\Big(\frac{2\mu_1(\zeta-1)(1+R-0.03\zeta)}{1-2\mu_1(\zeta-1)}\Big)^2\\
&+ \Big(\frac{(\zeta-1)(2R\mu_1 - 0.06\mu_1\zeta) - R + 0.06\zeta}{1-2\mu_1(\zeta-1)}\Big)^2\Big)^{\frac{1}{2}}\\
&\times \exp\Big(\frac{1}{\sqrt{3}}(\pi - \arctan(\frac{2\mu_1(\zeta-1)(1+R-0.03\zeta)}{2\mu_1(\zeta-1)(R-0.03\zeta) - R + 0.06\zeta}))\Big).
\end{aligned} \tag{2.29}$$

If we calculate the derivative at the point $z^* = 1$, we analyze the stability of the periodic solution. The derivative of the map (2.27) which is computed at the fixed point is $\frac{\partial P(\zeta,\mu_1)}{\partial \zeta}|_{\zeta=z^*} \approx 0.82$, which is less than one in modulus [109, 50, 108]. Then, we can assert that the perturbed system has a stable limit cycle by using the relation between map and the solution of the system.

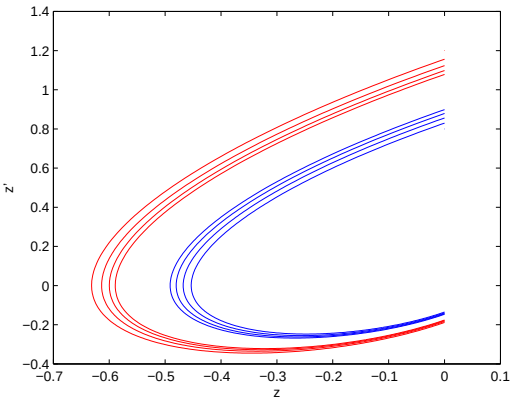

Figure 2.16: The red trajectory is a solution of the perturbed-system (2.25) with initial value $z(0) = 0, \quad z'(0) = 1.2$ and the blue one is a solution of the perturbed-system (2.25) with initial value $z(0) = 0, \quad z'(0) = 0.8$.

In Fig. 2.16, two different solutions of system (2.25) is drawn. The inner solution with the initial condition $z(0) = 0, \quad z'(0) = 0.8$ is drawn in blue curve and the outer solution with initial data $z(0) = 0, \quad z'(0) = 1.2$ is drawn in red curve. This two solutions approach limit cycle from inside and from outside, respectively. Moreover, we can conclude that system (2.25) has a stable discontinuous limit cycle.

In the **third example**, our aim is to present a mathematical model for the collision of two masses which are attached to the wall in one side and the remaining parts strike each other when the distance between masses is $x_3(t) - x_1(t) = 0.02 + \epsilon x_4(t)$. During collision velocities of the masses differ as $(w_4(\bar{\bar{\theta}}^+) - w_2(\bar{\bar{\theta}}^+)) - (w_4(\bar{\bar{\theta}}^-) - w_2(\bar{\bar{\theta}}^-)) = -(1+R)(w_4(\bar{\bar{\theta}}^-) - w_2(\bar{\bar{\theta}}^-))$, where $\bar{\bar{\theta}}$ is the time when two masses collide. However, our system does not have any dampers attached with the masses.

The motion of two masses is governed by the following system

$$\begin{aligned} w_1' &= w_2, \\ w_2' &= -0.2w_1 + 0.01, \\ w_3' &= w_4, \\ w_4' &= -0.055w_3 + 0.01, \\ \Delta(w_4 - w_2)|_{w_3 - w_1 = 0.02 + \epsilon w_4} &= -((1+R)(w_4 - w_2)). \end{aligned} \tag{2.30}$$

For $\epsilon = 0$, system has periodic solution with an initial value $w(0) = (-1, 0, 2, 0)$ which can be seen in the Fig. 2.17.

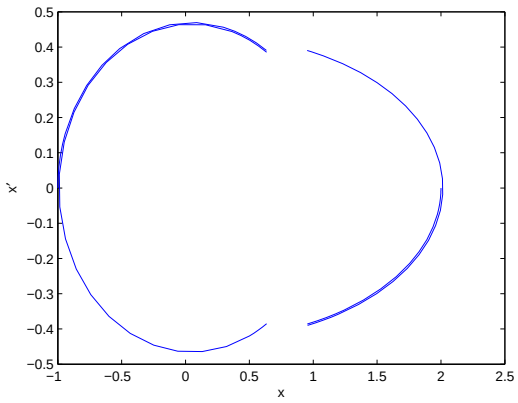

Figure 2.17: The phase portrait of the periodic solution of the non-perturbed system (2.30) with initial value $w(0) = (-1, 0, 2, 0)$

For the perturbed system with $\epsilon = 0.01$, we have defined the Poincaré map [50, 108] with two variables $M(x_2, x_4, \epsilon)$, the fixed point of the map $M(x_2, x_4, 0)$ corresponds to periodic solution of the system (2.30). We can understand that, it also corresponds to the performance of the coupled system which continues its motion in a harmony. For the perturbed system, we have a stable solution for one mass. For the remaining mass, we have an unstable solution. The stable solution can be observed in Fig. 2.18.

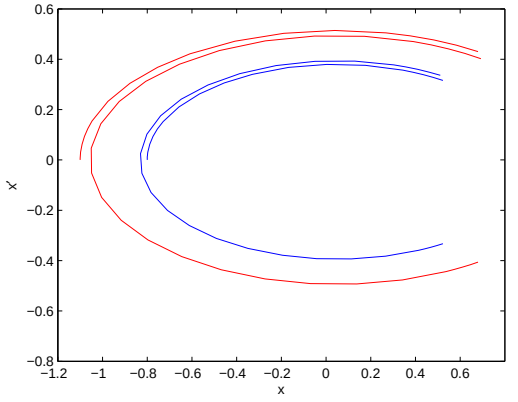

Figure 2.18: The blue curve is the phase portrait of the first mass for the perturbed system (2.30) corresponding to initial value $w(0) = (-0.8, 0, 1.75, 0)$ and red one is the phase portrait of the first mass for the perturbed system (2.30) with initial value $w(0) = (-1.1, 0, 2.1, 0)$

2.4 The suppression of chattering through impact deformations

In this section, by applying small variations on the surfaces of discontinuity and the coefficient of restitution in the models with chattering, we suppress chattering in such models. Then, the obtained model do not have infinite number of impact in a finite time. In other words, our idea is to substitute former models which are comprised of rigid flat surfaces of discontinuity and a constant coefficient of restitution with these which have the deformable surfaces of discontinuity and a variable coefficient of restitution. Then, our system with impact deformations will admit finite number of impacts in a finite time. As a consequence of that, our system become a more adequate modeling of the mechanisms with impacts, since chattering is not a realistic phenomenon (it is an idealize model). Chattering is one of the interesting phenomena for a system with impacts. In this study, chattering is comprehended as infinitely many impacts occur in a finite time. In the literature [22, 29, 61, 66, 90, 91], many investigations have been done to remove chattering from the system. In some papers, chattering has been suppressed in the system by applying variations on the excitation amplitude [29, 48]. In paper [91], chattering of a granular gas is considered. However, the suppression of chattering remains a huge problem for the mechanics and media. Our aim in this section is to suppress chattering in mechanical models by using impact deformations. Moreover, an assumption, which is mentioned in book of Nagaev [94], is also considered to suppress chattering in the system. We suppress the chattering in two different mechanical systems, which admit chattering, by using small modifications on surface of discontinuity and the coefficient of restitution to the models .

The first mechanical model, that we suppressed the chattering, is a bouncing bead model which starts a free fall from a height $x(0) = 10$ with the initial velocity $x'(0) = 0$. During the motion, the air resistance is neglected. When the bead reaches the level $x = 0,$ the impact occurs. After the impact, some energy is dissipated away. The motion of the bead is governed by the following system

$$\begin{aligned} x'' &= -g, \\ \Delta x'|_{x=0} &= -1.9x'. \end{aligned}$$

In system (2.31), the number 1.9 can be comprehended as follows $1.9 = 1 + 0.9$, where the coefficient of restitution is $R = 0.9$, and the level of the impact surface is $x = 0$.

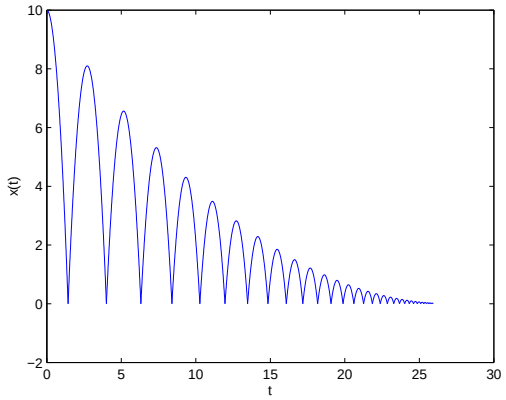

Figure 2.19: The time series of the motion which is governed by system (2.31) .

The time series of the motion can be seen in Fig. 2.19. In Fig. 2.19, one can observe that the height of the bead decreases but it cannot be zero during the motion as time increases. As time goes to infinity, the heights of the bead approaches to zero. As a consequence, the system preforms infinitely many jumps in a finite time. The velocity of the bead after the $k-th$ impact can be computed as $v_k = R^{k-1}v_1$, where v_1 is velocity of the bead after it first reaches the level $x = 0$ and R is the coefficient of restitution. The flight time between $k-th$ and $(k+1)-th$ bounces is $\tau_k = \dfrac{|2v_k|}{g} = R^{k-1}t_1$ and $t_1 = R\sqrt{\frac{8x_0}{g}}$, is the flight time between first bounce and second bounce. The bead stops after a time, $\tau = \sqrt{\dfrac{2x_0}{g}} + \displaystyle\sum_{k=1}^{\infty} R^{k-1}t_1 = \sqrt{\dfrac{2x_0}{g}}\dfrac{1+R}{1-R}$. The height of the bead after the $k-th$ impact is $x_k(t) = R^{2k}x_0$, where x_0 is the initial height of the bead. Additionally, the phase portrait of equation (2.31) with initial data $x(0) = 10$ and $x'(0) = 0$ is depicted in Fig. 2.20.

System (2.31) is not eligible for the real world applications. Because there is no such system which undergoes infinitely many impacts in a finite time in the real world. It

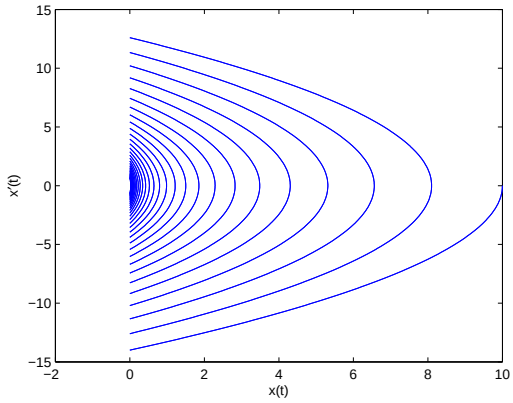

Figure 2.20: The phase portrait of system (2.31).

can be supposed that the number of strikes can be reduced to finite if elasticity and quasi elasticity are taken into account. One of the task of this study is to provide a model where quasi elasticity idea is expressed as deformable surfaces of impacts as well as the striking bodies are assumed not rigid flat and it has the variable coefficient of restitution [32, 89]. To verify that the bead undergoes finitely many strikes in a finite time, the variable coefficient of restitution and deformable surfaces are introduced with the model. This model is more realistic for the applications of the real world systems. Additionally, it enables us to have adequate results in the real world systems.

The system with impact deformations can be presented as follows:

$$\begin{aligned} x'' &= -g, \\ \Delta x'|_{x=-0.026|x'|} &= -(0.023x' + 1.9)x', \end{aligned} \tag{2.31}$$

with the initial condition $x(0) = 0.2$ and $x'(0) = 0$. In the system, $\psi(x') = 0.023x' + 0.9$ corresponds to the variable coefficient of restitution. When the bead reaches the surface $x = -0.026|x'|$, the impact occurs and the velocity of the bead changes proportional to the coefficient of restitution. It can be seen in Fig. 2.21 that after some time the trajectory of system (2.31) lies below the surface of meeting, $x = 0$, which is drawn as a red line. After the seventh bounce, the bead cannot reach the level $x = 0$ again, which can be observed from Fig. 2.21, Fig. 2.22 and Table 2.1. In the literature, this is considered as a stop in the motion [94]. One can suppose mechanically that the bead never leave the ground again. As a consequence of this

fact, the bead whose motion is governed by system (2.31) performs finitely many impacts in a finite time.

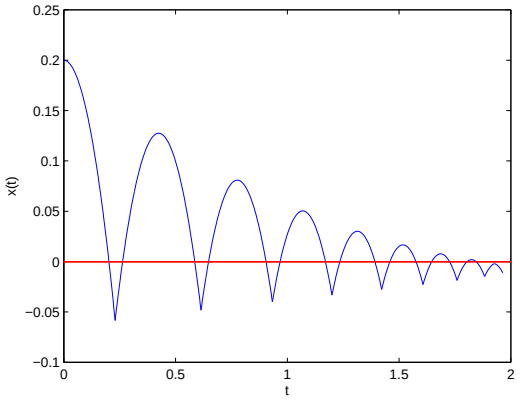

Figure 2.21: The time series of the motion which is governed by system (2.31).

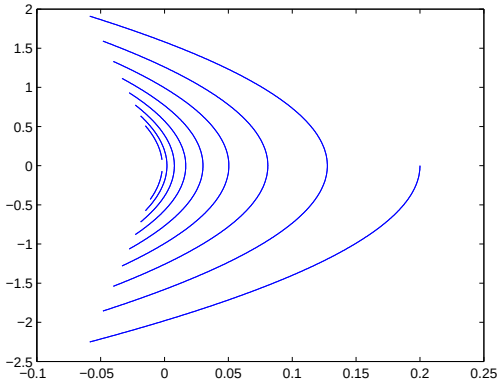

Figure 2.22: The phase portrait of system (2.31).

Observing the result of the simulation, which is depicted in Fig. 2.21, one can see that in larger impact velocities the displacement is larger. This is a fully agreement with Figs 2.3 and 2.11.

As a second mechanical model that we suppress chattering, we consider the linear inverted pendulum model, which impact against the rigid flat wall with a constant coefficient of restitution [60, 102]. The linear inverted pendulum is used in the modeling of various engineering applications, such as rings, printers, machine tools, dynamics of rigid standing structures, mooring buoy, moored vessels in a harbor against stiff fenders, and rolling railway wheel set [102]. The mechanical model of a linear inverted pendulum can be observed in Fig. 2.23. During the motion of the impacting

Table 2.1: The bouncing bead is starting its motion with height 0.2 and zero initial velocity, the deformation occurs only on surface where the bead meets. The numbers from 0 to 9 correspond to the number of bounce and the values from 0.2 to -0.001923 correspond to the heights of the bead in each bounce.

Number of bounce	Height (unit)	Number of bounce	Height (unit)
0	0.2	5	0.01564
1	0.1275	6	0.006795
2	0.08041	7	0.001702
3	0.04966	8	-0.001923
4	0.03022	9	

pendulum, we will take the wall at the position $x = 1$ as an impacting surface.

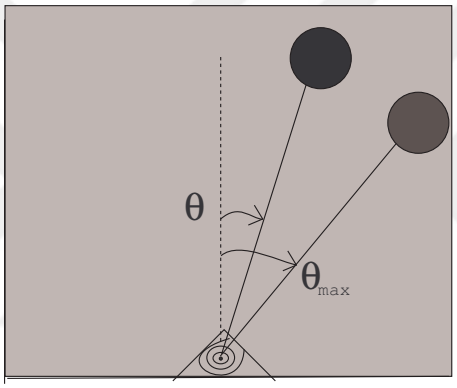

Figure 2.23: The linear inverted pendulum impacting on a rigid flat surface.

The motion is governed by the following system

$$\begin{aligned} x'' + 0.01x' - x &= 0.01\sin(2t), \\ \Delta x'|_{x=1} &= -(1+R)x', \end{aligned} \tag{2.32}$$

where $x = \theta/\theta_{max}$ is the normalized angle, $c = 0.01$ is the viscous damping which varies from zero to unity, $0.01\sin(2t)$ is the harmonic excitation representing the horizontal acceleration of the base and $x = 1$ is the surface of discontinuity. It is reasonable to take the coefficient of restitution as 0.9 in practical applications [102]. The time series and the phase portrait corresponding to system (2.32) with the initial condition $x(0) = 0$ and $x'(0) = 0$ are depicted in Figs 2.24 and 2.25, respectively.

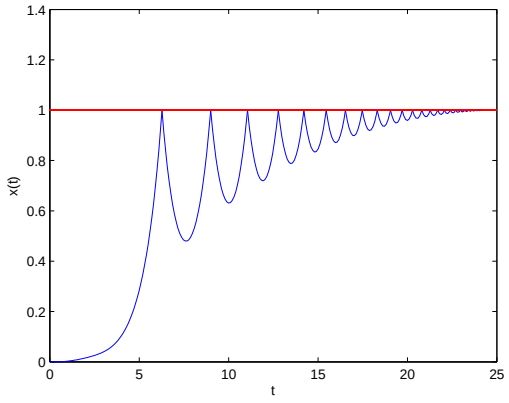

Figure 2.24: The time series of the motion which is governed by system (2.32).

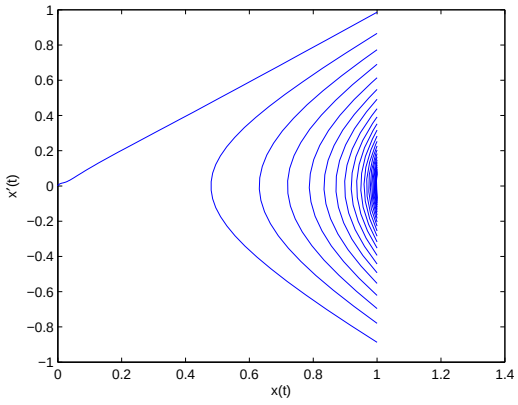

Figure 2.25: The phase portrait of system (2.32).

In Fig. 2.24, one can observe that the pendulum performs infinitely many strikes in a finite time. In papers [29, 66], the detailed mathematical investigations are presented for the model. Our aim in this chapter to remove chattering from the system. In order to suppress chattering in the system, we can consider that the impacting wall is deformable, and the coefficient of restitution is variable.

Let us consider the following model of linear inverted pendulum, where the coefficient of restitution is variable and the walls are deformable. During the motion, one of the walls, which is at the position $x = 1 + 0.1x'$, is considered. The motion can be

governed by the following system

$$\begin{aligned} x'' + 0.01x' - x &= 0.01\sin(2t), \\ \Delta x'|_{x=1+0.1x'} &= -(1 + R - 0.01x')x'. \end{aligned} \tag{2.33}$$

The time series and the phase portrait of system (2.33) with the initial condition $x(0) = 0$ and $x'(0) = 0$ are drawn in Figs 2.26 and 2.27, respectively.

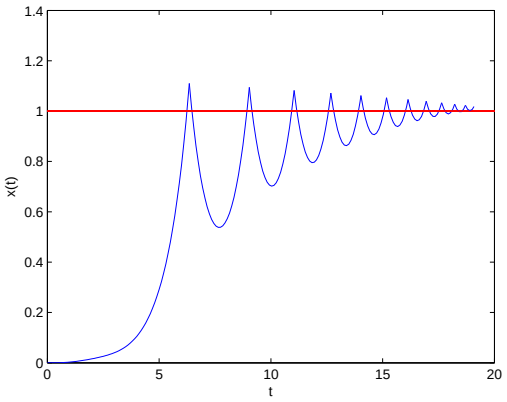

Figure 2.26: The time series of the motion which is governed by system (2.33).

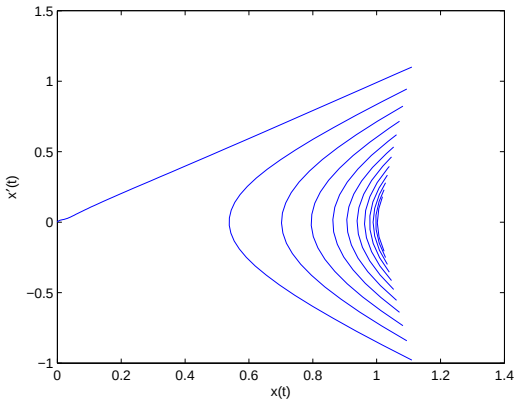

Figure 2.27: The phase portrait of system (2.33).

It can be derived from Fig. 2.26 that at large impact velocities the displacement is larger which is a good agreement with the reality and our proposals made in previous sections. It is observed in Fig. 2.26 that after some time interval the pendulum cannot reach the wall which lies at position $x = 1$. This is understood as the termination of the motion [94]. It can be concluded that the pendulum exerts finitely many impacts

in a finite time to the wall. Thus, this is called the suppression of chattering. It can be comprehended through Table 2.2 that after tenth impact, the pendulum cannot meet with the wall which lies at the level $x = 1$, again.

Table 2.2: The first column where the numbers emerge is corresponding to the number of bounce and the second column where decimals emerge is corresponding to the displacement of the pendulum.

Number of bounce	Displacement	Number of bounce	Displacement
0	0	6	0.9388
1	0.5382	7	0.9619
2	0.702	8	0.9787
3	0.7952	9	0.9888
4	0.8628	10	0.9979
5	0.8628	11	1.002

2.5 Discussion

In the real world, the interacting surfaces are not necessarily rigid flat, and the coefficient of restitution is not constant for the vibro-impact systems. In the light of this fact, we have presented a new model for the viscoelastic mechanisms with impacts by utilizing differential equations with variable moments of impulses. The Kelvin-Voigt viscoelastic model has been illustrated as an example for the contact motion. Two of the most important characteristics of the colliding bodies which are the dependence of the coefficient of restitution on the pre-impact velocity and the presence of deformable surfaces are investigated. We call these systems system with *impact deformations*. We replace CMKVM with CMID if the contact time is short for CMKVM. The theoretical results are actualized by extended examples and simulations. By using the qualitative theory for the differential equations with variable moments of impacts, we have examined the existence of periodic solutions and their stability for systems whose surfaces are not rigid flat and the coefficient of restitution is variable. We compare the models, which have chattering phenomena, with the existing ones in literature. As a particular outcome of this study, the suppression of chattering is achieved by using impact deformations. As a consequence of suppression of chatter-

ing, we can adapt our models to the real world applications. Many researches can be done on deformable surfaces and the variable coefficient of restitution. For example, the grazing bifurcation [32], which occurs for low impact velocities, is widely investigated in impacting systems with rigid flat surfaces. However, it is still remaining as an open problem for impacting systems with deformable surfaces.

A granular gas can be treated as an assembly of identical bouncing ball, each of the granules are colliding inelastically with the walls of the container and the ambient balls. Therefore, some of the results presented here may apply to the study of high-temperature or low density vibrated granular gases as well [91, 102].

A huge number of the viscoelastic mechanisms with deformable surfaces of impacts are presented in the literature. Actually, theory of the mechanisms can be converted to the models of impulsive system with impacts at variable moments [5, 109]. Several examples for these mechanisms are provided in this study. We hope that our proposals will throw light on the existing power of the theory and it is also expected that the results will expedite the course of the investigations, and give new opportunities for the theoretical analysis of impact mechanisms.

CHAPTER 3

DISCONTINUOUS DYNAMICAL SYSTEMS WITH GRAZING POINTS

3.1 Introduction

Due to the non-smoothness of the vibro-impact systems, they can be considered as an example for non-linear dynamical systems which exhibits complicated dynamics. In the literature, grazing became an attractive properties of the dynamics [31, 33, 93]. Two different definitions have been found for the grazing in the literature. One of the definition is that the grazing takes place when a trajectory touches the barrier tangentially [31, 33], [34], [70, 71, 75, 77]. In [97]-[100], the grazing is defined as getting close of the velocity to zero near the barrier. Our definition in this thesis is similar to that one given in [31, 34, 75].

In the study [36], grazing is taken into account as a boundary which divides regions of distinct dynamics. They examine the case that the trajectory meets an event triggering hypersurface tangentially . The optimization, continuation and shooting methods are improved and they are exemplified for the transient and grazing phenomena. It is illustrated by applying robotics and power electronics. In the study [106], the grazing cycle and its linearization for hybrid systems are determined by utilizing a numerical continuation method. By means of this, the normal-form coefficients have been calculated, which give a rise to chaos and period-adding cascade. The necessary and sufficient conditions of the discontinuous boundary are expounded in [70]. In [77], by utilizing non-stick mapping, the necessary and sufficient conditions in a linear oscillator with a periodical force and dry friction are attained for the grazing.

By constructing special maps, Nordmark map [97]-[100] and zero time discontinuity mapping [19, 33, 93], the existence of cycles and the stability of them are examined in mechanics.

In the present study, the dynamics with grazing points are modeled by applying differential equations with variable moments of impacts and utilizing the methods of which is initiated in [2, 3, 5]. As a consequence of the methods, the role of the mappings [97]-[100] is removed in the analysis. At the grazing point, the trajectory may touch the barrier tanegentially and the tangent plane drawn to the barrier at that point may be parallel to one or more than one coordinate axes. In particular, it implies that its velocity diminishes to zero [97]-[100]. . Then, one can say that this is an axial grazing. Otherwise, it is non-axial grazing. This study covers examples and theoretical results for both axial and non-axial grazing.

In [89], by simulations and experiments, it is demonstrated that restitution coefficient depends on the impact velocity of the particle by considering both the plastic and viscoelastic deformations of particles occurring at high and low impact velocities, respectively. In [87], it is proposed that for the large percentage of materials with linear elastic range, at low impact velocities, the restitution coefficient takes the form $R(v) = 1 - av$, where v is the impact velocity and a is a constant. Additionally, for low impact velocities the restitution law can be considered quadratic [37]. For this reason, we will utilize variable restitution coefficients in the impacting models in the present study.

For analysis of autonomous differential equations, it is eligible to use the features of dynamical systems. They are continuation of solutions in both time directions, the group property, continuity and differentiability in parameters. The studies of discontinuous dynamical systems with transversal intersections of orbits with surfaces, $B-$ smooth discontinuous flows, is presented in [2, 3, 5]. In the present research, the dynamics is obtained for systems with grazing orbits. Moreover, the adaptation of the definitions of orbital stability and asymptotic phase is done for the grazing cycles. The theorem of orbital stability is proved, which can not be underestimated for theory of impact mechanisms.

The remaining part of the present chapter can be organized as follows. In Section 3,

some necessary notations, definitions and theorems to specify discontinuous dynamical systems is introduced . In Section 3, it is demonstrated how the dynamics can be linearized around grazing orbits. In Section 4, the theorem of orbital stability is adapted for grazing cycles of discontinuous dynamics. In Section 5, the small parameter analysis is autilized near grazing orbits and bifurcation of cycles is obtained. In last three sections, examples are presented to realize the theoretical results, analytically and numerically. Finally, Conclusion covers a summary of the present study.

3.2 Discontinuous dynamical systems

Let $\mathbb{R}$, $\mathbb{N}$ and $\mathbb{Z}$ be the sets of all real numbers, natural numbers and integers, respectively. Consider the set $D \in \mathbb{R}^n$ such that $D = \cup D_i$, where D_i, $i = 1, 2, \ldots, k$, components of D, are disjoint open connected subsets of $\mathbb{R}^n$. To describe the surface of discontinuity, we present a function $\Phi : D^r \to \mathbb{R}^n$ which is two times continuously differentiable. The set can be defined as $\Gamma = \Phi^{-1}(0)$ and is a closed subset of $\bar{D}$, where $\bar{D}$ is the closure of D. Denote $\partial\Gamma$ as the boundary of Γ. One can easily see that $\Gamma = \cup_{i=1}^{k} \Gamma_i$, where Γ_i are parts of the surface of discontinuity in the components of D. Denote $\tilde{\Gamma} = J(\Gamma)$, $\tilde{\Phi}(x) = \Phi(J^{-1}(x))$. Denote an $r-$ neighborhood of D in $\mathbb{R}^n$ for a fixed $r > 0$ as D^r. Let Γ^r be the $r-$ neighborhood of Γ in $\mathbb{R}^n$, for a fixed $r > 0$ and define functions $J : \Gamma^r \to D^r$ and $\tilde{J} : \tilde{\Gamma}^r \to D^r$, such that, $J(\Gamma), \tilde{J}(\tilde{\Gamma}) \subset D$. Assume that a function $f(x) : D^r \to \mathbb{R}^n$ is continuously differentiable in D^r. Set the gradient vector of Φ as $\nabla\Phi(x)$.

The next definitions will be used in the remaining part of the study. Let $x(t-)$ be the left limit position of the trajectory and $x(t+)$ be the right limit of the position of the trajectory at the moment t. Define $\Delta x(t) := x(t+) - x(t-)$ as the jump operator for a function $x(t)$ such that $x(t) \in \Gamma$ and t is a discontinuity moment. In other words, the discontinuity moment t is the moment when the trajectory meets the surface of discontinuity Γ. The function $I(x)$ will be used in the next part of the chapter which is defined as $I(x) := J(x) - x$, for $x \in \Gamma$.

The following assumptions are needed throughout this study.

(C1) $\nabla\Phi(x) \neq 0$ for all $x \in \Gamma$,

(C2) $J \in C^1(\Gamma^r)$ and $\det\left[\frac{\partial J(x)}{\partial x}\right] \neq 0$, for all $x \in \Gamma^r \setminus \partial\Gamma$,

(C3) $\Gamma \bigcap \tilde{\Gamma} \subseteq \partial\Gamma \cap \partial\tilde{\Gamma}$,

(C4) $\langle \nabla\Phi(x), f(x)\rangle \neq 0$ if $x \in \Gamma \setminus \partial\Gamma$,

(C5) $\langle \nabla\tilde{\Phi}(x), f(x)\rangle \neq 0$ if $x \in \tilde{\Gamma} \setminus \partial\tilde{\Gamma}$,

(C6) $J(x) = x$ for all $x \in \partial\Gamma$,

(C7) $\tilde{J}(x) = x$ for all $x \in \partial\tilde{\Gamma}$.

It can be easily verified that $\tilde{\Gamma} = \{x \in D | \tilde{\Phi}(x) = 0\}$ and $\tilde{J}(x) \neq x$ on $\tilde{\Gamma}$ since of $(C2)$. Condition $(C1)$ implies that for every $x_0 \in \Gamma$, there is a number j and a function $\phi_{x_0}(x_1, \ldots, x_{j-1}, x_{j+1}, \ldots, x_n)$ such that Γ is the graph of the function $x_j = \phi_{x_0}(x_1, \ldots, x_{j-1}, x_{j+1}, \ldots, x_n)$ in a neighborhood of x_0. The same assertion is true for every $x_0 \in \tilde{\Gamma}$. Moreover, $\nabla\tilde{\Phi}(x) \neq 0$, for all $x \in \tilde{\Gamma}$, can be verified by utilizing the condition $(C2)$. The conditions $(C2), (C6), (C7)$, imply that the equality $\tilde{J}(x) = x$, is true for all $x \in \partial\tilde{\Gamma}$.

Let $\mathscr{A}$ be an interval in $\mathbb{Z}$. We say that the strictly ordered set $\theta = \{\theta_i\}, i \in \mathscr{A}$, is a $B-$*sequence* [5] if one of the following alternatives holds: (i) $\theta = \emptyset$, (ii) θ is a nonempty and finite set, (iii) θ is an infinite set such that $|\theta_i| \to \infty$ as $i \to \infty$. In what follows, θ is assumed to be a $B-$sequence .

The main object of our discussion is the following system,

$$\begin{aligned} x' &= f(x), \\ \Delta x|_{x\in\Gamma} &= I(x). \end{aligned} \tag{3.1}$$

In order to define a solution of (3.1), we need the following function and spaces.

A function $\phi(t) : \mathbb{R} \to \mathbb{R}^n,\ n \in \mathbb{N}$, θ is a $B-$sequence, is from the set $PC(\mathbb{R}, \theta)$ if it : (i) is left continuous, (ii) is continuous, except, possibly, points of θ, where it has discontinuities of the first kind.

A function $\phi(t)$ is from the set $PC^1(\mathbb{R}, \theta)$ if $\phi(t), \phi'(t) \in PC(\mathbb{R}, \theta)$, where the derivative at points of θ is assumed to be the left derivative. If $\phi(t)$ is a solution of (3.1), then it is required that it belongs to $PC^1(\mathbb{R}, \theta)$ [5].

We say that $x(t) : \mathscr{I} \to \mathbb{R}^n, \mathscr{I} \subset \mathbb{R}$, is a solution of (3.1) on $\mathscr{I}$ if there exists an extension $\tilde{x}(t)$ of the function on $\mathbb{R}$ such that $\tilde{x}(t) \in PC^1(\mathbb{R}, \theta)$, the equality $x'(t) = f(x(t)),\ t \in \mathscr{I}$, is true if $x(t) \notin \Gamma$, $x(\theta_i+) = J(x(\theta_i))$ for $x(\theta_i) \in \Gamma$ and $x(\theta_i+) \in \tilde{\Gamma}$, $\theta_i \in \mathscr{I}$. If θ_i is a discontinuity moment of $x(t)$, then $x(\theta_i) \in \Gamma$, for $\theta_i > 0$ and $x(\theta_i) \in \tilde{\Gamma}$, for $\theta_i < 0$. If $x(\theta_i) \in \partial\Gamma$ or $x(\theta_i) \in \partial\tilde{\Gamma}$, then $x(\theta_i)$ is a point of discontinuity with zero jump.

Definition 1 *A point x^* from $\partial\Gamma$ or $\partial\tilde{\Gamma}$ is a grazing point of system* (3.1) *if* $\langle \nabla\Phi(x^*), f(x^*)\rangle = 0$ *or* $\langle \nabla\tilde{\Phi}(x^*), f(x^*)\rangle = 0$, *respectively. If at least one of coordinates of $\nabla\tilde{\Phi}(x^*)$ is zero then the grazing is axial, otherwise it is non-axial.*

Definition 2 *An orbit $\gamma(x^*) = \{x(t, 0, x^*) | x^* \in D,\ t \in \mathbb{R}\}$ of (3.1) is grazing if there is at least one grazing point on the orbit.*

Consider a solution $x(t) : \mathbb{R} \to \mathbb{R}^n$ and $\{\theta_i\}$ be the moments of the discontinuity, they are the moments where solution $x(t)$ intersects Γ as time increases and the moments when the solution it intersects $\tilde{\Gamma}$ as time decreases.

A solution $x(t) = x(t, 0, x_0),\ x_0 \in D$ of (3.1) locally exists and is unique if the conditions $(C1) - (C3)$ are valid [5].

In the following part of the chapter, let $\|\cdot\|$ be the Euclidean norm, that is for a vector $x = (x_1, x_2, \ldots, x_n)$ in $\mathbb{R}^n$, the norm is equal to $\sqrt{x_1^2 + x_2^2 + \ldots + x_n^2}$.

The following condition for (3.1) guarantees that any set of discontinuity moments of the system constitutes a $B-$ sequence and we call the condition $B-$ *sequence condition*.

(C8) $\sup_D \|f(x)\| < +\infty$, and $\inf_{x_0 \in \tilde{\Gamma}}(x_0, y(\zeta, 0, x_0)) > 0$.

In [5], some other $B-$ sequence conditions are provided.

We will request for discontinuous dynamical systems that any sequence of discontinuity moments to be a $B-$ sequence.

Let us set the system

$$y' = f(y) \tag{3.2}$$

for the possible usage in the remaining part of the study.

Consider a solution $y(t, 0, x_0)$, $x_0 \in \tilde{\Gamma}$, of (3.2). Denote the first meeting point of the solution with the surface Γ, provided the point exists, by $y(\zeta, 0, x_0)$. The following conditions are sufficient for the continuation property.

(C9) (a) Every solution $y(t, 0, x_0)$, $x_0 \in D$, of (3.2) is continuable to either ∞ or Γ as time increases,
(b) Every solution $y(t, 0, x_0)$, $x_0 \in D$, of (3.2) is continuable to either $-\infty$ or $\tilde{\Gamma}$ as time decreases.

To verify the continuation of the solutions of (3.1), the following theorems can be applied.

Theorem 1 *[5] If the conditions $(C8)$ and $(C9)$ are valid, then, every solution $x(t) = x(t, 0, x_0)$, $x_0 \in D$ of (3.1) is continuable on $\mathbb{R}$.*

Now, we will present a condition which is sufficient for the *group property*.

(C10) For all $x_0 \in D$, the solution $y(t, 0, x_0)$ of (3.2) does not intersect $\tilde{\Gamma}$ before it meets the surface Γ as time increases.

In other words, for each $x_0 \in D$ and a positive number s such that $y(s, 0, x_0) \in \tilde{\Gamma}$, there exists a number r, $0 \leq r < s$, such that $y(r, 0, x_0) \in \Gamma$.

It is easy to verify that the condition $(C10)$ is equivalent to the assertion that for all $x_0 \in D$, the solution $y(t, 0, x_0)$ of (3.2) does not intersect Γ before it meets the surface $\tilde{\Gamma}$ as time decreases. In other words, for each $x_0 \in D$ and a negative number s such that $y(s, 0, x_0) \in \tilde{\Gamma}$, there exists a number r, $s < r \leq 0$, such that $y(r, 0, x_0) \in \tilde{\Gamma}$.

Theorem 2 *(The group property) Assume that conditions (C1)-(C10) hold. Then, $x(t_2, 0, x(t_1, 0, x_0)) = x(t_2 + t_1, 0, x_0)$, for all $t_1, t_2 \in \mathbb{R}$.*

Proof. Denote by $\xi(t) = x(t+\bar{t})$, for a fixed $\bar{t} \in \mathbb{R}$. It can be verified that the sequence $\{\theta_i - \bar{t}\}$ is a set of discontinuity moments of $\xi(t)$ and the function is a solution of (3.1)

[5]. The next step is to show that the following equality $x(-t, 0, x(t, 0, x_0)) = x_0$, holds for all $x_0 \in D$ and $t \in \mathbb{R}$. Consider the case $t > 0$. If the set of discontinuity moments $\{\theta_i\}$ is empty, the proof is same with that for continuous dynamical systems [30]. Because of the condition $(C2)$, which corresponds to invertibility of the jump function J, the equality $x(\theta_i, 0, x(\theta_i+)) = x(\theta_i)$, holds for all $i \in \mathscr{A}$. Assuming that $\theta_{-1} < 0 < \theta_1$, we should verify $x(-\theta_1, 0, x(\theta_1, 0, x_0)) = x_0$. Denote by $\bar{x}(t) = x(t, 0, x(\theta_1))$. The point $x(\theta_1)$ lies on the discontinuity surface Γ. By condition $(C3)$ the solution $\bar{x}(t)$ is a trajectory of $y' = f(y)$ for decreasing t. Condition $(C10)$, part (a), implies that the trajectory $\bar{x}(t)$ cannot meet with $\tilde{\Gamma}$ if $t > -\theta_1$ as time decreases. That is, $\bar{x}(-\theta_1) = x_0$ as the dynamics is continuous. The proof for $t < 0$ can be done in a similar way.

Remark 1 *For the application of the results, it is possible to take the initial moment as* $t_0 = 0$, *without being the discontinuity moment since of the group property. Then* $x_0 \notin \Gamma \cup \tilde{\Gamma}$.

Denote by $\widehat{[a, b]}$, $a, b \in \mathbb{R}$, the interval $[a, b]$, whenever $a \leq b$ and $[b, a]$, otherwise. Let $x_1(t) \in PC(\mathbb{R}_+, \theta^1)$, $\theta^1 = \{\theta_i^1\}$, and $x_2(t) \in PC(\mathbb{R}_+, \theta^2)$, $\theta^2 = \{\theta_i^2\}$, be two different solutions of (3.1).

Definition 3 *The solution* $x_2(t)$ *is in the* $\epsilon-$*neighborhood of* $x_1(t)$ *on the interval* $\mathscr{I}$ *if*

- *the sets* θ^1 *and* θ^2 *have same number of elements in* $\mathscr{I}$;
- $|\theta_i^1 - \theta_i^2| < \epsilon$ *for all* $\theta_i^1 \in \mathscr{I}$;
- *the inequality* $||x_1(t) - x_2(t)|| < \epsilon$ *is valid for all t, which satisfy* $t \in \mathscr{I} \setminus \cup_{\theta_i^1 \in \mathscr{I}}(\theta_i^1 - \epsilon, \theta_i^1 + \epsilon)$.

The topology defined with the help of $\epsilon-$ neighborhoods is called the B-topology. It can be apparently seen that it is Hausdorff and it can be considered also if two solutions $x_1(t)$ and $x_2(t)$ are defined on a semi-axis or on the entire real axis.

Definition 4 *The solution $x_0(t) = x(t, 0, x_0), t \in \mathbb{R}, x_0 \in D$, of (3.1) B-continuously depends on x_0 for increasing t if there corresponds a positive number δ to any positive ϵ and a finite interval $[0, b],\ b > 0$ such that any other solution $x(t) = x(t, 0, \tilde{x})$ of (3.1) lies in $\epsilon-$neighborhood of $x_0(t)$ on $[0, b]$ whenever $\tilde{x} \in B(x_0, \delta)$. Similarly, the solution $x_0(t)$ of (3.1) B-continuously depends on x_0 for decreasing t if there corresponds a positive number δ to any positive ϵ and a finite interval $[a, 0],\ a < 0$ such that any other solution $x(t) = x(t, 0, \tilde{x})$ of (3.1) lies in $\epsilon-$neighborhood of $x_0(t)$ on $[a, 0]$ whenever $\tilde{x} \in B(x_0, \delta)$. The solution $x_0(t)$ of (3.1) B-continuously depends on x_0 if it continuously depends on the initial value, x_0, for both increasing and decreasing t.*

If conditions (C1)-(C7) hold, then each solution $x_0(t) : \mathbb{R} \to \mathbb{R}^n$, $x_0(t) = x(t, 0, x_0)$, of (3.1) continuously depends on x_0 [5].

3.2.1 B-equivalence to a system with fixed moments of impulses

In order to facilitate the analysis of the system with variable moments of impulses (3.1), a *B-equivalent system* [5] to the system with variable moments of impulses will be utilized in our study. Below, we will construct the B-equivalent system.

Let $x(t) = x(t, 0, x_0 + \Delta x)$ be a solution of system (3.1) neighbor to $x_0(t)$ with small $\|\Delta x\|$. If the point $x_0(\theta_i)$ is a $(\beta)-$ or $(\gamma)-$ type point, then it is a boundary point. For this reason, there exist two different possibilities for the near solution $x(t)$ with respect to the surface of discontinuity. They are:

$(N1)$ The solution $x(t)$ intersects the surface of discontinuity, Γ, at a moment near to θ_i,

$(N2)$ The solution $x(t)$ does not intersect Γ, in a small time interval centered at θ_i.

Consider a solution $x_0(t) : \mathscr{I} \to \mathbb{R}^n$, $\mathscr{I} \subseteq \mathbb{R}$, of (3.1). Assume that all discontinuity points θ_i, $i \in \mathscr{A}$ are interior points of $\mathscr{I}$. There exists a positive number r, such that r-neighborhoods of $D_i(r)$ of $(\theta_i, x_0(\theta_i))$ do not intersect each other. Consider r is sufficiently small and so that every solution of (3.2) which satisfies condition $(N1)$

and starts in $D_i(r)$ intersects Γ in $G_i(r)$ as t increases or decreases. Fix $i \in \mathscr{A}$ and let $\xi(t) = x(t, \theta_i, x)$, $(\theta_i, x) \in D_i(r)$, be a solution of (3.2), $\tau_i = \tau_i(x)$ the meeting time of $\xi(t)$ with Γ and $\psi(t) = x(t, \tau_i, \xi(\tau_i) + J(\xi(\tau_i)))$ another solution of (3.2). Denoting by $W_i(x) = \psi(\theta_i) - x$, one can find that it is equal to

$$W_i(x) = \int_{\theta_i}^{\tau_i} f(\xi(s))ds + J(x + \int_{\theta_i}^{\tau_i} f(\xi(s))ds) + \int_{\tau_i}^{\theta_i} f(\psi(s))ds \tag{3.3}$$

and maps an intersection of the plane $t = \theta_i$ with $D_i(r)$ into the plane $t = \theta_i$.

Let us present the following system of differential equations with impulses at fixed moments, whose impulse moments, $\{\theta_i\}$, $i \in \mathscr{A}$, are the moments of discontinuity of $x_0(t)$,

$$\begin{aligned} y' &= f(y), \\ \Delta y|_{t=\theta_i} &= W_i(y(\theta_i)). \end{aligned} \tag{3.4}$$

The function f is the same as the function in system (3.1) and the maps W_i, $i \in \mathscr{A}$, are defined by equation (3.3). If $\xi(t) = x(t, \theta_i, x)$ does not intersect Γ near θ_i then we take $W_i(x) = 0$.

Let us introduce the sets $F_r = \{(t, x) | t \in I, \|x - x_0(t)\| < r\}$, and $\bar{D}_i(r)$, $i \in \mathscr{A}$, closure of an $r-$ neighborhood of the point $(\theta_i, x_0(\theta_i+))$. Write $D^r = F_r \cup (\cup_{i\in\mathscr{A}} D_i(r)) \cup (\cup_{i\in\mathscr{A}} \bar{D}_i(r))$. Take $r > 0$ sufficiently small so that $D^r \subset \mathbb{R} \times D$. Denote by $D(h)$ an h-neighborhood of $x_0(0)$. Assume that conditions $(C1) - (C10)$ hold. Then systems (3.1) and (3.4) are B-equivalent in D^r for a sufficiently small r [5]. That is, if there exists $h > 0$, such that:

1. for every solution $y(t)$ of (3.4) such that $y(0) \in D(h)$, the integral curve of $y(t)$ belongs to D^r and there exists a solution $x(t) = x(t, 0, y(0))$ of (3.1) which satisfies

$$x(t) = y(t), \;\; t \in [a, b] \setminus \cup_{i=-k}^{m} \widehat{(\tau_i, \theta_i]}, \tag{3.5}$$

   where τ_i are moments of discontinuity of $x(t)$. One should precise that we

assume $\tau_i = \theta_i$, if $x(t)$ satisfies $(N2)$. Particularly,

$$lx(\theta_i) = \begin{cases} y(\theta_i), & \text{if } \theta_i \leq \tau_i, \\ y(\theta_i^+), \text{otherwise,} \end{cases}$$
$$y(\tau_i) = \begin{cases} x(\tau_i), & \text{if } \theta_i \geq \tau_i, \\ x(\tau_i^+), \text{otherwise.} \end{cases} \tag{3.6}$$

2. Conversely, if (3.4) has a solution $y(t) = y(t, 0, y(0)), y(0) \in D(h)$, then there exists a solution $x(t) = x(t, 0, y(0))$ of (3.1) which has an integral curve in D^r, and (3.5) holds.

A solution $x_0(t)$ satisfies (3.1) and (3.4) simultaneously.

Consider a solution $x_0(t) : \mathbb{R} \to \mathbb{R}^n$, $x_0(t) = x(t, 0, x_0),\ x_0 \in D$ with discontinuity moments $\{\theta_i\}$. Fix a discontinuity moment θ_i. At this discontinuity moment, the trajectory may be on Γ and $\tilde{\Gamma}$. All possibilities of discontinuity moment should be analyzed. For this reason, we should investigate the following six cases:

$(\alpha)\ \ x_0(\theta_i) \in \Gamma \setminus \partial\Gamma,$

$(\alpha')\ \ x_0(\theta_i) \in \tilde{\Gamma} \setminus \partial\tilde{\Gamma},$

$(\beta)\ \ x_0(\theta_i) \in \partial\Gamma\ \&\ \langle \nabla\Phi(x_0(\theta_i)), f(x_0(\theta_i))\rangle \neq 0,$

$(\beta')\ \ x_0(\theta_i) \in \partial\tilde{\Gamma}\ \&\ \langle \nabla\tilde{\Phi}(x_0(\theta_i)), f(x_0(\theta_i))\rangle \neq 0,$

$(\gamma)\ \ x_0(\theta_i) \in \partial\Gamma\ \&\ \langle \nabla\Phi(x_0(\theta_i)), f(x_0(\theta_i))\rangle = 0,$

$(\gamma')\ \ x_0(\theta_i) \in \partial\tilde{\Gamma}\ \&\ \langle \nabla\tilde{\Phi}(x_0(\theta_i)), f(x_0(\theta_i))\rangle = 0.$

If a discontinuity point $x_0(\theta_i)$ satisfy the case $(\alpha),\ ((\alpha'))$ the case $(\beta),\ ((\beta'))$ and the case $(\gamma), ((\gamma'))$ we will call it an $(\alpha)-$ type point, a $(\beta)-$ type point and a $(\gamma)-$ type point, respectively.

Besides, we present the following definition which is compliant with Definition 2.

Definition 5 *If there exists a discontinuity moment, θ_i, $i \in \mathscr{A}$, for which one of the cases (γ) or (γ') is valid, then the solution $x_0(t) = x(t, 0, x_0)$, $x_0 \in \mathbb{R}^n$ of (3.1) is called a grazing solution and $t = \theta_i$ is called a grazing moment.*

Next, we consider *the differentiability properties of grazing solutions*. The theory for the smoothness of discontinuous dynamical systems' solutions without grazing phenomenon is provided in [5].

Denote by $\bar{x}(t), j = 1, 2, \ldots, n$, a solution of (3.4) such that $\bar{x}(0) = x_0 + \Delta x$, $\Delta x = (\xi_1, \xi_2, \ldots, \xi_n)$, and let η_i be the moments of discontinuity of $\bar{x}(t)$.

The following conditions are required in what follows.

(A) For all $t \in [0, b] \setminus \cup_{i \in \mathscr{A}} \widehat{(\eta_i, \theta_i]}$, the following equality is satisfied

$$\bar{x}(t) - x_0(t) = \sum_{i=1}^{n} u_i(t)\xi_i + O(\|\Delta x\|), \tag{3.7}$$

where $u_i(t) \in PC([0, b], \theta)$.

(B) There exist constants $\nu_{ij}, j \in \mathscr{A}$, such that

$$\eta_j - \theta_j = \sum_{i=1}^{n} \nu_{ij}\xi_i + O(\|\Delta x\|); \tag{3.8}$$

(C) The discontinuity moment η_j of the near solution approaches to the discontinuity moment $\theta_j, j \in \mathscr{A}$, of grazing one as ξ tends to zero.

The solution $\bar{x}(t)$ has a linerization with respect to solution $x_0(t)$ if the condition (A) is valid and, moreover, if the point $x_0(\theta_i)$ is of $(\alpha)-$ or $(\beta)-$ type, then the condition (B) is fulfilled. For the case $x_0(\theta_i)$ is of $(\gamma)-$ type the condition (C) is true.

The solution $x_0(t)$ is $K-$differentiable with respect to the initial value x_0 on $[0, b]$ if for each solution $\bar{x}(t)$ with sufficiently small Δx the linearization exists. The functions $u_i(t)$ and ν_{ij} depend on Δx and uniformly bounded on a neighborhood of x_0.

It is easy to see that the differentiability implies $B-$continuous dependence on solutions to initial data.

Define the map $\zeta(t, x)$ as $\zeta(t, x) = x(t, 0, x)$, for $x \in D$.

A K-smooth discontinuous flow is a map $\zeta(t, x) : \mathbb{R} \times D \to D$, which satisfies the following properties:

(I) The group property:

(i) $\zeta(0,x) : D \to D$ is the identity;

(ii) $\zeta(t,\zeta(s,x)) = \zeta(t+s,x)$ is valid for all $t, s \in \mathbb{R}$ and $x \in D$.

(II) $\zeta(t,x) \in PC^1(\mathbb{R})$ for each fixed $x \in D$.

(III) $\zeta(t,x)$ is K-differentiable in $x \in D$ on $[a,b] \subset \mathbb{R}$ for each a, b such that the discontinuity points of $\zeta(t,x)$ are interior points of $[a,b]$.

In [5], it was proved that if the conditions of Theorem 1 and (C1)-(C10) are fulfilled, then system (3.1) defines a B-smooth discontinuous flow [5] if there is no grazing points for the dynamics. It is easy to observe that the B-smooth discontinuous flow is a subcase of the K-smooth discontinuous flow. In the next section, we will construct a variational system for (3.1) in the neighborhood of grazing orbits. That is, we will assume that some of the discontinuity points are $(\gamma)-$ type points. Linearization around a solution and its stability will be taken into account. Thus, analysis of the discontinuous dynamical systems with grazing points will be completed.

3.3 Linearization around grazing orbits and discontinuous dynamics

The object of this section is to verify $K-$ differentiability of the grazing solution. Consider a grazing solution $x_0(t) = x(t,0,x_0),\ x_0 \in D$, of (3.1). We will demonstrate that one can write the variational system for the solution $x_0(t)$ as follows:

$$\begin{aligned} u' &= A(t)u, \\ \Delta u|_{t=\theta_i} &= B_i u(\theta_i), \end{aligned} \tag{3.9}$$

where the matrix $A(t) \in \mathbb{R}^{n\times n}$ of the form $A(t) = \frac{\partial f(x_0(t))}{\partial x}$. The matrices $B_i,\ i = 1,\ldots,n$, will be defined in the remaining part of the study. The matrix B_i is bivalued if θ_i is a grazing moment or of $(\beta)-$type.

The right hand side of the second equation in (3.9) will be described in the remaining part of the study for each type of the points. As the *linearization at a point of discontinuity*, we comprehend the second equation in (3.9).

3.3.1 Linearization at $(\alpha)-$ type points

Discontinuity points of (α) and (α') types are discussed in [5]. In this subsection, we will outline the results of the book.

Assume that $x(\theta_i)$ is an $(\alpha)-$type point. It is clear that the $B-$ equivalent system (3.4) can be applied in the analysis. The functions $\tau_i(x)$ and $W_i(x)$, are described in Subsection 3.2.1. Differentiating $\Phi(x(\tau_i(x))) = 0$, we have

$$\frac{\partial \tau_i(x_0(\theta_i))}{\partial x_j} = -\frac{\Phi_x(x_0(\theta_i))\frac{\partial x_0(\theta_i)}{\partial x_{0j}}}{\Phi_x(x_0(\theta_i))f(x_0(\theta_i))}. \tag{3.10}$$

Then, considering (3.3), we get the following equation,

$$\frac{\partial W_i(x_0(\theta_i))}{\partial x_{0j}} = (f(x_0(\theta_i)) - f(x_0(\theta_i) + J(x_0(\theta_i))))\frac{\partial \tau_i}{\partial x_{0j}} + \frac{\partial I}{\partial x}(e_j + f\frac{\partial \tau_i}{\partial x_{0j}}), \tag{3.11}$$

where $e_j = (\underbrace{0, \ldots, 1}_{j}, \ldots, 0)$.

The matrix $B_i \in \mathbb{R}^{n\times n}$ in equation (3.9) is defined as $B_i = W_{ix}$, where W_{ix} is the $n \times n$ matrix of the form $W_{ix} = [\frac{\partial W_i(x_0(\theta_i))}{\partial x_1}, \frac{\partial W_i(x_0(\theta_i))}{\partial x_2}, \ldots, \frac{\partial W_i(x_0(\theta_i))}{\partial x_n}]$. Its vector-components $\frac{\partial W_i(x_0(\theta_i))}{\partial x_{0j}}, \quad j = 1, \ldots, n$, evaluated by (3.11). Moreover, the components of the gradient $\nabla\tau_i$ have to be evaluated by formula (3.10).

3.3.2 Linearization at $(\beta)-$ type points

In what follows, denote $n \times n$ zero matrix by O_n. In the light of the possibilities $(N1)$ and $(N2)$, the matrix B_i in (3.1) can be expressed as follows:

$$B_i = \begin{cases} W_{ix}, & \text{if} \quad (N1) \text{ is valid,} \\ O_n, & \text{if} \quad (N2) \text{ is valid,} \end{cases} \tag{3.12}$$

where W_{ix} is evaluated by formula (3.11) and $\nabla\tau(x)$ evaluated by formula (3.10).

The differentiability properties for the cases (α') and (β') can be investigated similarly.

3.3.3 Linearization at a grazing point

Fix a discontinuity moment θ_i and assume that one of the cases (γ) or (γ') is satisfied. We will investigate the case (γ). The case (γ') can be considered in a similar way.

Considering condition $(C1)$ with the formula (3.10), it is easy to see that one coordinate of it is infinity at a grazing point. This gives arise singularity in the system, which makes the analysis harder and the dynamics complex. Through the formula (3.10), one can see that the singularity is just caused by the position of the vector field with respect to the surface of discontinuity and the impact component of the dynamical system does not participate in the appearance of the singularity. To handle with the singularity, we will rely on the following conditions.

$(A1)$ A grazing point is isolated. That is, there is a neighborhood of the point with no other grazing points.

$(A2)$ The map $W_i(x)$ in (3.3) is differentiable at the grazing point $x = x_0(\theta_i)$.

$(A3)$ The function $\tau_i(x)$ does not exceed a positive number less than $\theta_{i+1} - \theta_i$ near a grazing point, $x_0(\theta_i)$, on a set of points which satisfy condition $(N1)$.

In the present study, we analyze the case, when the impact functions neutralize the singularity caused by transversality. That is, the triad: impact law, the surface of discontinuity and the vector field is specially chosen, such that condition $(A2)$ is valid. Presumably, if there is no of this type of suppressing, complex dynamics near the grazing motions may appear [33, 70, 97, 98]. In the examples stated in the remaining part of the study, one can see the verification of $(A2)$, in details.

Let us prove the following assertion.

Lemma 1 *If conditions* $(C1)$, $(C4)$, $(C6)$, $(C8)$ *and* $(A3)$ *hold. Then,* $\tau_i(x)$ *is continuous near a grazing point* $x_0(\theta_i)$, *on a set of points, which satisfy condition* $(N1)$.

Proof. Let $x_0(\theta_i)$ be a grazing point. If $\bar{x}$ is not a point from the orbit of the grazing solution, the continuity of $\tau_i(x)$ at the point $x = \bar{x}$ can be proven using similar

technique presented in [5]. Now, the continuity at $x_0(\theta_i)$ is taken into account. On the contrary, assume that $\tau_i(x)$ is not continuous at the point $x = x_0(\theta_i)$. Then, there exists a positive number ϵ_0 and a sequence $\{x_n\}_{n\in\mathbb{Z}}$ such that $\tau_i(x_n) > \epsilon_0$ whenever $x_n \to x_0(\theta_i)$, as $n \to \infty$. Moreover, from condition $(A3)$, one can assert that there exists a subsequence $\tau_i(x_{n_k})$ which converges to a number $\epsilon_0 \leq \tau_0 < \theta_{i+1} - \theta_i$. Without loss of generality, assume that the subsequence converges the point where the sequence $\{x_n\}_{n\in\mathbb{Z}}$ converges. Since of the continuity of solutions in initial value, $x(\tau_i(x_n), 0, x_n)$ approaches to $x(\tau_0, 0, x(\theta_i))$. But $x(\tau_i(x_n), 0, x_n)$ is on the surface of discontinuity Γ, $x(\tau_0, 0, x_0(\theta_i)) \notin \Gamma$. This contradicts with the closeness of the surface of discontinuity Γ. The continuity at other points of the grazing orbit is valid by the group property. $\square$

Since of $B-$equivalence of systems (3.1) and (3.4), we will consider linearization around $x_0(t)$ as solution of the system (3.4), consequently, only formula (3.7) will be needed. Finally, the linearization matrix for the grazing point also has to be defined by the formula (3.12), where W_{ix} exists by condition $(A2)$. The following lemma is needed in the remaining part.

Lemma 2 *Assume that the partial derivatives* $\dfrac{\partial W_i(x)}{\partial x_j^0}$, $j = 1, 2, \ldots, n$ *exist in a neighborhood of the grazing point and they are continuous at the point [11]. Then, the function* $W_i(x)$ *is differentiable at* x^*.

In what follows, we will consider only grazing motions such that condition $(A2)$ holds. Consequently, the continuous dependence on initial data is valid. More precisely, $B-$ continuous dependence on initial data is true. Now, if conditions $(C1) - (C10)$ and $(A1), (A2)$ are assumed, the system (3.1) defines a $K-$ smooth discontinuous flow for dynamics with grazing points.

3.3.4 Linearization around a grazing periodic solution

Let $\Psi(t) : \mathbb{R} \to D$ be a periodic solution of (3.1) with period $\omega > 0$ and $\theta_i,\ i \in \mathbb{Z}$, are the points of discontinuity which satisfy $(\omega, p)-$ property, i.e. $\theta_{i+p} = \theta_i + \omega, p$ is a natural number.

Let us fix a solution $x(t) = x(t, 0, \Psi(0) + \Delta x)$ and assume that linearization of $\Psi(t)$ with respect to $x(t)$ exists and is of the form

$$\begin{aligned} u' &= A(t)u, \\ \Delta u|_{t=\theta_i} &= B_i u. \end{aligned} \tag{3.13}$$

The matrix B_i is determined by (3.12). It is known that $A(t+\omega) = A(t)$, $t \in \mathbb{R}$. But, the sequence B_i may not be periodic in general, since of (3.12). This makes the analysis of the neighborhood of $\Psi(t)$ difficult. For this reason, we suggest the following condition.

(A4) For each sufficiently small $\Delta x \in \mathbb{R}^n$, the variational system (3.13) satisfies $B_{i+p} = B_i$, $i \in \mathbb{Z}$. There exist a finite number $m \leq 2^l$, where l is the number of points of $(\beta)-$ or $(\gamma)-$ type in the interval $[0, \omega]$, of the periodic sequences B_i.

The assumption $(A4)$ is valid for many low dimensional models of mechanics and those which can be decomposed into low dimensional subsystems. To distinguish periodic sequences B_i in the assumption $(A4)$, we will apply the notation $B_i = D_i^{(j)}$, $i \in \mathbb{Z}$ and $j = 1, 2, \ldots, m$.

If the condition $(A4)$ is not fulfilled, then complex dynamics near a periodic motion may appear. This case can be investigated either by methods developed through mappings applications [25, 106] or it requests additional development of our present results.

In the next example, we will demonstrate that the system constitutes $K-$ smooth discontinuous flow although it has grazing points in the phase space.

Example 1 *(K-smooth discontinuous flow with grazing points). Consider an impact model*

$$\begin{aligned} y_1' &= y_2, \\ y_2' &= -y_1 + 0.001 y_2, \end{aligned} \tag{3.14a}$$

$$\begin{aligned} \Delta y_2|_{y \in \Gamma_1} &= -y_2 - R_1 y_2^2, \\ \Delta y_2|_{y \in \Gamma_2} &= -(1 + R_2) y_2, \end{aligned} \tag{3.14b}$$

with the domain $D = \mathbb{R}^2$, $R_1 = \exp(-0.0005\pi)$ *and* $R_2 = 0.9$. *In the paper [37], it is stated that the coefficient of restitution for low velocity impact still remains as an open problem. In the study [9], by considering Kelvin-Voigt model for the elastic impact, we derived quadratic terms of the velocity in the impact law. This arguments make the quadratic term for the impulse equation* (3.14b) *reasonable.*

Let us describe the set of discontinuity curves by $\Gamma = \Gamma_1 \cup \Gamma_2$. *The components* Γ_1 *and* Γ_2 *are intervals of the vertical lines* $y_1 = \exp(0.00025\pi)$ *and* $y_1 = 0$, *respectively and they will be precised next. Fix a point* $P = (0, \bar{y}_2) \in D$, *with* $\bar{y}_2 > 1$. *Let* $y(t, 0, P)$ *be a solution of (3.14a) and it meets with the vertical line* $x_1 = \exp(0.00025\pi)$, $x_2 > 0$ *at the point* $P_2 = (\exp(0.00025\pi), y_2(\theta_1, 0, P))$, *where* θ_1 *is the meeting moment with the line. Consider the point on the* $\tilde{\Gamma}_1$ *which is* $Q_2 = (\exp(0.00025\pi), -R_1 y_2(\theta_1, 0, P_2)^2)$ *and denote* $Q_1 = (0, y_2(\theta_2, 0, Q_2))$, *where* θ_2 *is the moment of meeting of the solution* $y(t, 0, Q_2)$ *with the vertical line* $x_1 = 0$, $x_2 < 0$. *We shall need also the point* $P_1 = (0, -R_2 y_2(\theta_2, 0, Q_2))$. *Finally, we obtain the region* G *in yellow and blue between the vertical lines and graphs of the solutions in Figure 3.1. The region* G *contains discontinuous trajectories and outside of this region all trajectories are continuous. Moreover, both region* G *and its complement are invariant.*

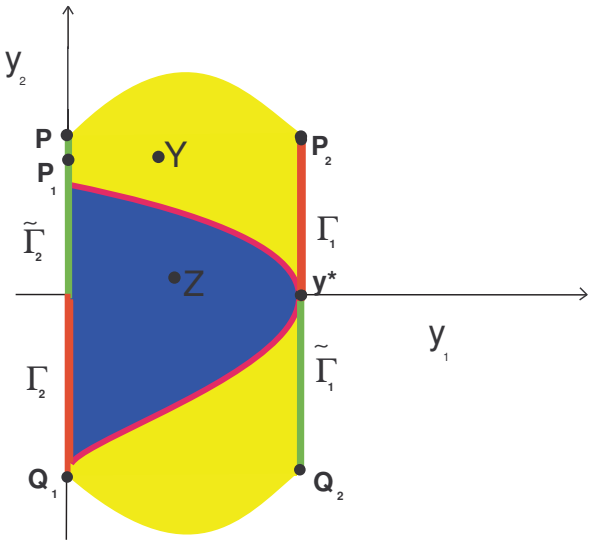

Figure 3.1: The region G for system (3.14) is depicted in details. The curves of discontinuity $\Gamma = \Gamma_1 \cup \Gamma_2$ and $\tilde{\Gamma} = \tilde{\Gamma}_1 \cup \tilde{\Gamma}_2$ are drawn as vertical lines in red and green, respectively and the grazing orbit in magenta.

Define $\Gamma_1 = \{(y_1, y_2)|\ y_1 = \exp(0.00025\pi), \quad 0 \leq y_2 \leq y_2(\theta_1, 0, (0, \bar{y}_2))\}$, *and* $\Gamma_2 = \{(y_1, y_2)|\ y_1 = 0,\ y_2(\theta_2, 0, -R_1 y_2((\theta_1, 0, (0, \bar{y}_2)))^2) \leq y_2 \leq 0\}$. *The boundary of the curve,* $\Gamma = \Gamma_1 \cup \Gamma_2$, *has of four points, they are*

$$\partial\Gamma = \{(0,0), (\exp(0.00025\pi), 0), (\exp(0.00025\pi), y_2(\theta_1, 0, (0, \bar{y}_2))),$$
$$(0, y_2(\theta_2, 0, -R_1 y_2(\theta_1, 0, (0, \bar{y}_2)))\}.$$

In the following part of the example, we will show that two of them, $y^* = (y_1^*, y_2^*) = (\exp(0.00025\pi), 0)$ *and the origin,* $(0, 0)$ *are grazing points. Moreover, it can be easily validated that other two points are of* $\beta-$*type.*

Issuing from system (3.14), the curve of discontinuity $\tilde{\Gamma}$ *consists of two components* $\tilde{\Gamma}_1$ *and* $\tilde{\Gamma}_2$. *The components are the following sets*

$$\tilde{\Gamma}_1 = \{(y_1, y_2)|\ y_1 = \exp(0.00025\pi),\ -R_1 y_2(\theta_1, 0, (0, \bar{y}_2))^2 \leq y_2 \leq 0\}$$

and

$$\tilde{\Gamma}_2 = \{(y_1, y_2)|\ y_1 = 0,\ 0 \leq -R_2 y_2(\theta_2, 0, Q_2)\}.$$

One can verify that the function

$$\Psi(t) = \begin{cases} \exp(0.0005t)\Big(\sin(t), \cos(t)\Big), & \text{if } t \in [0, \pi), \\ (0, 1), & \text{if } t = \pi, \end{cases} \tag{3.15}$$

is a discontinuous periodic solution of (3.14) with period $\omega = \pi$, *whose discontinuity points* $(0, 1)$ *and* $(0, -\exp(0.0005\pi))$ *belong to* $\tilde{\Gamma}$ *and* Γ, *respectively. The expression*

$$\langle \nabla\Phi((\exp(0.00025\pi), 0)), f((\exp(0.00025\pi), 0))\rangle$$
$$= \langle (1, 0), (0, -\exp(-0.00025\pi))\rangle = 0$$

verifies that y^* *is a* $(\gamma)-$*type point, i.e. a grazing point of the solution* $\Psi(t)$. *It is easily seen that the grazing is axial. Now, we can assert that the periodic solution (3.15) is a grazing solution in the sense of Definition 5. Its simulation is depicted in Figure 3.2.*

Since the complement of G *is invariant in both directions and consists of continuous trajectories of the linear system (3.14a), one can easily conclude that the complement is a continuous dynamical system [30]. Thus, to verify the dynamics for the whole*

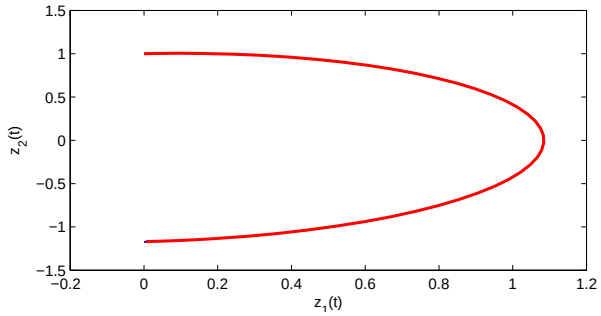

Figure 3.2: The grazing orbit of system (3.14).

system, one need to analyze it in the region G*. This set is bounded, consequently for solutions in it conditions* $(C8)$ *and* $(C9)$ *are fulfilled and by Theorem 1, they admit* $B-$*sequences and continuation property.*

Consider $\zeta(y_2) : [y_2(\theta_2, 0, Q_2), y_2(\theta_1, 0, P)] \to [y_2(\theta_2, 0, Q_2), y_2(\theta_1, 0, P)]$ *such that it is continuously differentiable, satisfies* $\zeta(y_2) = -R_2 y_2$ *in a neighborhood of* $y_2 = 0$ *and is the identity at the boundary points, i.e.* $\zeta(y_2(\theta_1, 0, P)) = y_2(\theta_1, 0, P)$ *and* $\zeta(y_2(\theta_1, 0, P)) = y_2(\theta_1, 0, P)$*. It is easily seen that such function exists. On the basis of this discussion, let us introduce the following system,*

$$\begin{aligned} y_1' &= y_2, \\ y_2' &= -y_1 + 0.001 y_2, \\ \Delta y_2|_{y\in\Gamma} &= \zeta(y_2) - y_2. \end{aligned} \tag{3.16}$$

It is apparent that system (3.16) is equivalent to (3.14) near the orbit of periodic solution $\Psi(t)$*. That is, they have the same trajectories there.*

Specifying (3.1) for (3.16), it is easy to obtain that $\Phi(y_1, y_2) = \tilde{\Phi}(y_1, y_2) = (y_1 - \exp(0.00025\pi))y_1$*,* $f(y_1, y_2) = (y_2, -y_1 + 0.001y_2)$ *and* $J(y) = (y_1, \zeta(y_2))$*.*

Now, we will verify that system (3.16) defines a $K-$ *smooth discontinuous flow. First, condition* $(C1)$ *is verified since* $\nabla\Phi_1(y) = \nabla\Phi_2(y) = (1, 0) \neq 0$*, for all* $y \in D$*. The jump function* $J(y) = (y_1, \zeta(y_2))$ *is continuously differentiable function. So, condition* $(C2)$ *is valid. It is true that* $\Gamma \cap \tilde{\Gamma} \subseteq \partial\Gamma \cap \partial\tilde{\Gamma}$*. Inequalities* $\langle \nabla\Phi_1(y), f(y)\rangle = \langle (1, 0), (y_2, -y_1 + 0.001y_2)\rangle = y_2 \neq 0$ *and* $\langle \nabla\Phi_2(y), f(y)\rangle = \langle (1, 0), (y_2, -y_1 + 0.001y_2)\rangle = y_2 \neq 0$*, if* $y \in \Gamma \setminus \partial\Gamma$*, validate the condition*

$(C4)$. *Moreover,* $\langle \nabla\tilde{\Phi}_1(y), f(y)\rangle = \langle (1,0),(y_2,-y_1+0.001y_2)\rangle = y_2 \neq 0$ *and* $\langle \nabla\tilde{\Phi}_2(y), f(y)\rangle = \langle (1,0),(y_2,-y_1+0.001y_2)\rangle = y_2 \neq 0$, *if* $y \in \tilde{\Gamma} \setminus \partial\tilde{\Gamma}$. *Conditions* $(C6)$ *and* $(C7)$ *hold as the function* ζ *is such defined. Thus, conditions* $(C1)-(C10)$ *have been verified. Consequently, the system* (3.14) *defines the* $K-$ *smooth discontinuous flow for all motions except the grazing ones. To complete the discussion, one need to linearize the system near the grazing solutions. First, we proceed with the linearization around the grazing periodic orbit (3.15).*

The solution, $\Psi(t)$ *has two discontinuity moments* $\theta_1 = \frac{\pi}{2}$ *and* $\theta_2 = \omega$ *in the interval* $[0,\omega]$. *The corresponding discontinuity points are of* $(\gamma)-$ *and* $(\alpha)-$ *types, respectively. Next, we will linearize the system at these points. The linearization at the second point exists [5] and the details of this will be analyzed in the next example. This time, we will focus on the grazing point* y^*.

First, we assume that $y(t) = y(t,0,y^*+\Delta y)$, $\Delta y = (\Delta y_1, \Delta y_2)$ *is not a grazing solution. Moreover, the solution intersects the line* Γ_1 *at time* $t = \xi$ *near* $t = \theta_1$ *as time increases. The meeting point* $\bar{y} = (\bar{y}_1, \bar{y}_2) = (y_1(\xi,0,(y^*+\Delta y)), y_2(\xi,0,(y^*+\Delta y))$, *is transversal one. It is clear* $\bar{y}_1 = \exp(0.00025\pi)$ *and* $\bar{y}_2 > 0$. *In order to find a linearization at the moment* $t = \theta_i$, *we use formula* (3.3) *for* $y(t)$, *and find that*

$$\begin{aligned}\frac{\partial W_i(y)}{\partial y_1^0} &= \int_{\theta_i}^{\tau(y)} \frac{\partial f(y(s))}{\partial y}\frac{\partial y(s)}{\partial y_1^0}ds + f(y(s))\frac{\partial \tau(y)}{\partial y_1^0} + J_y(y)\Big(e_1 + f(y(s))\frac{\partial \tau(y)}{\partial y_1^0}\Big)\\ &+ f(y(s)+J(y(s)))\frac{\partial \tau(y)}{\partial y_1^0} + \int_{\tau(y)}^{\theta_i} \frac{\partial f(y(s)+J(y(s)))}{\partial x}\frac{\partial y(s)}{\partial y_1^0}ds,\end{aligned} \tag{3.17}$$

where $e_1 = (1,0)^T$, T *denotes the transpose of a matrix. Substituting* $y = \bar{y}$ *to the formula* (3.17)*, we obtain that*

$$\begin{aligned}\frac{\partial W_i(y(\xi,0,y^*+\Delta y))}{\partial y_1^0} &= f(y(\xi,0,y^*+\Delta y))\frac{\partial \tau(y(\xi,0,y^*+\Delta y))}{\partial y_1^0}\\ &+J_y(y(\xi,0,y^*+\Delta y))\left(e_1 + f(y(\xi,0,y^*+\Delta y)))\frac{\partial \tau(y(\xi,0,y^*+\Delta y)))}{\partial y_1^0}\right)\\ &+ f(y(\xi,0,(J(y(\xi,0,y^*+\Delta y)))))\frac{\partial \tau(J(y(\xi,0,y^*+\Delta y)))}{\partial y_1^0}.\end{aligned} \tag{3.18}$$

Considering the formula (3.10) *for the transversal point* $\bar{y} = (\bar{y}_1, \bar{y}_2)$, *the first compo-*

nent $\dfrac{\partial\tau(\bar{y})}{\partial y_1^0}$ *can be evaluated as* $\dfrac{\partial\tau(\bar{y})}{\partial y_1^0} = -\dfrac{1}{\bar{y}_2}$. *From the last equality, it is seen how the singularity appears at the grazing point. Finally, we obtain that*

$$\frac{\partial W_i(\bar{y})}{\partial y_1^0} = \begin{bmatrix} \bar{y}_2 \\ -\bar{y}_1 - 0.001\bar{y}_2 \end{bmatrix} \Big(-\frac{1}{\bar{y}_2} \Big) + \begin{bmatrix} 1 & 0 \\ 0 & -2R_1\bar{y}_2 \end{bmatrix} \Bigg(e_1 + \begin{bmatrix} \bar{y}_2 \\ -\bar{y}_1 - 0.001\bar{y}_2 \end{bmatrix} \Big(-\frac{1}{\bar{y}_2} \Big) \Bigg) - \begin{bmatrix} -R_1(\bar{y}_2)^2 \\ -\bar{y}_1 + 0.001R_1(\bar{y}_2)^2 \end{bmatrix} \Big(-\frac{1}{\bar{y}_2} \Big) = \begin{bmatrix} \bar{y}_2 - R_1(\bar{y}_2)^2 \\ -\bar{y}_1 - 0.001(\bar{y}_2 - R_1(\bar{y}_2)^2) \end{bmatrix} \Big(-\frac{1}{\bar{y}_2} \Big) + \begin{bmatrix} 1 & 0 \\ 0 & -2R_1\bar{y}_2 \end{bmatrix} \begin{bmatrix} 0 \\ \dfrac{\bar{y}_1 + 0.001\bar{y}_2}{\bar{y}_2} \end{bmatrix}. \tag{3.19}$$

Calculating the righthand side of (3.19) *we have*

$$\frac{\partial W_i(\bar{y})}{\partial y_1^0} = \begin{bmatrix} -R_1\bar{y}_2 - 1 \\ 0.001(1 - R_1\bar{y}_2) + 2R_1(0.001\bar{y}_2 - \bar{y}_1) \end{bmatrix}. \tag{3.20}$$

The last expression demonstrates that the derivative is a continuous function of its arguments in a neighborhood of the grazing point. Since it is defined and continuous for the points, which are not from the grazing orbit by the last expression and for other points it can be determined by the limit procedure. Indeed, one can easily show that the derivative at the grazing point y^* *is*

$$\begin{bmatrix} -1 \\ 0.001 - 1.8\exp(0.00025\pi) \end{bmatrix}. \tag{3.21}$$

Similarly, all other points of the grazing orbit can be discussed.

Next, differentiating (3.3) *with* $y(t)$ *again we obtain that*

$$\frac{\partial W_i(y)}{\partial y_2^0} = \int_{\theta_i}^{\tau(y)} \frac{\partial f(y)}{\partial y}\frac{\partial y(s)}{\partial y_2^0}ds + f(y(s))\frac{\partial\tau(y)}{\partial y_2^0} + J_y(y)(e_2 + f(y(s))\frac{\partial\tau(y)}{\partial y_2^0}) + f(y + J(y))\frac{\partial\tau(y)}{\partial y_2^0} + \int_{\tau(y)}^{\theta_i} \frac{\partial f(y(s) + J(y(s)))}{\partial x}\frac{\partial y(s)}{\partial y_2^0}ds, \tag{3.22}$$

where $e_2 = (0,1)^T$. *Calculate the right hand side of* (3.22) *at the point* $\bar{y} = (\bar{y}_1, \bar{y}_2)$ *to obtain*

$$\begin{aligned}\frac{\partial W_i(y(\xi,0,y^*+\Delta y))}{\partial y_2^0} &= f(y(\xi,0,y^*+\Delta y))\frac{\partial \tau(y(\xi,0,y^*+\Delta y))}{\partial y_2^0} \\ &+ J_y(y(\xi,0,y^*+\Delta y))\left(e_2 + f(y(\xi,0,y^*+\Delta y)))\frac{\partial \tau(y(\xi,0,y^*+\Delta y))}{\partial y_2^0}\right) \\ &+ f(y(\xi,0,y^*+\Delta y))\frac{\partial \tau(y(\xi,0,y^*+\Delta y))}{\partial y_2^0}.\end{aligned} \tag{3.23}$$

To calculate the fraction $\dfrac{\partial \tau(y(\xi,0,y^*+\Delta y))}{\partial y_2^0}$ *in* (3.23)*, we apply formula* (3.10) *for the transversal point* $\bar{y} = (\bar{y}_1, \bar{y}_2)$. *The second component* $\dfrac{\partial \tau(\bar{y})}{\partial y_2^0}$ *takes the form* $\dfrac{\partial \tau(\bar{y})}{\partial y_2^0} = 0$. *This and formula* (3.23) *imply*

$$\frac{\partial W_i(\bar{y})}{\partial y_2^0} = \begin{bmatrix} 0 \\ -2R\bar{y}_2 \end{bmatrix}. \tag{3.24}$$

Similar to (3.21)*, one can obtain that*

$$\frac{\partial W_i(y^*)}{\partial y_2^0} = \begin{bmatrix} 0 \\ 0 \end{bmatrix}. \tag{3.25}$$

Joining (3.21) *and* (3.25)*, it can be obtained that*

$$W_{iy}(y^*) = \begin{bmatrix} -1 & 0 \\ 0.001 - 1.8\exp(0.00025\pi) & 0 \end{bmatrix}. \tag{3.26}$$

The continuity of the derivatives in a neighborhood of y^* *implies that the function* W *is differentiable at the grazing point* $y = y^*$, *and the condition* $(A2)$ *is valid.*

Now, on the basis of the discussion made above, one can obtain the bivalued matrix of coefficients for the grazing point as

$$B_1 = \begin{cases} O_2, & \textit{if (N1) is valid}, \\ \begin{bmatrix} -1 & 0 \\ 0.001 - 1.8\exp(0.00025\pi) & 0 \end{bmatrix}, & \textit{if (N2) is valid}. \end{cases}$$

The matrix $D_1^{(1)} = O_2$ *is for near solutions of (3.15) which are in the region where* Z *in, see Fig. 3.1, and do not intersect the curve of discontinuity* Γ_1. *The matrix*

$$D_1^{(2)} = \begin{bmatrix} -1 & 0 \\ 0.001 - 1.8\exp(0.00025\pi) & 0 \end{bmatrix}$$

is for near solutions of (3.15), which intersects the curve of discontinuity Γ_1. *They start in the subregion, where the point* Y *is placed. Thus, the linearization for* $\Psi(t)$ *at the grazing point exists. Moreover, since another point of discontinuity* $(0, \exp(0.0005\pi))$ *is not grazing, the linearization at the point exist as well as linearization at points of continuity [5, 105]. Consequently, there exist linearization around* $\Psi(t)$.

To verify condition $(A3)$, *consider a near solution* $y(t) = y(t, 0, \bar{y})$ *to* $\Psi(t)$, *where* $\bar{y} = (0, \bar{y}_2)$, $\bar{y}_2 > \Psi_2(0) = 1$, *which satisfy the condition* $(N1)$. *It is true that* $\theta_{i+1} - \theta_i = \dfrac{\pi}{2} = \dfrac{\omega}{2}$. *The first coordinate of the near solution is presented as*
$y_1(t) = \bar{y}\exp(0.0005t)\sin(t)$ *and*
$y_1(\frac{\omega}{2}) = y_1(\dfrac{\pi}{2}) = \bar{y}\exp(0.00025\pi) > \exp(0.00025\pi) = \Psi_1(\dfrac{\omega}{2})$. *Thus, the meeting moment of near solution* $y(t)$ *with the surface of discontinuity is less than* $\frac{\omega}{2}$. *So, it implies that* $0 < \tau(y) < \frac{\pi}{2} - \epsilon$ *for a small number* ϵ *if the first coordinate of* $\bar{y}$ *is close to* $\exp(0.00025\pi)$. *This validates condition* $(A3)$. *Now, Lemma 1 proves the condition* (C).

Now, let us take into account the point $(0, 0)$. *By utilizing Definition 1, we obtain that* $\langle \nabla\Phi((0,0)), f((0,0))\rangle = \langle (1,0), (0,0)\rangle = 0$. *That is, the origin is a grazing point. In the same time it is a fixed point of the system. For this particular grazing point, we can find the linearization directly. Indeed, all the near solutions satisfy the linear*

impulsive system,

$$\begin{aligned} x_1' &= x_2, \\ x_2' &= -x_1 + 0.001x_2, \\ \Delta x_2|_{x_1=0} &= -(1+R_2)x_2. \end{aligned} \tag{3.27}$$

Consider a solution $x(t) = x(t, 0, x_0)$*, where* $x_0 = (x_1^0, x_2^0) \neq (0, 0)$ *with moments of discontinuity* $\theta_i, i \in \mathbb{Z}$*, then the linearization system for the equation around the equilibrium is*

$$\begin{aligned} u_1' &= u_2, \\ u_2' &= -u_1 + 0.001u_2, \\ \Delta u_2|_{t=\theta_i} &= -(1+R_2)u_2. \end{aligned} \tag{3.28}$$

Indeed, if $u_1(t)$, $u_1(0) = e_1$, $u_2(t)$, $u_2(0) = e_2$, *are solutions of* (3.28)*, then one can see that* $x(t) - (0, 0) = x_1^0 u_1(t) + x_2^0 u_2(t)$*, for all* $t \in \mathbb{R}$.

We have obtained that linearization exists for both grazing solutions $\Psi(t)$*, and the equilibrium at the origin. Moreover, conditions* $(C1) - (C10)$ *are valid and all other solutions are B-differentiable in parameters [5]. Thus, the system* (3.14) *defines a* $K-$ *smooth discontinuous flow in the plane.*

In the next example, we will finalize the linearization around the grazing solution $\Psi(t)$.

Example 2 *(Linearization around the grazing discontinuous cycle). We continue analysis of the last example, and complete the variational system for* $\Psi(t)$.

Let us consider this time, the linearization at the non-grazing moment $\omega = \pi$*. The discontinuity point is* $c = (0, -\exp(0.0005\pi))$ *and it is of* $(\alpha)-$ *type, since*

$$\langle \nabla \Phi(c), f(c) \rangle$$

$$= \langle (1, 0)(-\exp(0.0005\pi), -0.001 \exp(0.0005\pi)) \rangle = -\exp(0.0005\pi) \neq 0.$$

Utilizing (3.10), the gradient can be computed as $\nabla \tau(c) = (\exp(-0.0005\pi), 0)$.

Then, utilizing $\nabla\tau(c)$ and formula (3.11), one can determine that the matrix of linearization at the moment π is

$$B_2 = \begin{bmatrix} \exp(-0.0005\pi) & 0 \\ 0.001 & 0 \end{bmatrix}.$$

From the monotonicity of the jump function, $-R_1 y_2^2$, it follows that the the yellow and blue subregions of G are invariant. Consequently, for each solution near to $\Psi(t)$, the sequences B_i is of two types $B_i = D_i^{(j)}$, $i \in \mathbb{Z}$ and $j = 1, 2$, where $D_{2i-1}^{(1)} = O_2$, $D_{2i-1}^{(2)} = D_1^{(2)} = \begin{bmatrix} -1 & 0 \\ 0.001 - 1.8\exp(0.00025\pi) & 0 \end{bmatrix}$, $D_{2i}^{(1)} = D_{2i}^{(2)} = \begin{bmatrix} \exp(-0.0005\pi) & 0 \\ 0.001 & 0 \end{bmatrix}$, $i \in \mathbb{Z}$. That is, the condition $(A4)$ is valid and the linearization around the periodic solution (3.15) on $\mathbb{R}$ is of two subsystems:

$$\begin{aligned} u_1' &= u_2, \\ u_2' &= -u_1 + 0.001u_2, \\ \Delta u|_{t=\theta_{2i-1}} &= D_{2i-1}^{(1)} u, \\ \Delta u|_{t=\theta_{2i}} &= D_{2i}^{(1)} u, \end{aligned} \tag{3.29}$$

and

$$\begin{aligned} u_1' &= u_2, \\ u_2' &= -u_1 + 0.001u_2, \\ \Delta u|_{t=\theta_{2i-1}} &= D_{2i-1}^{(2)} u, \\ \Delta u|_{t=\theta_{2i}} &= D_{2i}^{(2)} u, \end{aligned} \tag{3.30}$$

where $\theta_{2i-1} = \frac{(2i-1)\pi}{2}$ and $\theta_{2i} = i\pi$

The sequences $\{D_i^{(j)}\}$, $j = 1, 2$, are $2-$ periodic. It is appearant that system (3.29)+(3.30) is a $(\omega, 2)-$ periodic. Thus, the variational system for the grazing solution is constructed.

3.4 Orbital stability

In this section, we proceed investigation of the grazing periodic solution $\Psi(t)$. Analysis of orbital stability will be taken into account. Denote by $B(z,\delta)$, an open ball with center at z and the radius $\delta > 0$ for a fixed point $z \in \Gamma \setminus \partial\Gamma$. By condition (C3), the ball is divided by surface Γ into two connected open regions. Denote $c^+(z,\delta)$, for the region, where solution $x(t) = x(t,0,z)$ of (3.2) enters as time increases. The region is depicted in Figure 3.3.

Set the path of the periodic solution $\Psi(t)$ as

$$\eta := \{x \in D : x = \Psi(t), \quad t \in \mathbb{R}\}.$$

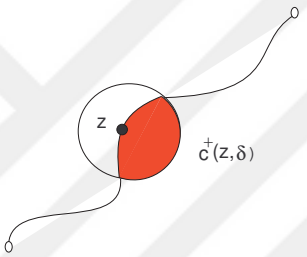

Figure 3.3: The region $c^+(z,\delta)$.

Define $dist(A,a) = \inf_{\alpha\in A} \|\alpha - a\|$, where A is a set, and a is a point.

Definition 6 *The periodic solution $\Psi(t) : \mathbb{R} \to D$ of (3.1) is said to be orbitally stable if for every $\epsilon > 0$, there is a $\delta = \delta(\epsilon) > 0$ such that $dist(x(t,0,x_0),\eta) < \epsilon$, for all $t \geq 0$, provided $dist(x_0,\eta) < \delta$ and $x_0 \notin \cup_i c^+(\Psi(\theta_i),\delta)$,for $i = 1,\ldots,m$, where m is the number of points $\Psi(\theta_i) \in \Gamma \setminus \partial\Gamma$.*

The point x_0 is not considered in regions $c^+(\Psi(\theta_i),\delta), i = 1,\ldots,m$, since solutions which start there move continuously on a finite interval, while $\Psi(t)$ experiences a non-zero jump at $t = \theta_i$ and this violates the continuity in initial value, in general. In the same time, we take into account any region adjoint to points of $\partial\Gamma$, since the jump of $\Psi(t)$ is zero there and, consequently, the continuous dependence in initial value is valid for all near points.

Definition 7 *The solution $\Psi(t) : \mathbb{R}_+ \to D$ of (3.1) is said to have asymptotic phase property if a $\delta > 0$ exists such that to each x_0 satisfying $dist(x_0, \eta) < \delta$ and $x_0 \notin \cup_i c^+(\Psi(\theta_i), \delta)$, for $i = 1, \ldots, m$, there corresponds an asymptotic phase $\alpha(x_0) \in \mathbb{R}$ with property: for all $\epsilon > 0$, there exists $T(\epsilon) > 0$, such that $x(t + \alpha(x_0), 0, x_0)$ is in ϵ-neighborhood of $\Psi(t)$ in $B-$topology for $t \in [T(\epsilon), \infty)$.*

Let us consider the following system, which will be needed in the following lemmas and theorem

$$\begin{aligned} x' &= A(t)x, \\ \Delta x|_{t=\zeta_i} &= B_i u, \end{aligned} \tag{3.31}$$

where $A(t)$ and B_i are $n \times n$ function-matrices, $A(t + \omega) = A(t)$, for all $t \in \mathbb{R}$ and there exists an integer p such that $\zeta_{i+p} = \zeta_i + \omega$ and $B_{i+p} = B_i$, for all $i \in \mathbb{Z}$.

Lemma 3 *Assume that system (3.31) has a simple unit characteristic multiplier and the remaining $n - 1$ ones are in modulus less than unity. Then, the system (3.31) has a real fundamental matrix $X(t)$, of the form*

$$X(t) = P(t) \begin{pmatrix} 1 & 0 \\ 0 & \exp(Bt) \end{pmatrix}, \tag{3.32}$$

where $P \in PC^1(\mathbb{R}, \theta)$ is a regular, ω-periodic matrix, and B is an $(n-1) \times (n-1)$ matrix with all eigenvalues have negative real parts.

Proof. Denote the matrix $X(t), X(0) = I$, as fundamental matrix of system (3.31). There is a matrix B_1 such that the substitution $x = P(t)z$, where
$P(t) = X(t)\exp(-B_1 t)$, transforms (3.31) to the following system with constant coefficient [5],

$$z' = \Lambda z. \tag{3.33}$$

The matrix $\exp(\Lambda\omega)$ has a simple unit eigenvalue and remaining $(n-1)$ ones are in modulus less than unity. Hence, there exists real nonsingular matrix M, which

satisfies

$$M^{-1}\exp(\Lambda\omega)M = \begin{bmatrix} 1 & 0 \\ 0 & C_1 \end{bmatrix}.$$

The remaining part of the proof is same as proof of Lemma 5.1.1 in [38]. □

Throughout this section, we will assume that $(A4)$ is valid. That is, the variational system (3.13) consists of m periodic subsystems. For each of these systems, we find the matrix of monodromy, $U_j(\omega)$ and denote corresponding Floquet multipliers by $\rho_i^{(j)}$, $i = 1,\ldots,n$, $j = 1,\ldots,m$. In the next part of the study, the following assumption is needed.

(A5) $\rho_1^{(j)} = 1$ and $|\rho_i^{(j)}| < 1$, $i = 2,\ldots,n$ for each $j = 1,\ldots,m$.

Lemma 4 *Assume that the assumptions (A4) and (A5) are valid. Then, for each $j = 1,\ldots,m$, the system (3.13) admits a fundamental matrix of the form*

$$U_j(t) = P_j(t)[1, \exp(H_j\omega)], \quad t \in \mathbb{R}, \tag{3.34}$$

where $P_j \in PC^1(\mathbb{R},\zeta)$ is a regular, ω-periodic matrix and H_j is an $(n-1)\times(n-1)-$ matrix with all eigenvalues have negative real parts.

The proof of Lemma 4, can be done similar to that of Lemma 3.

Theorem 3 *Assume that conditions $(C1)-(C7)$, $(C10)$, and the assumptions $(A1)-(A5)$ hold. Then ω- periodic solution $\Psi(t)$ of (3.1) is orbitally asymptotically stable and has the asymptotic phase property.*

Proof. Since of the group property, we may assume $\Psi(0)$ is not a discontinuity point. Then, one can displace the origin to the point $\Psi(0)$, and the coordinate system can be rotated in such a way that the tangent vector $\Psi_0' = \Psi'(0)$ points in the direction of the positive x_1 axis i.e. the coordinates of this vector are $\Psi_0' = (\Psi_{01}', 0,\ldots,0)$, $\Psi_{01}' > 0$.

Let $\theta_i, i \in \mathbb{Z}$, be the discontinuity moments of $\Psi(t)$. Denote the path of the solution by $\eta = \{x \in X : x = \Psi(t), t \in \mathbb{R}\}$. There exists a natural number p, such that $\theta_{i+p} = \theta_i + \omega$ for all i. Because of conditions $(C1)-(C7)$ and $K-$differentiability of

$\Psi(t)$ there exists continuous dependence on initial data and consequently there exists a neighborhood of η such that any solutions which starts in the set will have moments of discontinuity which constitute a $B-$ sequence with difference between neighbors approximately equal to the distance between corresponding neighbor moments of discontinuity of the periodic solution $\Psi(t)$. Consequently we can determine variational system for $\Psi(t)$, with points of discontinuity $\theta_i,\ i \in \mathbb{Z}$.

On the basis of discussion in Section 2.1, one can define in the neighborhood of η a $B-$ equivalent system of type (3.4). The variational system of it takes the form

$$\begin{aligned} z' &= A(t)z + r(t,z), \\ \Delta z|_{t=\theta_i} &= D_i^{(j)} z + q_i(z), \quad j = 1, 2, \ldots, m, \end{aligned} \tag{3.35}$$

where $r(t,z) = [f(\Psi(t)+z) - f(\Psi(t))] - A(t)z$ and $q_i(z) = W_i(\Psi(\theta_i)+z) - W_i(\Psi(\theta_i)) - D_i^{(j)}z$, are continuous functions, and matrices $D_i^{(j)}$ satisfy condition $(A4)$. The functions are continuously differentiable with respect to z. One can verify that $r(t,0) \equiv q_i(0) \equiv 0$ and $r(t+\omega, z) = r(t,z)$ for $t \in \mathbb{R}$. Moreover, the derivatives satisfy $r'(t,0) \equiv q'_{iz}(0) \equiv 0$ and the functions $r(t,z) \to 0$, $q_i(z) \to 0$, $r'_z(t,z) \to 0$ and $q'_{iz}(z) \to 0$, as $z \to 0$ uniformly in $t \in [0,\infty),\ i \geq 0$. Each system (3.35) for $j = 1, 2, \ldots, m$, corresponds to a region adjoint to initial value, x_0 such that these regions cover a neighborhood of x_0.

Fix a number j and denote $Y_j(t)$ the fundamental matrix of adjoint to (3.35) linear homogeneous system

$$\begin{aligned} y' &= A(t)y, \\ \Delta y|_{t=\theta_i} &= D_i^{(j)} y, \end{aligned} \tag{3.36}$$

of the form (3.34). One can verify that

$$Y_j(t)Y_j^{-1}(s) = P_j(t) \begin{pmatrix} 1 & 0 \\ 0 & \exp(H_j(t-s)) \end{pmatrix} P_j^{-1}(s), \tag{3.37}$$

for $-\infty < t, s < \infty$.

We can write

$$\begin{pmatrix} 1 & 0 \\ 0 & \exp(H_j(t-s)) \end{pmatrix} = \begin{pmatrix} 0 & 0 \\ 0 & \exp(H_j(t-s)) \end{pmatrix} + \begin{pmatrix} 1 & 0 \\ 0 & O_{n-1} \end{pmatrix},$$

where O_{n-1} is the $(n-1) \times (n-1)$ zero matrix. Then it can be driven

$$Y_j(t)Y_j^{-1}(s) = G_1^{(j)}(t,s) + G_2^{(j)}(t,s) = G^{(j)}(t,s),$$

where

$$G_1^{(j)}(t,s) = P_j(t) \begin{pmatrix} 0 & 0 \\ 0 & \exp(H_j(t-s)) \end{pmatrix} P_j^{-1}(s),$$

$$G_2^{(j)}(t,s) = P_j(t) \begin{pmatrix} 1 & 0 \\ 0 & O_{n-1} \end{pmatrix} P_j^{-1}(s).$$

Denote the eigenvalues of the matrix H_j by $\lambda_2^{(j)}, \ldots, \lambda_n^{(j)}$. By means of the Lemma 3 and 4, there exits a number $\alpha > 0$, such that $Re(\lambda_k^{(j)}) < -\alpha$, $k = 2, 3, \ldots, n$, where $Re(z)$ means the real part of the number, z. Taking into account that the matrices P_j and P_j^{-1} are regular and periodic, the following estimates can be calculated

$$|G_1^{(j)}(t,s)| \leq K^{(j)} \exp(-\alpha(t-s)), \tag{3.38}$$

$$|G_2^{(j)}(t,s)| \leq K^{(j)}, \tag{3.39}$$

where $K^{(j)}$ is a positive real constant.

Denote the first column of the fundamental matrix Y by χ^1. By the equation (3.34), χ^1 is equal to the first column of P_j, this means that it is a ω-periodic solution of (3.13).

By assumptions of the theorem the variational system (3.35) satisfies the conditions of Lemma 4, and one can verify that the following estimate is true [38]

$$|Y_j(t)| \leq K_1^{(j)} \exp(-\alpha t) \quad for \;\; t \geq 0, \tag{3.40}$$

where $K_1^{(j)}$ is a positive constant. Let us setup the following integral equation

$$z^{(j)}(t,a) = Y_j(t)a + \int_0^t G_1^{(j)}(t,s)r(s,z(s))ds - \int_t^\infty G_2^{(j)}(t,s)r(s,z(s))ds$$
$$+ \sum_{0<\theta_k<t} G_1^{(j)}(t,\theta_k+)q_k(z(\theta_k)) - \sum_{t<\theta_k<\infty} G_2^{(j)}(t,\theta_k+)q_k(z(\theta_k)), \tag{3.41}$$

where $a = [0, a_2, \ldots, a_n]$, $a_i \in \mathbb{R}$, $i = 2, 3, \ldots, n$, are orthogonal to $\Psi'(0)$, i.e. with the zero first coordinate.

Let $z_0^{(j)}(t,a) \equiv 0$, and consider the following successive approximations

$$z_k^{(j)}(t,a) = Y_j(t)a + \int_0^\infty G^{(j)}(t,s)r(s,z_{k-1}(s))ds + \sum_{k=1}^\infty G^{(j)}(t,\theta_k+)q_k(z_{k-1}(\theta_k)), \tag{3.42}$$

for $k = 1, 2, \ldots$. By using the approximation (3.42) and estimation (3.40), one can verify that

$$|z_1^{(j)}(t,a)| \le K_1^{(j)}|a|\exp(-\alpha t/2). \tag{3.43}$$

We will show that the bounded solution of (3.41) exists and satisfies (3.35). For arbitrary positive small number L, there exists a number $\delta = \delta(L)$ such that for $|z_1| < \delta$, $|z_2| < \delta$

$$|r(t,z_1) - r(t,z_2)| \le L|z_1 - z_2| \tag{3.44}$$

and

$$|q_i(z_1) - q_i(z_2)| \le L|z_1 - z_2|, \tag{3.45}$$

uniformly in $t \in [0,\infty)$.

Denote by $L_1 = 4K^{(j)}\Big(\dfrac{2}{\alpha} - \dfrac{1}{1-\exp(-\alpha\underline{\theta}/2)}\Big)$.

Next, by using mathematical induction, we are going to show that $z_s^{(j)}(t,a), s = 1, 2, \ldots,$ are defined for $t \in [0,\infty)$ and satisfy

$$|z_{s+1}^{(j)}(t,a) - z_s^{(j)}(t,a)| \le K_1^{(j)}|a|\exp(-\alpha t/2)/2^s,\ s = 0, 1, 2, \ldots, \tag{3.46}$$

if $L < L_1$. Utilizing Lemma 4 and inequalities (3.40), (3.44), (3.45) and $\theta_{i+1} - \theta_i \geq \underline{\theta}, i \in \mathbb{Z}$, one can verify that

$$|z_{k+1}^{(j)}(t,a) - z_k^{(j)}(t,a)| \leq K_1^{(j)}|a|L_1 \exp(-\alpha t/2)/(2^k\alpha). \tag{3.47}$$

As a consequence of (3.46), the sequence $z_{k+1}^{(j)}(t,a)$ converges uniformly on $t \in [0,\infty),\ |a| < \delta/2K_1^{(j)}$, and

$$|z_s^{(j)}(t,a)| \leq 2K_1^{(j)}|a| \exp(-\alpha t/2), s = 1,2,\ldots.$$

Therefore, the limit function $z^{(j)}(t,a)$ exists on the same domain, it is piecewise continuous, satisfies (3.41) and the following estimate

$$|z^{(j)}(t,a)| \leq 2K_1^{(j)}|a| \exp(-\alpha t/2). \tag{3.48}$$

Denote by $z(t) = z^{(j)}(t,a)$, for $j = 1,2,\ldots,m$. Next, we will verify that $z^{(j)}(t,a)$ satisfies (3.35). For it, differentiate (3.41)

$$\begin{aligned}
&z'(t) = Y_j'(t)a + G_1^{(j)}(t,t)r(t,z(t)) + G_2^j(t,t)r(t,z(t)) + \\
&\int_0^t G_{1t}^{(j)}(t,s)r(s,z(s))ds - \int_t^\infty G_{2t}^{(j)}(t,s)r(s,z(s))ds + \\
&\sum_{0<\theta_k<t} G_{1t}^{(j)}(t,\theta_k+)q_k(z(\theta_k)) - \sum_{t<\theta_k<\infty} G_{2t}^{(j)}(t,\theta_k+)q_k(z(\theta_k)) = \\
&A(t)Y_j(t)a + G^{(j)}(t,t)r(t,z(t)) + \int_0^\infty A(t)G^{(j)}(t,s)r(s,z(s))ds + \\
&\sum_{0<\theta_i<t} A(t)G^{(j)}(t,\theta_k+)q_k(z(\theta_k)) = A(t)z(t) + r(t,z(t)).
\end{aligned}$$

Fix θ_k, $k \in \mathbb{Z}$, then

$$z(\theta_k+)-z(\theta_k)=Y_j(\theta_k+)a+\int_0^{\theta_k}G_1^{(j)}(\theta_k+,s)r(s,z(s))ds$$
$$-\int_{\theta_k}^{\infty}G_2^{(j)}(\theta_k+,s)r(s,z(s))ds+\sum_{0\le\theta_i<\theta_k}G_1^{(j)}(\theta_k+,\theta_i+)q_i(z(\theta_i+))$$
$$-\sum_{\theta_k<\theta_i<\infty}G_2^{(j)}(\theta_k+,\theta_i+)q_i(z(\theta_i+))-Y_j(\theta_k)a-\int_0^{\theta_k}G_1^{(j)}(\theta_k,s)r(s,z(s))ds$$
$$+\int_{\theta_k}^{\infty}G_2^{(j)}(\theta_k,s)r(s,z(s))ds-\sum_{0\le\theta_i<\theta_k}G_1^{(j)}(\theta_k,\theta_i+)q_i(z(\theta_i))$$
$$+\sum_{\theta_k\le\theta_i<\infty}G_2^{(j)}(\theta_k,\theta_i+)q_i(z(\theta_i+))=D_k^{(j)}z(\theta_k)+q_k(z(\theta_k)).$$

The above discussion proves that $z^{(j)}(t,a), j=1,,2,\ldots,m$, are bounded solutions of system (3.35).

We will determine the initial values of bounded solutions in terms of $(n-1)$ parameters $a_2^{(j)},\ldots,a_n^{(j)}, j=1,,2,\ldots,m$. Denote $a^{(j)}=[0,a_2^j,a_3^j,\ldots,a_n^j]$. By using (3.41), we obtain

$$z^{(j)}(0,a^{(j)})=Y_j(0)a^{(j)}-\int_0^{\infty}G_2^{(j)}(0,s)r(s,z(s))ds-$$
$$\sum_{0<\theta_k<\infty}G_2^{(j)}(0,\theta_k+)q_k(z(\theta_k))=P_j(0)a^{(j)}-P_j(0)\begin{pmatrix}1&0\\0&O_{n-1}\end{pmatrix}\times$$
$$\int_0^{\infty}P_j^{-1}(s)r(s,z(s))ds-\sum_{0<\theta_k<\infty}P_j^{-1}(s)q_k(z(\theta_k)).$$

In the way utilized in [38], one can show that the coordinates of the initial value $(x_1,\ldots,x_n)\in D$ of the solution $z^{(j)}$ satisfy the equation

$$x_1+\sum_{i=2}^{n}c_i^jx_i-h_j(x_2,\ldots,x_n)=0, \tag{3.49}$$

where $h_j\in C^1, j=1,,2,\ldots,m$.

One can see that equation (3.49) determines $(n-1)$ dimensional hypersurfaces $S^j\subset D$, $j=1,2,\ldots,m$, in a neighborhood of the origin such that each solution which

starts at the surface satisfies inequality (3.48). From the analytical representation, it follows that the equation of the tangent space of S^j at the origin is described by the equation $x_1 + \sum_{i=2}^{n} c_i^j x_i$ and the first coordinate of the gradient of the left hand side in (3.49) is unity. Moreover, the path η intersects S^j transversely. This and condition $(A4)$ imply that the path of every solution $\phi(t)$ near $\Psi(t)$ intersects one of the manifolds $S^j, j = 1, 2, \ldots, m$, at some $\bar{t} \in [0, 2\omega]$.

Because of the continuous dependence on initial values, a $\delta(\epsilon) > 0$ exists for a given $\epsilon > 0$, such that if $dist(x^0, \eta_\delta) < \delta(\epsilon)$, then the solution $\phi(t, x^0)$ is defined on $[0, 2\omega]$, and $dist(\phi(t, x^0), \eta) < \epsilon \leq \epsilon_1$ for $t \in [0, 2T]$. Therefore, the path of $\phi(t, x^0)$ intersects S^j for some $j = 1, 2, \ldots, m$ and $t_1 \in [0, 2\omega]$. The solution $\phi(t, \phi(t_1, x^0)) = \phi(t + t_1, x^0)$ has its initial value in S^j, consequently, satisfies (3.48). In the light of the $B-$ equivalence, the corresponding solution $x(t), x(0) = \phi(0) - \Psi(0)$, of (3.35) satisfies the property that for all $\epsilon > 0$, there exists $T(\epsilon)$ such that $x(t)$ is in an $\epsilon-$ neighborhood of $\Psi(t)$ for $t \in [T(\epsilon), \infty)$. That is, the solution $\Psi(t)$ is orbitally asymptotically stable and there exists an asymptotical phase. □

Definitions of the orbital stability and an asymptotic phase as well as theorem of orbital stability for non-grazing periodic solutions are also presented in [113]. In our study, we suggest the orbital stability theorem for grazing periodic solutions, its proof and formulate the definitions for the stability. They are different in many aspects from those provided in [113]. It is valuable that they also valid, if the solution is non-grazing.

To shed light on our theoretical results, we will present the following examples.

Example 3 *We continue with the system presented in Examples 1 and 2. In Example 1, we verified that system (3.16)defines a $K-$ smooth discontinuous flow in the plane and the variational system (3.29)+(3.30) around the grazing periodic solution, $\Psi(t)$ is approved.*

Using systems (3.29) and (3.30), one can evaluate the Floquet multipliers as $\rho_1^{(1)} = 1$, $\rho_2^{(1)} = 0.8551$, $\rho_1^{(2)} = 1$ and $\rho_2^{(2)} = 0$. This verifies condition $(A5)$.

The conditions $(C1) - (C7)$ and $(C10)$ are validated and the assumptions (A4) and (A5) verified. By using Theorem 3, we can assert that the solution, $\Psi(t)$ is orbitally

asymptotically stable. The stability is illustrated in Fig. 3.4. The red one is for a trajectory of the discontinuous periodic solution (3.15) of (3.14) and the blue one is for the near solution of (3.14) with initial value $y_0 = (0.8, 1.2)$. *It can be observed from Fig. 3.4 that the blue trajectory approaches the red one as time increases.*

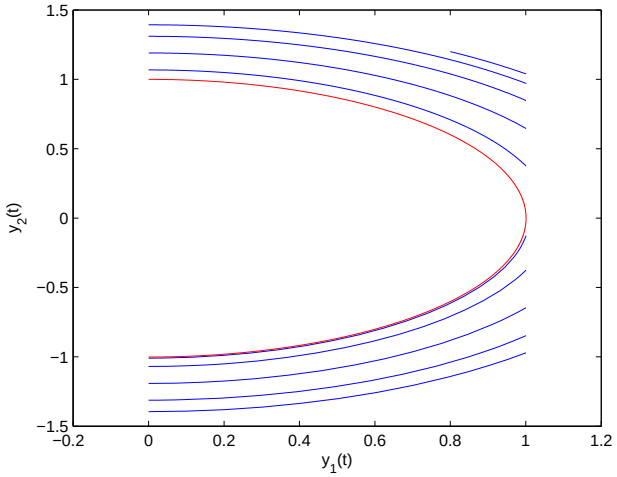

Figure 3.4: The red discontinuous cycle of (3.14) axially grazes Γ at $(0.00025\pi), 0)$ and $(0, -\exp(-0.0005\pi))$ is an (α)-type point. The blue arcs are of the trajectory with initial value $(0.8, 1.2)$. It is seen that it approaches the grazing one as time increases.

Example 4 *(A periodic solution with a non-axial grazing). We will take into account the following autonomous system with variable moments of impulses*

$$\begin{aligned} x_1' &= x_2, \\ x_2' &= -x_1, \\ \Delta x_1|_{x\in\Gamma} &= \frac{1}{\sqrt{2}} - x_1 + K(x_2 - x_1)^2, \\ \Delta x_2|_{x\in\Gamma} &= \frac{1}{\sqrt{2}} - x_2 + K(x_2 - x_1)^2, \end{aligned} \tag{3.50}$$

where $\Gamma = \{(x_1, x_2)|x_1 + x_2 = \sqrt{2}\}$, $\tilde{\Gamma} = \{(x_1, x_2)|x_1 = x_2\}$ *and* $K = 0.11$. *It is easy to verify that the point* $x^* = (\frac{1}{2}, \frac{1}{2})$ *is a grazing point since of the equality* $\langle \nabla\Phi(x^*), f(x^*)\rangle = \langle (1, 1), (\frac{1}{2}, -\frac{1}{2})\rangle = 0$ *and it is non-axial graziness. We assume that the domain is the plane.*

The solution $\Psi(t) = (\sin(t), \cos(t))$, $t \in \mathbb{R}$ *is a grazing one, since the point* $x^* =$

$\Psi(\frac{\pi}{4})$ *is from its orbit. The cycle and the line of discontinuity are depicted in Figure 3.5.*

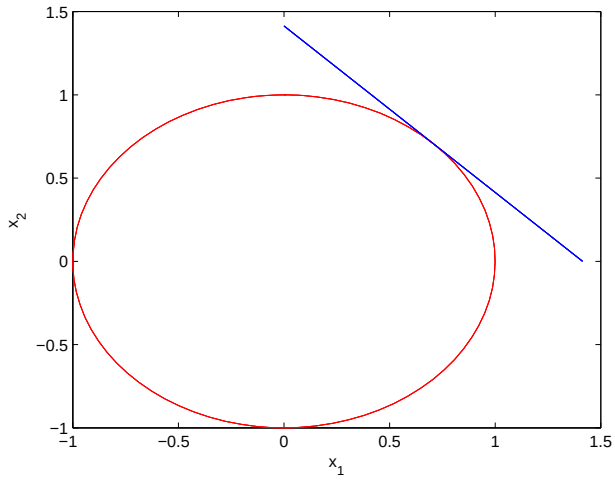

Figure 3.5: The red curve is the orbit of $\Psi(t)$ which grazes non-axially the line of discontinuity.

Let us consider the linearization at the grazing point x^* *next. We will consider the near solution* $x(t) = x(t, 0, x^* + \Delta x)$. *Denote* $t = \xi$, *the moment when the solution meets the surface of discontinuity* Γ *at the point* $\bar{x} = x(\xi) = x(\xi, 0, x^* + \Delta x)$. *Taking into account formulae* (3.17), (3.18) *with* (3.50), *one can obtain the following matrix*

$$\frac{\partial W_i(x(\xi,0,x^*+\Delta x))}{\partial x_1^0} = \begin{bmatrix} \bar{x}_2 \\ -\bar{x}_1 \end{bmatrix} \frac{1}{\bar{x}_1 - \bar{x}_2} + \begin{bmatrix} -2K(\bar{x}_2 - \bar{x}_1) & -2K(\bar{x}_2 - \bar{x}_1) \\ -2K(\bar{x}_2 - \bar{x}_1) & -2K(\bar{x}_2 - \bar{x}_1) \end{bmatrix}$$
$$\times \left(e_1 + \begin{bmatrix} \bar{x}_2 \\ -\bar{x}_1 \end{bmatrix} \frac{1}{\bar{x}_1 - \bar{x}_2} \right) + \begin{bmatrix} -\frac{1}{\sqrt{2}} + K(\bar{x}_2 - \bar{x}_1)^2 \\ \frac{1}{\sqrt{2}} - K(\bar{x}_2 - \bar{x}_1)^2 \end{bmatrix} \frac{1}{\bar{x}_1 - \bar{x}_2}. \tag{3.51}$$

Calculating the right hand side of the expression (3.51), *we obtain that*

$$\frac{\partial W_i(x(\xi,0,x^*+\Delta x))}{\partial x_1^0} = \begin{bmatrix} \frac{-\sqrt{2}+0.22}{2\sqrt{2}} \\ \frac{\sqrt{2}+0.22}{2\sqrt{2}} \end{bmatrix}. \tag{3.52}$$

Using similar method with that of the first one, the second derivative can be computed

as

$$\frac{\partial W_i(x(\xi,0,x^*+\Delta x))}{\partial x_2^0} = \begin{bmatrix} \dfrac{\sqrt{2}+0.22}{2\sqrt{2}} \\ \dfrac{-\sqrt{2}+0.22}{2\sqrt{2}} \end{bmatrix}. \tag{3.53}$$

Combining (3.52) *and* (3.53)*, we can obtain the following matrix for the linearization at the grazing point* x^*,

$$W_{ix}(x^*) = \begin{bmatrix} \dfrac{-\sqrt{2}+0.22}{2\sqrt{2}} & \dfrac{\sqrt{2}+0.22}{2\sqrt{2}} \\ \dfrac{\sqrt{2}+0.22}{2\sqrt{2}} & \dfrac{-\sqrt{2}+0.22}{2\sqrt{2}} \end{bmatrix}. \tag{3.54}$$

It is appearant that the matrix $W_{ix}(x^*)$ *is continuous with respect to its arguments, since it is constant if the point* $x^* + \Delta x$ *is not from the orbit of the grazing solution. Since of the limit procedure, it is the same constant for all points of the grazing solution. Thus, the Jacobian is constant matrix in a neighborhood of the grazing point and condition* $(A2)$ *is valid.*

Now, let us check the validity of the condition $(A3)$*. Consider a near solution* $x(t) = x(t,0,\bar{x})$*, to the grazing cycle* $\Psi(t)$*, where* $\bar{x} = (0,\bar{x}_2)$*,* $\bar{x}_2 > \Psi_2(0) = 1$*. So, the near solution* $x(t)$ *satisfies the condition* $(N1)$*. For the grazing periodic solution, it is true that* $\theta_{i+1} - \theta_i = 2\pi = \omega$*. The grazing solution* $\Psi(t) = x(t,0,(0,1))$*, touches the line of discontinuity* Γ *at* $t = \frac{\omega}{8}$*. The first coordinate of the near solution is* $x_1(t) = \bar{x}_2 \sin(t)$*, and* $x_1(\frac{\omega}{8}) = \bar{x}_2 \sin(\frac{\omega}{8}) = \dfrac{\bar{x}_2}{\sqrt{2}} > \Psi_1(\frac{\omega}{8}) = \dfrac{1}{\sqrt{2}}$*. Consequently, the near solution* $x(t)$ *meets the line of discontinuity* Γ *before the moment* $\frac{\omega}{8}$*. This implies that* $0 < \tau(x) < \frac{\pi}{4} - \epsilon$*, for a small positive* ϵ *whenever* $x_1(t)$ *is close to* $\frac{1}{\sqrt{2}}$*. Thus, the condition* $(A3)$ *is valid and Lemma 1 proves condition* (C)*.*

In the light of the above discussion, the bivalued matrix of coefficients for the grazing point is easily obtained as

$$B_1 = \begin{cases} O_2, & \text{if (N1) is valid,} \\ \begin{bmatrix} \dfrac{-\sqrt{2}+0.22}{2\sqrt{2}} & \dfrac{\sqrt{2}+0.22}{2\sqrt{2}} \\ \dfrac{\sqrt{2}+0.22}{2\sqrt{2}} & \dfrac{-\sqrt{2}+0.22}{2\sqrt{2}} \end{bmatrix}, & \text{if (N2) is valid.} \end{cases} \tag{3.55}$$

It is appearant that the interior of the grazing orbit is invariant. Let us show that the external part of the unit circle is positively invariant. It is sufficient to demonstrate that $J_1(x_1)^2 + J_2(x_2)^2 > 1$ *for any* $(x_1, x_2) \in \Gamma$. *Denote* $x_1 = z$ *and* $x_2 = \sqrt{2} - z$ *and consider the formula*

$$F(z) = J_1(z)^2 + J_2(\sqrt{2}-z)^2 = (\frac{1}{\sqrt{2}} + 0.11(\sqrt{2}-2z)^2)^2 + (\frac{1}{\sqrt{2}} + 0.11(\sqrt{2}-2z)^2)^2,$$

where $F(\frac{1}{\sqrt{2}}) = 1$. *It is easy to calculate that* $F'(\frac{1}{\sqrt{2}}) = 0$ *and* $F''(\frac{1}{\sqrt{2}}) = 0.88\sqrt{2} > 0$. *Consequently,*

$$F(z) - F(\frac{1}{\sqrt{2}}) = F(z) - 1 = \frac{1}{2}F''(\frac{1}{\sqrt{2}})(z - \frac{1}{\sqrt{2}})^2 + o(\|z - \frac{1}{\sqrt{2}}\|^2) > 0,$$

if z *is close to* $\frac{1}{\sqrt{2}}$. *Thus, near the grazing point, the external region is invariant. From this discussion, since of the formula* (3.55)*, we can conclude that the condition* $(A4)$ *is valid. Taking into account it with the expression* (3.55)*, the linearization system for* (3.50) *around the grazing solution* $\Psi(t)$ *is obtained as*

$$\begin{aligned} u_1' &= u_2, \\ u_2' &= -u_1, \\ \Delta u(2\pi i) &= D_i^{(j)} u, \end{aligned} \tag{3.56}$$

where $D_i^{(1)} = O_2$ *and* $D_i^{(2)} = \begin{bmatrix} \dfrac{-\sqrt{2}+0.22}{2\sqrt{2}} & \dfrac{\sqrt{2}+0.22}{2\sqrt{2}} \\ \dfrac{\sqrt{2}+0.22}{2\sqrt{2}} & \dfrac{-\sqrt{2}+0.22}{2\sqrt{2}} \end{bmatrix}$, $i \in \mathbb{Z}$.

To finalize stability analysis, consider the first system in (3.56)*, with matrices* $D_i^{(1)} = O_2$. *Its multipliers are* $\rho_1^{(1)} = \rho_2^{(1)} = 1$ *and it constitutes the linearization for the orbits which are inside the circle. The system does not give a decision by orbital stability theorem, Theorem 3. Nevertheless, from the simple analysis [105] result, we know that the grazing orbit is stable with respect to inside orbits of the system. The*

linearization of orbits which are outside of the circle has multipliers $\rho_1^{(2)} = 1$ *and* $\rho_2^{(2)} = -0.15$. *It means that the periodic solution is orbitally stable with respect to solutions outside of the circle. Summarizing the discussion, we can conclude that the periodic solution is stable. The stability result is observed through simulations and it is seen in Fig. 3.6.*

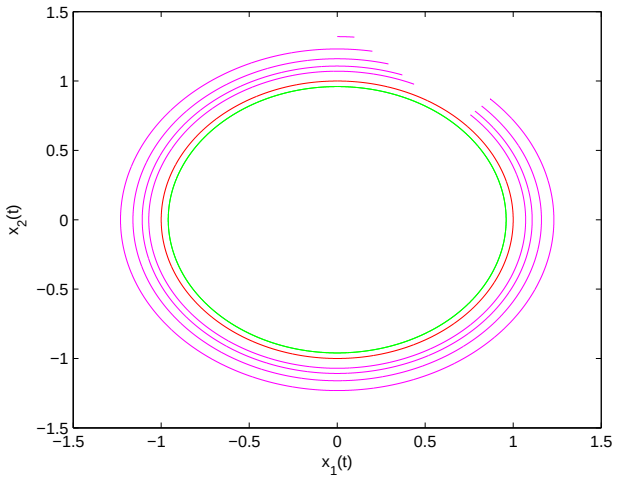

Figure 3.6: The red orbit of system (3.50) non-axially grazes the surface Γ. The magenta trajectory with initial point $(0, 1.32)$ approaches the cycle as time increases. The green cycle with initial point $(0, 0.96)$ demonstrates the inside stability of the grazing orbit.

3.5 Small parameter analysis and grazing bifurcation

In this part, we will discuss existence and bifurcation of cycles for perturbed systems, if the generating one admits a grazing periodic solution. In continuous dynamical systems, a small parameter may cause a change in the number of periodic solutions in critical cases. In the present analysis, we will demonstrate that the change may happen in *non-critical* cases, since of the non-transversality. That is why, one can say that *grazing bifurcation* is under discussion. Let us deal with the following system

$$\begin{aligned} x' &= f(x) + \mu g(x, \mu), \\ \Delta x|_{x \in \Gamma(\mu)} &= I(x) + \mu K(x, \mu), \end{aligned} \tag{3.57}$$

where $x \in \mathbb{R}^n, t \in \mathbb{R}, \Gamma(\mu) = \{x |\ \Phi(x) + \mu\phi(x,\mu) = 0\}$, $\mu \in (-\mu_0, \mu_0)$, and μ_0 is a sufficiently small positive number. Functions $f(x), I(x)$ and $\Phi(x)$ are continuously differentiable up to second order, $g(x,\mu), K(x,\mu)$ are continuously differentiable in x and μ. The function $\phi(x,\mu)$ is continuously differentiable in x up to second order and to first order in μ. We assume that the generating system for (3.57) is the system (3.1) with all conditions assumed for the system, earlier. The main assumption of this section is that (3.1) admits a $\omega-$periodic solution, $\Psi(t)$. Let $\Psi(0) = (\zeta_1^0, \zeta_2^0, \ldots, \zeta_n^0)$ be the initial value of the solution.

Our aim is to find conditions that verify the existence of periodic solutions of (3.57) with a period $\mathscr{T}$ such that for $\mu = 0$, the periodic solutions of (3.57) are turned down to $\Psi(t)$. It is common for the autonomous systems that the period $\mathscr{T}$ does not coincide with ω. Thus, in the remaining part of the study, we will consider the period $\mathscr{T}$ as an unknown variable.

Due to the fact that $\Psi(0)$ is not an equilibrium, there exits a number $j = 1, 2, \ldots, n$, such that $f_j(\zeta_1^0, \zeta_1^0, \ldots, \zeta_n^0) \neq 0$. In other words, the vector field is transversal to line $x_j = \zeta_j^0$ near the point. Hence, to try points near to $\Psi(0)$ for the periodicity, it is sufficient to consider those with $j-$th coordinate is equal to ζ_j^0, [85]. For the discontinuous dynamics, the choice of the fixed coordinate can be made easier if the surface of discontinuity is provided with a constant coordinate. We will demonstrate this in examples. Denote the initial values of the intended periodic solution by $\zeta_1, \zeta_2, \ldots, \zeta_n$. Assume that one initial value ζ_j is known, i.e. ζ_j^0. Thus, the problem contains $n-$many unknowns, they can be presented as $\zeta_1, \zeta_2, \ldots, \zeta_{j-1}, \zeta_{j+1}, \ldots, \zeta_n, \mathscr{T}$. Denote solution of (3.57) by $x_s(t, \zeta_1, \zeta_2, \ldots, \zeta_n, \mu)$ with initial conditions $x_s(0, \zeta_1, \zeta_2, \ldots, \zeta_n, \mu) = \zeta_s$. To determine the unknowns, we will consider the Poincaré criterion, which can be written as

$$\mathscr{S}_k(\mathscr{T}, \zeta_1, \zeta_2, \ldots, \zeta_n, \mu) \equiv x_k(\mathscr{T}, \zeta_1, \zeta_2, \ldots, \zeta_n, \mu) - \zeta_k = 0,\ k = 1, 2, \ldots, n, \tag{3.58}$$

where $\zeta_j = \zeta_j^0$. The equations (3.58) are satisfied with $\mu = 0, \mathscr{T} = \omega, \zeta_i = \zeta_i^0, i = 1, 2, \ldots, n$, since $\Psi(t)$ is the periodic solution.

The following condition for the determinant is also needed in the remaining part study.

(A6)

$$\begin{vmatrix} \frac{\partial(\mathscr{S}_1(\omega,\zeta_1^0,\zeta_2^0,...,\zeta_{j-1}^0,\zeta_{j+1}^0,...,\zeta_n^0,0))}{\partial\mathscr{T}} & \cdots & \frac{\partial(\mathscr{S}_1(\omega,\zeta_1^0,\zeta_2^0,...,\zeta_{j-1}^0,\zeta_{j+1}^0,...,\zeta_n^0,0))}{\partial\zeta_n} \\ \frac{\partial(\mathscr{S}_2(\omega,\zeta_1^0,\zeta_2^0,...,\zeta_{j-1}^0,\zeta_{j+1}^0,...,\zeta_n^0,0))}{\partial\mathscr{T}} & \cdots & \frac{\partial(\mathscr{S}_2(\omega,\zeta_1^0,\zeta_2^0,...,\zeta_{j-1}^0,\zeta_{j+1}^0,...,\zeta_n^0,0))}{\partial\zeta_n} \\ \vdots & \ddots & \vdots \\ \frac{\partial(\mathscr{S}_n(\omega,\zeta_1^0,\zeta_2^0,...,\zeta_{j-1}^0,\zeta_{j+1}^0,...,\zeta_n^0,0))}{\partial\mathscr{T}} & \cdots & \frac{\partial(\mathscr{S}_n(\omega,\zeta_1^0,\zeta_2^0,...,\zeta_{j-1}^0,\zeta_{j+1}^0,...,\zeta_n^0,0))}{\partial\zeta_n} \end{vmatrix} \neq 0 \quad (3.59)$$

Theorem 4 *Assume that condition* $(A6)$ *is valid. Then, (3.57) admits a non-trivial periodic solution, which converges in the* $B-$ *topology to the non-trivial* ω*-periodic solution of (3.57) as* μ *tends to zero.*

We will present the following examples to realize our theoretical results.

Example 5 *In this example, we will consider the perturbed system in case the generating system has a graziness. To show that, let us take into account the following perturbed system*

$$\begin{aligned} x_1' &= x_2, \\ x_2' &= -0.001x_2 - x_1, \\ \Delta x_2|_{x\in\Gamma_1} &= -(1 + R_1x_2 + \mu x_2)x_2, \\ \Delta x_2|_{x\in\Gamma_2} &= -(1 + R_2 + \mu(x_2 - \exp(0.001\pi/2))x_2. \end{aligned} \quad (3.60)$$

It is easy to see that the system (3.60) is of the form (3.57). For $\mu = 0$*, the generating system became (3.14). For the perturbed system (3.60), we will investigate existence of the periodic solution around the grazing periodic solution of (3.14) with the help of Theorem 4.*

There are two sorts of possible periodic solutions of (3.60) around the grazing one. One of them has two impulse moments during the period since it crosses both lines of discontinuity, i.e. $x_1 = 0$ *and* $x_1 = \exp(0.00025\pi)$*. The other sort is the periodic solution which does not intersect the line* $x_1 = \exp(0.00025\pi)$ *and intersects the line* $x_1 = 0$*. We will show the existence of both type of periodic solutions if* $|\mu|$ *sufficiently small.*

Let us start with the second type, assume that the solution for the perturbed system exists and it starts at the point $(0, x_{02}), x_{02} < 1$ *and does not intersect the line* $x_1 =$

$\exp(0.00025\pi)$. *Denote the initial values of the periodic solution by* ζ_1 *and* ζ_2. *Since the periodic solution necessarily intersects the line* $x_1 = 0$, *one can choose* $\zeta_1 \equiv \zeta_1^0 = 0$. *By specifying the formula in* (3.58) *for the system* (3.60), *it is easy to obtain the following expressions*

$$\begin{aligned} \mathscr{S}_1(\mathscr{T}, 0, \zeta_2, \mu) &= x_1(\mathscr{T}, 0, \zeta_2, \mu) = 0, \\ \mathscr{S}_2(\mathscr{T}, 0, \zeta_2, \mu) &= x_2(\mathscr{T}, 0, \zeta_2, \mu) - \zeta_2 = 0. \end{aligned} \tag{3.61}$$

Next, taking the derivative of the expressions in (3.61), *we can obtain the following*

$$\begin{vmatrix} \frac{\partial(\mathscr{S}_1(\mathscr{T},0,\zeta_2,\mu))}{\partial\mathscr{T}} & \frac{\partial(\mathscr{S}_1(\mathscr{T},0,\zeta_2,\mu))}{\partial\zeta_2} \\ \frac{\partial(\mathscr{S}_2(\mathscr{T},0,\zeta_2,\mu))}{\partial\mathscr{T}} & \frac{\partial(\mathscr{S}_2(\mathscr{T},0,\zeta_2,\mu))}{\partial\zeta_2} \end{vmatrix} = \begin{vmatrix} \frac{\partial x_1(\omega,0,\zeta_2^0,0)}{\partial\mathscr{T}} & \frac{\partial x_1(\omega,0,\zeta_2^0,0)}{\partial\zeta_2} \\ \frac{\partial x_2(\omega,0,\zeta_2^0,0)}{\partial\mathscr{T}} & \frac{\partial x_2(\omega,0,\zeta_2^0,0)}{\partial\zeta_2} - 1 \end{vmatrix}. \tag{3.62}$$

The determinant (3.62) *is calculated by means of the monodromy matrix of (3.14), with the impulse matrix* $D_1^{(1)} = O_2$, *i.e.*

$$\begin{bmatrix} 1 & -0.0317 \\ 1.0158 & -0.1014 \end{bmatrix}. \tag{3.63}$$

Taking into account the system (3.66) *with* (3.63) *at* $\zeta_2 = \zeta_2^0$ *and* $\mathscr{T} = \omega$ *for* $\mu = 0$, *one can derive that*

$$\begin{vmatrix} \frac{\partial\mathscr{S}_1(\omega,0,\zeta_2^0,0)}{\partial\mathscr{T}} & \frac{\partial\mathscr{S}_1(\omega,0,\zeta_2^0,0)}{\partial\zeta_2} \\ \frac{\partial\mathscr{S}_2(\omega,0,\zeta_2^0,0)}{\partial\mathscr{T}} & \frac{\partial\mathscr{S}_2(\omega,0,\zeta_2^0,0)}{\partial\zeta_2} - 1 \end{vmatrix} = -0.0317\exp(0.00025\pi) \neq 0. \tag{3.64}$$

This verifies condition $(A6)$. *Thus, condition* $(A6)$ *is valid, then by utilizing Theorem* (4), *we can assert that the system (3.57) admits a non-trivial periodic solution, which converges in the* $B-$ *topology to the non-trivial* ω*-periodic solution of (3.1) as* μ *tends to zero.*

Now, let us verify that system (3.60) has a circle which intersects the line $x_1 = \exp(0.00025\pi)$ *in the neighborhood of* $(\exp(0.00025\pi), 0)$. *So, the periodic solution will attain two discontinuity moments in a period. Denote the initial values of*

the periodic solution by ζ_1 *and* ζ_2*. To apply the condition* $(A6)$*, fix one initial value* $\zeta_1 = \zeta_1^0 = 0$ *of the intended periodic solution and in the light of the expressions* (3.58)

$$\begin{aligned} \mathscr{S}_1(\mathscr{T}, 0, \zeta_2, \mu) &= x_1(\mathscr{T}, 0, \zeta_2, \mu) = 0, \\ \mathscr{S}_2(\mathscr{T}, 0, \zeta_2, \mu) &= x_2(\mathscr{T}, 0, \zeta_2, \mu) - \zeta_2 = 0. \end{aligned} \tag{3.65}$$

Taking the derivative of the expressions (3.65) *with respect to variables* $\mathscr{T}$ *and* ζ_2*, one can obtain the following*

$$\begin{vmatrix} \frac{\partial(\mathscr{S}_2(\mathscr{T},0,\zeta_2,\mu))}{\partial \mathscr{T}} & \frac{\partial(\mathscr{S}_1(\mathscr{T},0,\zeta_2,\mu))}{\partial \zeta_2} \\ \frac{\partial(\mathscr{S}_2(\mathscr{T},0,\zeta_2,\mu))}{\partial \mathscr{T}} & \frac{\partial(\mathscr{S}_2(\mathscr{T},0,\zeta_2,\mu))}{\partial \zeta_2} \end{vmatrix} = \begin{vmatrix} \frac{\partial x_1(\omega,0,\zeta_2^0,0)}{\partial \mathscr{T}} & \frac{\partial x_1(\omega,0,\zeta_2^0,0)}{\partial \zeta_2} \\ \frac{\partial x_2(\omega,0,\zeta_2^0,0)}{\partial \mathscr{T}} & \frac{\partial x_2(\omega,0,\zeta_2^0,0)}{\partial \zeta_2} - 1 \end{vmatrix}. \tag{3.66}$$

To determine the above determinant, the monodromy matrix of (3.13) with the jump matrix $D_i^{(2)}$ *can be evaluated as*

$$\begin{bmatrix} 1 & 0.01 \\ 0 & 0.704 \end{bmatrix}. \tag{3.67}$$

For $\mu = 0$*, with the values* ω *and* ζ_2^0 *the determinant* (3.66) *can be determined as*

$$\begin{aligned} &\begin{vmatrix} \frac{\partial(\mathscr{S}_1(\omega,0,\zeta_2^0,0))}{\partial \mathscr{T}} & \frac{\partial(\mathscr{S}_1(\omega,0,\zeta_2^0,0))}{\partial \zeta_2} \\ \frac{\partial(\mathscr{S}_2(\omega,0,\zeta_2^0,0))}{\partial \mathscr{T}} & \frac{\partial(\mathscr{S}_2(\omega,0,\zeta_2^0,0))}{\partial \zeta_2} \end{vmatrix} = \begin{vmatrix} 0 & 0.01 \\ -\exp(0.00025\pi) & -0.296 \end{vmatrix} \\ &= 0.01\exp(25.10^{-5}\pi) \neq 0. \end{aligned} \tag{3.68}$$

This verifies condition $(A6)$*. So, By Theorem 4, we can conclude that the perturbed system* (3.60) *admits a non-trivial* $\mathscr{T}(\mu)-$ *periodic solution which converges in the* $B-$ *topology to the non-trivial* ω*-periodic solution of (3.14) as* μ *tends to zero such that* $\mathscr{T}(0) = \omega$*.*

In Fig. 3.7, some numerical results are provided to show the solutions of system (3.60) with $\mu = 0.05$*.*

The periodic solutions for $\mu \neq 0$ *are not grazing. For* $\mu = 0$*, we have one periodic solution which is orbitally stable, and for* $\mu < 0$*, there exist two periodic solutions.*

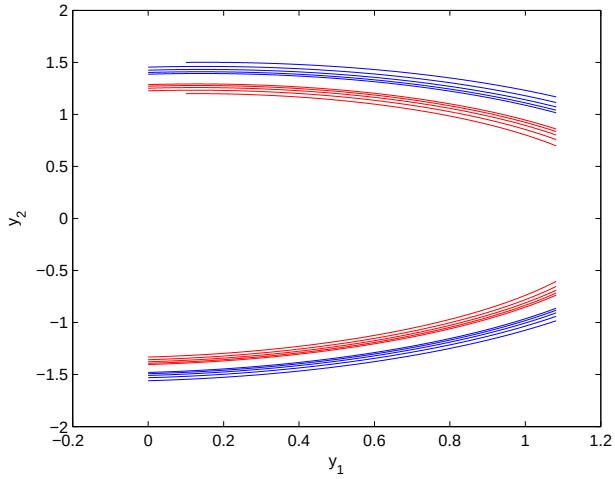

Figure 3.7: The red arcs are the trajectory of the system (3.60) with initial value $(0, 1.2)$ and the blue arcs are the orbit with initial value $(0, 1.5)$. Through simulation, we observe that the trajectories approach to the periodic solution of (3.60) as time increases.

One of them has one discontinuity moment in each period, in other words, the cycle does not intersect the surface of discontinuity around grazing point and it is orbitally stable and the other one has two discontinuity moments in each period. This means, the number of periodic solutions increases by variation of μ, around $\mu = 0$. So, we will call that bifurcation of periodic solution from a grazing cycle.

Example 6 *Let us consider the following system with variable moments of impulses and a small parameter*

$$\begin{aligned} x_1' &= x_2, \\ x_2' &= -0.0001[x_2^2 + (x_1 - 1)^2 - (1 + \mu)^2]x_2 - x_1 + 1, \\ \Delta x_2|_{x\in\Gamma} &= -(1 + Rx_2 + \mu x_2^3)x_2 + \mu^2, \end{aligned} \tag{3.69}$$

where $R = 0.9$ and $\Gamma = \{x | x_1 = 0, x_2 \leq 0\}$. It is easy to see that system (3.69) is of the form (3.57) and $\Phi(x_1, x_2) = x_1 = 0$. The system has a periodic solution

$$\Psi_\mu(t) = (1 + (1 + \mu)\cos(t), -(1 + \mu)\sin(t)), \tag{3.70}$$

where $t \in \mathbb{R}$ for $\mu \in (-2, 0]$.

The generating system of (3.69) has the following form

$$\begin{aligned} x_1' &= x_2, \\ x_2' &= -0.0001[x_2^2 + (x_1 - 1)^2 - 1]x_2 - x_1 + 1, \\ \Delta x_2|_{x\in\Gamma} &= -(1 + Rx_2)x_2, \end{aligned} \tag{3.71}$$

and admits the periodic solution $\Psi_0(t) = (1 + \cos(t), -\sin(t))$. *By means of the equality* $\langle \nabla\Phi(x^*), f(x^*)\rangle = \langle (1,0),(0,1)\rangle = 0$ *with* $x^* = (0,0) \in \partial\Gamma$, *it is easy to say that* x^* *is a grazing point of* $\Psi_0(t)$.

Let us start with the linearization of system (3.71) *around the periodic solution* $\Psi_0(t)$. *Consider a near solution* $y(t) = y(t, 0, y^* + \Delta y)$, *where* $\Delta y = (\Delta y_1, \Delta y_2)$, *to the periodic solution* $\Psi_0(t)$. *Assume that* $y(t)$ *satisfies condition* $(N1)$, *and it meets the surface of discontinuity* Γ *at the moment* $t = \xi$ *and at the point* $\bar{y} = y(\xi, 0, y^* + \Delta y)$. *Considering the formula* (3.10) *for the transversal point* $\bar{y} = (\bar{y}_1, \bar{y}_2)$, *the first component* $\dfrac{\partial\tau(\bar{y})}{\partial y_1^0}$ *can be evaluated as* $\dfrac{\partial\tau(\bar{y})}{\partial y_1^0} = -\dfrac{1}{\bar{y}_2}$. *From the last equality, the singularity is seen at the grazing point. By taking into account* (3.17) *with* (3.71) *and* $\dfrac{\partial\tau(\bar{y})}{\partial y_1^0}$, *we obtain that*

$$\frac{\partial W_i(\bar{y})}{\partial y_1^0} = \begin{bmatrix} R\bar{y}_2 - 1 \\ -10^{-4}R[(-\bar{y}_2^2 + (\bar{y}_1 - 1)^2 - 1) - 2(((\bar{y}_1 - 1)^2 - 1))] \end{bmatrix}. \tag{3.72}$$

Similarly, taking into account the formula (3.22), *one can evaluate that*

$$\frac{\partial\tau(\bar{y})}{\partial y_2^0} = 0.$$

This and formula (3.23) *imply*

$$\frac{\partial W_i(\bar{y})}{\partial y_2^0} = \begin{bmatrix} 0 \\ -2R\bar{y}_2 \end{bmatrix}. \tag{3.73}$$

Joining (3.72) *and* (3.73), *the matrix* $W_{iy}(\bar{y})$ *can be obtained as*

$$W_{iy}(\bar{y}) = \begin{bmatrix} R\bar{y}_2 - 1 & 0 \\ -0.0003R(\bar{y}_2^2 + (\bar{y}_1 - 1)^2 - 1) & -2R\bar{y}_2 \end{bmatrix}. \tag{3.74}$$

The last expression implies continuity of the partial derivatives near the grazing point. This validates condition $(A2)$.

Then, evaluating the matrix in (3.74) *at* $\bar{y} = y^* = (0, 0)$, *it is easy to obtain*

$$W_{iy}(y^*) = \begin{bmatrix} -1 & 0 \\ 0.0003R & 0 \end{bmatrix}, \tag{3.75}$$

and

$$B_i = \begin{cases} \begin{bmatrix} -1 & 0 \\ 0.0003R & 0 \end{bmatrix}, & \text{if} \quad (N1) \text{ is valid,} \\ O_2, & \text{if} \quad (N2) \text{ is valid.} \end{cases} \tag{3.76}$$

To verify condition $(A3)$, *let us specify the region*

$$H = \{(y_1, y_2) | y_2 < \sqrt{1 - (y_1 - 1)^2},\ 0 \leq y_1 \leq 1\}.$$

For the grazing solution $\Psi_0(t)$, *we have that* $\theta_{i+1} - \theta_i = 2\pi$. *Consider a near solution* $y(t) = (y_1(t), y_2(t)) = y(t, 0, \bar{y})$ *to* $\Psi(t)$. *To satisfy the condition* $(N1)$, *take* $\bar{y} = (\bar{y}_1, \bar{y}_2) \in H$. *The orbit of* $y(t)$ *is below the grazing orbit. Fix points* $y = (y_1, y_2) \in H$ *and* $\psi = (\psi_1, \psi_2)$ *of the orbits* $y(t)$ *and* $\Psi_0(t)$, *respectively such that* $0 \leq y_1 = \psi_1 \leq 1$ *and* $\psi_2 < 0$. *Since of the equation* $y_1' = y_2$, *the speed of* $y_1(t)$ *at* (y_1, y_2) *is larger than the speed of* $\Psi_1(t)$ *at* (ψ_1, ψ_2). *Consequently, one can find that* $\tau(y) \leq \frac{\pi}{4} < 2\pi$ *for* $y \in H$. *Thus, the condition* $(A3)$ *is valid and Lemma 1 verifies the condition* (C).

It is easy to demonstrate that the condition $(A4)$ *is valid such that near solutions to the grazing one are either continuous or discontinuous. That is, they don't intersect the line of discontinuity* Γ *or intersect it permanently near to the grazing point and by means of the formula* (3.76), *the linearization system for* (3.71) *around the grazing cycle* $\Psi_0(t)$ *consists of the following two subsystems*

$$\begin{aligned} u_1' &= u_2, \\ u_2' &= -0.0001 \sin(2t) u_1 + 0.0002 \sin^2(t) u_2, \end{aligned} \tag{3.77}$$

and

$$\begin{aligned} u_1' &= u_2, \\ u_2' &= -0.0001\sin(2t)u_1 + 0.0002\sin^2(t)u_2, \\ \Delta u|_{2\pi i} &= \begin{bmatrix} -1 & 0 \\ 0.0003R & 0 \end{bmatrix} u. \end{aligned} \tag{3.78}$$

The system (3.77) + (3.78) *is* $(2\pi, 1)$ *periodic. The Floquet multipliers of system* (3.77) + (3.78) *are* $\rho_1^{(1)} = 1$, $\rho_2^{(1)} = 0.939$, $\rho_1^{(2)} = 1$, $\rho_2^{(2)} = 0.912$. *Thus, condition* $(A5)$ *is validated. Moreover, the conditions* $(C1) - (C7)$ *and* $(A1), (A2)$ *can be verified utilizing similar way presented in Example 1. Consequently, Theorem 3 authenticates that the grazing periodic solution (cycle),* $\Psi_0(t)$ *of the system* (3.71) *is orbitally stable. The simulation results demonstrating the orbital stability of* $\Psi_0(t)$ *are depicted in Figure 3.8.*

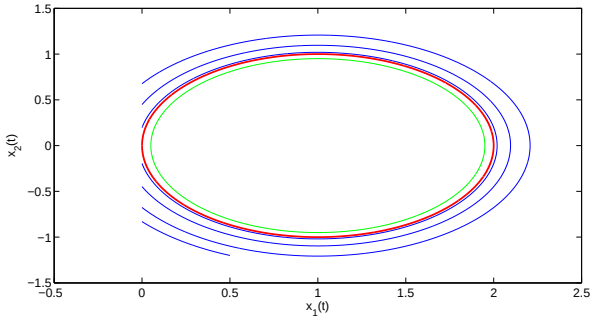

Figure 3.8: The grazing cycle of system (3.71) is in red. The blue arcs are the trajectory of the system with initial point $(0.5, 1.2)$ and the green continuous orbit is with initial value $(0.1, 0)$. They demonstrate stability of the grazing solution.

Next, we will investigate two sorts of periodic solutions of system (3.69) with a period $\mathscr{T}$ *near to* 2π. *The first one is continuous and the second admits discontinuities once on a period. For those solutions, corresponding linearization systems around the grazing cycle* $\Psi_0(t)$ *are* (3.77) *and* (3.78)*, respectively. Let us start with the continuous periodic solutions of (3.69). For continuous periodic solution, we will consider the linearization system* (3.77).

To apply Theorem 4, denote $\Psi_0(0) = (\zeta_1^0, 0)$. *That is, consider* $\zeta_2^0 = 0$. *Then, applying the above discussion, obtain that the Poincarè condition admits the form of the*

following equations,

$$\begin{aligned}\mathscr{S}_1(\mathscr{T},\zeta_1,\mu) &= x_1(\mathscr{T},\zeta_1,\mu) - x_1 = 0,\\ \mathscr{S}_2(\mathscr{T},\zeta_1,\mu) &= x_2(\mathscr{T},\zeta_1,\mu) = 0.\end{aligned} \tag{3.79}$$

Because solutions of the system (3.71) *have continuous derivatives with respect to the time, phase variables and parameters, we can calculate the following determinant*

$$\begin{vmatrix} \dfrac{\partial \mathscr{S}_1(\omega,\zeta_1^0,0)}{\partial \mathscr{T}} & \dfrac{\partial \mathscr{S}_1(\omega,\zeta_1^0,0)}{\partial x_1^0} \\ \dfrac{\partial \mathscr{S}_2(\omega,\zeta_1^0,0)}{\partial \mathscr{T}} & \dfrac{\partial \mathscr{S}_2(\omega,\zeta_1^0,0)}{\partial x_1^0} \end{vmatrix}. \tag{3.80}$$

First, we need the monodromy matrix of the system (3.77)*. It is*

$$\begin{bmatrix} 0.939 & -0.0001407 \\ -0.0003165 & 1 \end{bmatrix}. \tag{3.81}$$

It is easy to see that first column of the determinant (3.80) is computed by utilizing (3.71) and the second column is evaluated by means of the first column of the matrix (3.81). From this discussion, one can obtain that the determinant (3.80) *is equal to*

$$\begin{vmatrix} 0 & -0.061 \\ 1 & -0.0003165 \end{vmatrix} = 0.061 \neq 0. \tag{3.82}$$

Thus, in the light of Theorem 4, we can conclude that for sufficiently small $|\mu|$ *there exists a unique periodic solution of the system*

$$\begin{aligned} x_1' &= x_2,\\ x_2' &= -0.0001[x_2^2 + (x_1-1)^2 - (1+\mu)^2]x_2 - x_1 + 1. \end{aligned} \tag{3.83}$$

It is exactly the cycle (3.70) with a period $\mathscr{T} = 2\pi$*. If* $\mu < 0$*, the solution is separated from the set* Γ*. Consequently, it is a periodic continuous solution of the equation (3.69). It is orbitally stable by the theorem for continuous dynamics [30], since of the continuous dependence of multipliers on the parameter. The function* $\Psi_\mu(t), \mu > 0$*, intersects* Γ *and can not be a solution of equation (3.69). Thus, the system does not admit a continuous periodic solution near to* $\Psi_0(t)$*, if the parameter is positive.*

Considering those solutions which have one moment of discontinuity in a period, one can find that the corresponding linearization of $\Psi_0(t)$ *is the system* (3.78).

The monodromy matrix of (3.78) *can be evaluated as*

$$\begin{bmatrix} 0.939 & -0.00052 \\ -0.000427 & 1 \end{bmatrix}. \tag{3.84}$$

It can be easily observed that the discontinuous solution intersects the line $x_1 = 0$. *For this reason, one can specify the first coordinate of the initial value as* $\zeta_1 = \zeta_1^0 \equiv 0$. *In the light of these discussions and the formula* (3.58)*, the following equations are obtained:*

$$\begin{aligned} \mathscr{S}_1(\mathscr{T}, 0, \zeta_2, \mu) &= x_1(\mathscr{T}, 0, \zeta_2, \mu) = 0, \\ \mathscr{S}_2(\mathscr{T}, 0, \zeta_2, \mu) &= x_2(\mathscr{T}, 0, \zeta_2, \mu) - \zeta_2 = 0. \end{aligned} \tag{3.85}$$

Then, taking the derivative of the system (3.85) *with respect to* $\mathscr{T}$ *and* ζ_2*, and calculating it at* $\mathscr{T} = \omega$, $\zeta_2 = \zeta_2^0 = 0$, *and for* $\mu = 0$, *the following determinant is obtained*

$$\begin{vmatrix} \dfrac{\partial \mathscr{S}_1(\omega, 0, \zeta_2^0, 0)}{\partial \mathscr{T}} & \dfrac{\partial \mathscr{S}_1(\omega, 0, \zeta_2^0, 0)}{\partial \zeta_2} \\ \dfrac{\partial \mathscr{S}_2(\omega, 0, \zeta_2^0, 0)}{\partial \mathscr{T}} & \dfrac{\partial \mathscr{S}_2(\omega, 0, \zeta_2^0, 0)}{\partial \zeta_2} \end{vmatrix} = \begin{vmatrix} 0 & -0.0006 \\ 1 & 0.0009 \end{vmatrix} = -0.0006 \neq 0. \tag{3.86}$$

Thus, condition $(A6)$ *holds. Then, utilizing Theorem 4, it is easy to conclude that for sufficiently small* μ *there exists a unique periodic solution of the system (3.69) with a period* $\approx 2\pi$. *It is true that for positive as well as negative* μ. *Moreover, these solutions are orbitally asymptotically stable because of the continuous dependence of solutions on parameter and initial values and they meet the discontinuity line transversally.*

For each fixed $\mu \neq 0$, *solutions near to the periodic ones intersect the line of discontinuity* Γ *transversally once during the time approximately equal to the period. That is, the smoothness which is requested for the application of the Poincarè condition is valid, since the smoothness for the grazing point has already been verified. It is clear that there can not be another solutions with period close to* 2π. *Thus, one can make the following conclusion. The original system (3.69) admits two orbitally stable periodic solutions, continuous and discontinuous, if* $\mu < 0$. *There is a single orbitally stable continuous solution (grazing) if* $\mu = 0$. *Additionally, there is a unique*

discontinuous orbitally stable periodic solution for positive values of the parameter. Consequently, grazing bifurcation of cycles appears for the system with small parameter.

We have obtained regular behavior in dynamics near grazing orbits by Poincarè small parameter analysis. Nevertheless, outside the attractors irregular phenomena may be observed.

In Figure 3.9, the solutions of the system (3.69) with parameter $\mu = -0.2$ *are depicted through simulations. The red arcs are the trajectory of the system (3.69) with initial value* $(0.7, 0.05)$ *and the blue arcs are the trajectory of the system (3.69) with initial value* $(0.4, 0.05)$*. It is seen that both red and blue trajectories approach the discontinuous periodic solution of (3.69), as time increases. So, the discontinuous cycle is orbitally stable trajectory. Moreover, the green one is a continuous periodic trajectory of (3.69) with initial value* $(0, 0.05)$ *and it is orbitally asymptotically stable. To sum up, there exists two periodic solutions of (3.69) for the parameter* $\mu = -0.2$*, one is continuous, the other one is discontinuous and both solutions are orbitally asymptotically stable.*

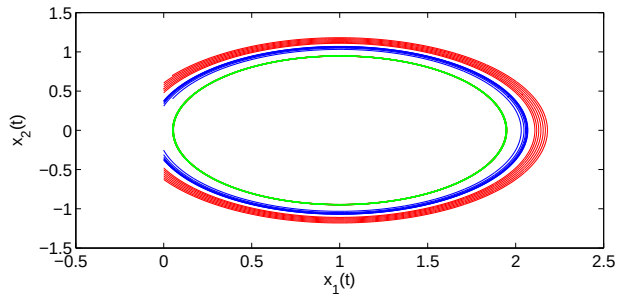

Figure 3.9: The blue, red and green arcs constitute the trajectories of system (3.69) with $\mu = -0.2$. The first two approach as time increases to the discontinuous limit cycle and the third one is the continuous limit cycle itself.

In Fig. 3.10, the red arcs are the orbit of the system with initial value $(0, 0.1)$ *and the blue arcs are the trajectory of it with initial value* $(0, 0.4)$*. Both trajectories approach to the discontinuous cycle of system (3.69), as time increases. Thus, Fig. 3.10 illustrates the existence of the orbitally stable discontinuous periodic solution if* $\mu = 0.2$*.*

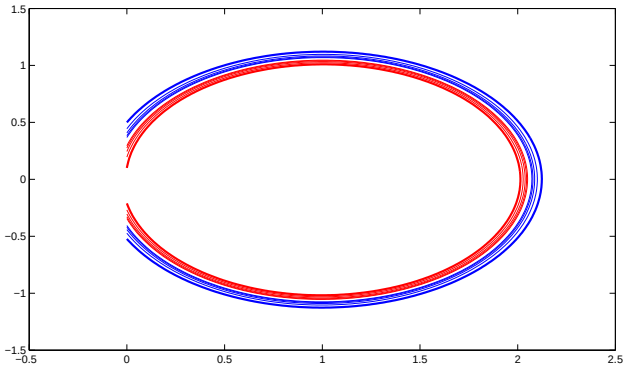

Figure 3.10: The red and blue arcs constitute the trajectories of the system (3.69) with $\mu = 0.2$. Both orbits approach to the discontinuous limit cycle, as time increases.

3.6 Conclusion

In literature, the dynamics in the neighborhood of the grazing points [19, 25, 31, 33, 34, 39, 40] is generally analyzed through maps of the Poincaré type. The main analysis is conducted on complex dynamics behavior such as chaos and bifurcation [19, 25, 31, 33, 34, 39]. However, there is still no sufficient conditions for the discontinuous motion to admit main features of dynamical systems : the group property, continuous and differentiable dependence on initial data and continuation of motions, which are useful for both local and global analysis. Variational systems for grazing solutions have not been considered in general as well as orbital stability theorem and regular perturbation theory around cycles, despite, particular cases can be found in specialized papers. See, for example, [20]. To investigate these problems in the present study, we have applied the method of $B-$ equivalence and results on discontinuous dynamics developed and summarized in [5]. In our analysis the grazing singularity is observed through the gradient of the time function $\tau(x)$, since some of its coordinates are infinite. We have found the components of the discontinuous dynamical system that is the vector field, surfaces of discontinuity and the equations of jump such that interacting they neutralize the effect of singularity. Then, we linearize the system at the grazing moments and this brings the dynamics to regular analysis and make suitable for the application. By means of the linearization, the theory can be understood as a part of the general theory of discontinuous dynamical system. Thus, we have considered grazing phenomena as a subject of the general theory of

discontinuous dynamical systems [5], discovered a partition of set of solutions near grazing solution such that we determine linearization around a grazing solution is a collection of several linear impulsive systems with fixed moments of impulses. This constitutes the main novelty of the present study. To linearize a solution around the grazing one, a system from the collection is to be utilized. This result has been applied to prove the orbital stability theorem. The way of analysis in [2, 3, 5] continues in the present study and it admits all attributes which are proper for continuous dynamics [30]. That is why, we believe that the method can be extended for introduction and research of graziness in other types of dynamics such as partial and functional differential equations and others. Next, we plan to apply the present results and the method of investigation for problems initiated in [19, 31, 33, 34].

3.6.1 An example: Van der Pol oscillators generated from grazing dynamics

In this example, we take into account two coupled Van der Pol equations with impacts. The main novelty is that the degenerated system for the model admits an oscillation with zero impact velocity. To prove presence of oscillations, beside the perturbation method, the newly developed linearization for dynamics with grazing has been applied. As different from the theoretical results such as Nordmark mapping and Zero time discontinuity mapping, the grazing is examined through another method of discontinuous dynamics, which diminishes the role of mappings in the analysis. The rich diversity of changes in the dynamics is observed under regular perturbations, since of the grazing discontinuity. By means of the simulation results, the analytical studies are visualized.

Van der Pol oscillator has been found many applications in biology [38], electronics and mechanics [8]. Van der Pol oscillator is used to model the vacuum tube circuits in the early stages of the electronics technology. Van der Pol and his coworkers analyzed the electrical circuits inserting vacuum tubes and they determined limit cycles of them. Moreover, the output of the system became a cycle with the frequency of the applied signal when a signal is applied to these circuits with frequency near to that of the limit cycle. Such phenomenon give a rise to the entrainment of the cycle with the signal. He developed various types of electronic circuit models for the investigation

of the heart dynamics and the external applied signal is found to be as an analogous to the situation that the heart is driven with a peacemaker. He was seeking to stabilize the irregular beatings of the heart by means of his entrainment study. The Van der Pol oscillator can be seen as a impact oscillator with a non-linear damping force. In literature, a wide ranges of works have been conducted on it. In [38], the qualitative analysis for the existence and non-existence of periodic solution of the oscillator has been investigated. By applying numerical methods, the cycles of the oscillator has been examined [84, 121]. In the paper [8], the limit cycles for the impacting Van der Pol oscillator has been obtained. By applying the generalized eigenvalue method, the stability of it is determined analytically.

In this study, the degenerated system is uncoupled which consists of a harmonic and Van der Pol oscillators. The harmonic oscillator has a grazing cycle which is orbitally stable from outside and stable from inside and the Van der Pol has a stable focus. The perturbed system contains two coupled Van der Pol oscillators. It is proved that this system admits a discontinuous torus which is considered as a Cartesian product of one continuous and discontinuous cycles. Then, it is called bifurcation of discontinuous torus.

We want to show how the results, derived in [6], are efficient for the analysis of the regular dynamics around the grazing cycle of the impacting Van der Pol oscillators. In the light of the theoretical results of the paper, we will investigate the grazing in the degenerated oscillators, and the persistence of the stable cycle under regular perturbation. We consider a *harmonic oscillator with impacts* as a degenerated one for the Van der Pol oscillator. That is, the degenerated oscillator *is not* a Van der Pol oscillator. The system, which we will analyze in this study, has the nonlinearities in both the vector field and the jump function. By applying newly developed linearization and perturbation theory, the orbital stability in the system of coupled Van der Pol oscillators have been examined.

In [38], the Van der Pol oscillator has been considered as a perturbed *harmonic oscillator*. For that, by applying averaging method, an approximate periodic solution of the oscillator has been obtained analytically. Moreover, by applying Dulac's criterion, it has been determined that there exists no periodic solution in the region $|x_1| < 1$. In

this study, by considering deformable surfaces and the velocity dependent coefficient of restitution and by utilizing the theories which are initiated in [6], the existence of the orbitally stable discontinuous cycle of the oscillator inside the region is obtained.

It is hard to analyze the cycles of the systems with grazing points since of the singularity in the Poincare mapping. In the literature, in order to analyze these systems, some different methods are applied such as Nordmark mapping [97] and other types of mappings [33, 31]. These mappings are made up of the composition of several discrete or continuous motions. In this investigation, we have proposed a method, which was presented in [5], converts systems with variable moments to those with fixed moments by preserving dynamical properties of the original system. There is a huge difference between these two approaches, because by applying the method, B-equivalent method, the role of mappings are diminished in the analysis and it indicates that how the method is efficient for the analysis and makes the investigations close to the existing theory of differential equations with impulses and ordinary differential equations. In our concern, science develops in various directions and by different methods. The strength of science is determined by the diversity of methods. For this reason, besides the methods realized in [31, 98], the application of B-equivalent method, which converts the differential equations with variable moments of impulses to those with fixed moment by saving dynamical properties of the original ones, has to be also realized to enrich the analysis and results for the grazing phenomenon.

In such papers [31, 33, 34, 97, 98], generally the complex behavior around the grazing solution or grazing points investigated. The way of study for the grazing is far more different in many senses from that ones in the literature because the aim of the present study is to find regular behaviors around it. The results, which are based on the linearization technique around grazing solutions, are fully analogues to the existing results in ordinary differential equations [38]. Until now, the theories obtained for differential equations [5] with impulses is very analogues to that for ordinary differential equations and in this study and the papers [6], some sufficient conditions, which proceed the existing results of impulsive system, are obtained for the systems with grazing.

Earlier, [6], we have considered discontinuous dynamics with grazing points. Some

sufficient conditions are obtained to define a discontinuous flow. Orbital stability definition is considered for those systems and orbital stability theorem is proved for the systems with grazing. In the literature, it is first time that orbital stability theorem is taken into account for discontinuous dynamics with grazing. Then, by applying regular perturbation [85] to the system, the orbitally stable oscillation for the model is examined. The aim of the present study is to show the applicability of the results, [6]. The approach of this study is different in many aspects from those in the literature, because the singularity, which is caused by the grazing, is suppressed in the system by harmonizing the vector field, the surface of discontinuity and the jump function. This allows us to consider the dynamics with grazing as a regular one. In the literature, the grazing is investigated through mapping approach and in this study, by utilizing special linearization technique the role of mapping is eliminated in the analysis. Also, it is a seminal study that the Van der Pol equation is taken into account with the grazing.

This study is devoted to show the existence of orbitally stable discontinuous cycle of the following perturbed system

$$\begin{aligned} &x'' + \mu(1-x^2)x' + x = 0, \\ &y'' + a(1-y^2)y' + y + \mu x = 0, \\ &\Delta x'|_{x\in\Gamma_\mu} = -(1+Rx')x', \end{aligned} \tag{3.87}$$

where $'$ stands for the derivative with respect to time, Γ_μ is the surface of discontinuity which is defined by $\Gamma_\mu = \{(x, x', y, y')|x = 1-\mu, \mu > 0\}$, the coefficient a is a positive constant and R is the coefficient of restitution. It is seen that the system (3.87) contains coupled Van der Pol oscillators.

The technique, which was developed in the paper [6], will be used in the present study. For models with impacts in the literature, the scientists generally formalize the jump equation by means of the Newton's coefficient of restitution which varies between zero and unity. That is, $x'_+ = -Rx'_-$, where x'_- and x'_+, denote the velocity before and after an impact, respectively. In this study, the coefficient of restitution will be taken into account as variable, in other words we will consider a velocity dependent coefficient of restitution. Many researches [56, 89, 110] have been conducted on the variable coefficient of restitution. In [89], the velocity dependent coefficient of restitution is analyzed through simulations and in [116], some experimental results

are obtained. The relation between the restitution and impact velocity is depicted for two different models in [60]. It is exhibited in [56] that the restitution coefficient is not constant at each cycle and every test. In this study, the impact function is considered as velocity dependent, the idea behind this is carefully analyzed in the paper [9].

The degenerated system for (3.87) is

$$\begin{aligned} &x'' + x = 0, \\ &y'' + a(1-y^2)y' + y = 0, \\ &\Delta x'|_{x\in\Gamma_0} = -(1+Rx')x'. \end{aligned} \tag{3.88}$$

It consists of the following two uncoupled oscillators

$$\begin{aligned} &x'' + x = 0, \\ &\Delta x'|_{x=1} = -(1+Rx')x', \end{aligned} \tag{3.89}$$

and

$$y'' + a(1-y^2)y' + y = 0. \tag{3.90}$$

The first equation is a harmonic oscillator with impacts and the second one is a Van der Pol oscillator. It is easy to demonstrate that $\Psi_1(t) = \cos(t)$ is a periodic solution of (3.89). The importance of the present research is connected to a difficulty in the analysis of the degenerated system, since the cycle is a *grazing* one.

Due to the fact that the linearization technique for the grazing oscillators has not been developed properly, yet, there are difficulties in the perturbation method. In the paper [6], a linearization system with two compartments is obtained for the grazing cycles of discontinuous dynamical system. In that paper, some sufficient conditions for the orbital stability and regular perturbations for the grazing cycle of those systems are presented. This study aims to show how these results are applicable and efficient for the discontinuous dynamics.

In the remainder, a perturbed system is taken into account as a couple of two Van der Pol equations. A harmonic oscillator with impacts is considered as a generating model. For that system, it is verified that there is a continuous grazing plane cycle and by applying linearization technique, developed in [6], it is demonstrated that the cycle is orbitally stable from outside and stable from inside. Then, by utilizing the

small parameter, the system (3.87) is obtained as two Van der Pol oscillators which are connected unilaterally. For this system, we obtain a discontinuous torus as a Cartesian product of two cycles, discontinuous and continuous ones. Moreover, it is approved that the cycle is orbitally stable with continuous and discontinuous coordinates such that if one interpret Cartesian product of two cycles as torus, we can formulate the main result as a bifurcation of a discontinuous torus. We would like to emphasize on as a particular result of the present study which concerns the oscillator (3.89). It is proved that it admits a unique continuous cycle which is stable. However, when it is perturbed, the generated oscillator admits a discontinuous cycle which is orbitally stable. In other words, it is asymptotically stable. That is, grazing in the degenerated model is a reason when perturbation creates discontinuity as well as it "improves" stability.

In the last section in this study, we will discuss the case when the Van der Pol oscillator in the generating system (3.88) admits a limit cycle and the generating system (3.88) admits two unit multipliers. This case can be comprehended as a critical one for the perturbation theory. Since the orbital stability theorem [38] as well as the small parameter method [38, 85] are hard to be applied. This problem can be taken into account by utilizing the results which are obtained in [5] Section 7.2. In this study, through simulations, we obtain that the continuous torus is transformed to discontinuous one under the regular perturbation. We have present this discussion at the end of the study to demonstrate the future work.

The rest of the example can be outlined as follows. In Section 2, we give a brief summary for the discontinuous dynamical system with grazing. The degenerated system with grazing is described. Section 3 covers the information about dynamics in harmonic oscillator with a grazing point. A recently developed linearization method [6] around grazing solutions has been utilized for the system (3.89) to examine orbitally stability. Section 4, is the main part of the study. By applying results of [6], the orbitally stable cycle for the perturbed system (3.87) has been obtained. Finally, bifurcation of discontinuous torus is observed and utilizing simulation tools, we have visualized the results of the present study. Section 5 includes a detailed summary of this study and some future works about the problem.

Defining variables as $x = x_1$, $x' = x_2$, $y = x_3$, $y' = x_4$, the system (3.88) can be rewritten as

$$\begin{aligned} x_1' &= x_2, \\ x_2' &= -x_1, \\ x_3' &= x_4, \\ x_4' &= -a(1-x_3^2)x_4 - x_3, \\ \Delta x_2|_{x\in\Gamma_0} &= -(1+Rx_2)x_2. \end{aligned} \tag{3.91}$$

Due to the fact that the generating system is an uncoupled one, The generating system (3.91) can be decomposed into following two systems,

$$\begin{aligned} x_1' &= x_2, \\ x_2' &= -x_1, \\ \Delta x_2|_{x\in\Gamma_0} &= -(1+Rx_2)x_2, \end{aligned} \tag{3.92}$$

and

$$\begin{aligned} x_3' &= x_4, \\ x_4' &= -a(1-x_3^2)x_4 - x_3. \end{aligned} \tag{3.93}$$

In the following part of the study, we will consider the stable oscillations of (3.91). It will be demonstrated in the following part that the fixed point of the equation (3.90) is a stable focus. In Fig. 3.12, the blue arc is drawn for the solution of (3.93) with initial value $(0.2, 0)$, which starts outside, approaches the fixed point $(0, 0)$ of the system (3.93).

First, we will show that, the model (3.89) has a grazing cycle, which is of the form $\Psi_1(t) = \cos(t)$. To accomplish it, we will consider Definition 1. We have $\langle \nabla\Phi(\Psi_1(0), \Psi_1'(0)), (\Psi_1'(0), -\Psi_1(0))\rangle = \langle (1,0),(0,1)\rangle = 0$, then we can say that the cycle $\Psi_1(t) = \cos(t)$, of the system (3.89) is a grazing one. In the next section, we will consider the linearization around the grazing cycle of the impacting harmonic oscillator (3.89).

Considering the system (3.91) with (3.1), one can determine that the barrier is $\Gamma_0 = \{(x_1, x_2, x_3, x_4)|x_1 = 1\}$, and it is defined by $\Phi(x_1, x_2, x_3, x_4) = x_1 - 1 = 0$ and the vector field is $f(x_1, x_2, x_3, x_4) = (x_2, -x_1, x_4, -a(1-x_3^2)x_4 - x_3)$.

Denote the cycle of the system (3.91) by $\Psi(t) = (\cos(t), -\sin(t), \Psi_3(t), \Psi_4(t))$,

where $\Psi_3(t) = 0$ and $\Psi_4(t) = 0$ is the fixed point of the system (3.93). To save the integrity of this study, it is important to see that the cycle, $\Psi(t)$, of the system (3.91) is a grazing one and the point $\Psi(0)$ is grazing.

Indeed, it is easy to verify that

$$\langle \nabla\Phi(x^*), f(x^*)\rangle = \langle (1,0,0,0), (0,1,-a(1-(\Psi_3(0))^2)\Psi_4(0) - \Psi_3(0))\rangle = 0,$$

and applying Definitions 1 and 5, one can conclude that the cycle $\Psi(t)$ grazes the surface of discontinuity Γ_0 at the point $\Psi(0)$.

3.6.1.1 Dynamics in the harmonic oscillator with the grazing point

Next, we will consider the linearization around the periodic solution $\Psi_1(t) = \cos(t)$ of the impacting system (3.89). Denoting the meeting moment of the solution $x(t) = x(t, 0, x_0)$ of (3.89) with a barrier $x = 1$ by $t = \theta$, we obtain for $\Delta x'(\theta) = x'_+ - x'_-$, where x'_- and x'_+ are velocities before and after impact, respectively. In order to analyze the stability of the grazing cycle $\bar{\Psi}(t) = (\Psi_1(t), \Psi'_1(t))$, it is urgent to consider the linearization around the cycle. There exist two different types of solutions near the grazing cycle. Some of them do not meet the surface of discontinuity and others intersect the surface of discontinuity near the grazing point $(\Psi_1(0), \Psi'_1(0))$, transversely.

For the continuous solutions, the linearization around the periodic solution $\bar{\Psi}(t)$ is

$$\begin{aligned} u'_1 &= u_2, \\ u'_2 &= -u_1. \end{aligned} \tag{3.94}$$

The fundamental matrix of (3.94) is $U(t)$, where $U(0) = I_2$, I_2, is 2×2 identity matrix. It is easy to verify by using techniques [38, 85] that the grazing cycle is stable with respect to the continuous inside solutions.

To obtain a linearization for the outside solutions to the cycle, it is important to consider a near solution $x(t) = x(t, \theta_i, \Psi(\theta_i)+\Delta x) = (x_1(t), x_2(t))$, to $\bar{\Psi}(t)$ of the differential part of the last system, near the moment $t = \theta_i$. The solution $x(t)$ meets the barrier at a moment $t = \xi_i$ near to $t = \theta_i$ at the point $(x_1, x_2) = (x_1(\xi_i), x_2(\xi_i))$. Let also, $\tilde{x}(t) = (\tilde{x}_1(t), \tilde{x}_2(t))$ be a solution of the equation such that $\tilde{x}(\xi_i) = x(\xi_i) + J(x(\xi_i))$,

where $J(x_1, x_2) = (x_1, 0.6x_2^2)$, it is easy to determine that $R = 0.6$ in (3.92) Define the following map

$$W_i(x) = \int_{\theta_i}^{\xi_i} \begin{bmatrix} x_2(s) \\ x_1(s) \end{bmatrix} ds + J\left(x + \int_{\theta_i}^{\xi_i} \begin{bmatrix} x_2(s) \\ -x_1(s) \end{bmatrix} ds \right) + \int_{\xi_i}^{\theta_i} \begin{bmatrix} \tilde{x}_2(s) \\ -\tilde{x}_1(s) \end{bmatrix} ds.$$

Now, we will carry on with examining the near discontinuous solution to the grazing cycle. It is too hard to analyze the systems with variable moments of impulses (3.92) for this reason, we should propose another system which preserves the dynamical properties of (3.92). For it, by applying $B-$ equivalence technique which is initiated in [5] and revised for the discontinuous dynamics with grazing points in [6], we will obtain a system with fixed moments of impacts to the system (3.92) which preserves dynamical properties of (3.92). Then, the $B-$equivalent system has the form

$$\begin{aligned} x_1' &= x_2, \\ x_2' &= -x_1, \\ \Delta x|_{t=\theta_i} &= W_i(x(\theta_i)), \end{aligned} \tag{3.95}$$

where $x = (x_1, x_2)^T$, T is the transpose of a matrix, $\theta_i = 2\pi i$, $i \in \mathbb{Z}$ and the maps $W_i(x(\theta_i))$, $i \in \mathbb{Z}$, is precised in (3.95). It is easy to verify that the cycle $\bar{\Psi}(t) = (\Psi_1(t), \Psi_1'(t)) = (\cos(t), -\sin(t))$ is a solution of system (3.95), as well [5].

Due to the construction of the map W_i, the solutions of (3.92) and (3.95) coincide except the intervals $\widehat{[\theta_i, \xi_i]}$, $i \in \mathbb{Z}$, where $\widehat{[\theta_i, \xi_i]} = [\theta_i, \xi_i]$ whenever $\theta_i < \xi_i$ and $\widehat{[\theta_i, \xi_i]} = [\xi_i, \theta_i]$, otherwise. By applying the method presented in [6], the derivative of the map (3.95) with respect to the first component of the initial value can be obtained as

$$\begin{aligned} \frac{\partial W_i(\bar{x})}{\partial x_1^0} = \begin{bmatrix} \bar{x}_2 \\ -\bar{x}_1 \end{bmatrix} \left(\frac{-1}{\bar{x}_2}\right) + \begin{bmatrix} 1 & 0 \\ 0 & 1.2\bar{x}_2 \end{bmatrix} \left(e_1 + \begin{bmatrix} \bar{x}_2 \\ -\bar{x}_1 \end{bmatrix} \left(\frac{-1}{\bar{x}_2}\right) \right) - \\ \begin{bmatrix} -0.6(\bar{x}_2)^2 \\ -\bar{x}_1 - \bar{x}_2 \end{bmatrix} \left(\frac{-1}{\bar{x}_2}\right) = \begin{bmatrix} -1 - 0.6\bar{x}_2 \\ 0.6\bar{x}_2 - 1.2\bar{x}_1 \end{bmatrix}, \end{aligned} \tag{3.96}$$

where $e_1 = (1, 0)^T$. Through the last expression, we can conclude that the derivative is a continuous function in its arguments in a neighborhood of the grazing point. Due to the fact that the point $\bar{x}$ is a transversal one, we get

$$\lim_{\bar{x} \to x^*} \frac{\partial W_i(\bar{x})}{\partial x_1^0} = \begin{bmatrix} -1 \\ -1.2 \end{bmatrix}. \tag{3.97}$$

By considering the theory which is originated in paper [6], we have the following linearization matrix at x^*,

$$W_{ix}(x^*) = \begin{bmatrix} -1 & 0 \\ -1.2 & 0 \end{bmatrix}. \tag{3.98}$$

Taking into account the above calculations, the linearization system for (3.89) around the periodic solution $\bar{\Psi}(t)$, can be obtained as

$$\begin{aligned} u_1' &= u_2, \\ u_2' &= -u_1, \\ \Delta u|_{t=\theta_i} &= W_{ix}(x^*)u, \end{aligned} \tag{3.99}$$

where the matrix $W_{ix}(x^*)$ calculated in (3.98). Then, one can evaluate the multipliers as $\rho_1 = 1$ and $\rho_2 = 0$. In the light of Theorem 5.1 in the paper [6], since one multiplier is unity and one is inside the unit disc, it is easy to conclude that the solution, $\bar{\Psi}(t)$ is orbitally stable with respect to outside impacting solution [5]. One can observe in Fig. 3.11 that the near inside solutions are continuous and the outside ones are discontinuous and the green one is drawn for the grazing cycle and the cycle is stable with respect to inside solution and orbitally stable with respect to outside solutions [6]. In Fig. 3.11 and 3.12, the solutions of the system (3.91) are depicted. Because both systems are separated from the each other, the trajectories of the system can be drawn separately as seen in Figs. 3.11 and 3.12.

The Fig. 3.11 is depicted for the solutions of an impacting harmonic oscillator which is subdued impacts at variable moments. The grazing cycle is pictured in green and the solutions with initial values $(x_1(0), x_2(0)) = (-1.8, 0)$ and $(x_1(0), x_2(0)) = (-0.9, 0)$ are drawn in blue and red, respectively. The blue curves approach the the green cycle as time increases and the inside cycle, which is drawn in red preserves its distance to the grazing cycle of the harmonic oscillator. It illustrates that the grazing cycle is orbitally stable with respect to impacting solutions and stable with respect to the non impacting solutions.

In Fig. 3.12, the solution of a non-impacting Van der Pol equation (3.93) with the constant $a = 1$ is depicted with initial value $(x_3(0), x_4(0)) = (0, 0.03)$ in blue. From the simulation, one can observe the the solution approaches the fixed point, $(0, 0)$ of the system (3.93). Thus, the fixed point is a stable focus.

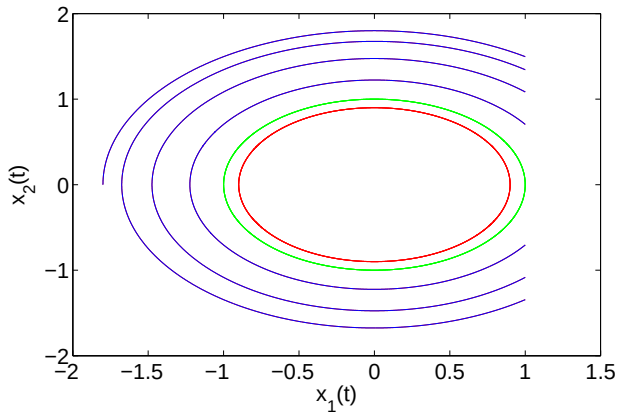

Figure 3.11: The blue and red arcs are for the solutions of system (3.92) with initial values $(x_1(0), x_2(0)) = (-1.8, 0)$ and $(x_1(0), x_2(0)) = (-0.9, 0)$, respectively. The green circle is for the grazing cycle of (3.92). It is apparent that the cycle is stable with respect to inside solution and orbitally stable with respect to outside solution.

In Fig. 3.13 the coordinates $x_1(t) - x_3(t) - x_4(t)$ of system (3.91) with initial values $(x_1(0), x_2(0), x_3(0), x_4(0)) = (0, 1.3, 0, 0.03)$ and $(x_1(0), x_2(0), x_3(0), x_4(0)) = (0, 0.9, 0, 0.03)$ are pictured in blue and red, respectively. It is hard to see in Fig. 3.13 how the solutions behave. For this reason, one should consider the Fig. 3.12 in order to observe that there exists a stable focus of the Van der Pol oscillator which is modeled through the system (3.93). It is seen in Fig. 3.13 that the trajectories are attracted by the circle in the plane $x_4 = 0$.

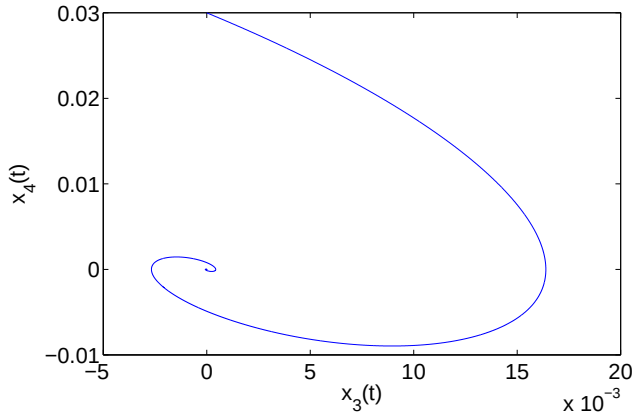

Figure 3.12: (a)The blue arc is drawn for the solution of system (3.93) with initial value $(x_3(0), x_4(0)) = (0, 0.03)$.

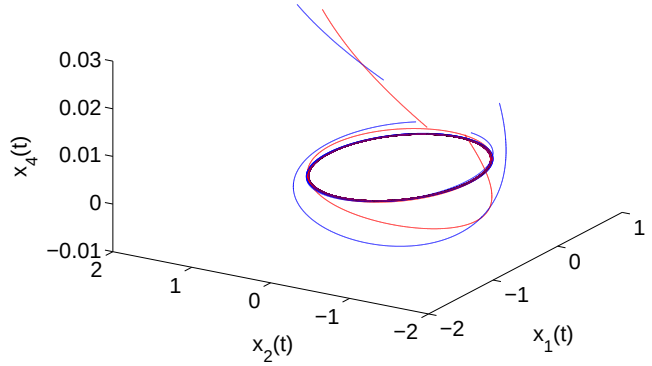

Figure 3.13: (b)The blue and red arcs are pictured for the coordinates $x_1(t) - x_2(t) - x_4(t)$ of the solution of the system (3.91) with initial values $(x_1(0), x_2(0), x_3(0), x_4(0)) = (0, 1.8, 0, 0.03)$ and $(x_1(0), x_2(0), x_3(0), x_4(0)) = (0, 0.9, 0, 0.03)$, respectively.

3.6.1.2 Regular perturbations: The bifurcation of torus

In this section, by applying regular perturbations to the model (3.88), we obtain the system (3.87). It is easy to see that the system (3.87) is a coupled system although the equations of the system (3.88) are uncoupled. Next, the existence of orbitally stable discontinuous periodic motion of (3.88) will be analyzed.

By applying the Dulac's criterion [38] through analysis of the expression $\mu(1 - x_1^2)$, we have obtained that there is no continuous periodic solutions of (3.92) near the unit circle for small $\mu \neq 0$.

Next, the aim of the present study is to examine the existence of orbitally stable discontinuous periodic solution of Van der Pol's equation (3.100) near to the grazing cycle. Defining variables as $x = x_1$, $x' = x_2$, $y = x_3$, $y' = x_4$, the system (3.87) can be rewritten as

$$\begin{aligned} x_1' &= x_2, \\ x_2' &= -x - \mu(1 - x_1^2)x_2, \\ x_3' &= x_4, \\ x_4' &= -a(1 - x_3^2)x_4 - x_3 - \mu x_1, \\ \Delta x_2|_{x \in \Gamma_\mu} &= -(1 + Rx_2)x_2. \end{aligned} \tag{3.100}$$

Let us construct the following map in order to determine the periodic solution of

the perturbed system (3.100). Denote by γ_1, γ_2, γ_3 and γ_4 the initial values of the intended solution (periodic solution of the perturbed system) and τ the period of it. Let $\gamma_1^0, \gamma_2^0, \gamma_3^0, \gamma_4^0$ be an initial value of the periodic solution $\Psi(t)$ of the generating system (3.91). Fix one initial value of the cycle of the perturbed system $\gamma_2 = \gamma_2^0 = 0$. In order to investigate the existence of the periodic solution, we will consider the following equations

$$\begin{aligned}
\mathcal{P}_1(\tau, \gamma_1, \gamma_2^0, \gamma_3, \gamma_4, \mu) &= x_1(\tau, \gamma_1, \gamma_2^0, \gamma_3, \gamma_4, \mu) - \gamma_1 = 0, \\
\mathcal{P}_2(\tau, \gamma_1, \gamma_2^0, \gamma_3, \gamma_4, \mu) &= x_2(\tau, \gamma_1, \gamma_2^0, \gamma_3, \gamma_4, \mu) = 0, \\
\mathcal{P}_3(\tau, \gamma_1, \gamma_2^0, \gamma_3, \gamma_4, \mu) &= x_3(\tau, \gamma_1, \gamma_2^0, \gamma_3, \gamma_4, \mu) - \gamma_3 = 0, \\
\mathcal{P}_4(\tau, \gamma_1, \gamma_2^0, \gamma_3, \gamma_4, \mu) &= x_4(\tau, \gamma_1, \gamma_2^0, \gamma_3, \gamma_4, \mu) - \gamma_4 = 0.
\end{aligned} \tag{3.101}$$

To solve the equations in (3.101), it request that the following determinant should not be equal to zero.

$$D = \left| \begin{array}{ccc} \frac{\partial \mathcal{P}_1(\tau,\gamma_1,\gamma_2^0,\gamma_3,\gamma_4,\mu)}{\partial \tau} & \cdots & \frac{\partial \mathcal{P}_1(\tau,\gamma_1,\gamma_2^0,\gamma_3,\gamma_4,\mu)}{\partial \gamma_4} \\ \vdots & \ddots & \vdots \\ \frac{\partial \mathcal{P}_4(\tau,\gamma_1,\gamma_2^0,\gamma_3,\gamma_4,\mu)}{\partial \tau} & \cdots & \frac{\partial \mathcal{P}_4(\tau,\gamma_1,\gamma_2^0,\gamma_3,\gamma_4,\mu)}{\partial \gamma_4} \end{array} \right|_{(\tau,\gamma_1,\gamma_2,\gamma_3,\gamma_4,\mu)=(2\pi,1,0,\gamma_3^0,\gamma_4^0,0)} =$$
$$\left| \begin{array}{ccc} \frac{\partial x_1(\tau,\gamma_1,\gamma_2^0,\gamma_3,\gamma_4,\mu)}{\partial \tau} & \cdots & \frac{\partial x_1(\tau,\gamma_1,\gamma_2^0,\gamma_3,\gamma_4,\mu)}{\partial \gamma_4} \\ \vdots & \ddots & \vdots \\ \frac{\partial x_4(\tau,\gamma_1,\gamma_2^0,\gamma_3,\gamma_4,\mu)}{\partial \tau} & \cdots & \frac{\partial x_4(\tau,\gamma_1,\gamma_2^0,\gamma_3,\gamma_4,\mu)}{\partial \gamma_4} - 1 \end{array} \right|_{(\tau,\gamma_1,\gamma_2,\gamma_3,\gamma_4,\mu)=(2\pi,1,0,\gamma_3^0,\gamma_4^0,0)} . \tag{3.102}$$

The determinant is computed as

$$D = P \times Q, \tag{3.103}$$

where

$$P = \left| \begin{array}{cc} x_2(\tau, \gamma_1, \gamma_2^0, \gamma_3, \gamma_4, \mu) & \frac{\partial x_1(\tau,\gamma_1,\gamma_2^0,\gamma_3,\gamma_4,\mu)}{\partial \gamma_1} \\ -x_1(\tau, \gamma_1, \gamma_2^0, \gamma_3, \gamma_4, \mu) & \frac{\partial x_2(\tau,\gamma_1,\gamma_2^0,\gamma_3,\gamma_4,\mu)}{\partial \gamma_1} \end{array} \right|_{(\tau,\gamma_1,\gamma_2,\gamma_3,\gamma_4,\mu)=(2\pi,1,0,\gamma_3^0,\gamma_4^0,0)} \tag{3.104}$$

and

$$Q = \left| \begin{array}{cc} \frac{\partial x_3(\tau,\gamma_1,\gamma_2^0,\gamma_3,\gamma_4,\mu)}{\partial \gamma_3} - 1 & \frac{\partial x_3(\tau,\gamma_1,\gamma_2^0,\gamma_3,\gamma_4,\mu)}{\partial \gamma_4} \\ \frac{\partial x_4(\tau,\gamma_1,\gamma_2^0,\gamma_3,\gamma_4,\mu)}{\partial \gamma_3} & \frac{\partial x_4(\tau,\gamma_1,\gamma_2^0,\gamma_3,\gamma_4,\mu)}{\partial \gamma_4} - 1 \end{array} \right|_{(\tau,\gamma_1,\gamma_2,\gamma_3,\gamma_4,\mu)=(2\pi,1,0,\gamma_3^0,\gamma_4^0,0)}, \tag{3.105}$$

The determinant P in (3.104), by means of the monodromy matrix, $\begin{bmatrix} 0 & 0 \\ 0 & 1 \end{bmatrix}$, of (3.99) is evaluated as

$$P = \left| \begin{array}{cc} \frac{\partial \mathcal{P}_1(\tau,\gamma_1,\gamma_2^0,\mu)}{\partial \tau} & \frac{\partial \mathcal{P}_1(\tau,\gamma_1,\gamma_2^0,\mu)}{\partial \gamma_1} \\ \frac{\partial \mathcal{P}_2(\tau,\gamma_1,\gamma_2,\mu)}{\partial \tau} & \frac{\partial \mathcal{P}_2(\tau,\gamma_1,\gamma_2^0,\mu)}{\partial \gamma_1} \end{array} \right|_{(\tau,\gamma_1,\mu)=(2\pi,1,0)} = \left| \begin{array}{cc} 0 & -1 \\ -1 & 0 \end{array} \right| = -1. \quad (3.106)$$

Next, let us continue with the determinant Q in (3.105). To calculate it, we should consider the linearization for the system (3.93) around the fixed point $(0, 0)$. Then, by applying theory of ordinary differential equations, the linearization for (3.93) at the fixed point $(0, 0)$ can be obtained in the form,

$$\begin{aligned} u_3' &= u_4, \\ u_4' &= -u_3 - u_4, \end{aligned} \quad (3.107)$$

with the fundamental matrix $\tilde{U}(t)$, where $\tilde{U}(0) = I_2$. By considering (3.107), the monodromy matrix is obtained as

$$\exp(-\pi) \begin{bmatrix} \cos(1.7320\pi) & \sin(1.7320\pi) \\ -\sin(1.7320\pi) & \cos(1.7320\pi) \end{bmatrix}. \quad (3.108)$$

With the monodromy matrix (3.108), the determinant Q, is evaluated as

$$Q = \exp(-\pi) \left| \begin{array}{cc} \cos(1.7320\pi) - 1 & \sin(1.7320\pi) \\ -\sin(1.7320\pi) & \cos(1.7320\pi) - 1 \end{array} \right| = 0.0012. \quad (3.109)$$

Combining (3.106) with (3.109), the determinant (3.103) is computed as

$$D = P \times Q = -0.0012 \neq 0. \quad (3.110)$$

Thus, by applying the results of the paper [6] which is given as Theorem 5.1, we can assert that there exists a cycle of the perturbed system (3.100) for sufficiently small $\mu > 0$ and $\mu < 0$, as well.

Because of the continuous dependence in initial value for the fundamental matrix of (3.100) and continuity of the matrix $W_{ix}(x^*)$ [6], the multipliers of the perturbed system become in the form that one is equal to unity and all others are less than unity. Thus, the cycle of the perturbed system is orbitally stable.

In the previous part, we have demonstrated that there exists an orbitally stable periodic solution of the perturbed system (3.100). Now, to actualize the theoretical result, we will present the following simulations and they are drawn for $R = 0.6$, $a = 1$ and $\mu = 0.1$. In Fig. 3.16, the two dimensional projection of the solutions of the perturbed system, the coordinates $x_1(t)$ and $x_2(t)$, are simulated with initial conditions $x_1(0) = 0$, $x_2(0) = 1.02$, $x_3(0) = 0$, $x_4(0) = 0.2$, and $x_1(0) = 0$, $x_2(0) = 1.6$, $x_3(0) = 0$, $x_4(0) = 0.02$, in blue and red, respectively. In Figs 3.14, 3.15 and 3.16, with the same initial conditions, the coordinates $x_1(t) - x_2(t)$, $x_1(t) - x_2(t) - x_3(t)$ and $x_1(t) - x_3(t) - x_4(t)$, for the solution of (3.100) are pictured, respectively. In Fig. 3.14, it is easy to see that the outside solution drawn in blue approaches the discontinuous periodic solution of (3.100) and the inside solution drawn in red approaches the discontinuous periodic solution of (3.100), as time increases. In the figure, one can conclude that the discontinuous periodic solution is orbitally asymptotically stable.

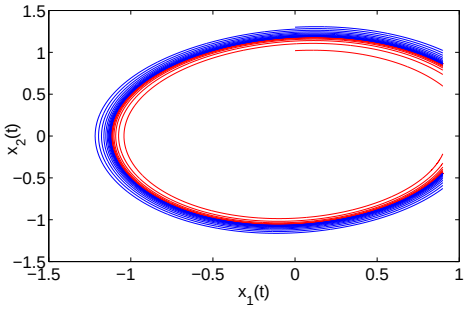

Figure 3.14: The coordinates $x_1(t)$, $x_2(t)$ of the solutions of the system (3.100).

In Fig. 3.15, the coordinates $x_1(t) - x_2(t) - x_3(t)$ are depicted. To make the visualization better, we consider the projection of the solutions of (3.100) with initial values $x(0) = (0, 1.02, 0, 0.02)$ and $x(0) = (0, 1.4, 0, 0.02)$ onto the $x_1 - x_2$ plane. In the Fig. 3.14, the blue one is for the solution with initial value $x(0) = (0, 1.02, 0, 0.02)$ and the red one is for that with initial value $x(0) = x(0) = (0, 1.4, 0, 0.02)$. One can observe that both approach the discontinuous periodic solution of the perturbed system (3.100) as time increases.

In Fig. 3.11, the degenerated oscillator has a stable continuous cycle, which grazes the surface of discontinuity, Γ_0. In Fig. 3.14, by applying regular perturbations to the surface of discontinuity and vector field, the orbitally stable discontinuous cycle of the Van der Pol equation is obtained. Moreover, in 3.13, one can see through simulation

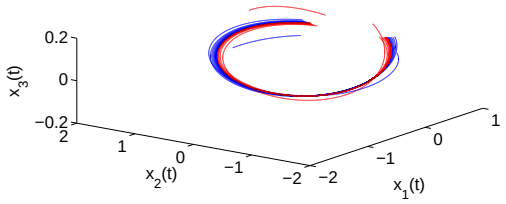

Figure 3.15: Three dimensional projection on the space $x_1 - x_2 - x_3$, the coordinates $x_1(t)$, $x_2(t)$ and $x_3(t)$, of the solutions of the system (3.100).

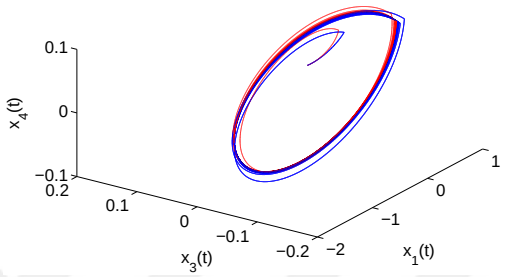

Figure 3.16: Three dimensional projection on the space $x_1 - x_3 - x_4$, the coordinates $x_1(t), x_3(t)$ and $x_4(t)$ of the solutions of system (3.100).

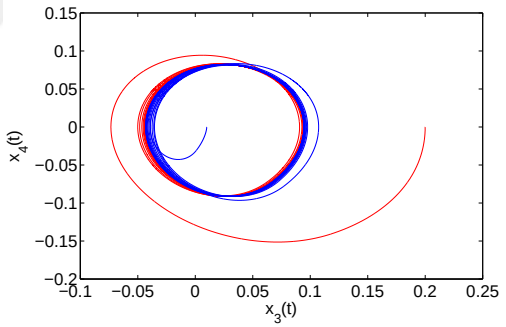

Figure 3.17: The coordinates $x_3(t)$, $x_4(t)$ of the solutions of the system (3.100). Coordinates of the solutions of system (3.100) which approach to the corresponding coordinate of the limit cycle.

that the origin is a stable focus for the system (3.93), but by applying perturbation to the system, one can see in Fig. 3.17 that, an orbitally stable continuous cycle for the the third and fourth equations of (3.100) is obtained.

Let us sum up the above discussion. As μ slightly changes from zero, the Cartesian product of the circle, $(\cos(t), -\sin(t))$, and focus, $(0, 0)$, of the system (3.91) became the Cartesian product of discontinuous and continuous cycles of system (3.100) (see

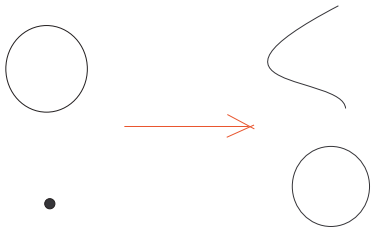

Figure 3.18: The generating system has a trajectory which is a Cartesian product of a grazing continuous cycle and a stable focus. Under regular perturbation, they are transformed to discontinuous and continuous cycles, respectively.

Fig. 3.18). One can consider the Cartesian product of cycles as a discontinuous torus (see Fig. 3.19). This is why, one can say about *the bifurcation of the discontinuous torus from the cycle and the equilibrium*.

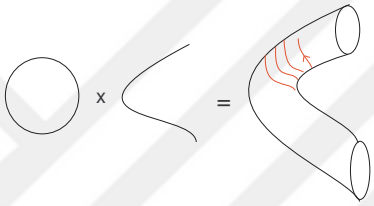

Figure 3.19: The Cartesian product of discontinuous and continuous cycles can be considered as a discontinuous torus.

3.6.1.3 Discussion

In the literature, the existence of the periodic solutions of Van der Pol oscillators and their stability are analyzed numerically and qualitatively. It is not new to examine coupled Van der Pol oscillators even if they are discontinuous. However, the main difficulty in the present study is caused by the grazing in the degenerated system, which is a harmonic oscillator with a grazing cycle. The difficulty with grazing is that it may cause a singularity in the linearization system. However, in this study, the singularity is suppressed in the system with the compliance of the vector field, the surface of discontinuity and the jump function. As different from the existing results, the orbitally stable cycle for the Van der Pol oscillator exists inside the region $|x_1| < 1$. By considering impacting Van der Pol oscillator, the discontinuous orbitally stable cycle of that system is obtained. This study demonstrates that how the results initiated in the paper [6] is eligible to analyze multi-dimensional and non-linear mechanical

systems. In this study, we obtained a discontinuous orbitally stable cycle for the impacting Van der Pol oscillator. By applying the periodic solution as a perturbation for other non-impacting Van der Pol's oscillator, the discontinuous cycle is extended to the four dimensional space. Thus, we have verified the existence of discontinuous cycle for the perturbed system and demonstrated that the cycle is orbitally stable.

One of the most popular method to prove the stability of a cycle is to evaluate the Floquet multipliers of the linearization system along the cycle. It can be applied only the cycle is located precisely. Particularly, when the cycle is near to a critical point, the theory of bifurcation can be utilized to prove the stability [114]. Borg [18] and Cronin [28] proved the existence of a stable cycle in their studies, although, it is not precisely located in a region. If the dimension of the equation is larger than two, the conditions of Cronin become complicated and need computer verification. The method of Borg and Cronin is applied in three dimensional equations by Sheerman [112]. The phase-asymptotic orbital stability is a method that presents powerful kind of stability for the applications. Some other ways of investigations that prove the orbital stability by means of a computer is considered in [67].

Even if one can prove the existence of periodic solution for perturbed system, the studies of Borg and Cronin should be developed for the systems with grazing and impact. It is worth noticing that methods developed in the book [5] and demonstrated in [6] will give possibility to analyze not only regular but also critical cases for the models with grazing points.

In this part, we will consider the critical case when both systems (3.92) end (3.93) admit orbitally stable cycles.

It is demonstrated in the book [38] that the system (3.93) has orbitally stable cycle with the parameter $a < 0$.

Denote the quasi-periodic solution of (3.91) by $\Psi(t) = (\cos(t), \sin(t), x_3(t), x_4(t))$. In Fig. 3.12, one can observe that the blue solution with initial value $x(0) = (-2.1, 0, 2.3, 0)$ which starts outside approaches the cycle and the red one with initial value $x(0) = (-1.98, 0, 2.1, 0)$ which starts inside approaches the cycle as time increases.

Let us verify Definition 1 for $\Psi(t)$. For it, the expression $\langle \nabla\Phi(x^*), f(x^*)\rangle = 0$, should be valid at the grazing point $x^* = \Psi(0)$. It is easy to verify that $\langle (1,0,0,0), (0,1,-2(1-(x_3(0))^2)x_4(0) - x_3(0))\rangle = 0$, then we can conclude that the cycle $\Psi(t)$ grazes the surface of discontinuity Γ_0 at the point $\Psi(0)$. So, we can say that $\Psi(0)$ is grazing and by Definition 5, $\Psi(t)$ is a grazing quasi-periodic solution.

In Figs. 3.11 and 3.20, the solutions of system (3.91) are depicted. Because both systems are separated from the each other, the trajectories of these systems can be drawn separately as seen in Figs. 3.11 and 3.20. The Fig. 3.11 is pictured for the impacting harmonic oscillator which is subdued impacts at variable moments. In Fig. 3.20, a non-impacting Van der Pol oscillator is simulated and it is easy to see that the outside as well as inside solutions which are drawn in blue and red, respectively, approach the cycle of the Van der Pol's oscillator as time increases. In Fig. 3.21 the coordinates $x_1(t) - x_3(t) - x_4(t)$ of system (3.91) with initial values $(x_1(0), x_2(0), x_3(0), x_4(0)) = (-1.4, 0, 1.9, 0)$ and $(x_1(0), x_2(0), x_3(0), x_4(0)) = (-0.98, 0, 2.1, 0)$ are visualized in blue and red, respectively. To obtain a better visualization, one should consider the Fig. 3.20 in order to observe that there exists orbitally stable cycle of the Van der Pol oscillator which is modeled through the system (3.93).

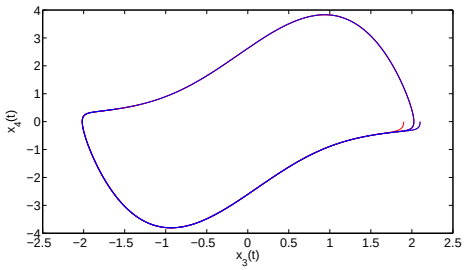

Figure 3.20: The red arc is for solution of system (3.93) with initial value $(x_3(0), x_4(0)) = (1.9, 0)$ and the blue one is for the same with initial value $(x_3(0), x_4(0)) = (2.1, 0)$.

In Fig. 3.22, the coordinates $x_1(t) - x_2(t) - x_3(t)$ are depicted. To obtain a better view, we consider the projections of the solutions of (3.91) with initial values $x(0) = (-2.1, 0, 1.9, 0)$ and $x(0) = (-2.3, 0, 2.3, 0)$ onto the $x_1 - x_2$ plane. In the Fig. 3.23, the blue and red ones are for the solution with initial values $x(0) = (-2.1, 0, 1.9, 0)$ and $x(0) = (-2.3, 0, 2.3, 0)$, respectively. One can observe that both approach the discontinuous periodic solution of the perturbed system (3.100) as time increases.

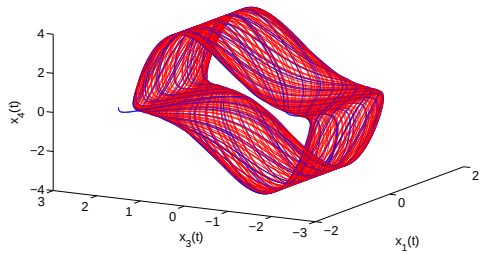

Figure 3.21: The red arc is for the coordinates $x_1(t) - x_3(t) - x_4(t)$ of system (3.91) with initial value $(x_1(0), x_2(0), x_3(0), x_4(0)) = (-1.4, 0, 1.9, 0)$ and the blue one is for the same coordinates of system (3.91) with initial value $(x_1(0), x_2(0), x_3(0), x_4(0)) = (-0.98, 0, 2.1, 0)$.

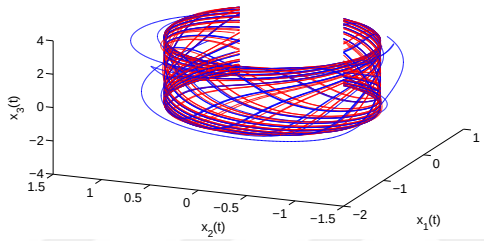

Figure 3.22: Three dimensional projection, the coordinates $x_1(t)$, $x_2(t)$ and $x_3(t)$, of the system (3.100), on the $x_1 - x_2 - x_3$ plane.

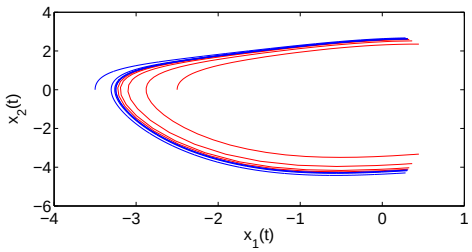

Figure 3.23: (b) The coordinates $x_1(t)$, $x_2(t)$ of the system (3.100).

In Figs 3.22, and 3.24, with the same initial conditions the three dimensional projections, the coordinates $x_1(t) - x_2(t) - x_3(t)$, and $x_1(t) - x_3(t) - x_4(t)$ respectively, for the solutions of (3.100) are pictured. In Fig. 3.25, the coordinates $x_3(t)$, $x_4(t)$ of the system (3.100) are depicted.

Moreover, the impacting part of the system (3.100) admits a periodic grazing solution which is orbitally stable with respect to outside and stable with respect to inside solution. For the generating system, there exist two continuous cycles the Cartesian product of them constitutes a continuous torus. It is worth mentioning that the cycles

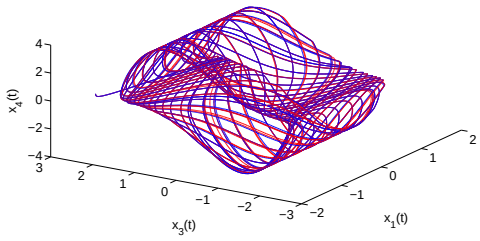

Figure 3.24: (a)Three dimensional projection, the coordinates $x_1(t), x_3(t)$ and $x_4(t)$ of the system (3.100), on the $x_1 - x_3 - x_4$ plane.

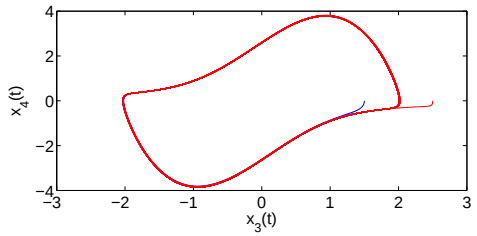

Figure 3.25: (b)The coordinates $x_3(t)$, $x_4(t)$ of the system (3.100).

of the generating system as well as perturbed system are, in general, with incommensurate periods because of the autonomous character of the systems. Under regular perturbation, there are two orbitally stable cycles one is discontinuous and other is continuous. So, one can say about bifurcation of discontinuous torus. In this example, since there are two unit multipliers of the degenerated system, one can not apply orbital stability theorem to examine the stability of the cycle. This is why, we consider only simulation analysis. In the future, utilizing the methods of small parameter for critical cases [38, 85, 92, 96], which were developed for discontinuous dynamics in [5], the stability of the cycle for the critical cases can be examined.

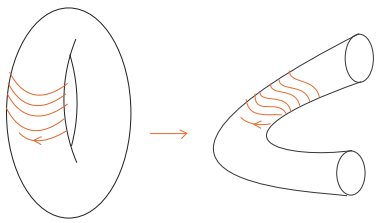

Figure 3.26: The system (3.91) has two stable continuous cycles and Cartesian product of them constitutes a continuous torus under regular perturbation, while the system (3.100) admits one discontinuous and one continuous cycles and Cartesian product of them is a torus which is discontinuous. Under variation of the parameter μ, one can see the transformation of the torus from continuous to discontinuous.

CHAPTER 4

GRAZING SOLUTIONS OF NON-AUTONOMOUS SYSTEMS

Grazing is a popular phenomenon in theoretical analysis as well as applications [31, 36, 53, 75, 77],[97]-[100]. In literature, grazing is understood as a particular case which makes the dynamics around it complicated such as the appearance of chaos through period adding [97] and bifurcation [31]. Many investigations are conducted on grazing, some of them are: in [100], the existence of periodic solution for the higher dimensional mechanical systems are investigated, in the studies [31, 33], the authors define the grazing bifurcation for the systems of differential equations with discontinuous right hand side and analyze the stability of periodic grazing solutions and in [36], grazing is defined as a bounding case which divides the regions with quite different dynamical behaviors and point, the system trajectory makes tangential contact with an event. It is observed that by finding smallest parameter alteration necessary to induce grazing, a basis for an optimization technique is obtained.

In the literature, two different approaches have been utilized to define grazing phenomenon. One of them is that grazing is the case when a trajectory meets with zero velocity to the surface of discontinuity [97]-[100]. The other is that the trajectory meets the surface of discontinuity tangentially [31, 33, 34, 75]. In the present study, to develop theory for non-autonomous systems with grazing points, we will take into account the comprehension of the authors who assert that the solutions intersect the surface of discontinuity tangentially at the grazing point. Our approach is maximally close to the way of investigations like ordinary differential equations.

In literature some special non-autonomous systems are taken into account. They consist of a non-autonomous vector-field and autonomous surfaces. In this present part of

the study, we will consider a special non-autonomous system with non-autonomous surfaces of discontinuity such that the surfaces are defined by $t = \tau_i(x)$, $i \in \mathbb{Z}$. For such systems, we introduce definitions such as a grazing point for the non-autonomous system, the continuous/ discontinuous grazing point and a proper linearization for non-autonomous impulsive systems near the periodic solution which has grazing points is constructed. Moreover, the theoretical results are supported by examples and simulations.

4.1 Preliminaries

Let $\mathbb{R}$, $\mathbb{N}$ and $\mathbb{Z}$ be the sets of all real numbers, natural numbers and integers, respectively. Let $G \subset \mathbb{R}^n$ be an open, bounded and connected set. Introduce the following system of differential equations with variable moments of impulses

$$\begin{aligned} x' &= f(t,x), \\ \Delta x|_{t=\tau_i(x)} &= J_i(x), \end{aligned} \tag{4.1}$$

where $(t,i,x) \in \mathbb{R}\times\mathbb{Z}\times G$, the function $f(t,x)$ is continuous on $\mathbb{R}\times G$, continuously differentiable in x and $T-$ periodic, i.e. $f(t+T,x) = f(t,x)$, functions J_i and $\tau_i(x)$, $i \in \mathbb{Z}$, are defined on G and continuously differentiable on G. The following equality $J_{i+p} = J_i$ for a natural number p is valid and $\tau_i(x)$ has $(T,p)-$property, i.e. $\tau_i(x) + T = \tau_{i+p}(x)$ for all $i \in \mathbb{Z}, x \in G$. Denote by $I_i(x) = J_i(x) + x$.

Let $\langle , \rangle$ be the dot product.

Consider a solution $x(t)$ of (4.1). Denote θ_i, $i \in \mathbb{Z}$, if $\theta_i = \tau_i(x(\theta_i))$. That is, $t = \theta_i$ is the moment of the intersection of the solution $x(t)$ with the surface $t = \tau_i(x)$. Regardless, if $x(t)$ has a discontinuity at the moment or not, we call the $t = \theta_i$ the *moment of discontinuity*.

Denote by $\nabla\tau_i(x) = (\frac{\partial\tau_i(x)}{\partial x_1}, \frac{\partial\tau_i(x)}{\partial x_2}, \ldots, \frac{\partial\tau_i(x)}{\partial x_n})$ the gradient of the function $\tau_i(x)$. Let us introduce the main object of the present discussion.

Definition 8 *A point $(\theta_i, x(\theta_i))$, $i \in \mathbb{Z}$, is a grazing if $\langle \nabla\tau_i(x(\theta_i)), f(\theta_i, x(\theta_i))\rangle = 1$. It is a continuous grazing point provided $I(x(\theta_i)) = 0$, otherwise it is discontinuous*

one.

Definition 9 *A solution $x(t)$ of (4.1) is grazing if it has a grazing point $(\theta_i, x(\theta_i))$.*

Assume that (4.1) admits a grazing $T-$periodic solution $\Psi(t)$ with discontinuity moments θ_i, $i \in \mathbb{Z}$, such that $\theta_{i+p} = \theta_i + T, i \in \mathbb{Z}$.

Consider the system of ordinary differential equations

$$x' = f(t, x), \tag{4.2}$$

which is a part of (4.1).

Let us formulate the following conditions which are sufficient for existence, uniqueness and continuation of solutions of (4.1) [5].

(N1) For any $c \in G$, $i \in \mathbb{Z}$, the inequality $\tau_i(c + J_i(c)) < \tau_i(c)$ is valid;

(N2) for all $x \in G$, $\tau_i(x) < \tau_{i+1}(x)$.

In what follows, let $\|\cdot\|$ be the Euclidean norm, that is for a vector $x = (x_1, x_2, \ldots, x_n)$ in $\mathbb{R}^n$, the norm is equal to $\sqrt{x_1^2 + x_2^2 + \ldots + x_n^2}$.

We need also the following assertions.

(N3) There exist positive numbers C and N with $CN < 1$ such that

$$\max_{(t,x)\in\mathbb{R}\times G} \|f(t,x)\| \leq C, \quad \max_{x\in G} \left\| \frac{\partial \tau_i(x)}{\partial x} \right\| \leq N.$$

(N4) for all $x \in G$ and $i \in \mathbb{Z}$, $\max\limits_{0\leq\sigma\leq 1} \langle \dfrac{\partial \tau_i(x + \sigma I_i(x))}{\partial x}, I_i(x) \rangle \leq 0.$

Suppose that conditions $(N1)-(N4)$ are fulfilled. Then, every solution $x(t) : I \to G$ of (4.1) intersects each of the surfaces of discontinuity $t = \tau_i(x), i \in \mathbb{Z}$, at most once [5].

Denote by $\widehat{[a, b]}$, $a, b \in \mathbb{R}$, the interval $[a, b]$, whenever $a \leq b$ and $[b, a]$, otherwise. Let $x_1(t) \in PC(\mathbb{R}_+, \theta^1)$, $\theta^1 = \{\theta_i^1\}$, and $x_2(t) \in PC(\mathbb{R}_+, \theta^2)$, $\theta^2 = \{\theta_i^2\}$, be two different solutions of (4.1).

Definition 10 *The solution $x_2(t)$ is in the $\epsilon-$neighborhood of $x_1(t)$ on the interval I if*

- $|\theta_i^1 - \theta_i^2| < \epsilon$ *for all* $\theta_i^1 \in \mathbb{R}$*;*
- *the inequality* $||x_1(t) - x_2(t)|| < \epsilon$ *is valid for all t, which satisfy* $t \in \mathbb{R} \setminus \cup_{\theta_i^1 \in \mathbb{R}}(\theta_i^1 - \epsilon, \theta_i^1 + \epsilon)$.

The topology defined with the help of $\epsilon-$ neighborhoods is called the B-topology [5]. One can easily see that it is Hausdorff and it can be considered also if two solutions $x_1(t)$ and $x_2(t)$ are defined on a semi-axis or on the entire real axis.

It is too complicated to invesitgate the systems with variable moments of impulses. To facilitate our analysis, an important method is presented in [5] which reduces the systems with variable moments of impulses to those with fixed moments of impulses. The system with fixed moment of impulses is named a ***B-equivalent system*** to the system with variable moments of impulses. In order to construct a B-equivalent system near the integral curve of $\Psi(t)$, we will consider the following way.

Consider a point $(\theta_i, x) \in \mathbb{R} \times G$ with a fixed ξ, on the periodic solution with a fixed $i \in \mathbb{Z}$. Let $\xi_i = \xi_i(x)$ be the meeting moment of the solution $x(t) = x(t, \theta_i, x)$ of (4.2). Additionally, assume that the solution $x_1(t) = x(t, \theta_i, x(\theta_i))$ of (4.2) exists on $\widehat{[\theta_i, \xi_i]}$. Due to the differentiability of the functions $\tau_i(x)$, it is true that near solutions meets the surface near to the periodic solution. The map $W : x \to x_1(\xi)$ can be constructed as

$$W_i(x) = \int_{\theta_i}^{\xi_i} f(u, x(u))du + J_i(x + \int_{\theta_i}^{\xi_i} f(u, x(u))du) + \int_{\xi_i}^{\theta_i} f(u, x_1(u))du. \quad (4.3)$$

Let us take into consideration the following system of differential equations with fixed moments of impulses

$$\begin{aligned} y' &= f(t, y), \\ \Delta y|_{t=\theta_i} &= W_i(y), \end{aligned} \quad (4.4)$$

which is $B-$ equivalent in $G \subset \mathbb{R}^n$ to (4.1). It is easy to see that $\Psi(t)$ is also a solution of (4.4) as well. In the following part, we will consider the system (4.4) instead of (4.1) to construct a linearization system around $\Psi(t)$.

Since of the way of construction of $W_i(x)$ systems (4.1) and (4.4) are $B-$equivalent in the neighborhood of $\Psi(t)$. That is, if $x(t) : U \to G$ is a solution of (4.1), then is coincides with a solution $y(t) : U \to G$ when $y(t_0) = x(t_0)$, for $t_0 \in U \setminus \cup_{i\in\mathbb{Z}}\widehat{[\theta_i, \xi_i]}$. Particularly, $x(\theta_i) = y(\theta_i+),\ x(\xi_i) = y(\xi_i),$ if $\theta_i > \xi_i$, $x(\theta_i) = y(\theta_i),\ x(\xi_i+) = y(\xi_i),$ if $\theta_i < \xi_i$.

4.2 Differentiability of the solutions

In this part of the study, we will analyze the differential dependence of solutions on initial conditions for the differential equations with variable moments of impulses with emphasis on grazing points.

Denote by $x_j(t), j = 1, 2, \ldots, n,$ solutions of (4.1) with $x^j(t_0) = x_0 + \xi e_j = (x_1^0, x_2^0, \ldots, x_{j-1}^0, x_j^0 + \xi, x_{j+1}^0, \ldots, x_n^0),\ \xi \in \mathbb{R}$, and let η_i^j be the moments of discontinuity of $x_j(t)$.

The solution $x(t)$ is $B-$differentiable with respect to $x_0^j,\ j = 1, 2, \ldots, n$, on $[t_0, T]$, if there exists $\delta > 0$, such that if $(t_0, x^j(t_0) \in D(t_0, \delta) \cap G$, where $D(t_0, \delta) = \{(t_0, x) : \|x - x_0\| < \delta\}$ is a disc with center at (t_0, x_0) and with radius $\delta > 0$, then

(A) there exist constants $\nu_{ij}, i \in \mathbb{Z}$, such that

$$\theta_i - \eta_i^j = \nu_{ij}\xi + o(|\xi|); \tag{4.5}$$

(B) for all $t \in [a, b]\setminus \cup_{i\in\mathbb{Z}}\ \widehat{(\theta_i, \eta_i^j]}$, the following equality is satisfied

$$x^j(t) - x(t) = u_j(t)\xi + o(|\xi|), \tag{4.6}$$

where $u_j(t) \in PC([t_0, T], \theta)$. The pair $\{u_j, \{\nu_{ij}\}_i\}$ is said to be a $B-$ derivative of $x(t)$ with respect to x_0^j on $[a, b]$.

Due to the complexity of analysis, which appears since of the grazing phenomenon, we will only discuss the linearization for periodic solutions.

The object of maining part is to find conditions for the smoothness of the grazing solution. In other words, for the existence of linearization around a grazing periodic

solution $\Psi(t)$ with a period T, and with discontinuity moments θ_i, $i = 1, 2, \ldots, p$, on the interval $[0, T]$.

We will construct the variational system in a neighborhood of the periodic solution $\Psi(t)$ as follows:

$$\begin{aligned} u' &= A(t)u, \\ \Delta u|_{t=\theta_i} &= D_i u(\theta_i), \end{aligned} \tag{4.7}$$

where the matrix $A(t) \in \mathbb{R}^{n\times n}$ of the form $A(t) = \frac{\partial f(t,x)}{\partial x}|_{x=\Psi(t)}$. The matrices $D_i,\ i = 1, \ldots, n$ will be defined in the remaining part of the study. Solutions of the variational equation (4.7) are the $B-$ derivatives, $(u_j(t)),\ j = 1, 2, \ldots, n$.

We will call the second equation in (4.7) a linearization at discontinuity moments, $\theta_i, i \in \mathbb{Z}$. In what follows, we will consider the linearization at both the transversal and tangential discontinuity points.

4.2.1 Linearization at a transversal point

In this part, our aim is to give information about the matrices D_i and the gradient $\nabla\theta_i(x)$ if the discontinuity point $(\theta_i + jT, \Psi(\theta_i + jT))$, $j \in \mathbb{Z}$, is a transversal one which means $\nabla\tau_i(\Psi(\theta_i + jT))f(\theta_i + jT, \Psi(\theta_i + jT)) \neq 1$. In the following part of the study, we will consider the discontinuity points, for $j = 0$, $(\theta_i, \Psi(\theta_i))$, as discontinuity moments. The linearization in these circumstances is described in [5]. The $T-$ periodic solution $\Psi(t)$ has $p-$ many discontiunity moment in each period and assume that the $k-$th many of them are grazing and the remaining $p - k-$many of them are transversal moments.

Fix a transversal discontinuity point $(\theta_i, \Psi(\theta_i))$, $i = k + 1, \ldots, p$. The following equation is driven by considering the equation $\theta_i(x) = \tau_i(x(\theta_i(x)))$, [5]

$$\nabla\theta_i(\Psi(\theta_i)) = \frac{\nabla\tau_i(\Psi(\theta_i))U(\theta_i)}{1 - \nabla\tau_i(\Psi(\theta_i))f(\theta_i, \Psi(\theta_i))}, \tag{4.8}$$

where $U(t)$, is a fundamental matrix of $u' = f_x(t, x(t))u$ with $U(\kappa) = I$, where I is $n \times n$ identity matrix.

By taking into account derivative of the B-map defined by (4.3) with respect to x we can determine the matrix D_i as

$$\begin{aligned} D_i = &(f(\theta_i, \Psi(\theta_i)) - f(\theta_i, \Psi(\theta_i)))\theta_i'(\Psi(\theta_i)) + J(\Psi(\theta_i)))\theta_i'(x) + \\ &J_{ix}(I + f(\theta_i, \Psi(\theta_i))\theta_i'(\Psi(\theta_i))). \end{aligned} \tag{4.9}$$

4.2.2 Linearization at a grazing point

Assume that the periodic solution $\Psi(t)$ intersects the surface of discontinuity $t = \tau_l(x)$ at the moment, $t = \theta_l$, $1 \leq l \leq k$, tangentially. That is, $(\theta_l + jT, \Psi(\theta_l + jT))$, $j \in \mathbb{Z}$, are grazing points of the periodic solution $\Psi(t)$.

Let us consider the grazing point $(\theta_l, \Psi(\theta_l))$. In the remainder, we will compute the derivatives of functions $\theta_l(x)$ and $W_l(x)$, at the grazing point which are described in the previous part of the study. One can observe from the equality (4.8), there exists two different possibility for the $\nabla\theta_l(x)$, first is at least one of the coordinate of the gradient $\nabla\theta_l(x)$ is infinity or all its coordinates are finite numbers. The complexity arises when at least one of the coordinate is infinity. It can be observed that the singularity is caused by the vector field and the surface of discontinuity. In order to handle with the complexity, the following conditions should be asserted.

(A1) A grazing point is isolated.

(A2) The matrix $W_i(x)$ is a differentiable at $(\theta_l, \Psi(\theta_l))$.

Next, we consider the case when the singularity appears at gradient $\nabla\theta_l(x)$ at the grazing point $(\theta_l, \Psi(\theta_l))$ and we consider that how the impact function eliminate the singularity in the whole system. To suppress the singularity, the harmony of impact law, vector fields and the surface of discontinuity is important. If these components do not work in an harmony, some complex situations may appear. This complex situations are not taken into account in this thesis. Our concern is to determine regular behaviour around the grazing solutions of impulsive systems Let us present the following assumption, which is needed to approve the existence of $B-$ derivatives at the grazing point and in the neighborhood of it.

In the following example, we will take into account the linearization of a function $\theta_l(x)$ at a grazing point.

Example 7 *Consider the following one dimensional system*

$$\begin{aligned} x' &= 4 - \sin(t), \\ \Delta x|_{t=\tau_i(x)} &= -4\pi + 1 - \frac{17}{16}x^2, \end{aligned} \tag{4.10}$$

where $\tau_i(x) = \frac{1}{4}\arctan(x) + i\pi$, $i \in \mathbb{Z}$ *and* $G = (-16, 16)$.

It is easy to verify by substituting (4.10) *that the following expression,*

$$\Psi(t) = \begin{cases} 0 & if \quad t = 0, \\ 4t + \cos(t) - 4\pi + 1 & if \quad t \in (0, \pi], \end{cases} \tag{4.11}$$

defines a $\pi-$*periodic solution of* (4.10)*. The solution is simulated in Figure 4.1.*

For the point $(\zeta_1, \Psi((\zeta_1))) = (0, 0)$*, one can get* $\langle \nabla\tau_0(\Psi((\zeta_1))), f(\zeta_1, \Psi((\zeta_1)))\rangle = \langle \frac{1}{4}, 4\rangle = 1$*. That is,* $(\zeta_1, \Psi((\zeta_1))) = (0, 0)$ *is a grazing point. Denote the grazing point by* $(t^*, x^*) = (0, 0)$.

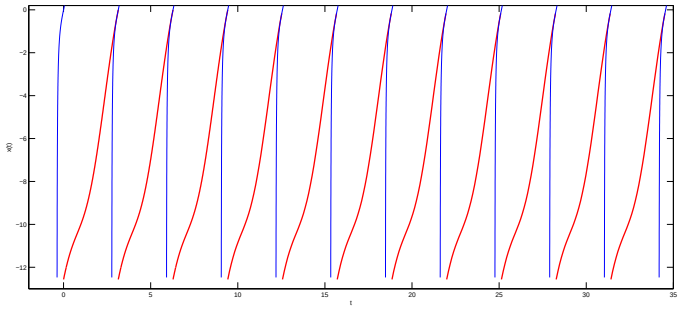

Figure 4.1: The red curves correspond to the periodic solution, $\Psi(t)$, of system (4.10) and the blue curves are the surfaces of discontinuity, $t = \tau_i(x),\ i = 0, 1, 2, \ldots, 11$.

The periodic solution $\Psi(t)$ *has one discontinuity point* $(\zeta_1, \Psi((\zeta_1))) = (0, 0)$ *in the period interval* $[0, \pi]$*, which is a grazing point. Our aim in this example is to verify the existence, uniqueness and extension of solutions of (4.10) and derive the linearization for (4.10) around the grazing periodic orbit,* $\Psi(t)$*. The moments* $t = i\pi$, $i \in \mathbb{Z}$*, are also grazing.*

Let us verify the conditions $(N1)-(N4)$. *For any* $\tilde{x}\in G$, *and* $i\in\mathbb{Z}$, *because* $\tau_i(x)$ *is increasing function and* $\tilde{x}>\tilde{x}-4\pi+1-\frac{17}{16}\tilde{x}^2$, *it is true that* $\tau_i(\tilde{x}-4\pi+1-\frac{17}{16}\tilde{x}^2)<\tau_i(\tilde{x})$. *This validates the condition* $(N1)$. *It is appearant that* $(N2)$ *is also true. There exists positive numbers* $N=1/4$ $C=4$, *with the inequality* $CN<1$, *which is true for all point in the domain* G *except the grazing points* $(i\pi,0)$, $i\in\mathbb{Z}$. *The differentiability in the grazing point will be expressed in details further. The following ones can be estimated as*

$$\max_{(t,x)\in I\times G}\|f(t,x)\|=\max_{(t,x)\in\mathbb{R}\times G}\|4-\sin(t)\|\leq 4,\max_{x\in G}\|\frac{\partial\tau_i(x)}{\partial x}\|=$$

$$\max_{x\in G}\|\frac{1}{4(x^2+1)}\|\leq\frac{1}{4}.$$

So, $(N3)$ *is verified. For all* $x\in G$ *and* $i\in\mathbb{Z}$, *we have*

$$\max_{0\leq\sigma\leq 1}\langle\frac{\partial\tau_i(x+\sigma I_i(x))}{\partial x},I_i(x)\rangle=\max_{0\leq\sigma\leq 1}\langle\frac{1}{1+(x+\sigma(-\frac{64\pi+33}{16}))^2},-\frac{64\pi+33}{16}\rangle\leq 0.$$

This verifies condition $(N4)$.

Now, we will continue with the linearization at the point $(\zeta_1,\Psi((\zeta_1)))=(0,0)$. *The grazing point is isolated as well. First, consider a near solution of* (4.10) $\bar{x}(t)=x(t,0,\Delta x)$ *to* $\Psi(t)$, *which meets the surface* $\tau_0(x)=\frac{1}{4}\arctan(x)$, *at the point* $(\frac{1}{4}\arctan(\bar{x}),\bar{x})$. *Considering derivative of* (4.3) *with respect to a solution of* (4.10) *near to the periodic solution, we obtain that*

$$\frac{\partial W_i(x)}{\partial x}=\int\limits_{\xi_i}^{\theta_i(x)}\frac{\partial f(u,x_0(u))}{\partial x}\frac{\partial x_0(u)}{\partial x}du+f(\theta_i(x),x_0(\theta_i(x)))\frac{\partial\theta_i(x)}{\partial x}+$$

$$\frac{\partial J_i(x)}{\partial x}\Big(1+\int\limits_{\xi_i}^{\theta_i(x)}\frac{\partial f(u,x_0(u))}{\partial x}\frac{\partial x_0(u)}{\partial x}du+f(\theta_i,x_0(\theta_i(x)))\frac{\partial\theta_i}{\partial x}\Big)\tag{4.12}$$

$$+\int\limits_{\theta_i}^{\xi_i}\frac{\partial f(u,x_1(u))}{\partial x}\frac{\partial x_1(u)}{\partial x}du-f(\theta_i(x),x_1(\theta_i(x)))\frac{\partial\theta_i(x)}{\partial x}.$$

Substituting $(\frac{1}{4}\arctan(\bar{x}),\bar{x})$ *to* (4.12), *we have*

$$\frac{\partial W_i(x)}{\partial x}=f(\theta_i(\bar{x}),x_0(\theta_i(\bar{x})))\frac{\partial\theta_i(\bar{x})}{\partial x}+\frac{\partial J_i(\bar{x})}{\partial x}\Big(1+$$

$$f(\theta_i(\bar{x}),x_0(\theta_i(\bar{x})))\frac{\partial\theta_i(\bar{x})}{\partial x}\Big)f(\theta_i(\bar{x}),x_1(\theta_i(\bar{x})))\frac{\partial\theta_i(\bar{x})}{\partial x}.\tag{4.13}$$

Next, we will evaluate the derivative $\frac{\partial \theta_i(\bar{x})}{\partial x}$. *To do it, the formula* (4.8) *will be taken into account, and the derivative is calculated as* $\frac{\partial \theta_i(\bar{x})}{\partial x} = \frac{1}{4\tan^2(4\bar{t})+2\sin(2\bar{t})}$. *It is easy to see that as* $\bar{t}$ *tends to zero the fraction diverges to infinity. Moreover, it is easy to see that* $\bar{x} = x(\bar{t})$ *Thus, at the grazing point singularity appears, to cope with the singularity we will utilize the compliance of vector field and the jump function and we consider the equality* (4.13)*, and we get*

$$\begin{aligned} \frac{\partial W_i(\bar{x})}{\partial x} &= \frac{4-\sin(\bar{t})}{4\tan^2(4\bar{t})+\sin(\bar{t})} - \frac{\tan(4\bar{t})}{16}\Big(1+\frac{4-\sin(\bar{t})}{4\tan^2(4\bar{t})+2\sin(2\bar{t})}\Big) - \\ \frac{4-2\sin(2\bar{t})}{4\tan^2(4\bar{t})+2\sin(2\bar{t})} &= -\frac{4\bar{x}^3+4\bar{x}}{64\bar{x}^2+32\sin(0.5\tan(\bar{x}))}, \end{aligned} \tag{4.14}$$

calculating above expression as $\bar{x}$ *tends to the grazing point* $x^* = 0$, *we obtain that*

$$\lim_{\bar{x}\to x^*} \frac{\partial W_i(\bar{x})}{\partial x} = \lim_{\bar{x}\to 0} -\frac{4\bar{x}^3+4\bar{x}}{64\bar{x}^2+16\sin(0.5\tan(\bar{x}))} = Z, \tag{4.15}$$

where $Z = -\frac{1}{2}$.

In order to obtain a linearization system around grazing periodic solution $\Psi(t)$, *the differentiability of the functions* $W_i(x)$ *at the grazing point* x^* *should be verified. To accomplish it, we will verify the derivative of the function* $W_{ix}(x)$ *exists at the point* x^*. *The derivative can be calculated as follows*

$$W_{ix}(x^*) = \lim_{\bar{x}\to x^*} \frac{W_i(x) - W_i(x^*)}{x - x^*},$$

above equation can be calculated by applying Mean Value Theorem [11], we obtain that

$$W_{ix}(x^*) = \lim_{\bar{x}\to x^*} \frac{\frac{\partial W_i(\bar{x})}{\partial x}(x-x^*) - Z(x-x^*)}{x-x^*} + Z, \tag{4.16}$$

where $\bar{x}$ *lies in the interval* $(x^*-\epsilon, x^*+\epsilon)$, *for some positive* ϵ. *By means of expressions* (7) *with* (4.16) *it is easy to obtain that*

$$W_{ix}(x^*) = Z. \tag{4.17}$$

Then, we can conclude that the linearization exists at the grazing point and the derivative is continuous as well. This verifies condition $(A2)$.

Assume that the linearization of $\theta_l(x)$ at the grazing point, $(\theta_l, \Psi(\theta_l))$, exists in the above defined sense for each $l = 1, 2, \ldots, k$. Because of the previous discussion, the

gradient, $\nabla\theta_l(x)$, depends on the solution $x_1(t) = x(t, t_0, x_0 + \Delta x)$ of (4.1), neighbor to $\Psi(t)$, with small $\|\Delta x\|$.

Differentiating equation (4.3), we get the following one :

$$\begin{aligned}\frac{\partial W_l(\Psi(\theta_l))}{\partial x_j} &= (f(\theta_l, \Psi(\theta_l)) - f(\theta_l, \Psi(\theta_l)))\nabla\theta_l(\Psi(\theta_l)) \\ &+ J_{lx}(\Psi(\theta_l))(I + f(\theta_l, \Psi(\theta_l))\nabla\theta_l(\Psi(\theta_l))).\end{aligned} \tag{4.18}$$

Let us formulate one of them. Other constructive conditions will be investigated in our future investigations.

(N5) For each $\Delta x \in \mathbb{R}^n$, the variational system (4.7), around $\Psi(t)$ on $\mathbb{R}$, the linearization system is

$$\begin{aligned}u' &= A(t)u, \\ \Delta u|_{t=\theta_i} &= D_i u,\end{aligned} \tag{4.19}$$

such that $D_{i+p} = D_i$.

The following assertions can be verified in the way of presented in Theorem 6.1.1 in [5].

Theorem 5 *Assume that conditions* $(N1) - (N5)$ *are valid. Then the solution* $\Psi(t)$ *of* (4.1) *for each finite interval* $[0, a]$, $a > 0$, *has* $B-$ *derivatives with respect to initial conditions,* $(u_j(t))$, *which satisfies the variational equation* (4.7) *with initial values* $e_j = (\underbrace{0, 0, \ldots, 1}_{j}, 0, \ldots, 0)$, $j = 1, 2, \ldots, n$.

4.2.3 Stability of the grazing periodic solution

The system (4.19) is the variational system around the grazing periodic solution $\Psi(t)$. One can derive the matrix of monodromy, $U_j(T)$, and the corresponding Floquet multipliers ρ_i, $i = 1, 2, \ldots, n$. The next assumption is needed to verify the stability of the periodic solution, $\Psi(t)$.

(N6) $|\rho_i| < 1$, $i = 1, 2, \ldots, n$.

Theorem 6 *Assume that conditions* $(N1) - (N6)$ *and assumptions* $(A1)$ *and* $(A2)$ *are valid. Then,* $T-$ *periodic solution* $\Psi(t)$ *of (4.1) is asymptotically stable.*

The last theorem can be proved similarly to Theorem 7.2.1 in [5].

We will exhibit some examples to actualize our theoretical results in the following section.

4.3 Examples

Example 8 *In this example, we will continue to analyze the system in Example 7. We derive the linearization for* $\theta(x)$ *at the grazing point* $(\theta_l, \Psi(\theta_l)) = (0, 0)$ *there. Thus, the linearization for* $\Psi(t)$ *consists of a* $\pi-$ *periodic system,*

$$\begin{aligned} u' &= 0, \\ \Delta u|_{t=\pi i} &= Du, \end{aligned} \tag{4.20}$$

where coefficient D *by formula* (4.18)*, is equal to* $-\frac{1}{4}$*. The multiplier of the variational system (4.20)is* $\rho = \frac{3}{4}$*. It is inside the unit circle and condition* $(N6)$ *holds. The conditions* $(N1) - (N6)$ *are valid, then by Theorem 6, the periodic solution* $\Psi(t)$ *of (4.10) is asymptotically stable. The stability of the solution,* $\Psi(t)$*, is pictured in Fig. 4.2 through simulations.*

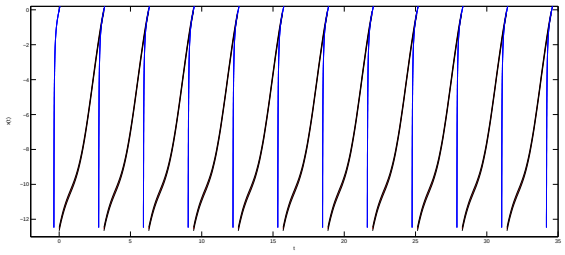

Figure 4.2: The black curves are the solutions of (4.10) with initial values $(-\pi/16, -1)$ and $(\pi/16, 1)$, respectively. The red one corresponds to the periodic solution $\Psi(t)$ and the blue curves are the surfaces of discontinuity, $t = \tau_i(x)$, $i = 0, 1, 2, \ldots, 11$.

Example 9 *In this example, we will consider the following system of differential equation with variable moment of impulse actions*

$$\begin{aligned} x_1' &= -x_1 + 4, \\ x_2' &= 2\pi \sin(2\pi t) + 1, \\ \Delta x_1|_{t=\tau_i(x)} &= -4(x_1 + 0.75x_1^2) - 1, \\ \Delta x_2|_{t=\tau_i(x)} &= 1 - 0.25x_2, \end{aligned} \tag{4.21}$$

where $\tau_i(x) = 0.25x_1 + i$. *For this system, denote by* $x = (x_1, x_2)$. *Let the domain of the system be* $G = \{(t, x) |\ t \in \mathbb{R},\ x_1 \in (-10, 10),\ x_2 \in (-2, 2)\}$. *System* (4.21) *is of the type* (4.1) *with* $f(t, x) = (-x_1 + 4, 2\pi \sin(2\pi t) + 1)$ *and* $J_i(x) = (-x_1 - 1, 1)$. *It is easy to observe that* $f(t, x)$ *is a* $1-$*periodic function.*

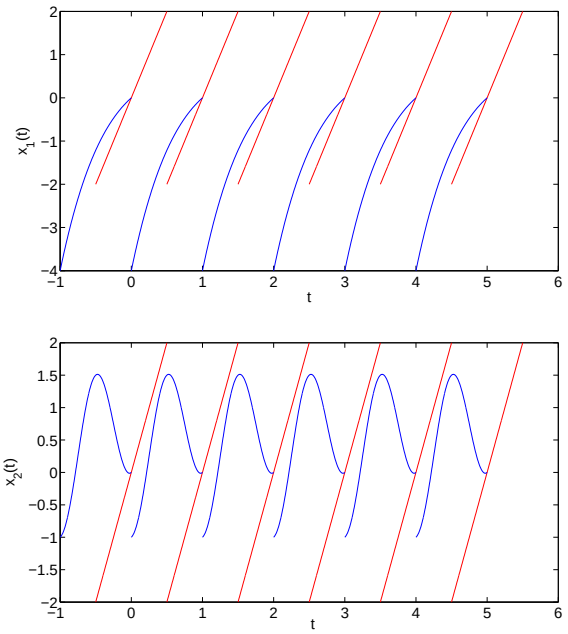

Figure 4.3: The above figure is for first component $x_1(t)$ of the periodic solution, $\Psi(t)$, with grazing points at $(i, 0, 0)$, $i \in \mathbb{Z}$ versus time, t and the second component $x_2(t)$ of the periodic solution, $\Psi(t)$, with grazing points at $(i, 0, 0)$, $i \in \mathbb{Z}$ versus time, t, is the right one.

It can be easily verified that the system admits a $1-$*periodic solution of the form*

$$\Psi(t) = \begin{cases} (0, 0) & if \quad t = 0, \\ (t\exp(-t) - \exp(-1), -\cos(2\pi t) + t - 1) & if \quad t \in (0, 1], \end{cases} \tag{4.22}$$

with discontinuity moments $\theta_i = i, i \in \mathbb{Z}$. It is easy to determine, utilizing the equality $\langle (4,0),(0.25,-2)\rangle = 1$, that $(\theta_1, \Psi(\theta_1)) = (0,0,0)$ is a grazing point. Moreover, by means of the periodicity of $\Psi(t)$, we can conclude that all moments $t = i\pi$, $i \in \mathbb{Z}$, are grazing ones. The components of periodic solution is simulated in Figure 4.3.

For ever point $(\tilde{x}_1, \tilde{x}_2) \in G$, the inequality $0.25(\tilde{x}_1 - 1) < 0.25\tilde{x}_1$ is true, this validates $(N1)$. The condition $(N2)$ is also valid because $\tau_i(x) = 0.25x_1 + i < 0.25x_1 + i + 1 = \tau_{i+1}(x)$. Due to the vector-field, surface of discontinuity and the jump function, it is easy to say that every solution which meets the surface of discontinuity in the neighborhood of the grazing periodic solution $\Psi(t)$ intersects the surface at most once. For this reason, there is no need to check $(N3)$.

Next, we will continue with the linearization of the system (4.21) *around the periodic solution $\Psi(t)$. To obtain it, first, we will consider the derivative of the formula* (4.3)*, then we get*

$$\begin{aligned}\frac{\partial W_i(x)}{\partial x_1^0} &= \int_{\xi_i}^{\theta_i(x)} \frac{\partial f(u,x_0(u))}{\partial x}\frac{\partial x_0(u)}{\partial x}du + f(\theta_i(x),x_0(\theta_i(x)))\frac{\partial \theta_i(x)}{\partial x} + \\ &\frac{\partial J_i(x)}{\partial x}\Big(\begin{bmatrix}1\\0\end{bmatrix} + \int_{\xi_i}^{\theta_i(x)} \frac{\partial f(u,x_0(u))}{\partial x}\frac{\partial x_0(u)}{\partial x}du + f(\theta_i,x_0(\theta_i(x)))\frac{\partial \theta_i}{\partial x}\Big) \\ &+ \int_{\theta_i}^{\xi_i} \frac{\partial f(u,x_1(u))}{\partial x}\frac{\partial x_1(u)}{\partial x}du - f(\theta_i(x),x_1(\theta_i(x)))\frac{\partial \theta_i(x)}{\partial x}.\end{aligned} \tag{4.23}$$

Consider a near solution $\tilde{x}(t)$ of (4.21) *to $\Psi(t)$. Assume that near solution meets the surface of discontinuity $t = \tau_i(x)$, at the point $\bar{x}$. Denote the meeting point by $\bar{x} = (\bar{x}_1, \bar{x}_2) = \tilde{x}(\tau_i(\bar{x}))$, substituting it to* (4.23)*, we have*

$$\begin{aligned}\frac{\partial W_i(\bar{x})}{\partial x_1^0} &= f(\theta_i(\bar{x}),\bar{x}(\theta_i(\bar{x})))\frac{\partial \theta_i(\bar{x})}{\partial x} + \frac{\partial J_i(\bar{x})}{\partial x}\Big(\begin{bmatrix}1\\0\end{bmatrix} + \\ &f(\theta_i(\bar{x}),\bar{x}(\theta_i(\bar{x})))\frac{\partial \theta_i(\bar{x})}{\partial x}\Big) + f(\theta_i(\bar{x}),x_1(\theta_i(\bar{x})))\frac{\partial \theta_i(\bar{x})}{\partial x}.\end{aligned} \tag{4.24}$$

Substitute the function $f(t,x)$ and the Jacobian $J_x(x)$ into (4.24)*, it is easy to obtain*

that

$$\frac{\partial W_i(\bar{x})}{\partial x_1^0} = \begin{bmatrix} \bar{x}_1 + 0.25 \\ 2\pi \sin(2\pi t) + 1 \end{bmatrix} \frac{\partial \theta_i(\bar{x})}{\partial x_1^0} + \frac{\partial J_i(\bar{x})}{\partial x} \Big(\begin{bmatrix} 1 \\ 0 \end{bmatrix} + \begin{bmatrix} \bar{x}_1 + 0.25 \\ 2\pi \sin(2\pi t) + 1 \end{bmatrix} \frac{\partial \theta_i(\bar{x})}{\partial x_1^0} \Big) + \begin{bmatrix} 0.75\bar{x}_1^2 - 1 + 0.25 \\ 2\pi \sin(2\pi t) + 1 \end{bmatrix} \frac{\partial \theta_i(\bar{x})}{\partial x_1^0}, \tag{4.25}$$

In order to evaluate above expression, we need to find the derivative $\frac{\partial \theta_i(\bar{x})}{\partial x_1^0}$*, by applying formula* (4.8)*, we obtain that* $\frac{\partial \theta_i(\bar{x})}{\partial x_1^0} = \frac{1}{\bar{x}_1}$*. It is easy to see that at the grazing point the derivative is infinity. To handle with it, we will apply a special jump function and vector field. Substituting the derivative to* (4.25)*, we get*

$$\frac{\partial W_i(\bar{x})}{\partial x_1^0} = \begin{bmatrix} \bar{x}_1 - 0.1\bar{x}_1^2 \\ 0 \end{bmatrix} \frac{1}{\bar{x}_1} + \begin{bmatrix} 0.2x_1 & 0 \\ 0 & 0 \end{bmatrix} \Big(\begin{bmatrix} 1 \\ 0 \end{bmatrix} + \begin{bmatrix} \bar{x}_1 + 0.25 \\ 2\pi \sin(2\pi t) + 1 \end{bmatrix} \frac{1}{\bar{x}_1} \Big) = \begin{bmatrix} 0.2x_1 - 0.8 & 0 \\ 0 & 0 \end{bmatrix} \tag{4.26}$$

By applying similar technique one can determine that

$$\frac{\partial W_i(\bar{x})}{\partial x_2^0} = \begin{bmatrix} 0 \\ 0 \end{bmatrix}. \tag{4.27}$$

Now, we will continue with the linearization around the grazing periodic solution $\Psi(t)$*.*

Depending on the position of the near solution, the variational system for the periodic solution, $\Psi(t)$*, is of the form*

$$\begin{aligned} u_1' &= -u_1, \\ u_2' &= 0, \\ \Delta u|_{t=\pi i} &= D_i u, \end{aligned} \tag{4.28}$$

where $D_i \equiv \begin{bmatrix} 0.8 & 0 \\ -0.1 & 0 \end{bmatrix}$*, and* $\theta_i = i$*,* $i \in \mathbb{Z}$*. System (4.28) is* $(1,1)-$ *periodic. The multipliers are equal to* $\rho_1 = 0.8, \quad \rho_2 = 0.3679$*. All of them are inside the unit circle, and by Theorem 6 one can conclude that the periodic solution is asymptotically stable. Considering the near solutions with initial values* $(-1, -3.2, -1.4)$ *and*

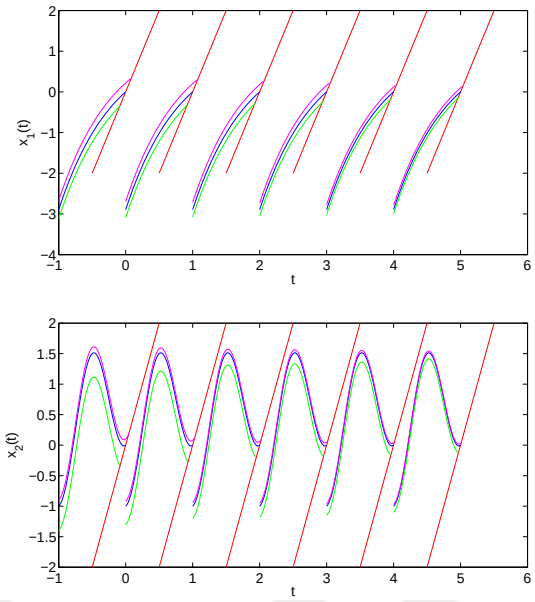

Figure 4.4: The above figures are for the first and second components of the periodic solution, $\Psi(t)$. Green curves are the solution $x_1(t)$ of (4.21) with initial values $(-1, -3.2, -1.4)$ and $(-1, -2.8, -0.8)$, and red curves are the grazing periodic solution, which have grazing point at $(i\pi, 0, 0)$, $i \in \mathbb{Z}$.. The bottom one is for the second component $x_2(t)$ of the periodic solution, $\Psi(t)$.

$(-1, -2.8, -0.8)$, *by using numerical simulation tools, we depicted the components of the near solutions to the components of* $\Psi(t)$ *in Figure 4.4.*

4.4 Regular perturbations around grazing periodic solution

Let D_x be a domain in $\mathbb{R}^n$ having compact closure, and let μ_0 be a fixed positive number. On the set

$$D = \{(x, t, i, \mu | x \in D_x,\ -\infty < t < \infty,\ i \in \mathbb{Z}, -\mu_0 < \mu < \mu_0\}.$$

we take into account the following system,

$$\begin{aligned} x' &= f(t, x) + \mu\phi(t, x, \mu), \\ \Delta x|_{t=\tau_i(x)+\mu\eta_i(x,\mu)} &= I_i(x) + \mu\theta_i(x, \mu), \end{aligned} \tag{4.29}$$

where the functions I_i, τ_i, θ_i and η_i have continuous partial derivatives of second order with respect to the variables $\mu, x_j,\ j = 1, 2, \ldots, n,\ f \in C^{(0,2)}(D) \cap C^{(1,2)}(D_0)$,

$\phi \in C^{(0,1,1)}(D) \cap C^{(1,2,2)}(D_0)$, where D_0 is the union of certain neighborhoods of the surfaces $t = \tau_i(x)$, $i \in \mathbb{Z}$. Moreover, we will assume that there exist a real number $T > 0$ and an integer $p > 0$ for which the following equalities are valid in the domain D :

$f(t+T,x) = f(t,x)$, $\phi(t+T,x,\mu) = \phi(t,x,\mu)$, $I_{i+p} = I_i$, $\theta_{i+p} = \theta_i$, $\tau_{i+p} = \tau_i + T$ and $\eta_{i+p} = \eta_i$.

The generating system is of the form

$$\begin{aligned} x' &= f(t,x), \\ \Delta x|_{t=\tau_i(x)} &= I_i(x). \end{aligned} \tag{4.30}$$

Assume that system (4.30) has a periodic solution $\Psi(t)$ with period T and satisfies the conditions $(N1)-(N5)$ and assumptions $(A1)$ and $(A2)$ are valid. If $|\mu|$ is sufficiently small, then (4.29) admits a $T-$ periodic solution which converges $\Psi(t)$ as $|\mu|$ tends to zero.

The next examples are presented to actualize our theoretical results and the increment of the periodic solution is demonstrated through simulation.

Example 10 *Let us consider the following one dimensional system with variable moments of impulses*

$$\begin{aligned} x' &= 4 - 2\sin(2t) + \mu\phi(t,x,\mu), \\ \Delta x|_{t=\tau_i(x)+\mu\kappa_i(x,\mu)} &= -4\pi - 1 - \frac{15}{16}x + \mu\eta_i(x,\mu), \end{aligned} \tag{4.31}$$

where μ is a sufficiently small parameter. The system is of the form (4.10) for $\mu = 0$. Considering the system (4.29)*, the functions and matrices can be determined as $A = 0$, $f(t) = 4 - 2\sin(2t)$, which is $\pi-$periodic, $I_i = -4\pi - 1 - \frac{15}{16}x$, $\mu = \frac{1}{32}$ and $\eta_i(x,\mu) = 2(x^2 - \tan^2(0.04) + \frac{15}{16}x)$.*

The generating system can be determined as in the form

$$\begin{aligned} x' &= 4 - 2\sin(2t), \\ \Delta x_2|_{t=\tau_i(x_1)} &= -4\pi - 1 - \frac{15}{16}x. \end{aligned} \tag{4.32}$$

The eigenvalue of the matrix of monodromy for it can be determined as ρ, which is not equal to one, so we can say that the system (4.31) *has a unique $T-$periodic solution, $\Psi_\mu(t)$ for μ sufficiently small.*

4.5 Conclusion

This study includes information about non autonomous system with non-fixed moments of impulses whose solutions have grazing points. By applying a novel technique, we construct a linearization system around the grazing periodic solution. Concrete mechanical models are demonstrated and some simulations are presented to visualize theoretical results. By applying regular perturbations, existence of periodic solution of these systems are investigated and exemplified. Grazing solutions are widely investigated in mechanical systems, but there is a few studies can be found in neural networks which includes graziness. However, the grazing bifurcation and graziness are not widely investigated for neural networks. Further, we will apply our methods to investigate the stability of neural networks model which has grazing points in other words which meets the threshold tangentially.

4.6 Horizontal and vertical grazing

Horizontal and vertical grazing should be considered because they cannot be taken into account by utilizing the existing results for the grazing phenomenon in the literature. In a geometrical sense, the horizontal grazing occurs when the surface of discontinuity has a tangent plane at the grazing point which is parallel to the time axis and the vertical grazing occurs whenever the tangent plane at the grazing point is perpendicular to the time axis. The horizontal and vertical grazing are depicted in Figures 4.5 and 4.6, respectively. The appropriate definitions of the horizontal and vertical grazing for non-autonomous system whose vector field and surfaces are defined by non-autonomous functions and the definition of horizontal grazing for non-autonomous system with cylindrical surface of discontinuity are given. The periodic solutions which have vertical or horizontal grazing are obtained in specific examples. The stabilities of them are examined by constructing proper linearization systems around the periodic solutions. The periodic solutions and their stabilities are observed through simulations and the results are depicted.

Take into account the following differential equation

$$x'' + a(t)x' + b(t)x = f(t, x, x'), \tag{4.33}$$

where $a(t)$ is a variable damping function, $b(t)$ is a variable spring function and $f(t, x, x')$ is a force applied to the system. Assume that it is subject to impacts with a cylindrical surface $\Gamma = \{(t, x, x')|\Phi(x, x') = 0\}$. The type of the barrier is common for impact mechanisms. To illustrate, the surfaces $x = X_0$ and $x' = X_0'$ in (t, x, x') are cylindrical surfaces. Thus, if the grazing occurs in the non-autonomous equation (4.33), then it is mainly a horizontal one as expected.

In the paper [101], the system of leaky integrate-and-fire neuron model is presented as

$$\begin{aligned} &\frac{du}{dt} = -ku + S(t), \\ &u(t^+) = 0 \quad \text{if} \quad u(t) = \Theta, \end{aligned} \tag{4.34}$$

where u is the internal state, k is the leaky parameter and $S(t)$ is the input time series which is positive. If the internal state u reaches the threshold Θ the spike occurs and the internal state immediately resets to the resting state $u = 0$. In the leaky integrate and fire neuron model, the grazing takes place whilst there exists a time T such that $\frac{du}{dt}_{t=T} = -ku + S(T) = 0$, (See Fig. 4.6, it is taken from the paper [101].) This demonstrates that the horizontal grazing can be observed in neural networks. Moreover, it is determined that the bifurcation results in the breaking of inter spike interval attractors. In [27], it is demonstrated that the grazing bifurcation can be utilized to find the Arnol'd tongue diagram for mode-locked responses and determined that the horizontal grazing phenomenon in integrate-and-fire neuron model causes the passing to a regular firing either from a fast firing or from a doublet firing and it causes the diminish of the stability of sub-threshold oscillations.

The presentation of the vertical grazing is beneficial since the method of analysis can be applied for models with singularities under impacts. Such systems can be seen in the models of electrically driven robot manipulator which has slower mechanical dynamics and faster electrical dynamics. In this type of systems, we should consider the problem in two parts such as one part is slower and one part is faster dynamics [122]. For which the vertical grazing can be utilized in the analysis of faster dynamics.

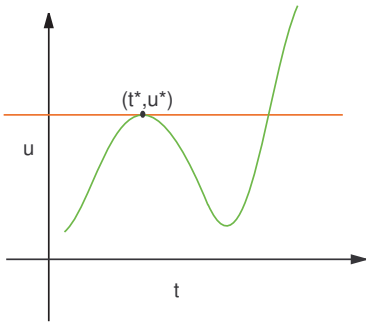

Figure 4.5: Horizontal grazing in neural networks [101].

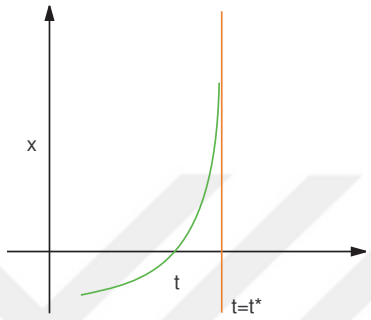

Figure 4.6: Vertical grazing.

4.7 Grazing non-autonomous system with variable impulse moments

Let $\mathbb{R}$, $\mathbb{N}$ and $\mathbb{Z}$ be the sets of all real numbers, natural numbers and integers, respectively. Let $G \subseteq \mathbb{R}^n$ be an open and connected set. The non-autonomous systems with variable moments of impulses consist of two different systems. One is that the vector field as well as surfaces are defined by non-autonomous functions and the other is the vector field defined as non-autonomous function bu the surfaces defined as an autonomous functions in other words the surfaces are cylindrical.

The first type can be considered as a following system

$$\begin{aligned} x' &= f(t,x), \\ \Delta x|_{t=\tau_i(x)} &= J_i(x), \end{aligned} \tag{4.35}$$

where $(t,i,x) \in \mathbb{R} \times \mathbb{Z} \times G$, the function $f(t,x)$ is continuously differentiable in x and t on $\mathbb{R} \times G$, and $T-$ periodic in t, i.e. $f(t+T,x) = f(t,x)$, functions $J_i(x)$ and $\tau_i(x)$, $i \in \mathbb{Z}$, are differentiable on G and $J_i(x)$ satisfies the following equality, $J_{i+p}(x) = J_i(x)$ for a natural number p and $\tau_i(x)$ has $(T,p)-$property, i.e. $\tau_i(x) + T = \tau_{i+p}(x)$ for all $i \in \mathbb{Z}$.

The other type of system can be defined by the following system of impulsive differential equations

$$\begin{aligned} x' &= f(t,x), \\ \Delta x|_{x\in\Gamma} &= J_i(x), \end{aligned} \tag{4.36}$$

where Γ is a cylindrical surface of discontinuity and defined as $\Gamma = \{(t,x)|\Phi(x) = 0,\ t \in \mathbb{R},\ x \in G\}$. The function $f(t,x)$ is continuously differentiable in x and t on $\mathbb{R}\times G$, and $T-$ periodic in t, i.e. $f(t+T,x) = f(t,x)$, functions $J_i(x)$ and $\Phi(x) = 0$ are differentiable on G and $J_i(x)$ satisfies the following equality, $J_{i+p}(x) = J_i(x)$ for a natural number p and for all $i \in \mathbb{Z}$.

To simplify the notation, we need the following system of ordinary differential equations

$$y' = f(t,y). \tag{4.37}$$

Assume that the conditions $(N1) - (N3)$ are valid. Then, the solution of (4.35) intersects the surfaces of discontinuity exactly once [5].

Consider a periodic solution $\Psi(t)$ of (4.35). Denote by θ_i, $i \in \mathbb{Z}$, the moment of meeting of a the periodic solution with the surface $t = \tau_i(x)$, $i \in \mathbb{Z}$. The intersection moments satisfy the property that $\theta_{i+p} = \theta_i + T$, $i \in \mathbb{Z}$, where p is a positive number.

Definition 11 *There is a horizontal grazing of the periodic solution $\Psi(t)$ of* (4.35) *at a point $(\theta_l, \Psi(\theta_l))$, $l = 1,2,\ldots,p$, if for some $j = 1,2,\ldots,n$, the conditions are fulfilled:*

(i) $f_j(\theta_l, \Psi(\theta_l)) = 0$,

(ii) a function

$t = \eta(x_j) \equiv \tau_l(\Psi_1(\theta_l), \Psi_2(\theta_l), \ldots, \Psi_{j-1}(\theta_l), x_j, \Psi_{j+1}(\theta_l), \ldots, \Psi_n(\theta_l))$ *is invertible near $x_j = x_j^0 = \Psi_j(\theta_l)$ for $x_j \le x_j^0$ or $x_j \ge x_j^0$, and the one sided derivative $[\eta^{-1}(t)]'_-|_{t=\theta_l}$ or $[\eta^{-1}(t)]'_+|_{t=\theta_l}$ is equal to zero, respectively.*

Definition 12 *A vertical grazing of the periodic solution $\Psi(t)$ of* (4.35) *at a point*

$(\theta_l, \Psi(\theta_l))$ *exits at the point* $(\theta_l, \Psi(\theta_l))$ $l = 1, 2, \ldots, p$, *if for some* $j = 1, 2, \ldots, n$, *the following conditions are fulfilled:*

(i) a function $x_j = \Psi_j(t)$ *is invertible near* $x_j = x_j^0 = \Psi_j(\theta_l)$ *for* $x_j \leq x_j^0$ *or/and* $x_j \geq x_j^0$, *and the one sided derivative* $[\Psi_j^{-1}(x_j)]'_-|_{x=x_j}$ *or/and* $[\Psi_j^{-1}(x_j)]'_+|_{x=x_j}$ *is equal to zero, respectively.*

(ii) $\tau_{lx_j}(\Psi(\theta_l)) = 0$.

Consider a periodic solution $\Psi(t)$ of (4.36). Denote by θ_i, $i \in \mathbb{Z}$, the meeting moments of $\Psi(t)$ with the surface $\Phi(x) = 0$. They satisfy the property for all $i \in \mathbb{Z}$, $\theta_{i+p} = \theta_i + T$, where p is a positive number.

Definition 13 *There is a horizontal grazing of the periodic solution* $\Psi(t)$ *of the system* (4.36) *at a point* $(\theta_l, \Psi(\theta_l))$, *where* $l = 1, 2, \ldots, p$, *if the equality at the point* $\langle \Phi(\Psi(\theta_l)), f(\theta_l, \Psi(\theta_l)) = 0$ *is valid.*

Next, we will construct $B-$equivalent system to the system (4.35) [5], which reduces the systems with variable moments of impulses to that with fixed moments of impulses. For the system (4.36), it can be obtained similarly. Consider a point $(\theta_i, x) \in \mathbb{R} \times G$ on the periodic solution with a fixed $i \in \mathbb{Z}$. Let $\xi_i = \xi_i(x)$ be the meeting moment of the solution $x(t) = x(t, \theta_i, x)$ of (4.37). Additionally, assume that the solution $x_1(t) = x(t, \theta_i, x(\theta_i))$ of (4.37) exists on $\widehat{[\theta_i, \xi_i]}$. The $B-$ map $W : x \to x_1(\xi)$ can be constructed as

$$W_i(x) = \int_{\theta_i}^{\xi_i} f(u, x(u))du + J_i(x + \int_{\theta_i}^{\xi_i} f(u, x(u))du) + \int_{\xi_i}^{\theta_i} f(u, x_1(u))du. \quad (4.38)$$

Let us take into account the following system of differential equations with fixed moments of impulses

$$\begin{aligned} y' &= f(t, y), \\ \Delta y|_{t=\theta_i} &= W_i(y). \end{aligned} \quad (4.39)$$

Due to the construction of $W_i(x)$ systems (4.35) and (4.39) are $B-$equivalent [5] in the neighborhood of $\Psi(t)$. That is, if $x(t) : U \to G$ is a solution of (4.35), then

coincides with a solution $y(t) : U \to G$ when $y(t_0) = x(t_0)$, for $t_0 \in U \setminus \cup_{i\in\mathbb{Z}}\widehat{[\theta_i, \xi_i]}$. Particularly, $x(\theta_i) = y(\theta_i+),\ x(\xi_i) = y(\xi_i),$ if $\theta_i > \xi_i$, $x(\theta_i) = y(\theta_i),\ x(\xi_i+) = y(\xi_i),$ if $\theta_i < \xi_i$. It is easy to see that $\Psi(t)$ is also a solution of (4.39) as well. In the remaining part of the study, we will consider (4.39) instead of (4.35).

Assume that the periodic solution $\Psi(t)$ of (4.35) meets the surface $t = \tau_i(x)$ at the moment $t = \theta_i$, transversally. Let us start with the derivative of the equation $\theta_i(x) = \tau_i(x(\theta_i(x)))$, [5],

$$\nabla\theta_i(\Psi(\theta_i)) = \frac{\nabla\tau_i(\Psi(\theta_i))U(\theta_i)}{1 - \nabla\tau_i(\Psi(\theta_i))f(\theta_i, \Psi(\theta_i))}, \tag{4.40}$$

where $U(t)$, is a fundamental matrix of $u' = f_x(t, \Psi(t))u$ with $U(\theta_i) = I$, where I is $n \times n$ identity matrix.

By taking the derivative of the B-map defined by (4.38) with respect to x, we can determine the matrix D_i as

$$\begin{aligned} D_i = W_{ix}(\Psi(\theta_i)) &= (f(\theta_i, \Psi(\theta_i)) - f(\theta_i, \Psi(\theta_i)))\theta_i'(\Psi(\theta_i)) \\ &+ J(\Psi(\theta_i))\theta_i'(x) + J_{ix}(I + f(\theta_i, \Psi(\theta_i))\theta_i'(\Psi(\theta_i))), \end{aligned} \tag{4.41}$$

where the Jacobian matrix can be obtained as $W_{ix}(\Psi(\theta_i)) = [\frac{\partial W_i}{\partial x_1}, \frac{\partial W_i}{\partial x_2}, \ldots, \frac{\partial W_i}{\partial x_n}]$.

It is easy to see that the linearization at the point $(\theta_i, \Psi(\theta_i))$ can be obtained as

$$\Delta u|_{t=\theta_i} = D_i u, \tag{4.42}$$

with $D_{i+p} = D_i,\ i \in \mathbb{Z}$.

For Examples 12 and 13, one can utilize the formulas (4.40) and (4.41) to obtain a linearization at the point $(\theta_i, \Psi(\theta_i)),\ i \in \mathbb{Z}$. For Example 11, we cannot apply formulas due to the appearance of singularity in the formula (4.41) at the grazing point. For this example, we will consider another approach to obtain a linearization at the grazing point.

Example 11 *In this example, the motion of one degree of freedom mechanical oscillator which is subjected to impacts with a rigid wall is considered and it can be*

expressed as

$$\begin{aligned} &x'' + 0.22x' + x = 1 + 0.22\sin(t), \\ &\Delta x'|_{(t,x,x')\in\Gamma} = -(1 + 0.9x')x', \end{aligned} \tag{4.43}$$

where the surface of discontinuity is $\Gamma = \{(t, x, x')|x = 0,\ t \in \mathbb{R}\}$. *System* (4.43) *admits* $2\pi-$ *periodic continuous solution of the form* $\Psi(t) = 1 - \cos(t)$. *Defining variables as* $x = x_1$ *and* $x' = x_2$, *we have*

$$\begin{aligned} &x_1' = x_2, \\ &x_2' = -0.22x_2 - x_1 + 1 + 0.22\sin(t), \\ &\Delta x_2|_{(t,x_1,x_2)\in\Gamma} = -(1 + 0.9x_2)x_2, \end{aligned} \tag{4.44}$$

where $\Gamma = \{(t, x_1, x_2)|x_1 = 0,\ t \in \mathbb{R}\}$ *and the points* $(\theta_i, \Psi(\theta_i), \Psi'(\theta_i)) = (2\pi i, 0, 0)$, $i \in \mathbb{Z}$, *are grazing as well. Denote by* $x(\theta_i) = (x_1(\theta_i), x_2(\theta_i))$. *The grazing periodic solution* $\Psi(t)$ *of* (4.44) *is depicted in blue in Figure 4.7. In what follows, we will apply formula* (4.41) *in the basis of system* (4.44).

Fix $i \in \mathbb{Z}$, *and consider a near solution* $x(t) = (x_1(t), x_2(t)) = x(t, \theta_i, \Psi(\theta_i) + \Delta x)$, *to* $\Psi(t)$ *of the differential part of the system* (4.44). *The solution* $x(t)$ *impacts the barrier at a moment* $t = \xi_i$ *near to* $t = \theta_i$ *and at the point* $(x_1, x_2) = (x_1(\xi_i), x_2(\xi_i))$. *Let also,* $\tilde{x}(t) = (\tilde{x}_1(t), \tilde{x}_2(t))$ *be a solution of the equation such that* $\tilde{x}(\xi_i) = x(\xi_i) + J(x(\xi_i))$. *Define the following map*

$$\begin{aligned} W_i(x) = &\int_{\theta_i}^{\xi_i} \begin{bmatrix} x_2(s) \\ x_1(s) - 0.22x_2(s) + 1 + 0.22\sin(s) \end{bmatrix} ds + J\Bigg(x + \\ &\int_{\theta_i}^{\xi_i} \begin{bmatrix} x_2(s) \\ -x_1(s) - 0.22x_2(s) + 1 + 0.22\sin(s) \end{bmatrix} ds\Bigg) + \\ &\int_{\xi_i}^{\theta_i} \begin{bmatrix} \tilde{x}_2(s) \\ -\tilde{x}_1(s) - 0.22\tilde{x}_2(s) + 1 + 0.22\sin(s) \end{bmatrix} ds. \end{aligned} \tag{4.45}$$

Let us start with a linearization for inside continuous solutions. The solutions, inside of the cycle, do not impact the barrier with non-zero velocity and are continuous. Thus, the linearization for these solutions is the following system [51],

$$\begin{aligned} &u_1' = u_2, \\ &u_2' = -u_1 - 0.22u_2. \end{aligned} \tag{4.46}$$

The multipliers of the system are $\rho_1^{(1)} = 0.5006 - 0.0191i$, $\rho_2^{(1)} = 0.5006 + 0.0191i$, *where* $i^2 = -1$. *Since the multipliers are inside the unit circle, the cycle* $\Psi(t)$ *is asymptotically stable with respect to inside continuous solutions.*

Now, we will continue with the linearization for the outside discontinuous solutions. The linearization system around the cycle $\Psi(t)$ *for solutions which are outside of the cycle has the form, [5],*

$$\begin{aligned} u_1' &= u_2, \\ u_2' &= -u_1 - 0.22u_2, \\ \Delta u|_{t=\theta_i} &= W_{ix}(x^*)u, \end{aligned} \tag{4.47}$$

where $\theta_i = 2\pi i$ *and* $u = (u_1, u_2)^T$, *where* T *denotes transpose of a matrix. The matrices* $W_{ix}(x^*)$ *will be evaluated below. Assume that the solution* $x(t)$ *meets the barrier at the moment* $t = \tau$ *and denote the meeting point as* $\bar{x} = x(\tau) = (x_1(\tau), x_2(\tau))$, *where* $x_1(\tau) = 0$, $x_2(\tau) < 0$ *and* $\tau \approx 2\pi$. *It is easy to see that any impacting solution near to* $\Psi(t)$ *meets the barrier transversely. Taking derivative of* (4.45) *and substituting* $x = \bar{x}$ *to the derivative, we obtain that*

$$\begin{aligned} &\frac{\partial W_i(\bar{x})}{\partial x_1^0} = \begin{bmatrix} \bar{x}_2 \\ -\bar{x}_1 - 0.22\bar{x}_2 + 1 + 0.22\sin(\tau) \end{bmatrix} \frac{\partial \xi_i(\bar{x})}{\partial x_1^0} + \begin{bmatrix} 1 & 0 \\ 0 & 1.96\bar{x}_2 \end{bmatrix} \times \\ &\left(e_1 + \begin{bmatrix} \bar{x}_2 \\ -\bar{x}_1 - 0.22\bar{x}_2 + 1 + 0.22\sin(\tau) \end{bmatrix} \frac{\partial \xi_i(\bar{x})}{\partial x_1^0} \right) - \\ &\begin{bmatrix} -0.98(\bar{x}_2)^2 \\ -\bar{x}_1 + 0.2156(\bar{x}_2)^2 + 1 + 0.22\sin(\tau) \end{bmatrix} \frac{\partial \xi_i(\bar{x})}{\partial x_1^0}. \end{aligned} \tag{4.48}$$

Moreover, differentiating $\Phi(x(\xi_i(x))) = 0$, *we have*

$$\frac{\partial \xi_i(x(\theta_i))}{\partial x_j} = -\frac{\Phi_x(x(\theta_i))\frac{\partial x(\theta_i)}{\partial x_{0j}}}{\Phi_x(x(\theta_i))f(\theta_i, x(\theta_i))},\ j = 1, 2, \tag{4.49}$$

for the transversal point $\bar{x} = (\bar{x}_1, \bar{x}_2)$, *the first component* $\frac{\partial \xi_i(\bar{x})}{\partial x_1^0}$ *can be evaluated as* $\frac{\partial \xi_i(\bar{x})}{\partial x_1^0} = -\frac{1}{\bar{x}_2}$. *From the last equality, it is seen how the singularity appears at the*

grazing point $x^* = (x_1^*, x_2^*) = (0, 0)$. *Finally, we obtain that*

$$\begin{aligned}
\frac{\partial W_i(\bar{x})}{\partial x_1^0} &= \begin{bmatrix} \bar{x}_2 \\ -\bar{x}_1 - 0.22\bar{x}_2 + 1 + 0.22\sin(\tau) \end{bmatrix} \left(\frac{-1}{\bar{x}_2}\right) + \begin{bmatrix} 1 & 0 \\ 0 & 1.96\bar{x}_2 \end{bmatrix} \\
&\left(e_1 - \begin{bmatrix} \bar{x}_2 \\ \bar{x}_1 + 0.22(\bar{x}_2 - \sin(\tau)) - 1 \end{bmatrix} \left(\frac{-1}{\bar{x}_2}\right) \right) \\
&+ \begin{bmatrix} 0.98(\bar{x}_2)^2 \\ \bar{x}_1 + 0.2156(\bar{x}_2)^2 - 1 - 0.22\sin(\tau) \end{bmatrix} \left(\frac{-1}{\bar{x}_2}\right) = \\
&\begin{bmatrix} -1 + 0.98\bar{x}_2 \\ 0.22 + 0.2156\bar{x}_2 + 1.96(\bar{x}_1 - 0.22\sin(\tau) + 0.22\bar{x}_2 - 1) \end{bmatrix},
\end{aligned} \tag{4.50}$$

where $e_1 = (1, 0)^T$.

The last expression demonstrates that the derivative is a continuous function of its arguments in a neighborhood of the grazing point. Since $\bar{x}$ *is a transversal point, one can evaluate the limit as*

$$\lim_{\bar{x} \to x^*} \frac{\partial W_i(\bar{x})}{\partial x_1^0} = B, \tag{4.51}$$

where $B = \begin{bmatrix} -1 \\ -1.74 \end{bmatrix}$.

To linearize system at the grazing point x^*, *we should verify that the function* $W_i(x)$ *is differentiable at* x^*. *The differentiability requests that the partial derivatives* $\frac{\partial W_i(x)}{\partial x_j^0}$, $j = 1, 2$, *exist in a neighborhood of the grazing point and they are continuous at the point [11]. To compute the derivative* $\frac{\partial W_i(x)}{\partial x_1^0}$ *at* x^*, *the following expression will be taken into account*

$$\begin{aligned}
\frac{\partial W_i(x_1^*, x_2^*)}{\partial x_1^0} = \lim_{x_1 \to x_1^*} \frac{W_i(x_1, x_2^*) - W_i(x_1^*, x_2^*)}{x_1 - x_1^*} = \\
\lim_{x_1 \to x_1^*} \frac{W_i(x_1, x_2^*) - W_i(x_1^*, x_2^*)}{x_1 - x_1^*} - B + B.
\end{aligned} \tag{4.52}$$

Applying the Mean Value Theorem [11], we obtain that

$$\lim_{x_1 \to x_1^*} \frac{\frac{\partial W_i(\zeta, x_2^*)}{\partial x_1^0}(x_1 - x_1^*) - B(x_1 - x_1^*)}{x_1 - x_1^*} + B, \tag{4.53}$$

where ζ *lies between* x_1 *and* x_1^*.

From (4.53)*, considering* (4.51)*, we have that*

$$\frac{\partial W_i(x_1^*, x_2^*)}{\partial x_1^0} = B. \tag{4.54}$$

So, the derivative exists and is continuous at x^*.

Now, let us check the existence and continuity of the derivative $\dfrac{\partial W_i(x)}{\partial x_2^0}$ *at* x^**. To accomplish these, we should continue with differentiating* (4.45) *again and substituting* $\bar{x} = (\bar{x}_1, \bar{x}_2)$*. Then, we obtain*

$$\begin{aligned}
\frac{\partial W_i(\bar{x})}{\partial x_2^0} &= \begin{bmatrix} \bar{x}_2 \\ -\bar{x}_1 - 0.22\bar{x}_2 + 1 + 0.22\sin(\tau) \end{bmatrix} \frac{\partial \xi_i(\bar{x})}{\partial x_2^0} + \begin{bmatrix} 1 & 0 \\ 0 & 1.96\bar{x}_2 \end{bmatrix} \times \\
&\left(e_2 + \begin{bmatrix} \bar{x}_2 \\ -\bar{x}_1 - 0.22(\bar{x}_2 - \sin(\tau)) + 1 \end{bmatrix} \frac{\partial \xi_i(\bar{x})}{\partial x_2^0} \right) \\
&+ \begin{bmatrix} 0.98(\bar{x}_2)^2 \\ \bar{x}_1 - 0.2156(\bar{x}_2)^2 - 1 - 0.22\sin(\tau) \end{bmatrix} \frac{\partial \xi_i(\bar{x})}{\partial x_2^0} = \\
&\begin{bmatrix} \bar{x}_2 - 0.98(\bar{x}_2)^2 \\ -\bar{x}_1 - 0.22(\bar{x}_2 - 0.98(\bar{x}_2)^2) \end{bmatrix} \frac{\partial \xi_i(\bar{x})}{\partial x_2^0} + \begin{bmatrix} 1 & 0 \\ 0 & 1.96\bar{x}_2 \end{bmatrix} \left(e_2 + \right. \\
&\left. \begin{bmatrix} \bar{x}_2 \\ -\bar{x}_1 - 0.22(\bar{x}_2 - \sin(\tau)) + 1 \end{bmatrix} \frac{\partial \xi_i(\bar{x})}{\partial x_2^0} \right)
\end{aligned} \tag{4.55}$$

where $e_2 = (0, 1)^T$*. To evaluate the derivative* $\frac{\partial \xi_i(\bar{x})}{\partial x_2^0}$ *in* (4.55)*, we apply formula* (4.49) *for the transversal point* $\bar{x} = (\bar{x}_1, \bar{x}_2)$ *and it is equal to* $\frac{\partial \xi_i(\bar{x})}{\partial x_2^0} = 0$*. This and formula* (4.55) *imply*

$$\lim_{\bar{x} \to x^*} \frac{\partial W_i(\bar{x})}{\partial x_2^0} = C, \tag{4.56}$$

where $C = \begin{bmatrix} 0 \\ 0 \end{bmatrix}$.

Similar to above discussion for the first derivative, one can obtain that $\frac{\partial W_i(x^*)}{\partial x_2^0} = C$ *and the derivative is continuous at* x^**. Thus, both derivatives* $\frac{\partial W_i(x)}{\partial x_1^0}$ *and* $\frac{\partial W_i(x)}{\partial x_2^0}$ *exist in a neighborhood of* x^* *and they are continuous at* x^**. That is,* $W_i(x)$ *is differentiable at* x^**. Since of the periodicity, the linearization can be obtained for all grazing moment* θ_i, $i \in \mathbb{Z}$.

Joining (4.54) *and* (4.56)*, it is obtained that*

$$W_{ix}(x^*) = \begin{bmatrix} -1 & 0 \\ -1.74 & 0 \end{bmatrix}. \tag{4.57}$$

The multipliers of (4.47) *are* $\rho_1 = 0$ *and* $\rho_2 = 0.5339$*. Due to the fact that the multipliers are less than unity in norm, we can conclude that the periodic solution* $\Psi(t)$ *is asymptotically stable. The near solutions to* $\Psi(t)$ *are depicted in Figure 4.7 with initial values* $(t_0, x_1^0, x_2^0) = (0, 0.05, 0)$ *and* $(t_0, x_1^0, x_2^0) = (0, 0, -0.9)$*, in magenta and green, respectively. It can be observed from Figure 4.7 that both green and magenta solutions approach the grazing periodic solution asymptotically as time increases.*

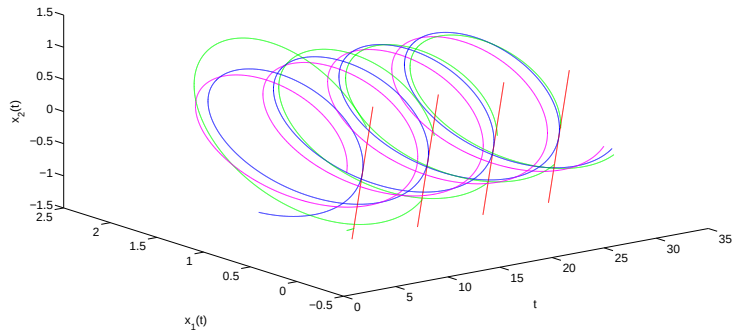

Figure 4.7: The blue one is the periodic solution $\Psi(t)$, the green curve is the near impacting solution of (4.44) with initial data $(0, 0, -0.9)$, and the magenta is the near non-impacting solution of (4.44) with initial data $(0, 0.05, 0)$.

Despite the grazing, the singularity is not obtained in the derivative (4.40) in Examples 12 and 13. So, the method presented in [5] can be utilized in the following examples to find a linearization at the grazing point.

Example 12 *We will consider the system*

$$\begin{aligned} x' &= 0, \\ \Delta x|_{t=\tau_i(x)} &= -0.2x, \end{aligned} \tag{4.58}$$

where $\tau_i(x) = 10arccos(x + 0.1) + i\pi$*. One can easily determine that the system has zero solution* $x(t) = 0$*. We will consider it as a* $\pi-$*periodic solution of* (4.58)*.*

By means of the fact that $\tau_i(x)$ *is an increasing function, it is easy to see that condition* $(N1)$ *is valid. For constants* $C = 1/11$, *and* $N = \frac{10}{\sqrt{0.99}}$, *such that* $CN < 1$ *and the following inequalities are valid* $\max_{(t,x)\in\mathbb{R}\times D} \|f(t,x)\| = 0 \leq C$, $\max_{x\in D} \|\frac{\partial \tau_i(x)}{\partial x}\| = \max_{x\in D} \|\frac{10}{\sqrt{1-(x+0.1)^2}}\| \leq N$, *and* $\max_{0\leq\sigma\leq 1}\langle \frac{\partial \tau_i(x+\sigma J_i(x))}{\partial x}, J_i(x)\rangle$
$= \max_{0\leq\sigma\leq 1} \frac{-2}{\sqrt{1-((1-0.2\sigma)x)^2}} \leq 0$. *So,* $(N2)$ *is valid. The condition* $(N3)$ *is also true for this example.*

The integral line $x(t) \equiv 0$ *is tangent to the surface* $t = \tau_0(x)$ *at the point* $(\theta_1, \Psi(\theta_1)) = (0,0)$. *Indeed, since the right hand side* $f(t,x)$ *is constantly zero, the condition* (i) *is valid. Take into account the function* $t = \eta(x) \equiv 10arccos(x + 0.1)$, *which is invertible near* $x = \Psi(\theta_1) = 0$, *for* $x \leq 0$ *and the one sided derivative* $[\eta^{-1}(t)]'_-|_{t=\theta_1} = 0.1\sin(\theta_1) = 0$. *So, it validates the condition* (ii). *Therefore, the zero solution has horizontal grazing at the point* $(\theta_1, \Psi(\theta_1)) = (0,0)$. *Moreover, one can validate easily that* $(\pi i, 0)$, $i \in \mathbb{Z}$ *are also horizontal grazing points.*

Let us obtain a linearization system around zero solution. For a solution, $x(t) = x(t,0,\bar{x})$, *with* $\bar{x} > 0$, *there exists no intersection with the surfaces of discontinuity. This is why, the linearization system has the form*

$$u' = 0. \tag{4.59}$$

Next, consider another solution $x(t) = x(t,0,\bar{x})$, *with* $\bar{x} < 0$ *of (4.58). One can easily find that the solution meets each of the surfaces of discontinuity. Due to the periodicity of the system, linearization near the zero solution at all points* $(i\pi, 0)$ *is the same, if exists. So, it is sufficient to consider the linearization around the grazing point* $(0,0)$ *for those points where* $\bar{x} < 0$. *Let us start with the function* $\theta(x) = 10arccos(x(\theta(x)) + 0.1)$. *By taking derivative of it, we get*

$$\theta'(x) = -10\frac{f(\theta(x), x(\theta(x)))\theta'(x) + 1}{\sqrt{1-(x(\theta(x)) + 0.1)^2)}}, \tag{4.60}$$

and substituting the grazing point into the equation (4.60)*, one can get* $\theta'(0) = -10/\sqrt{0.99}$.

The coefficients in the impulsive part of the linearization system have to be evaluated by formula

$$D_i = (f(\theta(0), x(\theta(0))) - f(\theta(0), x(\theta(0)) + J(x(\theta(0)))))\theta'(0)$$
$$+ J_x(1 + f(\theta(0), x(\theta(0))))\theta'(0) = -0.2,$$

for all $i \in \mathbb{Z}$.

So, linearization system for the intersecting solutions with initial value $\bar{x} < 0$ *can be determined as*

$$\begin{aligned} u' &= 0, \\ \Delta u|_{t=\pi i} &= -0.2u. \end{aligned} \tag{4.61}$$

Consider solutions with $\bar{x} < 0$. *The linearization for them is the system* (4.61) *and its multiplier can be evaluated as* $\rho = 0.8 < 1$, *and consequently solutions with negative initial values are attracted by the zero solution. Nevertheless, the solutions with positive initial values are constant. That is, one can say that the zero solution is stable for neighbors from above. On the basis of the discussion, one can conclude that zero solution is stable. It is pictured in Figure 4.8. The solutions* $\Psi(t) = 0$, *and* $x(t, 0, \bar{x})$ *with initial values* $\bar{x} > 0$ *and* $\bar{x} < 0$ *are depicted in black, red and magenta, respectively in Fig. 4.8 and the stability of the zero solution is apparently seen by virtue of simulation.*

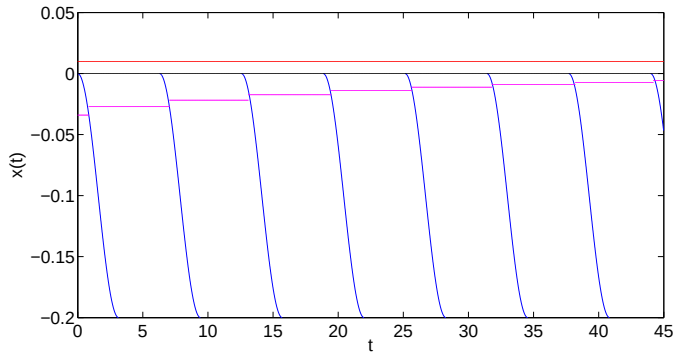

Figure 4.8: The blue curves are the discontinuity surfaces $t = \tau_i(x), i = 0, 1, 2, \ldots, 7$. The solutions $\Psi(t) = 0$, and $x(t, 0, \bar{x})$ with initial values $\bar{x} = 0.01$ and $\bar{x} = -0.03$ are depicted in black, red and magenta, respectively.

Through the last examples, it is seen that the tangent at the grazing point is parallel to the time axis. This approves why we call the phenomenon as *horizontal grazing*.

Example 13 *In order to demonstrate vertical grazing, we take into account the following system*

$$\begin{aligned} x' &= \frac{1}{\sqrt{i-t}},\ t \in [i-1, i), \\ \Delta x|_{t=\tau_i(x)} &= -1, \end{aligned} \tag{4.62}$$

where $f(t,x) = \frac{1}{\sqrt{i-t}}$ *and* $\tau_i(x) = \sqrt{16-x^2} - 3 + i$, $i \in \mathbb{Z}$. *The domain is equal to* $G = (-0.6, 0.6)$. *One can easily determine that the system has a* $1-$*periodic solution*

$$\Psi(t) = \begin{cases} -2 & if\ \ t = 0, \\ -2\sqrt{1-t} & if\ \ t \in (0,1]. \end{cases}$$

The integral curve of the solution is tangent to the curve of discontinuity $\tau_0(x) = \sqrt{1-x^2} + 1$ *at the point* $(\theta_1, \Psi(\theta_1))$, *and the tangent is vertical. That is, one can find that the function* $x = \Psi(t)$ *is invertible near* $x = \Psi(\theta_1) = 0$ *and for* $x < 0$, *and the left hand derivative is equal to* $[\Psi_j^{-1}(x_j)]'_-|_{x=x_j} = -2\frac{1}{2}x(\theta_1)^2 = 0$ *and let* $\tau_0(x) = \tau(x)$, *and* $\tau_x(x) = -\frac{x(\theta_1)}{\sqrt{16-x^2}} = 0$. *Conditions* (i) *and* (ii) *are verified and the periodic solution* $\Psi(t)$ *has vertical grazing at the point* $(\theta_1, \Psi(\eta_1))$. *Similarly, the points are* $(i, 0)$, $i \in \mathbb{Z}$ *are vertical grazing ones. The periodic solution,* $\Psi(t)$, *is exhibited through simulation in Fig. 4.9.*

Now, we will validate the conditions from $(N1)$ *to* $(N4)$. *Every solution which meets a discontinuity surface does not intersect the same one again, which validates* $(N1)$ *and instead of the equation* $x' = \frac{1}{\sqrt{i-t}}$, $t \in [i-1, i)$, *we will take into account the differential equation* $\frac{dt}{dx} = \frac{1}{\sqrt{i-t}}$, $t \in [i-1, i)$. *For* $C = 1$ *and* $N = 0.7$, *such that* $CN < 1$ *and the following inequalities are valid* $\max_{(t,x)\in\mathbb{R}\times D} \|f(t,x)\| = 1$, $\max_{x\in D} \|\frac{\partial \tau_i(x)}{\partial x}\| = \max_{x\in D} \|\frac{10}{\sqrt{1-(x+0.1)^2}}\| \leq N$, *and* $\max_{0\leq\sigma\leq 1} \langle \frac{\partial \tau_i(x+\sigma J_i(x))}{\partial x}, J_i(x) \rangle = \max_{0\leq\sigma\leq 1} \frac{-2}{\sqrt{1-((1-0.2\sigma)x)^2}} \leq 0$. *So,* $(N2)$ *is verified. Conditions* $(N3)$ *and* $(N4)$ *can be validated easily.*

Consider a near solution $x(t) = x(t, 0, \bar{x})$ *of* (4.62) *to* $\Psi(t)$ *with* $\bar{x} \neq 0$. *It is easy to determine that all near solutions intersects the surface of discontinuity* $\tau(x) = \tau_0(x)$. *We could not evaluate the derivative* $\theta'(x)$ *at the grazing point, by considering the original system. For this reason, let us interchange the dependent and independent*

variables in the equation. Consider the system

$$\frac{dt}{dx} = \sqrt{1-t}. \tag{4.63}$$

Since the function $\Psi(t)$ *is invertible on the interval* $[0,1]$*, its inverse satisfies the equation* (4.63)*, as well as the surface* $\tau_0(x)$ *can be written as* $X(t) = -\sqrt{16-(t-3)^2}$*, for negative values of* x*. It is easy to check that the solution*

$$\Psi^{-1}(x) = \begin{cases} 0 & if \;\; x = -2, \\ 1 - \frac{x^2}{4} & if \;\; x \in (-2, 0], \end{cases} \tag{4.64}$$

of the equation (4.63) *has a horizontal grazing point,* $(\Psi^{-1}(\theta_1), \theta_1) = (0, 1)$.

Introduce the function $\phi(t)$ *as an analogue of* $\theta(x)$ *for the last equation. It is easy to find that*

$$\theta'(0) = \frac{1}{\phi'(1)}, \tag{4.65}$$

since the functions are mutually inverse. Let us evaluate $\phi'(1)$*. Issuing from that* $\phi(t) = -\sqrt{16-(t(\phi(t))-3)^2}$*, we get* $\phi'(1) = -\frac{-2(t(\phi(1))-3)(\sqrt{1-t(\phi(1))}\phi'(1)+1)}{2\sqrt{16-(t(\phi(1))-3)^2}}$ *and* $\phi'(1) = -\frac{1}{\sqrt{3}}$*, i.e.* $\theta'(0) = -\sqrt{3}$*. Taking into account the periodicity of system* (4.62) *as well as* $\Psi(t)$*, one can conclude that* $\theta_i'(0)$*, is equal to* $-\sqrt{3}$*, for all* $i \in \mathbb{Z}$*. By utilizing this discussion and equation* (4.41)*, one can obtain that* $D_i \equiv D = -\sqrt{3}$.

Thus, the variational system for all solutions near $\Psi(t)$ *has the form*

$$\begin{aligned} u' &= 0, \\ \Delta u &= -\sqrt{3}u. \end{aligned} \tag{4.66}$$

The multiplier for (4.66) *can be found as* $\rho = -\sqrt{3} + 1$*, and it is less than one in absolute value. So, the periodic solution* $\Psi(t)$ *is asymptotically stable. One can observe through simulations results exhibited in Fig. 4.9 that near solutions approach to th orbit of the cycle* $\Psi(t)$ *as time increases.*

This section includes information about a non-autonomous system with non-fixed moments of impulses whose solutions have vertical and grazing points. For the horizontal grazing, a system with a non-autonomous vector field and a cylindrical surface of discontinuity is considered as an example and for the vertical grazing the systems

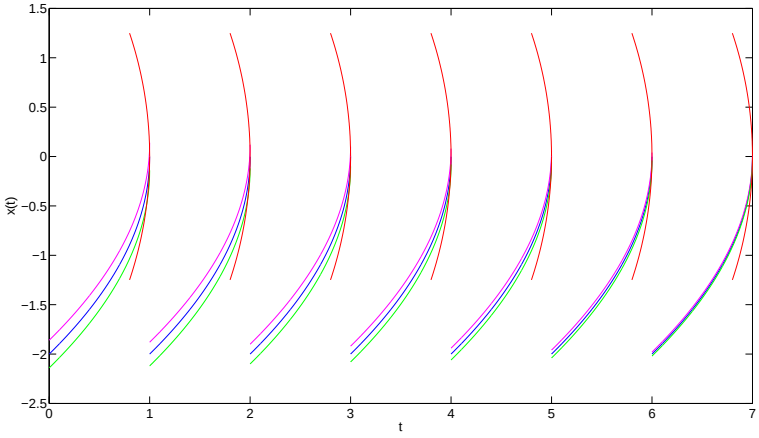

Figure 4.9: The blue curve is for the cycle $\Psi(t)$, the magenta and green curves are the solutions which start with an initial condition -1.9 and -2.1, respectively. The red curves are the surfaces of discontinuity $t = \tau_i(x)$, $i = 0, 1, \ldots, 6$.

with non-autonomous vector field and the surfaces of discontinuity is exemplified. By applying a novel technique, we construct a linearization system around the grazing periodic solution. Concrete models are demonstrated and some simulations are presented to visualize theoretical results. Grazing solutions are widely investigated in mechanical systems, but there is a few studies can be found in neural networks which includes grazing. Further, we will apply our methods to investigate the stability of neural network models which have grazing points in other words which meet the threshold tangentially.

4.8 Grazing periodic solutions of the system of differential equations with stationary impulses

In examples, we shall need non-constant restitution coefficients in impact mechanisms. It is presented in [24] numerically and through simulations that at low impact velocities $R(v) = 1 - av$, where v is the velocity before collision and a is a constant. For low impact velocities the restitution law can be considered velocity dependent [37]. In [61], it is observed through simulations and experiments that the coefficient of restitution depends on the impact velocity of the particle by considering both the viscoelastic and the plastic deformations of particles occurring at low and high velocities, respectively.

Our aim in this study is to seek some sufficient conditions for the linearization around a grazing periodic orbit. Then, by means of the linearization, we consider the stability of the grazing periodic solution. The stability of periodic solution of an impact system is generally investigated by applying the method of Poincare map. However, for the grazing solutions at the grazing point the Poincare map is not differentiable so this method is not applicable for the analysis of such systems. The stability of these solutions are widely investigated by constructing normal map and Nordmark map around the grazing periodic orbit [26, 65, 97, 100]. In the paper of [65], the author investigate the bifurcations of dynamical systems, represented by a second-order differential equation with periodic coefficients and an impact condition with grazing points. In [126], the non-differentiability of Poincare mapping for grazing impacts is considered. Considering solutions near a grazing orbit for a single-freedom- degree vibro-impact system, Nordmark derived a two dimensional local map which express the dynamics of an orbit near the grazing point. Nordmark also studied the dynamics of this map and obtained several important results [97]. In the paper [98], this analysis are generalized to n-dimensional impact oscillators and some conditions for the persistence or disappearance of a local attractor in the neighborhood of a grazing periodic solution are taken into account. The grazing bifurcations have been known in Russian literature as $C-$ bifurcations. Feigin [39] constructed a map to demonstrate existence and stability of periodic solution of system which undergoes the $C-$ bifurcation.

In our previous paper [6], discontinuous dynamics with grazing solutions is discussed. The group property, continuation of solutions, continuity and smoothness of motions are thoroughly analyzed. A variational system around a grazing solution which depends on near solutions is constructed. Stability of grazing cycles is examined by linearization. Small parameter method is extended for analysis of neighborhoods of grazing orbits, and grazing bifurcation of cycles is observed in an example. Linearization around an equilibrium grazing point is discussed. The mathematical background of the study relies on the theory of discontinuous dynamical systems [5]. Our approach is analogues to that one of the continuous dynamics analysis and results can be easily extended on functional differential, partial differential equations and others.

In the present study, the non-autonomous system with stationary impulse condition

has been taken into account. Due to the fact that the differential equation of the system is non-autonomous but the impulse equation is autonomous, this system can be named “half-autonomous system." In order to analyze these type of equations, we should request conditions which are in many senses different than those presented in [6]. In other words, our present research is slightly different than that for autonomous impulsive systems. For this reason, the problems of grazing solutions of half-autonomous systems is considered in a different part of this chapter.

The remaining part of the study is divided into four parts. The next section covers information of the half autonomous systems, grazing point and grazing solution. Some sufficient conditions are provided. The third section is about the linearization of the half autonomous system around the grazing periodic solution. The four section is related with the stability of the periodic solution. In the fifth, the small parameter analysis have been conducted on the neighborhood of grazing periodic solution. The last one is the discussion section which displays the sum of our work and possible future works related with our subject of discussion.

4.8.1 The grazing solutions

Let $\mathbb{R}$, $\mathbb{N}$ and $\mathbb{Z}$ be the sets of all real numbers, natural numbers and integers, respectively. Consider the open connected and bounded set $G \in \mathbb{R}^n$. Let $\Phi : G \to \mathbb{R}$ be a function, differentiable up to second order with respect to x, $S = \Phi^{-1}(0)$ is a closed subset of G. Define a continuously differentiable function $J : G \to G$ such that $J(S) \subset G$. The function $I(x)$ will be used in the following part of the study which is defined as $I(x) := J(x) - x$, for $x \in S$.

The following definitions will be utilized in the remaining part of the study. Let $x(\theta-)$ be the left limit of a function $x(t)$ at the moment θ, and $x(\theta+)$ be the right limit of the solution. Define $\Delta x(\theta) := x(\theta+) - x(\theta-)$ as the jump operator for $x(t)$ such that $x(\theta) \in S$ and $t = \theta$ is a moment of discontinuity. Discontinuity moments are the moments when the solution meets the surface of discontinuity.

In this study, we take into account the following system

$$\begin{aligned} x' &= f(t,x), \\ \Delta x|_{x\in S} &= I(x), \end{aligned} \tag{4.67}$$

where $(t,x) \in \mathbb{R}\times G$, the functions $f(t,x)$ is continuously differentiable with respect to x up to second order and continuous with respect to time. We will consider the surface of discontinuity as $\Gamma = \{(t,x)|\Phi(x) = 0\} \subseteq \mathbb{R}\times S$. We say that the system is with stationary impulse conditions, since the function $I(x)$ and the surface S do not depend on time.

For the convenience in notation, let us separate the differential equation of the impulse system as

$$y' = f(t,y). \tag{4.68}$$

Assume that the solution $x_0(t) = x(t,t_0,x_0)$, $t_0 \in \mathbb{R}$, $x_0 \in G$ of (4.67) intersects the surface of discontinuity Γ, at the moments $t = \theta_i,\ i \in \mathbb{Z}$.

Set the gradient vector of Φ with respect to x as $\nabla\Phi(x)$. The normal vector of Γ at a meeting moment, $t = \theta_i$, of the solution $x_0(t)$ can be determined as $\overrightarrow{n} = (0, \nabla\Phi(x_0(\theta_i))) \in \mathbb{R}^{n+1}$, where $\langle,\rangle$ means the dot product. For the tangency, the vectors $\overrightarrow{n}$ and $(1, f(\theta_i, x_0(\theta_i)))$ should be perpendicular to each other . That is, $\langle\nabla\Phi(x_0(\theta_i)), f(\theta_i, x_0(\theta_i))\rangle = 0$.

In what follows, let $\|\cdot\|$ be the Euclidean norm, that is for a vector $x = (x_1, x_2, \ldots, x_n)$ in $\mathbb{R}^n$, the norm is equal to $\sqrt{x_1^2 + x_2^2 + \ldots + x_n^2}$.

Consider the function $H(t,x) := \langle\nabla\Phi(x), f(t,x)\rangle$, with $(t,x) \in \mathbb{R}\times S$.

Let us start with the following definitions.

Definition 14 *A point $(\theta_i, x_0(\theta_i))$ is a grazing point and θ_i a grazing moment for a solution $x_0(t)$ of (4.67) if $H(\theta_i, x_0(\theta_i)) = 0$ and $I(x_0(\theta_i)) = 0$.*

Definition 15 *A solution $x_0(t)$ of (4.67) is grazing if it has a grazing point $(\theta_i, x_0(\theta_i))$. The moment θ_i is the grazing moment of the solution $x_0(t)$.*

Definition 16 *A point $(\theta_i, x_0(\theta_i))$ is a transversal point and θ_i a transversal moment for a solution $x_0(t)$ if $H(\theta_i, x_0(\theta_i)) \neq 0$.*

Figure 4.10 is drawn to illustrate the grazing phenomenon. The red line is a grazing solution $x_0(t)$ of (4.67), and it intersects the surface Γ at the point $P = (\theta_i, x_0(\theta_i))$. The yellow region is the tangent plane to the surface at the point. Vector v is tangent to the integral curve at P. It belongs to the tangent plane. This is why the point is grazing.

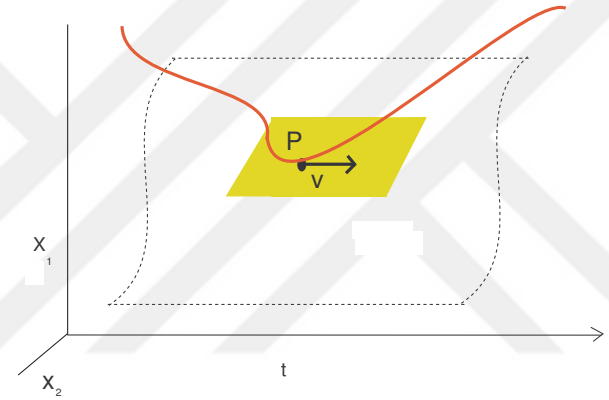

Figure 4.10: The red line is a grazing solution $x_0(t)$ of (4.67) with the grazing point $P = (\theta_i, x_0(\theta_i))$. The yellow region is the tangent plane to the surface Γ at the grazing point. Vector v is tangent to the integral curve at P.

In what follows, we will assume that the following condition is valid.

(H1) For each grazing point $(\theta_i, x_0(\theta_i))$ there is a number $\delta > 0$ such that $H(t, x) \neq 0$ and $J(x) \notin S$ if $0 < |t - \theta_i| < \delta$ and $0 < \|x - x_0(\theta_i)\| < \delta$.

It is also clear that function $H(t, x) \neq 0$ near a transversal point.

Consider a solution $x(t) = x(t, \theta_i, x_0 + \Delta x)$ of (4.67) with a small $\|\Delta x\|$. Because of the geometrical reasons caused by the tangency at the grazing point, this solution may not intersect the surface of discontinuity near $(\theta_i, x_0(\theta_i))$. For this reason there exist two different behavior of it with respect to the surface of discontinuity, they are:

(N1) The solution $x(t)$ intersects the surface of discontinuity Γ at a moment near to θ_i.

(N2) There is no intersection moments of $x(t)$ close to θ_i.

We say that $\theta = \{\theta_i\}$ is a $B-$*sequence* if one of the following alternatives holds: (i) $\theta = \emptyset$, (ii) θ is a nonempty and finite set, (iii) θ is an infinite set such that $|\theta_i| \to \infty$ as $i \to \infty$. In what follows, we will consider $B-$sequences.

In order to define a solution of (4.67), the following functions and sets are needed.

A function $\phi(t) : \mathbb{R} \to \mathbb{R}^n,\ n \in \mathbb{N}$, is from the set $PC(\mathbb{R}, \theta)$ if it : (i) is left continuous, (ii) is continuous, except, possibly, points of θ, where it has discontinuities of the first kind.

A function $\phi(t)$ is from the set $PC^1(\mathbb{R}, \theta)$ if $\phi(t), \phi'(t) \in PC(\mathbb{R}, \theta)$, where the derivative at points of θ is assumed to be the left derivative. If $\phi(t)$ is a solution of (4.67), then it is required that it belongs to $PC^1(\mathbb{R}, \theta)$. We say that $x(t) : \mathscr{I} \to \mathbb{R}^n, \mathscr{I} \subset \mathbb{R}$, is a solution of (4.67) on $\mathscr{I}$ if there exists an extension $\tilde{x}(t)$ of the function on $\mathscr{I}$ such that $\tilde{x}(t) \in PC^1(\mathbb{R}, \theta)$, the equality (4.68) $t \in \mathscr{I}$, is true if $x(t) \notin S$, $x(\theta_i+) = J(x(\theta_i))$ for $x(\theta_i) \in S$ and $\theta_i \in \mathscr{I}$.

4.8.1.1 B-equivalence to a system with fixed moments of impulses

The system with variable moments of impulses is a difficult task for the investigations. In order to facilitate the analysis, in [5], a powerful instrument was suggested which reduces the systems with variable moments of impulses to those with fixed moments of impulses, which preserves the dynamical properties of (4.67). The system with fixed moment of impulses is called a *B-equivalent system* to the system with variable moments of impulses. The B-equivalent system can be constructed as follows.

Consider a solution $x_0(t) : \mathscr{I} \to \mathbb{R}^n$, $\mathscr{I} \subseteq \mathbb{R}$, of (4.67). Assume that all discontinuity points θ_i of $x_0(t)$, $i \in \mathscr{A}$, are interior points of $\mathscr{I}$. Where $\mathscr{A}$ is an interval in $\mathbb{Z}$. There exists a positive number r, such that r-neighborhoods $G_i(r)$ of $(\theta_i, x_0(\theta_i))$ do not intersect each other. Fix $i \in \mathscr{A}$ and let $\xi(t) = x(t, \theta_i, x)$, $(\theta_i, x) \in G_i(r)$,

be a solution of (4.68), which satisfies $(N1)$, and $\tau_i = \tau_i(x)$ the meeting time of $\xi(t)$ with S and $\psi(t) = x(t, \tau_i, \xi(\tau_i) + J(\xi(\tau_i)))$ another solution of (4.68). Denote $W_i(x) = \psi(\theta_i) - x$ and one can define the map $W_i(x)$ as

$$W_i(x) = \int_{\theta_i}^{\tau_i} f(s, \xi(s))ds + J(x + \int_{\theta_i}^{\tau_i} f(s, \xi(s))ds) + \int_{\tau_i}^{\theta_i} f(s, \psi(s))ds \quad (4.69)$$

It is a map of an intersection of the plane $t = \theta_i$ with $G_i(r)$ into the plane $t = \theta_i$. Let us present the following system of differential equations with impulses at fixed moments, whose impulse moments, $\theta_i,\ i \in \mathscr{A}$, correspond to the points of discontinuity of $x_0(t)$,

$$\begin{aligned} y' &= f(t, y), \\ \Delta y|_{t=\theta_i} &= W_i(y(\theta_i)). \end{aligned} \quad (4.70)$$

The function f is the same as the function in system (4.70) and the map W_i, $i \in \mathscr{A}$, is defined by equation (4.69) if $x(t)$ satisfies condition $(N1)$. Otherwise, if a solution $x(t)$ satisfies $(N2)$, then we assume that it admits the discontinuity moment θ_i with zero jump such that $W_i(x(\theta_i)) = 0$.

Let us introduce the sets $F_r = \{(t, x)|t \in \mathscr{I}, \|x - x_0(t)\| < r\}$, and $G_i^+(r)$, $i \in \mathscr{A}$, an $r-$ neighborhood of the point $(\theta_i, x_0(\theta_i+))$. Write $G^r = F_1 \cup (\cup_{i\in\mathscr{A}} G_i(r)) \cup (\cup_{i\in\mathscr{A}} G_i^+(r))$. Take r sufficiently small so that $G^r \subset \mathbb{R} \times G$. Denote by $G(h)$ an h-neighborhood of $x_0(0)$.

Definition 17 *Systems (4.67) and (4.70) are said to be $B-$equivalent in G^r if there exists $h > 0$, such that:*

1. *for every solution $y(t)$ of (4.70) such that $y(0) \in G(h)$, the integral curve of $y(t)$ belongs to G^r there exists a solution $x(t) = x(t, 0, y(0))$ of (4.67) which satisfies*

$$x(t) = y(t), \ \ t \in [a, b] \setminus \cup_{i=-k}^{m} \widehat{(\tau_i, \theta_i]}, \quad (4.71)$$

where τ_i are moments of discontinuity of $x(t)$. Particularly:

$$\begin{aligned} x(\theta_i) &= \begin{cases} y(\theta_i), & \text{if } \theta_i \leq \tau_i, \\ y(\theta_i+), & \text{otherwise,} \end{cases} \\ y(\tau_i) &= \begin{cases} x(\tau_i), & \text{if } \theta_i \geq \tau_i, \\ x(\tau_i+), & \text{otherwise.} \end{cases} \end{aligned} \tag{4.72}$$

2. *Conversely, if (4.67) has a solution $x(t) = x(t, 0, x(0)), x(0) \in G(h)$, then there exists a solution $y(t) = y(t, 0, x(0))$ of (4.70) which has an integral curve in G^r, and (4.71) holds.*

The solution $x_0(t)$ satisfies (4.67) and (4.70) simultaneously.

4.8.2 Linearization around grazing solutions

The object of this section is to investigate the smoothness of the grazing solution. Consider a grazing solution $x_0(t) = x(t, 0, x_0),\ x_0 \in G$, of (4.67) which was introduced in the last section. We will demonstrate that one can write the variational system for the solution as follows:

$$\begin{aligned} u' &= A(t)u, \\ \Delta u|_{t=\theta_i} &= B_i u(\theta_i), \end{aligned} \tag{4.73}$$

where the matrix $A(t) \in \mathbb{R}^{n\times n}$ of the form $A(t) = \frac{\partial f(t,x_0(t))}{\partial x}$. We call the second equation in (4.73) as the *linearization at a moment of discontinuity or at a point of discontinuity*. It is different for transversal and grazing points. However, the first differential equation in (4.73) is common for all type of solutions. The matrices B_i will be described in the remaining part of the study for each type of the points.

4.8.2.1 Linearization at a transversal moment

Linearization at the transversal point has been analyzed completely in Chapter 6, [5]. Let us demonstrate the results shortly. The $B-$ equivalent system (4.70) is involved in

the analysis, since the solution $x_0(t)$ satisfies also the equation (4.70) at all moments of time, and near solutions do the same for all moments except small neighborhoods of the discontinuity moment θ_i. Consequently, it is easy to see that the system of variations around $x_0(t)$ for (4.67) and (4.70) are identical. Assume that $x(\theta_i)$ is at a transversal point. We consider the reduced B-equivalent system and use the functions $\tau_i(x)$ and $W_i(x)$, defined by equation (4.69), are presented in Subsection 4.8.1.1 for linearization. Differentiating $\Phi(x(\tau_i(x))) = 0$, we have

$$\frac{\partial \tau_i(x_0(\theta_i))}{\partial x_{0j}} = -\frac{\langle \Phi_x(x_0(\theta_i)), \frac{\partial x_0(\theta_i)}{\partial x_{0j}} \rangle}{\langle \Phi_x(x_0(\theta_i)), f(\theta_i, x_0(\theta_i)) \rangle}, j = 1, \ldots, n. \tag{4.74}$$

The Jacobian $W_{ix}(x_0(\theta_i)) = [\frac{\partial W_i(x_0(\theta_i))}{\partial x_{01}}, \frac{\partial W_i(x_0(\theta_i))}{\partial x_{02}}, \ldots, \frac{\partial W_i(x_0(\theta_i))}{\partial x_{0n}}]$ is evaluated by

$$\begin{aligned} &\frac{\partial W_i(x_0(\theta_i))}{\partial x_{0j}} = (f(\theta_i, x_0(\theta_i)) - f(\theta_i, x_0(\theta_i) + J(x_0(\theta_i)))) \frac{\partial \tau_i}{\partial x_{0j}} + \\ &\frac{\partial J}{\partial x_0}(e_j + f(\theta_i, x_0(\theta_i)) \frac{\partial \tau_i}{\partial x_{0j}}), \end{aligned} \tag{4.75}$$

where $e_j = (\underbrace{0, \ldots, 1}_{j}, \ldots, 0)$, $j = 1, 2, \ldots, n$. Next, by considering the second equation in (4.70) and using mean value theorem, one can obtain that

$$\Delta(x(\theta_i) - x_0(\theta_i)) = W_i(x(\theta_i) - x_0(\theta_i)) = W_{ix}(x_0(\theta_i))(x(\theta_i) - x_0(\theta_i)) + O(\|x(\theta_i) - x_0(\theta_i)\|).$$

From the last expression it is seen that the linearization at the transversal moment is determined with the matrix $B_i = W_{ix}(x_0(\theta_i))$.

4.8.2.2 Linearization at a grazing moment

Fix a discontinuity moment θ_i and assume that it is of grazing type. Considering Definition 8 with the formula (4.74), it is appearant that at least one coordinate of the gradient, $\nabla\tau(x)$, is infinity at the grazing point. This causes singularity in the system, which makes the analysis harder and the dynamics complex. Through the formula (4.74), one can see that the singularity is just caused by the position of the vector field with respect to the surface of discontinuity and the impact does not participate in the appearance of the singularity. To get rid of the singularity, we will consider the

following conditions.

$(A1)$ The map $W_i(x)$ in (4.69) is differentiable if $x = x_0(\theta_i)$.

$(A2)$ $\tau_i(x) < \theta_{i+1} - \theta_i - \epsilon$ for some positive ϵ on a set of points near $x_0(\theta_i)$, which satisfy condition $(N1)$.

The appearance of singularity in (4.74) does not mean that the Jacobian $W_{ix}(x)$ is infinity. Because, in order to find the Jacobian, not only the surface of discontinuity and the vector field are required, but the jump function is also needed. The regularity of the Jacobian can be arranged by means of the proper choice of the vector field, surface of discontinuity and jump function. In other words, if they are specially chosen, the map can be differentiable, and this validates condition $(A1)$. Thus, in the present study we analyze the case, when the impact functions neutralize the singularity. Presumably, if there is no of this type of suppressing, complex dynamics near the grazing motions may appear [97, 98, 70, 33]. In the examples stated in the remaining part of the study, one can see the verification of $(A1)$, in details.

There are many ways are suggested to investigate the existence and stability of periodic solution of systems with graziness in literature [99, 53]. They investigate them by constructing special maps around the grazing point. In this study, we suggest to investigate the existence and stability by using the method of Floquet multipliers for dynamics with continuous time. It is a well known method in literature [5, 113], but this is not widely applied to the analysis of the stability of grazing solutions because of the tangency of the grazing solution with the surface of discontinuity. This is the main novelty of our study.

By means of these discussions, one can conclude that the matrix B_i in (4.73) is the following

$$B_i = \begin{cases} W_{ix} & \text{if} \quad (N1) \text{ is valid,} \\ O_n & \text{if} \quad (N2) \text{ is valid,} \end{cases} \tag{4.76}$$

where O_n denotes the $n \times n$ zero matrix.

Denote by $\bar{x}(t), j = 1, 2, \ldots, n$, a solution of (4.70) with $\bar{x}(t_0) = x_0 + \Delta x$, $\Delta x = (\xi_1, \xi_2, \ldots, \xi_n)$, and let η_j be the moments of discontinuity of $\bar{x}(t)$.

The following conditions are required in what follows.

(A) For all $t \in \mathscr{I} \setminus \cup_{i \in \mathscr{A}} \widehat{(\eta_i, \theta_i]}$, the following equality is satisfied

$$\bar{x}(t) - x_0(t) = \sum_{i=1}^{n} u_i(t)\xi_i + O(\|\Delta x\|), \tag{4.77}$$

where $u_i(t) \in PC(\mathscr{I}, \theta)$ and $\mathscr{I}$ is a finite subset of $\mathbb{R}$.

(B) There exist constants $\nu_{ij}, j \in \mathscr{A}$, such that

$$\eta_j - \theta_j = \sum_{i=1}^{n} \nu_{ij}\xi_i + O(\|\Delta x\|); \tag{4.78}$$

(C) The discontinuity moment η_j of the near solution approaches to the discontinuity moment $\theta_j, j \in \mathscr{A}$, of grazing one as ξ tends to zero.

The solution $\bar{x}(t)$ has a linearization with respect to solution $x_0(t)$ if the condition (A) is valid. Moreover, if $x_0(\theta_i)$ is a grazing point, then the condition (C) is fulfilled and condition (B) is true if $x_0(\theta_i)$ is a transversal point.

The solution $x_0(t)$ is $K-$differentiable with respect to the initial value x_0 on $\mathscr{I}, t_0 \in \mathscr{I}$, if for each solution $\bar{x}(t)$ with sufficiently small Δx the linearization exists. The functions $u_i(t)$ and ν_{ij} depend on Δx and uniformly bounded on a neighborhood of x_0.

Lemma 5 *Assume that the conditions* $(H1)$ *and* $(A2)$ *are valid. Then, the function* $\tau_i(x)$ *is continuous on the set of points near a grazing point which satisfy condition* $(N1)$.

Proof. Let the point $(\theta_i, x_0(\theta_i)) \in \Gamma$ be a grazing one. First, consider a point $(\theta_i, \bar{x}), \bar{x} \neq x_0(\theta_i)$. By means of condition $(H1)$, the continuity of $\tau(x)$ at $\bar{x}$ can be verified by applying technique presented in [5]. Next, we will take into account the continuity at $(\theta_i, x_0(\theta_i))$. Contrarily, assume that $\tau_i(x)$ is not continuous at $x_0(\theta_i)$.

Moreover, assume without loss of generality that it is non-negative. Then, there exists a positive number ϵ_0 and a sequence x_k, $k \in \mathbb{Z}$ such that $\tau(x_k) > \epsilon_0$ and x_k tends to $x_0(\theta_i)$ as $k \to \infty$. Furthermore, by means of the condition $(A2)$, the subsequence $\tau(x_k)$ converges to a number τ_0, where $\epsilon_0 \leq \tau_0 < \theta_{i+1} - \theta_i$. Otherwise, one can take a subsequence of x_k. Due to the fact that the solutions are continuous with respect to initial data, $(\theta_i + \tau(x_k), x(\theta_i + \tau(x_k), \theta_i, x_k)) \in \Gamma$ approaches to $(\theta_i + \tau_0, x(\theta_i + \tau_0, \theta_i, x_0(\theta_i))$. However, the point $(\theta_i + \tau_0, x(\theta_i + \tau_0, \theta_i, x_0(\theta_i)) \notin \Gamma$ and $x(\theta_i + \tau_0, \theta_i, x_0(\theta_i) \notin S$, as well. Because of the closeness of S, we can say that it is impossible. $\square$.

The systems (4.67) and (4.70) are $B-$equivalent, for this reason it is acceptable to linearize system (4.70) instead of system (4.67) around $x_0(t) = x(t, t_0, x_0)$, which is a solution of both systems. Thus, by applying linearization to (4.70), the system (4.73) is obtained. Additionally, the linearization matrix B_i in (4.73) for the grazing point also has to be defined by the formula (4.76), where W_{ix} exists by condition $(A2)$.

On the basis of the discussion made in Subsections 4.8.2.1 to 4.8.2.2, one can conclude that the variational system for the solution $x_0(t)$ with the grazing points can be constructed as a system (4.73).

4.9 Stability of grazing periodic solutions

In this part of the study, by means of the discussions made in the previous part of the study, we will investigate the stability of a periodic solution. Consider the system (4.67) again and the function $f(t, x) : \mathbb{R} \times D \to \mathbb{R}^n$, where D is open connected subset of $\mathbb{R}^n$. Additionally assume that $f(t, x)$ is $T-$ periodic in time, i.e. $f(t + T, x) = f(t, x)$, for $T > 0$.

Let $\Psi(t) : \mathbb{R}_+ \to D$ be a periodic solution of (4.67) with period T and $\theta_i,\ i \in \mathbb{Z}$, be the points of discontinuity which satisfy $(T, p)-$ property, i.e. $\theta_{i+p} = \theta_i + T, p$ is a natural number.

Fix a solution $x(t) = x(t, t_0, \Psi(t_0) + \Delta x)$ and assume that the linearization of that

solution around $\Psi(t)$ exists and there are l many transversal and k many grazing discontinuity moments of $\Psi(t)$ in $[t_0, t_0 + T]$. It is easily seen that the matrix $A(t)$ in the variational system (4.73) for $\Psi(t)$ is $T-$periodic. However, in general, through the formula (4.76), the sequence B_i may not be periodic. For this reason, in what follows we assume the validity of the next condition.

(A3) For each $\Delta x \in \mathbb{R}^n$, the variational system for the near solution $x(t) = x(t, t_0, x_0 + \Delta x)$ to $\Psi(t)$ is one of the following m periodic homogeneous linear impulsive systems

$$\begin{aligned} u' &= A(t)u, \\ \Delta u|_{t=\theta_i} &= B_i^{(j)} u, \end{aligned} \tag{4.79}$$

such that $B_{i+p}^{(j)} = B_i^{(j)}$, $i \in \mathbb{Z},\ j = 1, \ldots, m$, where the number m cannot be larger than 2^k.

We will call the collection of m systems (4.79) *the variational system around the periodic grazing orbit*. This assumption is valid for many low dimensional models and those which can be decomposed into two dimensional subsystems.

So, the variational system (4.79) consists of m periodic subsystems. For each of these systems, we find the matrix of monodromy, $U_j(T)$ and denote corresponding Floquet multipliers by $\rho_i^{(j)}$, $i = 1, \ldots, n$, $j = 1, \ldots, m$. Next, we need the following assumption,

(A4) $|\rho_i^{(j)}| < 1$, $i = 1, \ldots, n$, for each $j = 1, \ldots, m$.

Theorem 7 *Assume that the conditions* $(H1)$, $(A1) - (A4)$ *are valid. Then* $T-$*periodic solution* $\Psi(t)$ *of (4.67) is asymptotically stable.*

Proof. Let $\theta_i, i \in \mathbb{Z}$, be the discontinuity moments of $\Psi(t)$. There exists a natural number p, such that $\theta_{i+p} = \theta_i + T$ for all $i \in \mathbb{Z}$. Because of conditions $(H1)$ and $B-$differentiability of $\Psi(t)$, there exists continuous dependence on initial data and consequently there exists a neighborhood of $(\theta_i, x_0(\theta_i))$ such that any solutions which

starts in the set will have moments of discontinuity which constitute a $B-$ sequence with difference between neighbors approximately equal to the distance between corresponding neighbor moments of discontinuity of the periodic solution $\Psi(t)$. For this reason, the variational system for $\Psi(t)$, can be determined through B-reduced system.

On the basis of above discussion, the variational system of $\Psi(t)$ takes the form

$$\begin{aligned} z' &= A(t)z + \phi(t,z), \\ \Delta z|_{t=\theta_i} &= B_i^{(j)} z + \psi_i(z), \quad j = 1, 2, \ldots, m, \end{aligned} \tag{4.80}$$

where $\phi(t,z) = [f(t,\Psi(t)+z) - f(t,\Psi(t))] - A(t)z$ and $\psi_i(z) = W_i(\Psi(\theta_i)+z) - W_i(\Psi(\theta_i)) - B_i^{(j)}z$, are continuous functions, and matrices $B_i^{(j)}$ satisfy condition $(A4)$.

Denote $Y_j(t)$, $j = 1, 2, \ldots, m$ the fundamental matrix of (4.81) adjoint to (4.80) linear homogeneous system

$$\begin{aligned} y' &= A(t)y, \\ \Delta y|_{t=\theta_i} &= B_i^{(j)} y. \end{aligned} \tag{4.81}$$

Due to the conditions $(A3)$ and $(A4)$, there exist numbers $K > 0$ and $\gamma > 0$ such that for all $j = 1, 2, \ldots, m$, the following estimate holds

$$\|Y_j(t,s)\| \leq Ke^{-\gamma(t-s)} \tag{4.82}$$

Any solution of (4.80) neighbor to the trivial one can be written as one of the following form

$$z(t,z_0) = Z(t,t_0)z_0 + \int_{t_0}^{t} Y_j(t,s)\phi(s,z(s,z_0))ds + \sum_{t_0 \leq \theta_i < t} Y_j(t,\theta_i)\psi_i(z(\theta_i,z_0)). \tag{4.83}$$

The functions $\phi(t,z)$ and $\psi(t,z)$ satisfy the inequalities

$$\|\phi(t,z)\| \leq l\|z\| \tag{4.84}$$

and

$$\|\psi_i(z)\| \leq l\|z\|, \tag{4.85}$$

for all $t > t_0$, $\|z\| < k$, $k > 0$. Using estimates (4.82), (4.84) and (4.85), we obtain that

$$\begin{aligned}\|z(t,z_0)\| &\leq Ke^{-\gamma(t-t_0)}\|z_0\| + \int_{t_0}^{t} Ke^{-\gamma(t-s)}l\|z(s,z_0)\|ds \\ &+ \sum_{t_0<\theta_i<t} Ke^{-\gamma(t-\theta_i)}l\|z(\theta_i,z_0)\|.\end{aligned} \tag{4.86}$$

There exists positive θ such that the inequality $\theta_{i+1} - \theta_i > \theta$ is true. By applying Gronwall-Bellman Lemma [5, 113], one can obtain the following estimate

$$\|z(t,t_0)\| \leq Ke^{-(\gamma - Kl - \frac{1}{\theta}ln(1+kl))(t-t_0)}\|z_0\|. \tag{4.87}$$

For sufficiently small l, it is true that $\gamma - Kl - \frac{1}{\theta}ln(1+kl) > 0$, any solution $z(t,z_0)$ of (4.80), with $\|z_0\| < \frac{l}{K}$ is defined for all $t \geq t_0$ and $\lim_{t\to\infty}\|z(t,z_0\| = 0$. Thus, the the trivial solution of (4.80) is exponentially stable. □

Example 14 *In this example, we consider the following system of differential equation with variable moments of impulses*

$$\begin{aligned}&x'' + 0.002x' + x = -1 - 0.002\sin(t), \\ &\Delta x'|_{x\in S} = -(1+0.9x')x',\end{aligned} \tag{4.88}$$

where $S = \{(x,x')|\Phi(x,x') = x = 0\}$. *Let us rewrite the system* (4.88) *in the form*

$$\begin{aligned}&x_1' = x_2, \\ &x_2' = -0.002x_2 - x_1 - 1 - 0.002\sin(t), \\ &\Delta x_2|_{x\in S} = -(1+0.9x_2)x_2,\end{aligned} \tag{4.89}$$

where $x = (x_1, x_2)$ *and the discontinuity surface* S *can be written in the form* $S = \{(x_1,x_2)|\Phi(x) = x_1 = 0\}$. *It has a periodic solution* $\Psi(t) = (-1+\cos(t), -\sin(t))$. *The orbit of which is pictured in Fig. 4.11*

The system (4.89) *has a discontinuity surface* $S = \{(x_1,x_2)|\ x_1 = 0,\ x_2 > 0\}$. *Then, it is easy to see that* $\Phi(x) = x_1^2$. *Consider the function* $H(t,x)$ *at the point* $(\theta_i, \Psi(\theta_i)) = (2\pi i, \Psi(2\pi i))$, $i \in \mathbb{Z}$. *It is true that* $H(2\pi i, \Psi(2\pi i)) = 0$, $J(\Psi(2\pi i)) =$

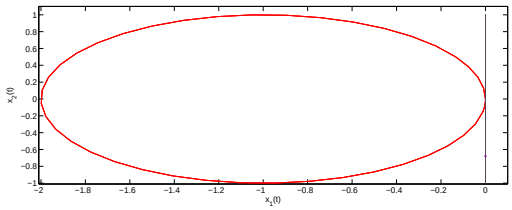

Figure 4.11: The periodic solution $\Psi(t)$ of (4.89) and the blue line is the surface of discontinuity S.

0 *and* $H(t,x) \neq 0$ *for some number* $\delta > 0$, *such that* $|t - 2\pi i| < \delta$ *and* $\|x - \Psi(2\pi i)\| < \delta$. *So, by means of Definitions 14 and 15, we can say that* $(\theta_i, \Psi(\theta_i)) = (2\pi i, \Psi(2\pi i)) = (2\pi i, 0, 0)$ *is a grazing point and the periodic solution* $\Psi(t)$ *contains the grazing point* $(2\pi i, 0, 0)$, *then we can say that* $\Psi(t)$ *is a grazing periodic orbit. Additionally, all points* $(2\pi i, \Psi(2\pi i)),\ i \in \mathbb{Z}$ *are grazing points. This validates the condition* $(H1)$.

In the remaining part, we will investigate the stability of the grazing orbit by the linearization of (4.89) *around the solution. Because the point* $(2\pi i, 0, 0)$ *is a grazing point, we will consider the linearization by applying formulas* (4.74) *and* (4.76). *By means of condition* $(H1)$, *it is true that the solutions intersects the surface of discontinuity transversely near the grazing one. For this reason, consider a point* $\bar{x} = (0, \bar{x}_2)$ *on the surface of discontinuity* Γ *near* $x^* = (0,0)$. *Because of the transversality of* $\bar{x}$, *the first component* $\frac{\partial \tau(\bar{x})}{\partial x_1}$ *of the gradient* $\nabla\tau(\bar{x})$ *can be determined by formula* (4.49), *it is obtained as* $\frac{\partial \tau(\bar{x})}{\partial x_1} = -\frac{1}{\bar{x}_2}$. *At the grazing point, the first component can be evaluated as* $\frac{\partial \tau(x^*)}{\partial x_1} = -\infty$.

First, we assume that $x(t) = x(t, 0, x^* + \Delta x)$, $\Delta x = (\Delta x_1, \Delta x_2)$ *is not a grazing solution. That is, the point* $x^* + \Delta x$ *is not an orbit point of* $\Psi(t)$. *Hence, the meeting point* $\bar{x} = (\bar{x}_1, \bar{x}_2) = (x_1(\xi, 0, (x^* + \Delta x)), x_2(\xi, 0, (x^* + \Delta x))$, *is transversal one. Moreover,* ξ *is the meeting moment with* Γ.

It is clear $\bar{x}_1 = 0$ *and* $\bar{x}_2 < 0$. *In order to find a linearization at the moment* $t = \theta_i$,

we use formula (4.69) *and find that*

$$\frac{\partial W_i(x)}{\partial x_1^0} = \int_{\theta_i}^{\tau(x)} \frac{\partial f(s,x(s))}{\partial x}\frac{\partial x(s)}{\partial x_1^0}ds + f(s,x(s))\frac{\partial \tau(x)}{\partial x_1^0} + J_x(x)(e_1+$$

$$f(s,x(s))\frac{\partial \tau(x)}{\partial x_1^0}) + f(s,x(s)+J(x(s)))\frac{\partial \tau(x)}{\partial x_1^0} + \int_{\tau(x)}^{\theta_i} \frac{\partial f(s,x(s)+J(x(s)))}{\partial x}\frac{\partial x(s)}{\partial x_1^0}ds, \tag{4.90}$$

where $e_1 = (1,0)^T$, T *denotes the transpose of a matrix. Substituting* $x = \bar{x}$ *to the formula* (4.90)*, we obtain that*

$$\frac{\partial W_i(x(\xi,0,x^*+\Delta x))}{\partial x_1^0} = f(\xi, x(\xi,0,x^*+\Delta x))\frac{\partial \tau(x(\xi,0,x^*+\Delta x))}{\partial x_1^0}$$
$$+J_x(x(\xi,0,x^*+\Delta x))\left(e_1 + f(\xi,x(\xi,0,x^*+\Delta x)))\frac{\partial \tau(x(\xi,0,x^*+\Delta x)))}{\partial x_1^0}\right)$$
$$+f(\xi,x(\xi,0,(J(x(\xi,0,x^*+\Delta x)))))\frac{\partial \tau(J(x(\xi,0,x^*+\Delta x)))}{\partial x_1^0}. \tag{4.91}$$

Considering the formula (4.49) *for the transversal point* $\bar{x} = (\bar{x}_1, \bar{x}_2)$*, the first component* $\frac{\partial \tau(\bar{x})}{\partial x_1^0}$ *can be evaluated as* $\frac{\partial \tau(\bar{x})}{\partial x_1^0} = -\frac{1}{\bar{x}_2}$*. From the last equality, it is seen how the singularity appears at the grazing point. By taking into account* (4.88) *with* (4.91)*, one can obtain that*

$$\frac{\partial W_i(\bar{x})}{\partial x_1^0} = \begin{bmatrix} \bar{x}_2 \\ -\bar{x}_1 - 0.002\bar{x}_2 - 1 - 0.002\sin(\xi) \end{bmatrix}\Big(-\frac{1}{\bar{x}_2}\Big) + \begin{bmatrix} 1 & 0 \\ 0 & -2R\bar{y}_2 \end{bmatrix}$$
$$\left(e_1 + \begin{bmatrix} \bar{x}_2 \\ -\bar{x}_1 - 0.002\bar{x}_2 - 1 - 0.002\sin(\xi) \end{bmatrix}\Big(-\frac{1}{\bar{x}_2}\Big)\right)$$
$$-\begin{bmatrix} -R(\bar{x}_2)^2 \\ -\bar{x}_1 + 0.002R(\bar{x}_2)^2 - 1 - 0.002\sin(\xi) \end{bmatrix}\Big(-\frac{1}{\bar{x}_2}\Big) =$$
$$\begin{bmatrix} \bar{x}_2 - R(\bar{x}_2)^2 \\ -\bar{x}_1 - 0.002(\bar{x}_2 - R(\bar{x}_2)^2) \end{bmatrix}\Big(-\frac{1}{\bar{x}_2}\Big) +$$
$$\begin{bmatrix} 1 & 0 \\ 0 & -2R\bar{x}_2 \end{bmatrix}\begin{bmatrix} 1 & \\ \dfrac{\bar{x}_1 + 0.1\bar{x}_2 - 1 - 0.002\sin(\xi)}{\bar{x}_2} & \dfrac{-\bar{x}_2}{\bar{x}_2} \end{bmatrix}. \tag{4.92}$$

Calculating the righthand side of (4.92) *we can obtain that*

$$\frac{\partial W_i(\bar{x})}{\partial x_1^0} = \begin{bmatrix} R\bar{x}_2 - 1 \\ 0.1(1 - R\bar{x}_2) + 2R(0.1\bar{x}_2 - \bar{x}_1 - 1 - 0.002\sin(\xi)) \end{bmatrix}. \tag{4.93}$$

Similarly, differentiating (4.69) *with* $x(t)$ *one can find that*

$$\begin{aligned} \frac{\partial W_i(x)}{\partial x_2^0} &= \int_{\theta_i}^{\tau(x)} \frac{\partial f(s,x)}{\partial x}\frac{\partial x(s)}{\partial x_2^0}ds + f(s,x(s))\frac{\partial \tau(x)}{\partial x_2^0} + J_x(x)(e_2 \\ &+ f(s,x(s))\frac{\partial \tau(x)}{\partial x_2^0}) + f(s,x+J(x))\frac{\partial \tau(x)}{\partial x_2^0} \\ &+ \int_{\tau(x)}^{\theta_i} \frac{\partial f(s,x(s)+J(x(s)))}{\partial x}\frac{\partial x(s)}{\partial x_2^0}ds, \end{aligned} \tag{4.94}$$

where $e_2 = (0,1)^T$. *Calculate the right hand side of* (4.94) *at the point* $\bar{x} = (\bar{x}_1, \bar{x}_2)$ *to obtain*

$$\begin{aligned} \frac{\partial W_i(x(\xi,0,x^*+\Delta x))}{\partial x_2^0} &= f(\xi, x(\xi,0,y^*+\Delta x))\frac{\partial \tau(x(\xi,0,x^*+\Delta x))}{\partial x_2^0} \\ &+ J_x(x(\xi,0,x^*+\Delta x))\left(e_2 + f(\xi,x(\xi,0,x^*+\Delta x)))\frac{\partial \tau(x(\xi,0,x^*+\Delta x))}{\partial x_2^0}\right) \\ &+ f(\xi,x(\xi,0,x^*+\Delta x))\frac{\partial \tau(x(\xi,0,x^*+\Delta x))}{\partial x_2^0}. \end{aligned} \tag{4.95}$$

To calculate the fraction $\dfrac{\partial \tau(x(\xi,0,x^*+\Delta x))}{\partial x_2^0}$ *in* (4.95)*, we apply formula* (4.49) *for the transversal point* $\bar{x} = (\bar{x}_1, \bar{x}_2)$. *The second component* $\dfrac{\partial \tau(\bar{x})}{\partial x_2^0} = 0$. *This and formula* (4.95) *imply*

$$\frac{\partial W_i(\bar{x})}{\partial x_2^0} = \begin{bmatrix} 0 \\ -2R\bar{x}_2 \end{bmatrix}. \tag{4.96}$$

Joining (4.93) *and* (4.56)*, the matrix* $W_{ix}(\bar{x})$ *can be obtained as*

$$W_{iy}(\bar{x}) = \begin{bmatrix} R\bar{x}_2 - 1 & 0 \\ 0.1(1 - R\bar{x}_2) + 2R(0.1\bar{x}_2 - \bar{x}_1 - 1 - 0.002\sin(\xi)) & -2R\bar{x}_2 \end{bmatrix}. \tag{4.97}$$

Taking into account formula (4.97)*, we can assert that the map* $W_i(x)$ *is differentiable at* $x = x^*$*. Thus, this verifies the condition* $(A1)$*. Let consider a near solution to* $(\theta_i, \Psi(\theta_i))$ *there are two possibility for the near solution it satisfies* $(N1)$ *an d* $(N2)$*. The meeting moment* $\tau(x)$ *can not been taken into account whenever it satisfies* $(N1)$*. So, to validate the condition condition* $(A2)$*, we should only consider those which satisfies* $(N2)$*. To verify it, let us take into account a solution of the first equation in* (4.88) *which starts at the point* $\bar{x} = (0, \bar{x}_2) \in S$*. The solution of* (4.88) *at* $\bar{x}$ *is the form*

$$x(t, 0, \bar{x}) = \frac{\bar{x}_2}{\sqrt{1-(0.01)^2}} \exp(0.01t) \sin(\sqrt{1-(0.01)^2}t).$$

This solution meets the surface $\mathscr{S}$ *at the moment* $\bar{t} = \frac{2\pi}{\sqrt{1-(0.01)^2}}$*, again. Thus, the meeting moment* $\tau_i(x) = \bar{t} < 2\pi - \epsilon$*, where* ϵ *is a small positive number and this verifies* $(A2)$*. Let us come back to the linearization part. The last expression* (4.97) *demonstrates that the Jacobian is continuous function of its arguments in a neighborhood of the grazing point. Indeed, it is defined and continuous for the points, which are not from the orbit of grazing solution. For the orbit points of the grazing solution the Jacobian can be determined by the limit procedure. We apply it when* $x \to x^*$*, as well as* $\xi \to 2\pi$*, where* 2π *is the first grazing discontinuity point of periodic solution* $\Psi(t)$*, then we obtain that*

$$W_{iy}(y^*) = \begin{bmatrix} -1 & 0 \\ 0.1 - 2R & 0 \end{bmatrix}. \tag{4.98}$$

Consequently, the function $W_i(x)$ *is differentiable at the grazing point* $x = x^*$ *and* $(A1)$ *is valid.*

Utilizing (4.76) *with above discussion, we obtain that*

$$B_1 = \begin{cases} \begin{bmatrix} -1 & 0 \\ 0.1 - 2R & 0 \end{bmatrix}, & if \quad \textit{(N1) is valid}, \\ O_2, & if \quad \textit{(N2) is valid}. \end{cases}. \tag{4.99}$$

On the basis of the above discussion, we can assert that the variational system con-

sists of $m = 2$ *linear homogenous subsystems:*

$$\begin{aligned} z' &= A(t)z, \\ \Delta z|_{t=\theta_i} &= B^{(1)}z, \end{aligned} \tag{4.100}$$

and

$$\begin{aligned} z' &= A(t)z, \\ \Delta z|_{t=\theta_i} &= B^{(2)}z, \end{aligned} \tag{4.101}$$

where $A(t) = \begin{bmatrix} 0 & 1 \\ -1 & -0.02 \end{bmatrix}$, $\theta_i = 2\pi i$, $B^{(1)} = O_2$ *and* $B^{(2)} = \begin{bmatrix} 0 & 0 \\ -0.6 & 0.4 \end{bmatrix}$. *One can check easily that* $A(t + 2\pi) = A(t)$, *for all* $t \in \mathbb{R}$, $B_i^{(1)} = B^{(1)}$, $B_i^{(2)} = B^{(2)}$, *and* $2\pi(i + 1) = 2\pi i + 2\pi$. *Thus,* $\{B_i^{(j)}\}$, $j = 1, 2$ *are* $1-$*periodic. Moreover, system* (4.100)+ (4.101) *is a* $(2\pi, 1)-$*periodic system this validates* $(A3)$. *The monodromy matrices for* (4.100) *and* (4.101) *have multipliers* $\rho_1^{(1)} = 0.9844$, $\rho_2^{(1)} = 0.9844$, $\rho_1^{(2)} = 0.9844$, $\rho_2^{(2)} = 0.098$. *Thus, the condition* $(A4)$ *is valid. Consequently, the conditions* $(H1)$ *and* $(A1) - (A4)$ *are valid, by means of Theorem 7, it is easy to say that the periodic solution* $\Psi(t)$ *is asymptotically stable. In Fig. 4.12, the red curve corresponds to the periodic solution* $\Psi(t)$, *the blue line is the discontinuity surfaces* S *and* $\tilde{S}$ *and the black curves are the phase portrait of a solution of* (4.89) *with initial value* $x_0 = (-0.01, 0.5)$. *One can observe that the black curves approach the red one as time increases.*

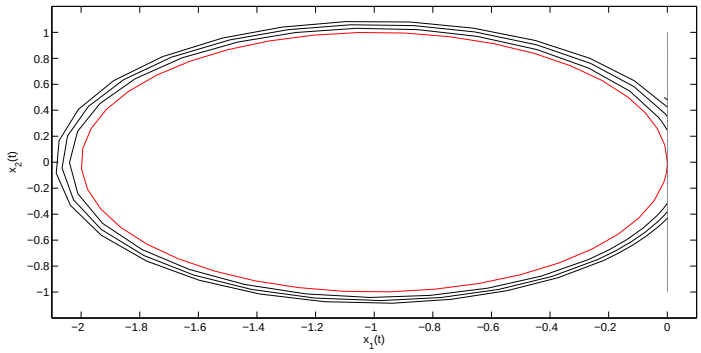

Figure 4.12: The red curve is the periodic solution $\Psi(t)$ of (4.89), the blue ones are the phase portrait of the solution of (4.89) with initial value $x_0 = (-0.01, 0.5)$. and the blue line is the surface of discontinuity S.

Example 15 *In this example, we take into account the following system*

$$\begin{aligned} &x'' - 0.05x' + x = -0.05\sin(t) + 1, \\ &\Delta x|_{(x,x')\in S} = 1 - \frac{1}{\sqrt{2}} - x + R(x' + x - 1)^2, \\ &\Delta x'|_{(x,x')\in S} = \frac{1}{\sqrt{2}} - x' + R(x' + x - 1)^2, \end{aligned} \tag{4.102}$$

where $R = 0.5$ *and* $S = \{(x, x')|x - x' = 1 - \sqrt{2}\}$. *It is easy to see that* $\Gamma = \mathbb{R} \times S$. *Defining variables as* $x = x_1$ *and* $x' = x_2$, *the system* (4.102), *can be rewritten as*

$$\begin{aligned} &x_1' = x_2, \\ &x_2' = 0.01x_2 - x_1 - 0.01\sin(t) + 1, \\ &\Delta x_1|_{(x_1,x_2)\in S} = 1 - \frac{1}{\sqrt{2}} - x_1 + R(x_2 + x_1 - 1)^2, \\ &\Delta x_2|_{(x_1,x_2)\in S} = \frac{1}{\sqrt{2}} - x_2 + R(x_2 + x_1 - 1)^2, \end{aligned} \tag{4.103}$$

where $S = \{(x_1, x_2)|x_1 - x_2 - 1 + \sqrt{2} = 0\}$. *It is easy to see that* $\Gamma = \mathbb{R} \times S$. *The system has a* $2\pi-$*periodic solution, that is* $\Psi(t) = (1 - \cos(t), \sin(t)), t \in \mathbb{R}$. *At time* $t = \frac{\pi}{4}$, *it has a grazing point of the form* $(\theta_i, \Psi(\theta_i)) = (\frac{\pi}{4} + 2\pi i, 1 - \frac{1}{\sqrt{2}}, \frac{1}{\sqrt{2}})$. *To verify it, we will consider* $\Phi(x_1, x_2) = x_1 - x_2 - 1 + \sqrt{2}$, *then the gradient of is* $\nabla\Phi(x_1, x_2) = (1, -1)$. *Taking into account formula* $H(t, x)$ *at* $(\frac{\pi}{4}, 1 - \frac{1}{\sqrt{2}}, 1 - \frac{1}{\sqrt{2}})$, *we obtain that*

$$H(\frac{\pi}{4}, 1 - \frac{1}{\sqrt{2}}, \frac{1}{\sqrt{2}}) = \langle(1, -1), (\frac{1}{\sqrt{2}}, \frac{0.01}{\sqrt{2}} - 1 + \frac{1}{\sqrt{2}} + 1 - 0.01\sin(\frac{\pi}{4})\rangle = 0.$$

In (4.13), *the periodic solution of* (4.103) *is depicted.*

Next, let us consider the linearization of (4.103) *at the grazing point* $(\theta_i, \Psi(\theta_i)))$. *Consider a solution* $x(t) = x(t, 0, \Psi(\theta_i) + \Delta x)$ *of* (4.103) *which is near to* $\Psi(t)$. *Denote the meeting moment of* $x(t)$ *with the surface of discontinuity* Γ *as* $t = \zeta$ *and the meeting point with* S *as* $\bar{x} = x(\zeta) = x(\zeta, 0, \Psi(\theta_i) + \Delta x)$. *It is easy to see that* $(\zeta, x(\zeta)) \in \Gamma$. *Then, taking into account formulae* (4.90) *and* (4.91) *with system*

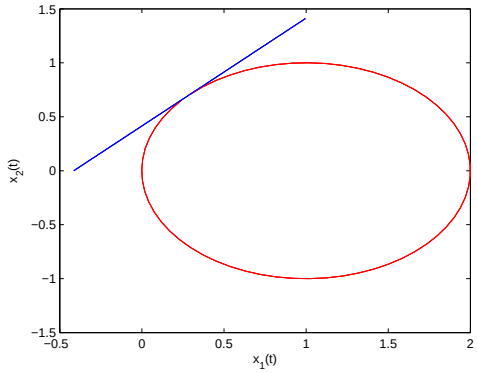

Figure 4.13: The red curve is the periodic solution $\Psi(t)$ of (4.103) and the blue line is the surface of discontinuity S.

(4.103), *we obtain that*

$$\frac{\partial W_i(\bar{x})}{\partial x_1^0} = \begin{bmatrix} \bar{x}_2 \\ -\bar{x}_1 + 0.01\bar{x}_2 + 1 + 0.01\sin(\zeta) \end{bmatrix} \Big(- \frac{1}{1.99\bar{x}_2 - \sqrt{2} + 1 - 0.01\sin(\zeta)} \Big)$$
$$+ 2K(x_1 + x_2 - 1) \begin{bmatrix} 1 & 1 \\ 1 & 1 \end{bmatrix} \Bigg(e_1 + \begin{bmatrix} \bar{x}_2 \\ -\bar{x}_1 + 0.01\bar{x}_2 - 1 - 0.01\sin(\zeta) \end{bmatrix} \times$$
$$\Big(- \frac{1}{1.99\bar{x}_2 - \sqrt{2} + 0.01\sin(\zeta)} \Big) \Bigg)$$
$$- \begin{bmatrix} \frac{1}{\sqrt{2}} + R(\bar{x}_2 + \bar{x}_1 - 1)^2 \\ -1 + \frac{1}{\sqrt{2}} - R(\bar{x}_2 + \bar{x}_1 - 1)^2 + 0.01(\frac{1}{\sqrt{2}} + R(\bar{x}_2 + \bar{x}_1 - 1)^2 - \sin(\zeta)) + 1 \end{bmatrix} \times$$
$$\Big(- \frac{1}{2\bar{x}_2 - 0.01\bar{x}_2 - \sqrt{2} + 0.01\sin(\zeta)} \Big). \tag{4.104}$$

Above equation is simplified as

$$\frac{\partial W_i(\bar{x})}{\partial x_1^0} = \begin{bmatrix} \frac{\sqrt{2}\bar{x}_2 - 1}{\sqrt{2}} + R(\bar{x}_2 - \sqrt{2})^2 \\ \frac{1 - \sqrt{2}\bar{x}_2}{\sqrt{2}} + 0.01(\frac{\sqrt{2}\bar{x}_2 - 1}{\sqrt{2}} + R(\bar{x}_2 - \sqrt{2})^2) \end{bmatrix} +$$
$$\begin{bmatrix} 2R(2\bar{x}_2 - \sqrt{2})\bar{x}_2 \\ 2R(2\bar{x}_2 - \sqrt{2})(-\bar{x}_1 + 0.01(\bar{x}_2 - \sin(\zeta)) - 1) \end{bmatrix} \times \tag{4.105}$$
$$\Big(- \frac{1}{2\bar{x}_2 - 0.01\bar{x}_2 - \sqrt{2} + 0.01\sin(\zeta)} \Big)$$

Calculating (4.105) *at* $(\theta_i, \Psi(\theta_i))$, *we obtain that*

$$\frac{\partial W_i(\Psi(\theta_i))}{\partial x_1^0} = \begin{bmatrix} -1-\sqrt{2}R \\ -0.505 \end{bmatrix}. \tag{4.106}$$

Similarly, one can obtain that

$$\begin{aligned} \frac{\partial W_i(\bar{x})}{\partial x_2^0} = & \begin{bmatrix} \bar{x}_2 - \frac{1}{\sqrt{2}} + R(\bar{x}_2 - \sqrt{2})^2 \\ \frac{1}{\sqrt{2}} - \bar{x}_2 + 0.01(\bar{x}_2 - \frac{1}{\sqrt{2}} + R(\bar{x}_2 - \sqrt{2})^2) \end{bmatrix} \\ & \begin{bmatrix} 2R(2\bar{x}_2 - \sqrt{2}) + 2R(2\bar{x}_2 - \sqrt{2})\bar{x}_2 \\ 2R(2\bar{x}_2 - \sqrt{2})(-\bar{x}_1 + 0.01\bar{x}_2 - 1 - 0.01\sin(\zeta)) \end{bmatrix} \times \\ & \Big(\frac{1}{2\bar{x}_2 - 0.01\bar{x}_2 - \sqrt{2} + 0.01\sin(\zeta)}\Big) \end{aligned} \tag{4.107}$$

and simply we obtain that

$$\frac{\partial W_i(\Psi(\theta_i))}{\partial x_2^0} = \begin{bmatrix} 1+\sqrt{2}R \\ 0.505 \end{bmatrix}. \tag{4.108}$$

Combining (4.106) *with* (4.108)*, we obtain the linearization matrix at* $(\theta_i, \Psi(\theta_i))$,

$$W_{ix}(\Psi(\theta_i)) = \begin{bmatrix} -1-\sqrt{2}R & 1+\sqrt{2}R \\ -0.505 & 0.505 \end{bmatrix}. \tag{4.109}$$

Utilizing (4.76) *with above discussion, we obtain that*

$$B_1 = \begin{cases} \begin{bmatrix} -1-\sqrt{2}R & 1+\sqrt{2}R \\ -0.505 & 0.505 \end{bmatrix} & if \quad \textit{(N1) is valid}, \\ O_2, & if \quad \textit{(N2) is valid}. \end{cases}. \tag{4.110}$$

In the light of the expression (4.109) *and the formula* (4.76)*, the variational system for* $\Psi(t)$ *can be obtained as*

$$\begin{aligned} u_1' &= u_2, \\ u_2' &= 0.01u_2 - u_1 \end{aligned} \tag{4.111}$$

and

$$\begin{aligned} u_1' &= u_2, \\ u_2' &= 0.01u_2 - u_1, \\ \Delta u|_{t=\frac{pi}{4}+2\pi i} &= \begin{bmatrix} -1-\sqrt{2}R & 1+\sqrt{2}R \\ -0.505 & 0.505 \end{bmatrix} u. \end{aligned} \tag{4.112}$$

It is easy to see that the variational system is $(2\pi, 1)$ *periodic system which verifies condition* $(A3)$ *and the eigenvalues of th monodromy matrix can be obtained as* $\rho_1^{(1)} = 0.908$, $\rho_2^{(1)} = -0.608$, $\rho_1^{(2)} = 0.879$, $\rho_2^{(2)} = -0.02$. *Thus, the assumption* $(A4)$ *is true. Using similar method presented in Example 14, it is easy to verify the conditions* $(A1)$ *and* $(A2)$. *In the light of the conditions* $(H1)$ *and* $(A1) - (A4)$, *By means of Theorem 7, we can conclude that the periodic solution* $\Psi(t)$ *of* (4.103) *is asymptotically stable. In Fig. 4.14, the red curve corresponds tı the periodic solution* $\Psi(t)$ *of* (4.103) *and the blue line is the surface of discontinuity* S. *The magenta curve is the near solution to* $\Psi(t)$ *of* (4.103) *with initial value* $(1, -1.1)$. *The magenta curve approaches to the red curve as time increases which verifies through simulation that the periodic solution is asymptotically stable.*

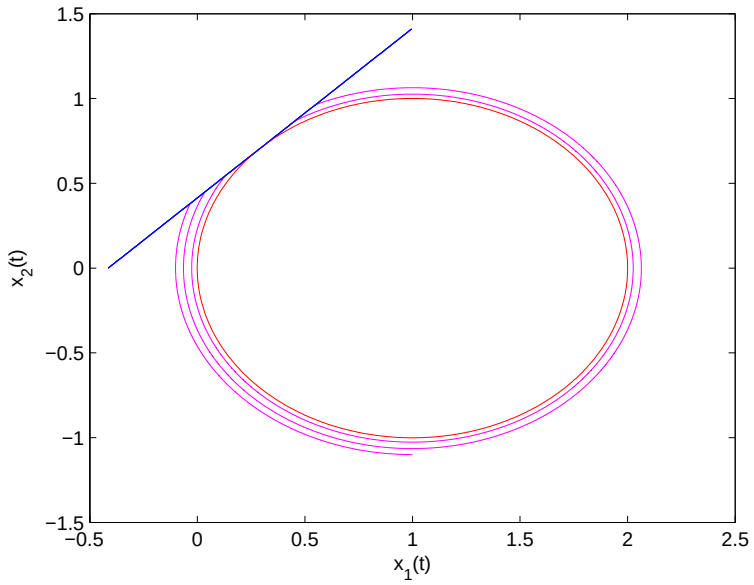

Figure 4.14: The red curve is the periodic solution $\Psi(t)$ of (4.103) and the blue line is the surface of discontinuity S. The magenta curve is the near solution to $\Psi(t)$ of (4.103) with initial value $(1, -1.1)$.

4.9.1 Regular perturbations around the grazing periodic solution

In the previous part of the study, we analyze the existence and stability of periodic solutions of non-autonomous systems with a stationary impulse condition. In this part, we will investigate the bifurcation of grazing periodic solutions by applying regular perturbation to the system. Under certain conditions, the perturbation gives rise the existence of periodic solution in impulsive systems. Due to the complexity of the grazing behavior, there may be different type of bifurcation scenarios. In this part of the study, we will demonstrate the increment in the number of periodic solutions with the variation of the parameter μ.

To make our investigations, we take into account the following perturbed system:

$$\begin{aligned} x' &= f(t,x) + \mu g(t,x,\mu), \\ \Delta x|_{x\in S(\mu)} &= I(x) + \mu K(x,\mu), \end{aligned} \tag{4.113}$$

where $(t,x) \in \mathbb{R}\times G$, $\mu \in (-\mu_0,\mu_0)$, μ_0 is a fixed positive number. The system (4.113) is $T-$periodic system, i.e. $f(t+T,x) = f(t,x)$ and $g(t+T,x,\mu) = g(t,x,\mu)$ with some positive number T. Additionally, $f(t,x)$ is two times differentiable in x, continuous in time and first order differentiable in μ. The function $K(x,\mu)$ is differentiable in x and μ and $I(x)$ is differentiable in x. The surface of discontinuity of (4.113), $S(\mu)$ is defined as $S(\mu) = \{x \in G| \quad \Phi(x) + \mu\phi(x,\mu) = 0\}$, where $\Phi(x)$ second order differentiable in x and $\phi(x,\mu)$ is second and first order differentiable in x and μ, respectively.

The generating system of (4.113) is the system (4.67). In the previous section, we assumed that the generating system has a periodic solution $\Psi(t)$. All assumptions and conditions $(H1)$, $(A1)-(A4)$ are also valid in this subsection.

Let us seek the periodic solutions of (4.113) around the grazing one. Generally, the investigation on the periodic solutions of such systems is carried out by utilizing Poincare map which is based on the values of solutions at the period moment. For this reason, we will analyze the existence of the periodic solution of (4.113) in the light of this map. But, it may not be differentiable near a grazing point [82, 25]. To handle with this problem, we make use of the condition $(A1)$. There can be m different linearization system can be appear around the grazing solution depending

on the grazing point. Fix some j, where $j \in 1, 2, \ldots, m$. Denote a solution of system (4.113) by

$$x_i^{(j)}(t, \gamma_1^{(j)}, \ldots, \gamma_n^{(j)}, \mu),\ i = 1, 2, \ldots, n, \tag{4.114}$$

with initial values

$$x_i^{(j)}(0, \gamma_1^{(j)}, \ldots, \gamma_n^{(j)}, \mu) = \gamma_i^{(j)},\ i = 1, 2, \ldots, n. \tag{4.115}$$

Moreover, considering the periodic solution $\Psi(t) = (\Psi_1(t), \ldots, \Psi_n(t))$ of the generating system, it is easy to obtain that

$$x_i^{(j)}(t, \Psi_1(0), \ldots, \Psi_n(0), 0) \equiv \Psi_i(t),\ i = 1, 2, \ldots, n. \tag{4.116}$$

In order to verify the existence of such periodic solution of (4.113), it is neccessary and sufficient to check the validity of the following equality

$$\mathscr{P}_i^{(j)}(\gamma_1^{(j)}, \ldots, \gamma_n^{(j)}) = x_i^{(j)}(T, \gamma_1^{(j)}, \ldots, \gamma_n^{(j)}, \mu) - \gamma_i^{(j)},\ i = 1, 2, \ldots, n. \tag{4.117}$$

By means of the equation (4.114) conditions (4.115) -(4.117) are satisfied for $\mu = 0$, $\gamma_i = \Psi_i(0)$, since the generating solution is periodic.

The following conditions for the determinant will be needed for the rest of the study.

(A5)

$$\begin{vmatrix} \frac{\partial \mathscr{P}_1^{(j)}(\gamma_1,\ldots,\gamma_n)}{\partial \gamma_1} & \cdots & \frac{\partial \mathscr{P}_1^{(j)}(\gamma_1,\ldots,\gamma_n)}{\partial \gamma_n} \\ \vdots & \ddots & \vdots \\ \frac{\partial \mathscr{P}_n^{(j)}(\gamma_1,\ldots,\gamma_n)}{\partial \gamma_1} & \cdots & \frac{\partial \mathscr{P}_n^{(j)}(\gamma_1,\ldots,\gamma_n)}{\partial \gamma_n} \end{vmatrix} \neq 0. \tag{4.118}$$

If this solution belongs to the proper subset, we will say it a periodic solution of the perturbed system. To find the solutions, we should verify the condition $(A5)$ and we have to see that (4.117) is solvable. In the set of the initial values which contains initial with that request linearizations.

Assume that the conditions $(H1)$ and $(A1) - (A5)$ are valid. Then, (4.67) admits a non-trivial m $T-$ periodic solution, which converges in the $B-$ topology to the T-periodic solution of (4.113) as μ tends to zero.

Let us verify the above assertion. Without loss of generality, assume that the moments of discontinuity of the periodic solution $\Psi(t)$ admits that $0 < \theta_1 < \ldots < \theta_p < T$ Let $x^{(j)}(t) = x(t, 0, x^{(j)}, \mu)$ be a solution of the perturbed system (4.113) with initial values $x^{(j)}(0) = x^{(j)}$. Fix j in the system (3.13) and fixed some solution $x^{(j)}(t)$, whose linearization is exactly that system. Taking into account the conditions and assumptions $(H1)$ and $(A1)-(A4)$, it is easy to verify that the discontinuity moments of $x^{(j)}(t)$ satisfy that $0 < \eta_1 < \ldots < \eta_p < T$ and there exists a neighborhood $\Psi(0)$ which does not intersect . Applying the formulas (4.114)-(4.117), the following can be obtained

$$\mathscr{P}^{(j)}(y, \mu) = X(T, 0, y, \mu) - y = 0. \tag{4.119}$$

It is satisfied with $y = z^{(j)}$. Now, let us apply implicit function theorem to verify the existence of the periodic solutions of (4.113) with the help of (4.119) in the neighborhood of $(\Psi(0), 0)$. For $\mu = 0$, it is easy to obtain the following variational system

$$\begin{aligned} u' &= A(t)u, \\ \Delta u(\theta_i) &= B_i^{j)} u(\theta_i), \end{aligned} \tag{4.120}$$

where $i \in \mathbb{Z}$ and $j = 1, \ldots, m$. The $K-$derivatives of the solution $x^{(j)}(t)$ in $x^{(j)}$ forms the fundamental matrix $Y^{(j)}(t, x^{(j)}(t), \mu)$, of the variational system (4.120) with $Y^{(j)}(0, x^{(j)}(t), \mu) = I$, where I is an identity matrix. The uniqueness of the periodic solution $\Psi(t)$ implies that

$$\mathscr{P}_y^{(j)}(y, \mu) = Z^{(j)}(T, 0, y, \mu) - I \neq 0. \tag{4.121}$$

Thus, the equation (4.119) has a unique solution in the neighborhood of $\Psi(0)$ for sufficiently small $|\mu|$. The suggested periodic solution of the perturbed system takes the form
$z^{(j)}(t) = z(t, 0, z^{(j)}(\mu), \mu)$, where $z^{(j)}(\mu)$ are the initial values of that solution which are obtained uniquely from the equation (4.119). This solution became closer to $\Psi(0)$ as μ tends to zero. Denote the number of grazing point of the periodic solution by β and it can be vary from 0 to m. The above part is verified only for a fixed j, bu it can be done for all possible $\beta-$many periodic solutions. Thus, we can conclude that the

system (4.67) admits a non-trivial $\beta-$ many $T-$ periodic solution, which converge in the $B-$ topology to the $T-$ periodic solution of (4.113) as $|\mu|$ tends to zero.

This assertion will be realized thoroughly in the next subsection which covers some application results about the present study. In the models, we are not going to approve rigorously existence of solutions and their stability. Nevertheless, we will check necessary conditions and we will verify the stability by means of simulations. The necessary conditions which says about the linearization make it possible to seek the periodic solutions and stability through simulations.

4.9.2 Some application results

The mechanical and electrical interpretation of the first model has not been determined, yet. However, this model contains a Van der Pol oscillator with a periodic external force which is connected unilaterally to another oscillator. The second one is provided with its full mechanical meaning. In this model, two mass m and M weakly connected to each other bi-laterally with a spring and a damper. The first mass, m, is subdued impacts with the rigid barrier and the other mass, M, connected to the wall with a spring and damper. The mechanical model for this can be observed from Fig. 4.15.

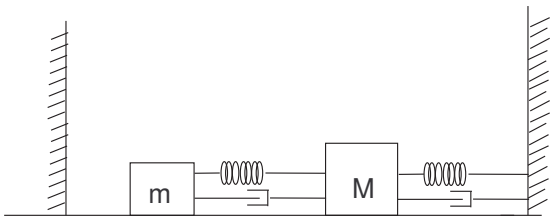

Figure 4.15: The mechanical model for two degree of freedom oscillator.

Let us start with the first model which has two coupled oscillator and they are connected to each other unilaterally.

Model 1: Consider the following perturbed system of differential equation with vari-

able moments of impulses:

$$\begin{aligned} &x'' + 0.002x' + x = -(1+\mu) - 0.002\sin(t), \\ &y'' - 2(1-y^2)y' + y = \mu\sin(t) + 0.01x_2, \\ &\Delta x'|_{x\in S} = -(1+0.5x')x', \end{aligned} \tag{4.122}$$

where $x = (x, x', y, y')$ $S = \{x|\Phi(x, x', y, y') = x = 0\}$. Defining the variables as $x_1 = x$, $x_2 = x'$, $x_3 = y$, and $x_4 = y'$, (4.122) can be rewritten as

$$\begin{aligned} &x_1' = x_2, \\ &x_2' = -0.002x_2 - x_1 - (1+\mu) - 0.002\sin(t), \\ &x_3' = x_4, \\ &x_4' = 2(1-y_3^2)y_4 - y_3 + \mu x_2, \\ &\Delta x_2|_{x\in S} = -(1+0.5x_2)x_2, \end{aligned} \tag{4.123}$$

where $x = (x_1, x_2, x_3, x_4)$ and the vector field is $f(x) = (x_2, -0.002x_2 - x_1 - (1+\mu) - 0.002\sin(t), x_4, 2(1-y_3^2)y_4 - y_3 + 0.01\sin(t))$ the discontinuity surface S can be written in the form $S = \{x|\Phi(x) = x_1 = 0\}$.

For $\mu = 0$, the system (4.123) is reduced to

$$\begin{aligned} &x_1' = x_2, \\ &x_2' = -0.002x_2 - x_1 - 1 - 0.002\sin(t), \\ &x_3' = x_4, \\ &x_4' = 2(1-x_3^2)x_4 - x_3 + \mu\sin(t), \\ &\Delta x_2|_{x\in S} = -(1+0.5x_2)x_2. \end{aligned} \tag{4.124}$$

Let us verify that the point $x^* = (0, 0, x_3(0), x_4(0))$ is a grazing point of the periodic solution, $\Psi(t) = (-1+\cos(t), -\sin(t), x_3(t), x_4(t))$. By considering the expression $\langle\Phi(x^*), f(x^*)\rangle = \langle(1,0,0,0), (0,-1,x_4(0), 2(1-x_3(0)^2)x_4 - x_3(0) + 0.01\sin(0))\rangle = 0$, we can conclude that the point x^* is grazing by Definition 1 which is stated in [6].

To consider the existence of the periodic solutions of the system (4.124), we should take into account the following impacting system

$$\begin{aligned} &x_1' = x_2, \\ &x_2' = -0.002x_2 - x_1 - 1 - 0.002\sin(t), \\ &\Delta x_2|_{x\in S} = -(1+0.5x_2)x_2. \end{aligned} \tag{4.125}$$

The grazing periodic solution of the system (4.125) is $\Psi(t) = (-1+\cos(t), -\sin(t))$, which has a grazing point at $(0, 0)$.

In the remainder, we will seek the periodic solutions of (4.126)

$$\begin{aligned} x_1' &= x_2, \\ x_2' &= -0.002x_2 - x_1 - (1+\mu) - 0.002\sin(t), \\ \Delta x_2|_{x\in S} &= -(1+0.5x_2)x_2. \end{aligned} \tag{4.126}$$

for sufficiently small μ. Two sorts of periodic solutions of (4.126) exist around the grazing one. One of them has no impulse during the period since it does not cross the line of discontinuity. The other sort is the periodic solution which intersects the line $x_1 = 0$. We will show the existence of both type of periodic solutions for a sufficiently small $|\mu|$.

Let us start with the second type. Denote the initial values of the intended periodic solution by ζ_1, ζ_2, ζ_3 and ζ_4. By specifying the formula for the system (4.123), it is easy to obtain the following expressions

$$\begin{aligned} \mathscr{P}_1^{(1)}(T,\zeta_1,\zeta_2,\zeta_3,\zeta_4,\mu) &= x_1(T,\zeta_1,\zeta_2,\zeta_3,\zeta_4,\mu) - \zeta_1 = 0, \\ \mathscr{P}_2^{(1)}(T,\zeta_1,\zeta_2,\zeta_3,\zeta_4,\mu) &= x_2(T,\zeta_1,\zeta_2,\zeta_3,\zeta_4,\mu) - \zeta_2 = 0, \\ \mathscr{P}_3^{(1)}(T,\zeta_1,\zeta_2,\zeta_3,\zeta_4,\mu) &= x_3(T,\zeta_1,\zeta_2,\zeta_3,\zeta_4,\mu) - \zeta_3 = 0, \\ \mathscr{P}_4^{(1)}(T,\zeta_1,\zeta_2,\zeta_3,\zeta_4,\mu) &= x_4(T,\zeta_1,\zeta_2,\zeta_3,\zeta_4,\mu) - \zeta_4 = 0. \end{aligned} \tag{4.127}$$

Next, taking the derivative of the expressions in (4.127), we can obtain the following

$$\begin{vmatrix} \frac{\partial \mathscr{P}_1^{(1)}(2\pi,0,0,x_3(2\pi),x_4(2\pi),0)}{\partial\zeta_1} & \cdots & \frac{\partial \mathscr{P}_1^{(1)}(2\pi,0,0,x_3(2\pi),x_4(2\pi),0)}{\partial\zeta_4} \\ \frac{\partial \mathscr{P}_2^{(1)}(2\pi,0,0,x_3(2\pi),x_4(2\pi),0)}{\partial\zeta_1} & \cdots & \frac{\partial \mathscr{P}_2^{(1)}(2\pi,0,0,x_3(2\pi),x_4(2\pi),0)}{\partial\zeta_4} \\ \frac{\partial \mathscr{P}_3^{(1)}(2\pi,0,0,x_3(2\pi),x_4(2\pi),0)}{\partial\zeta_1} & \cdots & \frac{\partial \mathscr{P}_3^{(1)}(2\pi,0,0,x_3(2\pi),x_4(2\pi),0)}{\partial\zeta_4} \\ \frac{\partial \mathscr{P}_4^{(1)}(2\pi,0,0,x_3(2\pi),x_4(2\pi),0)}{\partial\zeta_1} & \cdots & \frac{\partial \mathscr{P}_4^{(1)}(2\pi,0,0,x_3(2\pi),x_4(2\pi),0)}{\partial\zeta_4} \end{vmatrix} =$$

$$\begin{vmatrix} \frac{\partial x_1(2\pi,0,0,x_3(2\pi),x_4(2\pi),0)}{\partial\zeta_1} - 1 & \cdots & \frac{\partial x_1(2\pi,0,0,x_3(2\pi),x_4(2\pi),0)}{\partial\zeta_4} \\ \frac{\partial x_2(2\pi,0,0,x_3(2\pi),x_4(2\pi),0)}{\partial\zeta_1} & \cdots & \frac{\partial x_2(2\pi,0,0,x_3(2\pi),x_4(2\pi),0)}{\partial\zeta_4} \\ \frac{\partial x_3(2\pi,0,0,x_3(2\pi),x_4(2\pi),0)}{\partial\zeta_1} & \cdots & \frac{\partial x_3(2\pi,0,0,x_3(2\pi),x_4(2\pi),0)}{\partial\zeta_4} \\ \frac{\partial x_4(2\pi,0,0,x_3(2\pi),x_4(2\pi),0)}{\partial\zeta_1} & \cdots & \frac{\partial x_4(2\pi,0,0,x_3(2\pi),x_4(2\pi),0)}{\partial\zeta_4} - 1 \end{vmatrix} = \tag{4.128}$$

$$\begin{vmatrix} \frac{\partial x_1(2\pi,0,0,x_3(2\pi),x_4(2\pi),0)}{\partial\zeta_1} - 1 & \frac{\partial x_1(2\pi,0,0,x_3(2\pi),x_4(2\pi),0)}{\partial\zeta_2} \\ \frac{\partial x_2(2\pi,0,0,x_3(2\pi),x_4(2\pi),0)}{\partial\zeta_1} & \frac{\partial x_2(2\pi,0,0,x_3(2\pi),x_4(2\pi),0)}{\partial\zeta_4} - 1 \end{vmatrix} \times$$

$$\begin{vmatrix} \frac{\partial x_3(2\pi,0,0,x_3(2\pi),x_4(2\pi),0)}{\partial\zeta_3} - 1 & \frac{\partial x_3(2\pi,0,0,x_3(2\pi),x_4(2\pi),0)}{\partial\zeta_4} \\ \frac{\partial x_4(2\pi,0,0,x_3(2\pi),x_4(2\pi),0)}{\partial\zeta_3} & \frac{\partial x_4(2\pi,0,0,x_3(2\pi),x_4(2\pi),0)}{\partial\zeta_3} - 1 \end{vmatrix}$$

The third determinant (4.128) is calculated by means of the variational system, with the impulse matrix $D_1^{(1)} = O_2$, it is

$$\begin{aligned} u_1' &= u_2, \\ u_2' &= -0.002u_2 - u_1, \end{aligned} \tag{4.129}$$

where $U(0) = I_2$, I_2 is $2 \times 2-$identity matrix. By considering the variational system (4.129), the monodromy matrix can be computed as [51]

$$\begin{bmatrix} 1 & -0.0317 \\ 1.0158 & -0.1014 \end{bmatrix}. \tag{4.130}$$

Taking into account the system (4.124) with (4.130) at $\zeta_1 = \zeta_1^0 = 0$ and $\zeta_2 = \zeta_2^0 = 0$, $\zeta_1^0, \zeta_2^0, \zeta_3^0, \zeta_4^0$ are the values of the periodic solution of the generating system (4.124) at the period $T = 2\pi$ for $\mu = 0$, one can derive that

$$\begin{vmatrix} \frac{\partial x_1(2\pi,\zeta_1^0,\zeta_2^0,\zeta_3^0,\zeta_4^0,0)}{\partial\zeta_1} & \frac{\partial x_1(2\pi,\zeta_1^0,\zeta_2^0,\zeta_3^0,\zeta_4^0,0)}{\partial\zeta_2} \\ \frac{\partial x_2(2\pi,\zeta_1^0,\zeta_2^0,\zeta_3^0,\zeta_4^0,0)}{\partial\zeta_1} & \frac{\partial x_2(2\pi,\zeta_1^0,\zeta_2^0,\zeta_3^0,\zeta_4^0,0)}{\partial\zeta_2} \end{vmatrix} = 0.76\exp(\frac{0.01\pi}{2\sqrt{3.99}}) \neq 0. \tag{4.131}$$

Morever, the fourth determinant in (4.128) is calculated by means of the linearization of third and fourth equations in (4.123) with respect to its periodic solution. It is easy to say that the system admits an aymptotically stable periodic solution [38]. Thus, we can conclude that all eigenvalues of the monodromy matrix is less than unity and the fourth determinant (4.128) is not equal to zero. The product of third and fourth determinant is not zero and this verifies condition $(A5)$. Thus, condition $(A5)$ is valid, then we can assert that the system (4.123) admits a non-trivial periodic solution, which converges in the $B-$ topology to the non-trivial T-periodic solution of (4.124) as μ tends to zero which does not impact to the surface of discontinuity.

Now, let us verify that system (4.122) has a discontinuous periodic solution which intersects the line $x_1 = 0$ in the neighborhood of $(0, 0, x_3(2\pi), x_4(2\pi))$. So, the periodic solution will attain a discontinuity moment in a period. Denote the initial values of the periodic solution by ζ_1, ζ_2, ζ_3 and ζ_4. In the light of the expressions (4.117), one can write that

$$\begin{aligned}
\mathscr{P}_1^{(2)}(T, \zeta_1, \zeta_2, \zeta_3, \zeta_4, \mu) &= x_1(T, \zeta_1, \zeta_2, \zeta_3, \zeta_4, \mu) - \zeta_1 = 0, \\
\mathscr{P}_2^{(2)}(T, \zeta_1, \zeta_2, \zeta_3, \zeta_4, \mu) &= x_2(T, \zeta_1, \zeta_2, \zeta_3, \zeta_4, \mu) - \zeta_2 = 0, \\
\mathscr{P}_3^{(2)}(T, \zeta_1, \zeta_2, \zeta_3, \zeta_4, \mu) &= x_3(T, \zeta_1, \zeta_2, \zeta_3, \zeta_4, \mu) - \zeta_3 = 0, \\
\mathscr{P}_4^{(2)}(T, \zeta_1, \zeta_2, \zeta_3, \zeta_4, \mu) &= x_4(T, \zeta_1, \zeta_2, \zeta_3, \zeta_4, \mu) - \zeta_4 = 0.
\end{aligned} \tag{4.132}$$

Taking the derivative of the expressions (4.132) with respect to variables ζ_1, ζ_2, ζ_3

and ζ_4, one can obtain the following

$$\begin{vmatrix} \frac{\partial \mathscr{P}_1^{(2)}(2\pi,0,0,x_3(2\pi),x_4(2\pi),0)}{\partial \zeta_1} & \cdots & \frac{\partial \mathscr{P}_1^{(2)}(2\pi,0,0,x_3(2\pi),x_4(2\pi),0)}{\partial \zeta_4} \\ \frac{\partial \mathscr{P}_2^{(2)}(2\pi,0,0,x_3(2\pi),x_4(2\pi),0)}{\partial \zeta_1} & \cdots & \frac{\partial \mathscr{P}_2^{(2)}(2\pi,0,0,x_3(2\pi),x_4(2\pi),0)}{\partial \zeta_4} \\ \frac{\partial \mathscr{P}_3^{(2)}(2\pi,0,0,x_3(2\pi),x_4(2\pi),0)}{\partial \zeta_1} & \cdots & \frac{\partial \mathscr{P}_3^{(2)}(2\pi,0,0,x_3(2\pi),x_4(2\pi),0)}{\partial \zeta_4} \\ \frac{\partial \mathscr{P}_4^{(1)}(2\pi,0,0,x_3(2\pi),x_4(2\pi),0)}{\partial \zeta_1} & \cdots & \frac{\partial \mathscr{P}_4^{(2)}(2\pi,0,0,x_3(2\pi),x_4(2\pi),0)}{\partial \zeta_4} \end{vmatrix} =$$

$$\begin{vmatrix} \frac{\partial x_1(2\pi,0,0,x_3(2\pi),x_4(2\pi),0)}{\partial \zeta_1} - 1 & \cdots & \frac{\partial x_1(2\pi,0,0,x_3(2\pi),x_4(2\pi),0)}{\partial \zeta_4} \\ \frac{\partial x_2(2\pi,0,0,x_3(2\pi),x_4(2\pi),0)}{\partial \zeta_1} & \cdots & \frac{\partial x_2(2\pi,0,0,x_3(2\pi),x_4(2\pi),0)}{\partial \zeta_4} \\ \frac{\partial x_3(2\pi,0,0,x_3(2\pi),x_4(2\pi),0)}{\partial \zeta_1} & \cdots & \frac{\partial x_3(2\pi,0,0,x_3(2\pi),x_4(2\pi),0)}{\partial \zeta_4} \\ \frac{\partial x_4(2\pi,0,0,x_3(2\pi),x_4(2\pi),0)}{\partial \zeta_1} & \cdots & \frac{\partial x_4(2\pi,0,0,x_3(2\pi),x_4(2\pi),0)}{\partial \zeta_4} - 1 \end{vmatrix} = \tag{4.133}$$

$$\begin{vmatrix} \frac{\partial x_1(2\pi,0,0,x_3(2\pi),x_4(2\pi),0)}{\partial \zeta_1} - 1 & \frac{\partial x_1(2\pi,0,0,x_3(2\pi),x_4(2\pi),0)}{\partial \zeta_2} \\ \frac{\partial x_2(2\pi,0,0,x_3(2\pi),x_4(2\pi),0)}{\partial \zeta_1} & \frac{\partial x_2(2\pi,0,0,x_3(2\pi),x_4(2\pi),0)}{\partial \zeta_4} - 1 \end{vmatrix} \times$$

$$\begin{vmatrix} \frac{\partial x_3(2\pi,0,0,x_3(2\pi),x_4(2\pi),0)}{\partial \zeta_3} - 1 & \frac{\partial x_3(2\pi,0,0,x_3(2\pi),x_4(2\pi),0)}{\partial \zeta_4} \\ \frac{\partial x_4(2\pi,0,0,x_3(2\pi),x_4(2\pi),0)}{\partial \zeta_3} & \frac{\partial x_4(2\pi,0,0,x_3(2\pi),x_4(2\pi),0)}{\partial \zeta_3} - 1 \end{vmatrix}$$

Let us obtain a variational system for 4.124 around the grazing periodic solution $\Psi(t)$, to accomplish it let us consider a near solution to $\Psi(t)$. For a fixed $i \in \mathbb{Z}$, take into account a near solution $x(t) = x(t, \theta_i, \Psi(\theta_i) + \Delta x) = (x_1(t), x_2(t))$, to $\Psi(t)$ of the differential part of the last system, near the moment $t = \theta_i$, assuming that it impacts the barrier at a moment $t = \xi_i$ near to $t = \theta_i$ and at the point $(x_1, x_2) = (x_1(\xi_i), x_2(\xi_i))$. Let also, $\tilde{x}(t) = (\tilde{x}_1(t), \tilde{x}_2(t))$ be a solution of the equation $\tilde{x}(\xi_i) = x(\xi_i) + J(x(\xi_i))$, where $J(x_1, x_2) = (x_1, 0.98x_2^2)$. In the light of this, define the following map

$$\begin{aligned} W_i(x) = &\int_{\theta_i}^{\xi_i} \begin{bmatrix} x_2(s) \\ x_1(s) - 0.002x_2(s) + 1 + 0.002\sin(s) \end{bmatrix} ds + \\ &J\left(x + \int_{\theta_i}^{\xi_i} \begin{bmatrix} x_2(s) \\ -x_1(s) - 0.002x_2(s) + 1 + 0.002\sin(s) \end{bmatrix} ds \right) \\ &+ \int_{\xi_i}^{\theta_i} \begin{bmatrix} \tilde{x}_2(s) \\ -\tilde{x}_1(s) - 0.002\tilde{x}_2(s) + 1 + 0.002\sin(s) \end{bmatrix} ds. \end{aligned} \tag{4.134}$$

Taking into account the map (4.134), we can write a B-equivalent system to (4.124)

[5]

$$\begin{aligned} x_1' &= x_2, \\ x_2' &= -0.002x_2 - x_1 - 1 - 0.002\sin(t), \\ \Delta x|_{t=\theta_i} &= W_i(\Psi(\theta_i))x, \end{aligned} \tag{4.135}$$

$W_i(\Psi(\theta_i))$ will be precised below.

The construction of W_i allows that the solutions of (4.135) and (4.124) coincide except the time intervals $\widehat{[\theta_i, \xi_i]}$, $i \in \mathbb{Z}$, where $\widehat{[\theta_i, \xi_i]} = [\theta_i, \xi_i]$ whenever $\theta_i < \xi_i$ and $\widehat{[\theta_i, \xi_i]} = [\xi_i, \theta_i]$, otherwise. For this reason, system (4.135) can be used for the analysis of the stability of the periodic solution. For the transversal point $\bar{x} = (\bar{x}_1, \bar{x}_2)$, utilizing formula (3.10), the derivative $\dfrac{\partial \xi_i(\bar{x})}{\partial x_1^0}$ is computed as $\dfrac{\partial \xi_i(\bar{x})}{\partial x_1^0} = -\dfrac{1}{\bar{x}_2}$. In the last expression, one can see how the singularity appears at the grazing point $x^* = (x_1^*, x_2^*) = (0, 0)$. Then by means of the derivative, it is easy to obtain that

$$\begin{aligned} &\frac{\partial W_i(\bar{x})}{\partial x_1^0} = \begin{bmatrix} \bar{x}_2 \\ -\bar{x}_1 - 0.002\bar{x}_2 + 1 + 0.002\sin(\tau) \end{bmatrix} \Big(-\frac{1}{\bar{x}_2} \Big) + \begin{bmatrix} 1 & 0 \\ 0 & 1.96\bar{x}_2 \end{bmatrix} \Bigg(e_1 + \\ &\begin{bmatrix} \bar{x}_2 \\ -\bar{x}_1 - 0.002\bar{x}_2 + 1 + 0.002\sin(\tau) \end{bmatrix} \Big(-\frac{1}{\bar{x}_2} \Big) \Bigg) - \\ &\begin{bmatrix} -0.98(\bar{x}_2)^2 \\ -\bar{x}_1 - 0.0294(\bar{x}_2)^2 + 1 + 0.002\sin(\tau) \end{bmatrix} \Big(-\frac{1}{\bar{x}_2} \Big) \\ &= \begin{bmatrix} -1 + 0.98\bar{x}_2 \\ 0.002 + 0.0294\bar{x}_2 - 1.96(-\bar{x}_1 + 0.002\sin(\tau) - 0.002\bar{x}_2 + 1) \end{bmatrix}, \end{aligned} \tag{4.136}$$

where $e_1 = (1, 0)^T$.

From the last expression, it is easy to see that the derivative is a continuous function of its arguments in a neighborhood of the grazing point. Since $\bar{x}$ is a transversal point, we get

$$\lim_{\bar{x} \to x^*} \frac{\partial W_i(\bar{x})}{\partial x_1^0} = B, \tag{4.137}$$

where $B = \begin{bmatrix} -1 \\ -1.93 \end{bmatrix}$. To linearize system at the grazing point x^*, we should verify

that the function $W_i(x)$ is differentiable at $x^* = (\Psi_1(\theta_i), \Psi_2(\theta_i))$. The differentiability requests that the partial derivatives $\dfrac{\partial W_i(x)}{\partial x_j^0}$, $j = 1, 2$, exist in a neighborhood of the grazing point and they are continuous at the point. To compute the derivative $\dfrac{\partial W_i(x)}{\partial x_1^0}$ at x^*, the following expression will be taken into account

$$\begin{aligned}\frac{\partial W_i(x_1^*, x_2^*)}{\partial x_1^0} = \lim_{x_1 \to x_1^*} \frac{W_i(x_1, x_2^*) - W_i(x_1^*, x_2^*)}{x_1 - x_1^*} = \\ \lim_{x_1 \to x_1^*} \frac{W_i(x_1, x_2^*) - W_i(x_1^*, x_2^*)}{x_1 - x_1^*} - B + B.\end{aligned} \tag{4.138}$$

Applying the Mean Value Theorem, we obtain that

$$\lim_{x_1 \to x_1^*} \frac{\frac{\partial W_i(\zeta, x_2^*)}{\partial x_1^0}(x_1 - x_1^*) - B(x_1 - x_1^*)}{x_1 - x_1^*} + B, \tag{4.139}$$

where ζ lies between x_1 and x_1^*.

Similar to above discussion for the first derivative, one can obtain for the second derivative that $\dfrac{\partial W_i(x^*)}{\partial x_2^0} = \begin{bmatrix} 0 \\ 0 \end{bmatrix}$ and the derivative is continuous at x^*. Thus, both derivatives $\dfrac{\partial W_i(x)}{\partial x_1^0}$ and $\dfrac{\partial W_i(x)}{\partial x_2^0}$ exist in a neighborhood of x^* and they are continuous at x^*. That is, $W_i(x)$ is differentiable at x^*. Since of the periodicity, the linearization can be obtained for all grazing moment θ_i, $i \in \mathbb{Z}$.

Joining the derivatives, the one can obtain that

$$W_{ix}(x^*) = \begin{bmatrix} -1 & 0 \\ -1.93 & 0 \end{bmatrix}. \tag{4.140}$$

The above matrix will be called the linearization matrix at x^*.

For the near impacting solution, the linearization system can be obtained as

$$\begin{aligned} u_1' &= u_2, \\ u_2' &= -0.002u_2 - u_1, \\ \Delta u|_{t=2\pi i} &= W_{ix}(x^*)u, \end{aligned} \tag{4.141}$$

where $W_{ix}(x^*)$ is determined in (4.140). The monodromy matrix of the (4.141) is equal to

$$\begin{bmatrix} 0.0000 & 0.0017 \\ 0.0081 & 0.8546 \end{bmatrix} \tag{4.142}$$

For $\mu = 0$, taking into account (4.142), the determinant (3.66) can be obtained as

$$\begin{vmatrix} \frac{\partial \mathscr{P}_1^{(2)}(2\pi,0,0,0)}{\partial \zeta_1} & \frac{\partial \mathscr{P}_1^{(2)}(2\pi,0,0,0)}{\partial \zeta_2} \\ \frac{\partial \mathscr{P}_2^{(2)}(2\pi,0,0,0)}{\partial \zeta_1} & \frac{\partial \mathscr{P}_2^{(2)}(2\pi,0,0,0)}{\partial \zeta_2} \end{vmatrix} = \tag{4.143}$$

$$\begin{vmatrix} -1 & 0.0017 \\ 0.0081 & 0.8546 \end{vmatrix} = -0.02 \exp(0.001/\sqrt{3.99}) \neq 0. \tag{4.144}$$

Moreover, the determinant in (4.133) is calculated by means of the linearization of third and fourth equations in (4.123) with respect to its periodic solution. It is easy to say that the system admits an asymptotically stable periodic solution [38]. Thus, we can conclude that all eigenvalues of the monodromy matrix is less than unity and the fourth determinant (4.133) is not equal to zero. The product of third and fourth determinant is not zero and this verifies condition $(A5)$. This verifies condition $(A5)$. So, we can conclude that the perturbed system (4.122) admits a non-trivial periodic solution which converges in the $B-$ topology to the non-trivial T-periodic solution of (4.123) as μ tends to zero. Consequently, we can say that system (4.126) admits two periodic solutions with the variation of μ around zero. It means that the number of periodic solution increases with the help of the small change in μ. We will call this bifurcation of the grazing periodic solution. The discontinuous periodic solution is depicted for $\mu = 0.1$ in Fig. 4.17.

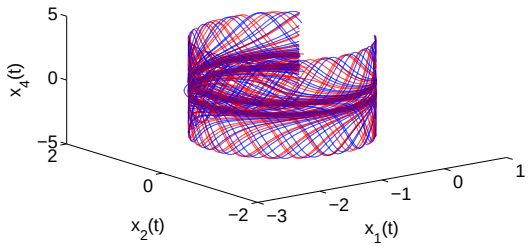

Figure 4.16: The coordinates $x_1(t), x_2(t)$ and $x_4(t)$ are depicted. The blue curve is for those coordinates of the solution with initial value $x(0) = (-2.3, 0, 2, 0)$ and the red one is for the same ones with the initial value $x(0) = (-2.01, 0, 2, 0)$.

In Fig. 4.16, we pictured the coordinates $x_2(t), x_3(t)$ and $x_4(t)$ the near solutions of the system (4.122) with the same initial data and in 4.19 the projection of the coordinates $x_3(t) - x_4(t)$ is depicted in order to demonstrate the existence of an asymp-

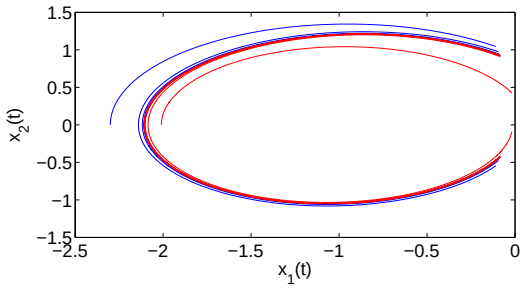

Figure 4.17: The blue curve is for the coordinates $x_1(t) - x_2(t)$ of the solution with initial value $x(0) = (-2.3, 0, 2, 0)$ and the red one is for the same ones with the initial value $x(0) = (-2.01, 0, 2, 0)$. One can see that these solutions (drawn in blue and red) approach asymptotically discontinuous periodic solution of the perturbed system and this picture is also the projection of Fig. 4.16 onto the $x_1(t) - x_2(t)$ plane.

totically stable periodic solution of the non-impacting part of the system (4.122)

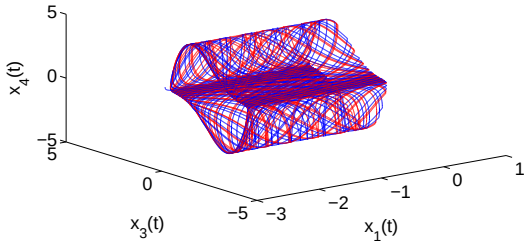

Figure 4.18: The coordinates $x_1(t), x_3(t)$ and $x_4(t)$ are depicted and blue and red ones are for the solution with initial values $x(0) = (-2.3, 0, 2, 0)$ and $x(0) = (-2.01, 0, 2, 0)$, respectively.

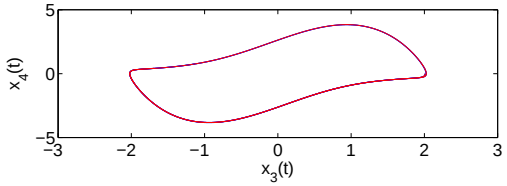

Figure 4.19: The projection of Fig. 4.18 onto the $x_3(t) - x_4(t)$ plane.

Model 2: Let us consider the mechanical problem which consists of two mass and they weakly coupled to each other with spring and damper and one of them impacts

against the rigid wall. The mathematical model for this problem is of the form

$$\begin{aligned} &mx'' + ax' + bx + \epsilon_1(x' - y') + \epsilon_2(x - y) = c\sin(t), \\ &My'' + Ay' + \epsilon_1(y' - x') + \epsilon_2(y - x) + B\frac{1}{16}y^3 = C, \\ &\Delta x'|_{x\in S} = -(1 + Rx')x', \end{aligned} \tag{4.145}$$

where $S = \{(x, x', y, y')|\Phi(x, x', y, y') = x + 1 = 0\}$, R is the coefficient of restitution which varies between zero and unity.

The system (4.145) can be normalized as

$$\begin{aligned} &x'' + \eta_1 x' + \eta_2 x + \mu_1(x' - y') + \mu_2(x - y) = \eta_3\sin(t), \\ &y'' + \xi_1 y' + \xi_2 y^3 - \mu_1(x' - y') - \mu_2(x - y) = \xi_3, \\ &\Delta x'|_{x\in S} = -(1 + Rx')x', \end{aligned} \tag{4.146}$$

where $\eta_1 = a/m$, $\eta_2 = b/m$, $\eta_3 = c/m$, $\xi_1 = A/M$, $\xi_2 = B/M$, $\xi_2 = C/M$, $\mu_1 = \epsilon_1/m$ and $\mu_2 = \epsilon_2/M$. The generating system corresponding to normalized system (4.146) takes the form

$$\begin{aligned} &x'' + \eta_1 x' + \eta_2 x = \eta_3\sin(t), \\ &y'' + \xi_1 y' + \xi_2 y^3 = \xi_3, \\ &\Delta x'|_{x\in S} = -(1 + Rx')x'. \end{aligned} \tag{4.147}$$

In this model, we will consider the case when the coefficients are $\eta_1 = 1$, $\eta_2 = 1$, $\eta_3 = 1$, $\xi_1 = 1$, $\xi_2 = 1/16$ and $\xi_3 = 4$ and the coefficient of restitution $R = 0.8$. Defining variables as $x = x_1$, $x' = x_2$, $y = x_3$ and $y' = x_4$, we can obtain that

$$\begin{aligned} &x_1' = x_2, \\ &x_2' = -x_2 - x_1 + \sin(t), \\ &x_3' = x_4, \\ &x_4' = -x_4 - \frac{1}{16}x_3^3 + 4, \\ &\Delta x_2|_{x\in S} = -(1 + 0.8x_2)x_2, \end{aligned} \tag{4.148}$$

where $x = (x_1, x_2, x_3, x_4)$ and $S = \{x|\Phi(x) = x_1 + 1 = 0\}$.

From the description, one can see that the model in (4.145) in the sense of analysis is quite similar to that for the model in (4.122). This is why, we will pass the detailed

analysis for the system (4.145) and we will present essential discussions related to the application of the assertion related with the small parameter analysis near grazing solution and provide final results what we have obtained through above calculations.

It is easy to see that the generating system (4.148) consists of two uncoupled oscillators, one of them is an impacting forced spring-mass-damper system and the other one is forced duffing oscillator. The system can be interpreted as the following subequations

$$\begin{aligned} x_1' &= x_2, \\ x_2' &= -x_2 - x_1 + \sin(t), \\ \Delta x_2|_{x\in S} &= -(1+0.8x_2)x_2, \end{aligned} \tag{4.149a}$$

and

$$\begin{aligned} x_3' &= x_4, \\ x_4' &= -x_4 - \frac{1}{16}x_3 + 4, \end{aligned} \tag{4.149b}$$

It is easy to verify that the first system, (4.149a), has a $2\pi-$periodic solution $\bar{\Psi}(t) = (-\cos(t), \sin(t))$ which grazes the surface of discontinuity at the moment $t = 0$ and at the point $\bar{\Psi}(0) = (-1, 0)$. The system (4.149b) has a fixed point $(4, 0)$. Thus, we have that $\Psi(t) = (-\cos(t), \sin(t), 4, 0)$ is a solution of the generating system, (4.148). In the following part, we will consider $\Psi(t)$ as $2\pi-$ periodic function. At the moment $t^* = 0$ and the point $x^* = (-1, 0, 4, 0) = \Psi(t^*)$ it i,s tru that $\langle \Phi(x*), f(t*, x*)\rangle = \langle (1, 0, 0, 0), (0, -1, 0, 0)\rangle = 0$. Now, we can conclude that the point $x^* = (-1, 0, 4, 0)$ is a *grazing point* and $\Psi(t)$ is grazing periodic solution.

Because the two systems, (4.149a) and (4.149b), are uncoupled, we will consider the linearization of these systems, separately. Let us start with the system (4.149a). There are two different type of solutions near the periodic solution due to the fact that the periodic solution, $\bar{\Psi}(t)$, is a grazing one. The first type is non-impacting and the other is impacting. We will continue with the non-impacting one. For those, the

linearization system has the form

$$\begin{aligned} u_1' &= u_2, \\ u_2' &= -u_2 - u_1. \end{aligned} \tag{4.150}$$

The characteristic multipliers of the system are $\rho_1^{(1)} = 0.0288 + 0.0322i$ and $\rho_2^{(1)} = 0.0288 - 0.0322i$. All characteristic multipliers are less than unity in magnitude. Now, we can conclude that the periodic solution, $\bar{\Psi}(t)$ is asymptotically stable with respect to inside (non-impacting) solutions.

Next, we will take into account the linearization of (4.149a) with respectt to impacting solutions. In the light of the the calculations done for Model 1, the linearization system can be obtained as

$$\begin{aligned} u_1' &= u_2, \\ u_2' &= -u_2 - u_1, \\ \Delta u(2\pi i) &= W_{ix}(\bar{\Psi}(2\pi i))u(2\pi i). \end{aligned} \tag{4.151}$$

Considering the formulas (3.10) and (3.11), the characteristic multipliers of the linearization system, (4.151) can be computed as $\rho_1^{(2)} = 0.0868$ and $\rho_2^{(2)} = 0$. Now, we can say that the characteristic multipliers are inside the unit disc, so the periodic solution is asymptotically stable with respect to impacting (outside) solutions.

Let us take into account the linearization of system (4.149b) at the fixed point, $(4, 0)$, and it is obtained as

$$\begin{aligned} u_3' &= u_4, \\ u_4' &= -u_4 - 3u_1. \end{aligned} \tag{4.152}$$

The characteristic multipliers of the system are (4.152) $\rho_3^{(1)} = 0.3679$ and $\rho_4^{(1)} = 0.3679$. Both are inside the unit disc, then it is easy to conclude that the fixed point, $(4, 0)$, is asymptotically stable.

In Fig. 4.20, the grazing periodic solution for system (4.149a) is depicted in green. The blue is depicted for the coordinates, $x_1(t)$ and $x_2(t)$ of the system (4.148) with initial value $(2.12, 0, 4, 3)$ and red is simulated for the coordinates, $x_1(t)$ and $x_2(t)$ of the system (4.148) with initial value $(0, 0, 4, 3)$. It is easy to see in Fig. 4.20 that bots solutions approach the green periodic solution asymptotically, as time increases.

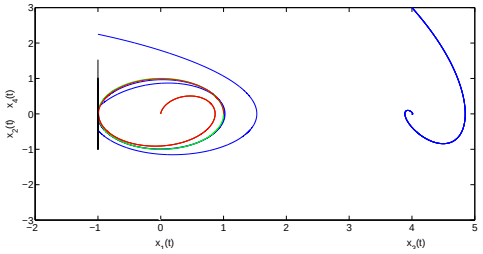

Figure 4.20: The green is for the grazing periodic solution of system (4.149a). The blue and red are for the coordinates, $x_1(t)$ and $x_2(t)$ of the system (4.148) with initial values $(2.12, 0, 4, 3)$ and $(0, 0, 4, 3)$, respectively.

In Figs. 4.21 and 4.22, the coordinates $x_1(t)$, $x_2(t)$ and $x_3(t)$ and $x_1(t)$, $x_3(t)$ and $x_4(t)$ of the system (4.148) are depicted, respectively. Taking into account both of the Figs., we can conclude that all near solutions approach to the grazing periodic solution, $\Psi(t)$, of the system (4.148) as time increases.

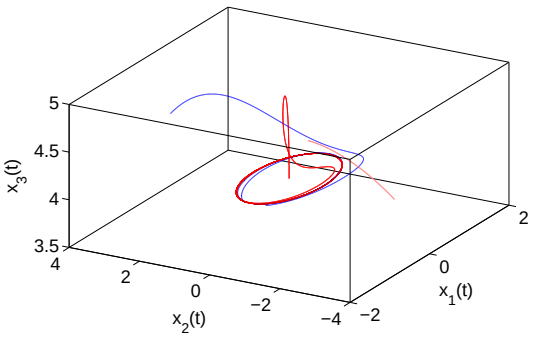

Figure 4.21: The blue and red are for the coordinates, $x_1(t)$, $x_2(t)$ and $x_3(t)$ of the system (4.148) with initial values $(2.12, 0, 4, 3)$ and $(0, 0, 4, 3)$, respectively.

If we consider the system with regular perturbation μ_1 and μ_2, we can see the existence of discontinuous periodic solution for the system (4.149a) which is orbitally asymptotically stable and the system (4.149a) has a continuous periodic solution.

Defining variables as $x = x_1$, $x' = x_2$, $y = x_3$ and $y' = x_4$, we can obtain that

$$\begin{aligned}
x_1' &= x_2, \\
x_2' &= -x_2 - x_1 + \sin(t) - \mu_1(x_4 - x_2) - \mu_2(x_1 - x_3), \\
x_3' &= x_4, \\
x_4' &= -x_4 - \frac{1}{16}x_3^3 + 4 + \mu_1(x_4 - x_2) + \mu_2(x_1 - x_3), \\
\Delta x_2|_{x \in S} &= -(1 + 0.8x_2)x_2,
\end{aligned} \tag{4.153}$$

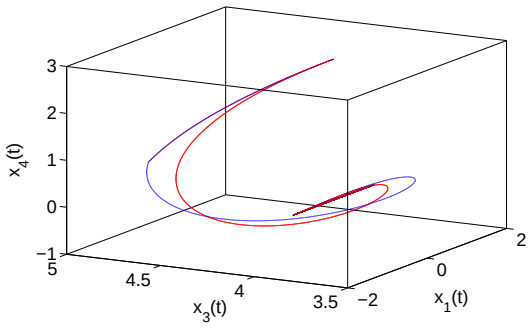

Figure 4.22: The blue and red are for the coordinates, $x_1(t)$, $x_3(t)$ and $x_4(t)$ of the system (4.148) with initial values $(2.12, 0, 4, 3)$ ans $(0, 0, 4, 3)$, respectively.

where $x = (x_1, x_2, x_3, x_4)$ and $S = \{x|\Phi(x) = x_1 + 1 = 0\}$.

Next, our aim to verify that the perturbed system (4.145) admits a periodic solution which approaches the periodic solution of the generating system (4.147) as μ_1 and μ_2 tend to zero. To accomplish it, we will use the formulas and assertions, given in subsection 4.9.1. Now, the independent variables are μ_1 and μ_2 which are not single. For this reason, it is worth saying that applying similar analysis, done for Model 1, it is easy to conclude that the perturbed system (4.145) has a periodic solution. Due to the continuity of the linearization system and the linearization matrix, we can say that the periodic solution is asymptotically stable. It can be observed in Figs 4.23, 4.24, 4.25 and 4.26.

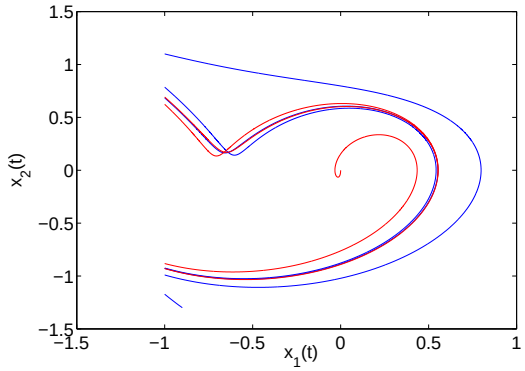

Figure 4.23: The blue and red are for the coordinates, $x_1(t)$, $x_2(t)$ for the solution of system (4.153) with initial values $(1, 0, 4.15, 0.1)$ and $(0, 0, 4.15, 0)$, respectively.

If we consider Fig. 4.25 as a projection to the $x_1 - x_2$ plane, we obtain Fig. 4.23 and additionally if we take into account 4.26 as a projection to the $x_3 - x_4$ plane, we get Fig. 4.23. In both couples of figures, it is easy to see that the solution of the system

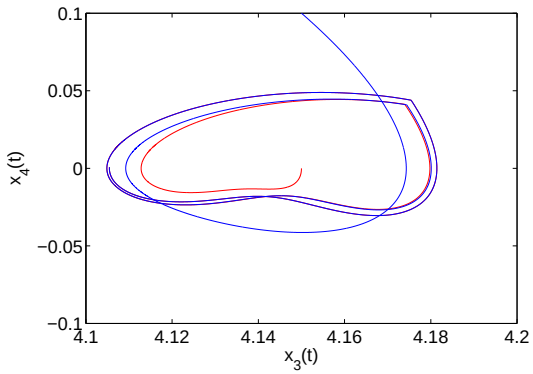

Figure 4.24: The blue and red are for the coordinates, $x_3(t)$, $x_4(t)$ for the solution of system (4.153) with initial values $(1, 0, 4.15, 0.1)$ and $(0, 0, 4.15, 0)$, respectively.

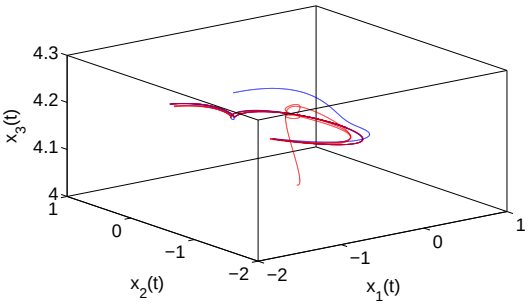

Figure 4.25: The blue and red are for the coordinates, $x_1(t)$, $x_2(t)$ $x_3(t)$, for the solution of system (4.153) with initial values $(1, 0, 4.15, 0.1)$ and $(0, 0, 4.15, 0)$, respectively.

is asymptotically stable.

Next, we will consider the following bi-laterally connected oscillator as a different from above results the periodic solutions of the non-impacting oscillator can not be determined analytically. For this reason, we will verify our results, which is obtained in Model 2 by using simulations. Let us consider the following system

$$\begin{aligned} &x'' + x' + x + \mu_1(x' - y') + \mu_2(x - y) = \sin(t), \\ &y'' + 2y' + \mu_1(y' - x') + \mu_2(y - x) + \frac{1}{16}y^3 + \sin(t) = 4, \\ &\Delta x'|_{x\in S} = -(1 + 0.8x')x', \end{aligned} \tag{4.154}$$

where $x = (x, x', y, y')$ $S = \{x|\Phi(x) = x = -1\}$. The generating system for 4.154

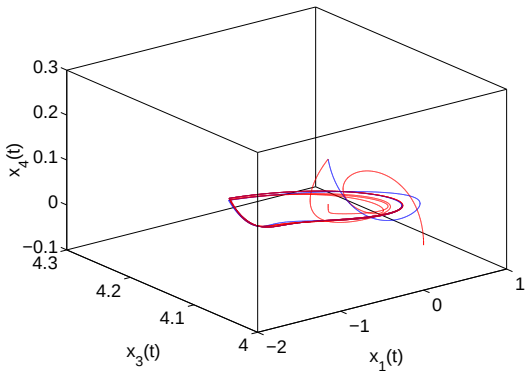

Figure 4.26: The blue and red are for the coordinates,$x_1(t)$, $x_3(t)$, $x_4(t)$ for the solution of system (4.153) with initial values $(1, 0, 4.14, 0.1)$ and $(0, 0, 4.15, 0)$, respectively.

is of the fomr

$$\begin{aligned} &x'' + x' + x = \sin(t), \\ &y'' + y' + \frac{1}{16}y^3 = 4 + \sin(t), \\ &\Delta x'|_{x\in S} = -(1 + 0.8x')x', \end{aligned} \tag{4.155}$$

Defining the variables $x = x_1$, $x' = x_2$, $y = x_3$ and $y' = x_4$, the systems (4.155) and (4.154) can be rewritten as

$$\begin{aligned} &x_1' = x_2, \\ &x_2' = -x' - x - \sin(t), \\ &x_3' = x_4, \\ &x_4' = -x_4 - \frac{1}{16}x_3^3 + 4 + \sin(t), \\ &\Delta x_2|_{x\in S} = -(1 + 0.8x_2)x_2, \end{aligned} \tag{4.156}$$

and

$$\begin{aligned} &x_1' = x_2, \\ &x_2' = -x' - x - \sin(t) - \mu_1(x_4 - x_2) - \mu_2(x_3 - x_1), \\ &x_3' = x_4, \\ &x_4' = -x_4 - \frac{1}{16}x_3^3 + \mu_1(x_4 - x_2) + \mu_2(x_3 - x_1) + 4 + \sin(t), \\ &\Delta x_2|_{x\in S} = -(1 + 0.8x_2)x_2, \end{aligned} \tag{4.157}$$

where $x = (x_1, x_2, x_3, x_4)$ and $S = \{x|\Phi(x) = x_1 = -1\}$. Similar to Model2, the

system (4.156) consists of two uncoupled oscillators and they are:

$$\begin{aligned} x_1' &= x_2, \\ x_2' &= -x' - x - \sin(t), \\ \Delta x_2|_{x\in S} &= -(1+0.8x_2)x_2, \end{aligned} \tag{4.158a}$$

$$\begin{aligned} x_3' &= x_4, \\ x_4' &= -x_4 - \frac{1}{16}x_3^3 + 4 + \sin(t). \end{aligned} \tag{4.158b}$$

In Model 2, it is obtained that the system (4.158a) has a grazing cycle which is of the form $\bar{\Psi}(t) = (-\cos(t), \sin(t))$. Since of the system (4.149b) has an equilibrium with charachteristic exponents having negative real part, by applying theorems for the existence of solutions of quasi-linear systems [38, 92], one can prove that the periodic solution of the system exists whenever the coefficient of x_3^3 in the system is sufficiently small. Taking into account the coefficient $1/16$ we obtain a 2π-periodic solution for that system which can be seen in the Fig. 4.27 and it is easy to observe that this solution is asymptotically stable. If one can determine the periodic solution $\tilde{\Psi(t)} = (\Psi_3(t), \Psi_4(t))$ of (4.158b) analytically, then it will be possible to evaluate its Floquet multipliers. However, for this case it is impossible to determine the periodic solution in an analytical way. For this reason, we have obtained some simulation results to verify our results.

Denote the $2\pi-$periodic solution of (4.156) by $\Psi(t)(-\cos(t), \sin(t), \Psi_3(t), \Psi_4(t))$. Utilizing the formula $\langle \Phi(x^*), f(t^*, x^*)\rangle$, at the grazing moment and point of the periodic solution
$(t^*, x^*) = (0, \Psi(0)) = (0, -1, 0, \Psi_3(0), \Psi_4(0))$, it is easy to verify that the point x^* and the moment t^* are grazing. So, the periodic solution, $\Psi(t)$, is a grazing one.

Figs. 4.28 and 4.29 are depicted to show the asymptotical properties of the system in there dimensional space. Considering the projection of 4.28 onto the $x_1 - x_2$ plane, we obtain the on the left part of the Fig. 4.27. Through the left part of the Fig. one can observe that 4.27, both solutions drawn in red and blue approach the discontinuous periodic solution, $\bar{\Psi}(t)$ of the system (4.158a) and from the right part, it is easy to see both solutions drawn in red and blue approach the continuous periodic solution, $\tilde{\Psi}(t)$ of the system (4.158b), as time increases.

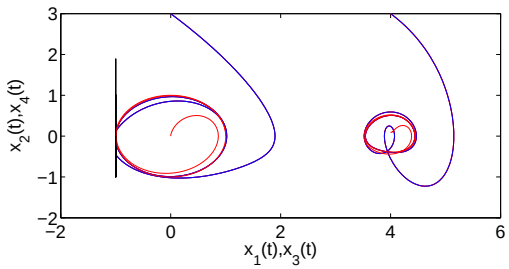

Figure 4.27: On the left part, the blue and red are for the coordinates, $x_1(t)$, $x_2(t)$ for the solution of system (4.156) with initial values $(1, 0, 4.15, 0.1)$ and $(0, 0, 4.15, 0)$, respectively. On the right part, the blue and red are for the coordinates, $x_3(t)$, $x_4(t)$ for the solution of system (4.156) with initial values $(1, 0, 4.15, 0.1)$ and $(0, 0, 4.15, 0)$, respectively.

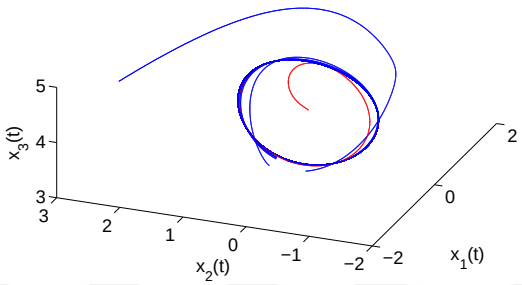

Figure 4.28: The blue and red are for the coordinates, $x_1(t)$, $x_2(t)$ $x_3(t)$, for the solution of system (4.156) with initial values $(1, 0, 4.15, 0.1)$ and $(0, 0, 4.15, 0)$, respectively.

In both Figs. 4.30, the outside and inside solutions which are drawn in blue and red, respectively approach the periodic solution of the system (4.157), as time increases. The Figs. 4.31 and 4.32 in drawn for the coordinates $x_1(t)$, $x_2(t)$ $x_3(t)$, and $x_1(t)$, $x_3(t)$, $x_4(t)$, repsectively. From that figures, one can see the asymptotic properties of the solutions of the perturbed system (4.157). In order to obtain better view, if one project the Figs. 4.31 and 4.32 into $x_1 - x_2$ and $x_3 - x_4$ planes, respectively, one can obtain the left and right parts of Fig. 4.30, respectively.

In general, the analysis of periodic solutions by using implicit function theorem is not applicable in systems which have graziness. Because grazing point may violate the differentiability of the Poincare map. For this in literature many methods have been used such as Nordmark map [97]-[100] and zero time discontinuity mapping (ZDM) [23]. By using special assumptions, we investigate the existence and stability of peri-

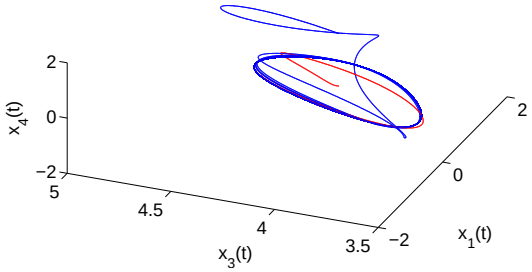

Figure 4.29: The blue and red are for the coordinates,$x_1(t)$, $x_3(t)$, $x_4(t)$ for the solution of system (4.156) with initial values $(1, 0, 4.14, 0.1)$ and $(0, 0, 4.15, 0)$, respectively.

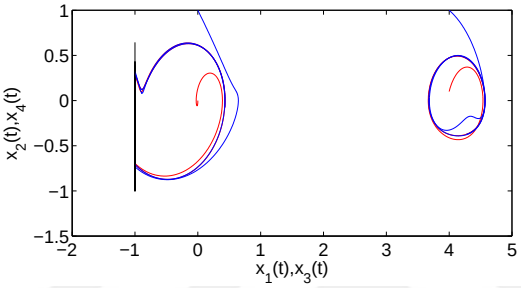

Figure 4.30: In the left, the blue and red are for the coordinates, $x_1(t)$, $x_2(t)$ for the solution of system (4.157) with initial values $(1, 0, 4.15, 0.1)$ and $(0, 0, 4.15, 0)$, respectively. In the right, the blue and red are for the coordinates, $x_3(t)$, $x_4(t)$ for the solution of system (4.157) with initial values $(1, 0, 4.15, 0.1)$ and $(0, 0, 4.15, 0)$, respectively.

odic solution of the perturbed system without disrupting the nature of the mechanisms with impacts.

4.9.3 Discussion

The singularity provided by grazing which appears in the Poincare map, if one want to analyze the problem of stability the following mapping approaches such as zero time discontinuity mapping [23] and Nordmark mapping [97]-[100] should be considered. In the literature, ss distinct from the mapping results, Ivanov [58],[59] analyzed the stability of the grazing periodic solution half autonomous systems under a parameter variation in the vector field through the variational system approach. As different from the theoretical results, the singularity in our analysis appears during the con-

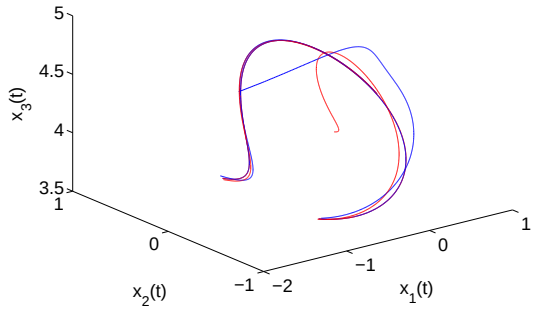

Figure 4.31: The blue and red are for the coordinates, $x_1(t)$, $x_2(t)$ $x_3(t)$, for the solution of system (4.153) with initial values $(1, 0, 4.15, 0.1)$ and $(0, 0, 4.15, 0)$, respectively.

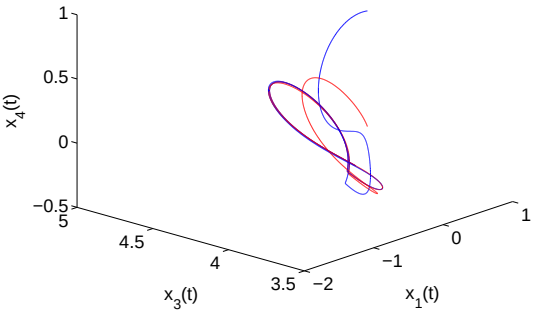

Figure 4.32: The blue and red are for the coordinates,$x_1(t)$, $x_3(t)$, $x_4(t)$ for the solution of system (4.153) with initial values $(1, 0, 4.14, 0.1)$ and $(0, 0, 4.15, 0)$, respectively.

struction of linearization at the moment of discontinuity. By harmonizing the vector field, the barrier and the jump equations, the singularity is suppressed in the system.

We provide some examples with simulations to demonstrate the practicability of our theoretical results. In addition, this work can be applied the integrate and fire neuron models which intersects the threshold tangentially. We propose that such phenomenon can be understood as the activity of a neuron cell transfers to the non-firing stage to firing stage.

By applying regular perturbations to the half autonomous system, we investigate the existence of periodic solution of the perturbed system. We derive rigorous mathematical method for the analysis of discontinuous trajectories near grazing orbits. If

there is no impacts in models, our results can be easily reduced to those for finite dimensional continuous dynamics. That is why, this method is convenient to investigate infinite dimensional problems and periodic solutions of functional differential equations and bifurcation theory.

In what follows, to emphasize the effectiveness of our results, we compare our way of investigation with that proposed in papers [58, 59]. In the paper [59], the following equation is taken into consideration

$$\ddot{q} = f(t, q, \dot{q}). \tag{4.159}$$

Model is subdued impacts with the law $\dot{q^+} = -e\dot{q^-}$, where $\dot{q^+}$ and $\dot{q^-}$, velocities before and after impacts, respectively. It is assumed that the system with the impact law has a periodic solution $q_0(t)$. It is assumed in the paper that t_0 is the initial moment and denoted the impacting time by $t'_i, i \in \mathbb{Z}$, such that $t_0 < t'_1 < t'_2 < \dots$. Moreover, it is notated that $\xi = q - q_0(t)$, $\eta = \dot{q} - \dot{q_0}(t)$, and it is asserted that they satisfy the following relation

$$\begin{bmatrix} \xi(t) \\ \eta(t) \end{bmatrix} = X(t, t_0) \begin{bmatrix} \xi_0 \\ \eta_0 \end{bmatrix} + O(\xi_0^2 + \eta_0^2), \tag{4.160}$$

where the fundamental matrix $X(t, t_0)$ satisfied the following variational system

$$\dot{X(t}, t_0) = A(t)X(t, t_0), \quad A(t) = \begin{bmatrix} 0 & 1 \\ f'_q & f'_{\dot{q}} \end{bmatrix}, \quad X(t_0, t_0) = I_2, \tag{4.161}$$

where I_2, is 2×2 identity matrix. The entries of the matrix $A(t)$ was computed along the periodic solution $q_0(t)$. In the remaining part, without loss of generality, it is assumed that $t_0 = 0$. By considering the formula (3.11) with (3.10), it is easy to compute the matrix in (4.163) and as well as applying B-equivalence technique, the linearization around the periodic solution $q_0(t)$, is considered with the following relations

$$\xi^+ = \xi^- I(\dot{q_0}(t_1)\Delta t_1)\Delta t_1 + u_1 \Delta t_1 = \frac{I(u_1, t'_1)}{u_1}\xi^-,$$

$$\eta^+ = \eta^- + f(t'_1, 0, u_1)\frac{-\xi^-}{u_1} - I(\eta^- + f(t'_1, 0, u_1)\frac{-\xi^-}{u_1}) - f(t'_1, 0, u_1)\frac{-\xi^-}{u_1}.$$

Simplifying above equations, we obtain that

$$\begin{aligned}
&\xi^+ = \frac{I(t_1', u_1)}{u_1}\xi^-, \\
&\eta^+ = (\frac{f(t_1', 0, u_1) - f(t_1', 0, u_1 + I(t_1', u_1))}{u_1} - \frac{I_u(t_1', u_1)f(t_1', 0, u_1)}{u_1})\xi^- + \\
&(1 + I_u(t_1', u_1))\zeta^-.
\end{aligned} \tag{4.162}$$

Above system can be obtained in the following matrix form

$$\begin{bmatrix} \xi^+ \\ \eta^+ \end{bmatrix} = B_1 \begin{bmatrix} \xi^- \\ \eta^- \end{bmatrix},$$

where

$$B_1 = \begin{bmatrix} \frac{I(t_1', u_1)}{u_1} & 0 \\ \frac{f(t_1', 0, u_1) - f(t_1', 0, u_1 + I(t_1', u_1))}{u_1} - \frac{I_u(t_1', u_1)f(t_1', 0, u_1)}{u_1} & 1 + I_u(t_1', u_1) \end{bmatrix}. \tag{4.163}$$

However in the paper [58], the relations in (4.162) is computed as

$$\begin{aligned}
&\xi^+ = q^+(t_1') - q^0(t_1') = \xi^-(1 + \frac{I(t_1', u_1)}{u_1}), \\
&\eta^+ = \dot{q}^+(t_1') - \dot{q}^0(t_1') = (\frac{f(t_1', 0, u_1) - f(t_1', 0, u_1 + I(t_1', u_1))}{u_1} - \\
&\frac{I_u(t_1', u_1)f(t_1', 0, u_1)}{u_1})\xi^- + (1 + I_u(t_1', u_1))\zeta^-.
\end{aligned} \tag{4.164}$$

The impact matrix can be computed through the relations of the paper [58] as

$$B_1 = \begin{bmatrix} -\frac{u_1 + I(t_1', u_1)}{u_1} & 0 \\ \frac{f(t_1', 0, u_1) - f(t_1', 0, u_1 + I(t_1', u_1))}{u_1} - \frac{I_u(t_1', u_1)f(t_1', 0, u_1)}{u_1} & 1 + I_u(t_1', u_1) \end{bmatrix}. \tag{4.165}$$

If your compare the results what we have obtained in (4.162) with those (4.164), what the Ivanov obtained in his paper, you can find first entry of the first row is slightly different than our result. Because, particularly, the formula (8) first equation, $\xi^+ = q^+(t_1') - q^0(t_1')$, in the paper [58] does not make sense.

CHAPTER 5

CONCLUSION

In this thesis, Kelvin-Voigt contact model is displaced by contact model with impact deformations for the investigation of mechanisms with contacts. Comparing these two model, appropriate coefficient of restitution and the surfaces of discontinuity obtained analytically and numerically. The obtained model with impact deformations is compared with the existing experimental data. It is observed that the obtained results are slightly similar with that of those in literature. In some mechanical models the chattering phenomenon is observed analytically and simulation and it is suppressed by utilizing models with impact deformations. The existence and stability of periodic solutions for some mechanical systems is investigated by means of differentiability properties impulsive systems analytically and through simulation results. A brief summary is done for the granular material to emphasize that our results can be applicable for the models with granular material. The grazing solutions of the impulsive systems are analyzed. For those, appropriate definitions are presented. The differentiability properties of impulsive system, orbital stability and small parameter method are considered for those systems. The K- smooth discontinuous flow is defined. Two different types of non autonomous impulsive systems is considered. One is with autonomous surfaces of discontinuity and impulse function and non-autonomous vector field. For those systems, we have used the term non-autonomous systems with stationary impact actions and the other type constitutes of non-autonomous vector field and surfaces of discontinuity with autonomous impulse function. For both non-autonomous systems, we have obtained definitions of grazing point, solution and moment. The asymptotical stability of grazing periodic solutions are considered by applying special linearization technique. Regular pertur-

bations around the grazing cycles of both systems are obtained and the existence of the asymptotically stable periodic solutions are examined. The appropriate definitions for the horizontal and vertical grazing is given and linearization around the periodic solutions of systems with horizontal or vertical grazing is obtained. The results of this thesis are exemplified through simulation results obtained from MATLAB [88].

This our results for the modeling study is also extend for other types of contact model in the form of Kelvin-Voigt contact model and the grazing phenomena can be observed also in impulsive systems with non stationary impact and the non-autonomous impulsive systems. These type of systems have been already considered in our next papers and the systems with discontinuous right hand side can be taking into account for the analysis of grazing solutions and stability. Moreover, the results of the section related with non-autonomous grazing phenomenon can be applied to the analysis of the neural networks which meet the threshold tangentially.

REFERENCES

[1] E. Akalin and M. Akhmet. The principles of b-smooth discontinuous flows. *Computers and Mathematics with Applications*, 49(7–8):981 – 995, 2005.

[2] M. Akhmet. On the smoothness of solutions of impulsive autonomous systems. *Nonlinear Analysis: Theory, Methods and Applications*, 60(2):311 – 324, 2005.

[3] M. Akhmet. Perturbations and hopf bifurcation of the planar discontinuous dynamical system. *Nonlinear Analysis: Theory, Methods and Applications*, 60(1):163 – 178, 2005.

[4] M. Akhmet. Li-yorke chaos in the system with impacts. *Journal of Mathematical Analysis and Applications*, 351(2):804 – 810, 2009.

[5] M. Akhmet. *Principles of discontinuous dynamical systems*. Springer, New York, 2010.

[6] M. Akhmet and A. Kıvılcım. Discontinuous dynamics with grazing points. *Communications in Nonlinear Science and Numerical Simulation*, 38:218 – 242, 2016.

[7] M. Akhmet and M. Turan. Bifurcation in a 3d hybrid system. *Communications in Applied Analysis*, 14:311–324, 2010.

[8] M. Akhmet and M. Turan. Bifurcation of discontinuous limit cycles of the van der pol equation. *Mathematics and Computers in Simulation*, 95:39 – 54, 2014. Discontinuous Differential Systems : Theory and Numerical Methods.

[9] M. U. Akhmet and A. Kıvılcım. The models with impact deformations. *Discontinuity, Nonlinearity, and Complexity*, 4(1):49–78, 2015.

[10] A. Andronow and C. Chaikin. *Theory of oscillations*. Princeton University Press, Princeton, 1949.

[11] T. M. Apostol. *Multi-variable calculus and linear algebra with applications to differential equations and probability*. Wiley, Moscow, 1969.

[12] I. Argatov. Mathematical modeling of linear viscoelastic impact: Application to drop impact testing of articular cartilage. *Tribology International*, 63:213 – 225, 2013. The International Conference on BioTribology 2011.

[13] J. Awrejcewicz and C.-H. Lamarque. *Bifurcation and chaos in nonsmooth mechanical systems*. World Scientific Series on Nonlinear Science Series A: Volume 45, New York, 2003.

[14] V. Babitsky. *Theory of Vibro-Impact System and Applications*. Springer, Berlin, 1998.

[15] A. L. Biance, F. Chevy, C. Clanet, G. Lagubeau, and D. Quere. On the elasticity of an inertial liquid shock. *Journal of Fluid Mechanics*, 554:47–66, 2006.

[16] S. Bishop. Impact oscillators. *Phil. Trans. R. Soc. Lon. A*, 347(1683):347 –351, 1994.

[17] B. Blazejczyk-Okolewska, K. Czolczynski, and T. Kapitaniak. Hard versus soft impacts in oscillatory systems modeling. *Communications in Nonlinear Science and Numerical Simulation*, 15(5):1358 – 1367, 2010.

[18] G. Borg. A condition for the existence of orbitally stable solutions of dynamical systems. *Journal of Differential Equations*, 153:3–12, 1960.

[19] A. Bouzerdoum and R. Pinter. Nonlinear lateral inhibition applied to motion detection in the fly visual system,. *Nonlinear Vision, CRC Press, Boca Raton, FL,*, pages 423–450, 1992.

[20] B. Brogliato. *Nonsmooth mechanics*. Springer-Verlag: London, 1999.

[21] B. Brogliato. *Impacts in Mechanical Systems*. Springer-Verlag Berlin Heidelberg, 2000.

[22] C. Budd and F. Dux. Chattering and related behaviour in impact oscillators. *Philosophical Transactions of the Royal Society of London A: Mathematical, Physical and Engineering Sciences*, 347(1683):365–389, 1994.

[23] C. J. Budd. Non-smooth dynamical systems and the grazing bifurcation. *Nonlinear Mathematics and its Applications*, pages 219–235, 1996.

[24] R. Burton. *Vibration and impact*. Addison-Wesley Publishing Company, New York, 1958.

[25] W. Chin, E. Ott, H. E. Nusse, and C. Grebogi. Grazing bifurcations in impact oscillators. *Phys. Rev. E*, 50:4427–4444, Dec 1994.

[26] W. Chin, E. Ott, H. E. Nusse, and C. Grebogi. Universal behavior of impact oscillators near grazing incidence. *Physics Letters A*, 201(2):197 – 204, 1995.

[27] S. Coombes, R. Thul, and K. Wedgwood. Nonsmooth dynamics in spiking neuron models. *Physica D: Nonlinear Phenomena*, 241(22):2042 – 2057, 2012. Dynamics and Bifurcations of Nonsmooth Systems.

[28] J. Cronin. A criterion for asymptotic stability. *Journal of Mathematical Analysis and Applications*, 74(1):247 – 269, 1980.

[29] L. Demeio and S. Lenci. Asymptotic analysis of chattering oscillations for an impacting inverted pendulum. *The Quarterly Journal of Mechanics and Applied Mathematics*, 59(3):419–434, 2006.

[30] M. Devaney, W. Hirsch, S. Smale, and L. Robert. *Differential Equations, Dynamical Systems, and an Introduction to Chaos*. Academic Press, Boston, 2013.

[31] M. di Bernardo, C. Budd, and A. Champneys. Grazing, skipping and sliding: Analysis of the non-smooth dynamics of the dc/dc buck converter. *Nonlinearity*, 11(4):859, 1998.

[32] M. di Bernardo, C. Budd, A. Champneys, and P. Kowalczyk. *Piecewise-smooth dynamical systems theory and applications*. Springer-Verlag, London, 2008.

[33] M. di Bernardo, C. J. Budd, and A. R. Champneys. Grazing bifurcations in n-dimensional piecewise-smooth dynamical systems. *Physica D*, 160:222–254, 2001.

[34] M. di Bernardo and S. J. Hogan. Discontinuity-induced bifurcations of piecewise smooth dynamical systems. *Philosophical Transactions of The royal society A*, 368:4915–4935, 2010.

[35] E. Dill. *Continuum mechanics, elasticity, plasticity, viscoelasticity*. Taylor and Francis Group, Portland OR, 2007.

[36] V. Donde and I. A. Hiskens. Shooting methods for locating grazing phenomena in hybrid systems. *International Journal of Bifurcation and Chaos*, 16(03):671–692, 2006.

[37] E. Falcon, C. Laroche, S. Fauve, and C. Coste. Behavior of one inelastic ball bouncing repeatedly off the ground. *The European Physical Journal B - Condensed Matter and Complex Systems*, 3(1):45–57, 1998.

[38] M. Farkas. *Periodic Motions*. Springer-Verlag, 1994.

[39] M. I. Feigin. Doubling of the oscillation period with c-bifurcations in piecewise continuous systems. *Journal of Applied Mathematics and Mechanics (Prikladnaya Matematika i Mechanika)*, 34:861–869, 1970.

[40] M. I. Feigin. On the structure of c-bifurcation boundaries of piecewise continuous systems. *Journal of Applied Mathematics and Mechanics (Prikladnaya Matematika i Mechanika)*, 42:820–829, 1978.

[41] A. C. Fischer-Cripps. *Introduction to Contact Mechanics*. Springer US, US, 2007.

[42] S. Foale and S. R. Bishop. Bifurcations in impact oscillations. *Nonlinear Dynamics*, 6(3):285–299, 1994.

[43] M. Forrestal, D. Frew, S. Hanchak, and N. Brar. Penetration of grout and concrete targets with ogive-nose steel projectiles. *International Journal of Impact Engineering*, 18(5):465 – 476, 1996.

[44] M. H. Fredriksson. Grazing bifurcations in multibody systems. *Nonlinear Anal.*, 30(7):4475–4483, Dec. 1997.

[45] J. Fu, M. Adams, G. Reynolds, A. Salman, and M. Hounslow. Impact deformation and rebound of wet granules. *Powder Technology*, 140(3):248 – 257, 2004. 1st International Workshop on Granulation (Granulation across the length scales: linking microscopic experiments and models to real process operation).

[46] B. C. Gegg, A. C. Luo, and S. C. Suh. Grazing bifurcations of a harmonically excited oscillator moving on a time-varying translation belt. *Nonlinear Analysis: Real World Applications*, 9(5):2156 – 2174, 2008.

[47] M. H. Ghayesh. Nonlinear dynamic response of a simply-supported kelvin–voigt viscoelastic beam, additionally supported by a nonlinear spring. *Nonlinear Analysis: Real World Applications*, 13(3):1319 – 1333, 2012.

[48] S. Giusepponi, F. Marchesoni, and M. Borromeo. Randomness in the bouncing ball dynamics. *Physica A: Statistical Mechanics and its Applications*, 351(1):142 – 158, 2005. New Horizons in Stochastic Complexity International Workshop on New Horizons in Stochastic Complexity.

[49] J. T. Gomez and A. Shukla. Multiple impact penetration of semi-infinite concrete. *International Journal of Impact Engineering*, 25(10):965 – 979, 2001.

[50] J. Guckenheimer and P. Holmes. *Nonlinear oscillations, dynamical systems, and bifurcations of vector Fields*. Springer, New York, 1983.

[51] P. Hartman. *Ordinary differential equations*. Classics in Applied Mathematics 38, Philadelphia: Society for Industrial and Applied Mathematics, edition =.

[52] K. S. Hedrih, V. Raicevic, and S. Jovic. Phase trajectory portrait of the vibro-impact forced dynamics of two heavy mass particles motions along rough circle. *Communications in Nonlinear Science and Numerical Simulation*, 16(12):4745 – 4755, 2011. SI:Complex Systems and Chaos with Fractionality, Discontinuity, and Nonlinearity.

[53] C. Hos and A. R. Champneys. Grazing bifurcations and chatter in a pressure relief valve model. *Physica D: Nonlinear Phenomena*, 241(22):2068 – 2076, 2012. Dynamics and Bifurcations of Nonsmooth Systems.

[54] K. Hunt and F. Crossley. Coefficient of restitution interpreted as damping in vibroimpact. *ASME Journal of Applied Mechanics*, 42:440–445, 1975.

[55] R. Ibrahim. *Vibro-impact dynamics modeling, mapping and applications*. Springer-Verlag, Berlin Heidelberg, 2009.

[56] R. A. Ibrahim. Recent advances in vibro-impact dynamics and collision of ocean vessels. *Journal of Sound and Vibration*, 333(23):5900–5916, 2014.

[57] J. Ing, E. Pavlovskaia, M. Wiercigroch, and S. Banerjee. Bifurcation analysis of an impact oscillator with a one-sided elastic constraint near grazing. *Physica D: Nonlinear Phenomena*, 239(6):312 – 321, 2010.

[58] A. Ivanov. Impact oscillations: Linear theory of stability and bifurcations. *Journal of Sound and Vibration*, 178(3):361 – 378, 1994.

[59] A. P. Ivanov. Non-linear dynamic and chaos in mechanical systems bifurcations in impact systems. *Chaos, Solitons and Fractals*, 7(10):1615 – 1634, 1996.

[60] R. Jackson, I. Green, and D. Marghitu. Predicting the coefficient of restitution of impacting elastic-perfectly plastic spheres. *Nonlinear Dynamics*, 60(3):217–229, 2010.

[61] H. M. Jaeger, S. R. Nagel, and R. P. Behringer. Granular solids, liquids, and gases. *Rev. Mod. Phys.*, 68:1259–1273, Oct 1996.

[62] K. Johnson. *Contact mechanic*. Cambridge University Press, UK, 1985.

[63] T. Kapitaniak and M. Wiercigroch. Periodic solution finder for an impact oscillator with a drift. *Pergamon, Oxford (special issue of Chaos, Solitons and Fractals*, 11(12):2411–2412, 2000.

[64] A. S. Khan and S. Huang. *Continuum Theory of Plasticity*. John Wiley and Sons Inc, New York, 1995.

[65] S. Kryzhevich. Grazing bifurcation and chaotic oscillations of vibro-impact systems with one degree of freedom. *Journal of Applied Mathematics and Mechanics*, 72(4):383 – 390, 2008.

[66] S. Lenci, L. Demeio, and M. Petrini. Response scenario and nonsmooth features in the nonlinear dynamics of an impacting inverted pendulum. *ASME. J. Comput. Nonlinear Dynam.*, 1(1):56–64, 2005.

[67] B. Li. Periodic orbits of autonomous ordinary differential equations: theory and applications. *Nonlinear Analysis: Theory, Methods and Applications*, 5:931–958, 1981.

[68] J. M. Luck and A. Mehta. Bouncing ball with a finite restitution: Chattering, locking, and chaos. *Phys. Rev. E*, 48:3988–3997, Nov 1993.

[69] A. Luo. *Singularity and dynamics on discontinuous vector fields*. Elsevier, (Monograph Series on Nonlinear Science and Complexity), Netherlands, volume 3 edition, 2006.

[70] A. Luo. *Singularity and Dynamics on Discontinuous Vectorfields*. Elsevier, Amsterdam, 2006.

[71] A. Luo. *Discontinuous Dynamical Systems on Time-varying Domains*. Higher Education Press, Beijing, 2009.

[72] A. Luo. *Nonlinear deformable-body dynamics*. Springer, Beijing, volume 3 edition, 2010.

[73] A. Luo. *Discontinuous dynamical systems*. Springer-Verlag, Beijing, 2012.

[74] A. Luo and Y. Guo. *Vibro-impact dynamics*. John Wiley and Sons, Ltd, United Kingdom, 2013.

[75] A. C. Luo. A theory for non-smooth dynamic systems on the connectable domains. *Communications in Nonlinear Science and Numerical Simulation*, 10(1):1 – 55, 2005.

[76] A. C. Luo. On grazing and strange attractors fragmentation in non-smooth dynamical systems. *Communications in Nonlinear Science and Numerical Simulation*, 11(8):922 – 933, 2006.

[77] A. C. Luo and B. C. Gegg. Grazing phenomena in a periodically forced, friction-induced, linear oscillator. *Communications in Nonlinear Science and Numerical Simulation*, 11(7):777 – 802, 2006.

[78] A. C. J. Luo and D. O'Connor. Mechanism of impacting chatter with stick in a gear transmission system. *International Journal of Bifurcation and Chaos*, 19(06):2093–2105, 2009.

[79] A. C. J. Luo and D. O'Connor. Periodic motions and chaos with impacting chatter and stick in a gear transmission system. *International Journal of Bifurcation and Chaos*, 19(06):1975–1994, 2009.

[80] G. Luo, X. Lv, and L. Ma. Periodic-impact motions and bifurcations in dynamics of a plastic impact oscillator with a frictional slider. *European Journal of Mechanics - A/Solids*, 27(6):1088 – 1107, 2008.

[81] G. Luo and J. Xie. Bifurcations and chaos in a system with impacts. *Physica D: Nonlinear Phenomena*, 148(3–4):183 – 200, 2001.

[82] G. Luo, J. Xie, X. Zhu, and J. Zhang. Periodic motions and bifurcations of a vibro-impact system. *Chaos, Solitons and Fractals*, 36(5):1340 – 1347, 2008.

[83] G. Luo, Y. Zhang, J. Xie, and J. Zhang. Periodic-impact motions and bifurcations of vibro-impact systems near 1:4 strong resonance point. *Communications in Nonlinear Science and Numerical Simulation*, 13(5):1002 – 1014, 2008.

[84] H. Y. M. Urabe and Y. Shinohara. Periodic solutions of van der pol's equation with damping coefficient $\lambda = 2 \approx 10,$. *J. Sci. Hiroshima Uni. Ser.*, 23:325–366, 1960.

[85] I. G. Malkin. *Some Problems in the Theory of Nonlinear Oscillations*. State Technical Publishing House, Moscow, 1956.

[86] D. Marhefka and D. Orin. A compliant contact model with nonlinear damping for simulation of robotic systems. *Systems, Man and Cybernetics, Part A: Systems and Humans, IEEE Transactions on*, 29(6):566–572, Nov 1999.

[87] D. Marhefka and D. Orin. A compliant contact model with nonlinear damping for simulation of robotic systems. *Systems, Man and Cybernetics, Part A: Systems and Humans, IEEE Transactions on*, 29(6):566–572, Nov 1999.

[88] MATLAB. Version 7.12.0 (r2011a). The MathWorks Inc., Natick, Massachusetts, 2011.

[89] S. McNamara and E. Falcon. Simulations of vibrated granular medium with impact-velocity-dependent restitution coefficient. *Phys. Rev. E*, 71:031302, Mar 2005.

[90] S. McNamara and W. R. Young. Inelastic collapse and clumping in a one-dimensional granular medium. *Physics of Fluids*, 4:496–504, Mar. 1992.

[91] S. McNamara and W. R. Young. Inelastic collapse in two dimensions. *Phys. Rev. E*, 50:R28–R31, Jul 1994.

[92] N. Minorsky. *Nonlinear oscillations*. Malabar, Fla. Krieger, Krieger, 1987.

[93] J. Molenaar, J. G. de Weger, and W. van de Water. Mappings of grazing-impact oscillators. *Nonlinearity*, 14(2):301, 2001.

[94] R. Nagaev. *Mechanical processes with repeated attenuated impacts*. World Scientific Publishing Co, Singapore, 1985.

[95] M. Nagurka and S. Huang. A mass-spring-damper model of a bouncing ball. In *American Control Conference, 2004. Proceedings of the 2004*, volume 1, pages 499–504 vol.1, June 2004.

[96] A. H. Nayfeh and B. Balachandran. *Applied Nonlinear Dynamics, Analytical, Computational, and Experimental Methods*. Wiley, 1995.

[97] A. B. Nordmark. Non-periodic motion caused by grazing incidence in an impact oscillator. *Journal of Sound and Vibration*, 145(2):279 – 297, 1991.

[98] A. B. Nordmark. Universal limit mapping in grazing bifurcations. *Phys. Rev. E*, 55:266–270, Jan 1997.

[99] A. B. Nordmark. Existence of periodic orbits in grazing bifurcations of impacting mechanical oscillators. *Nonlinearity*, 14(6):1517, 2001.

[100] A. B. Nordmark and P. Kowalczyk. A codimension-two scenario of sliding solutions in grazing–sliding bifurcations. *Nonlinearity*, 19(1):1, 2006.

[101] Y. Ono, K. Aihara, and H. Suzuki. Grazing bifurcation and mode-locking in reconstructing chaotic dynamics with a leaky integrate-and-fire model. *Artificial Life and Robotics*, 7(1):55–62, 2003.

[102] F. Paparella and G. Passoni. Absence of inelastic collapse for a 1d gas of grains with an internal degree of freedom. *Computers and Mathematics with Applications*, 55(2):218 – 229, 2008. Modeling GranularityModeling Granularity.

[103] T. Pavlidis. Stability of a class of discontinuous dynamical systems. *Information and Control*, 9(3):298 – 322, 1966.

[104] E. Pavlovskaia, M. Wiercigroch, and C. Grebogi. Modeling of an impact system with a drift. *Phys. Rev. E*, 64:056224, Oct 2001.

[105] L. Perko. *Differential Equations and Dynamical Systems*. Springer, 2001.

[106] P. T. Piiroinen, L. N. Virgin, and A. R. Champneys. Chaos and period-adding; experimental and numerical verification of the grazing bifurcation. *Journal of Nonlinear Science*, 14(4):383–404, 2004.

[107] L. Půst and F. Peterka. Impact oscillator with hertz's model of contact. *Meccanica*, 38(1):99–116, 2003.

[108] C. Robinson. *Dynamical systems: stability, symbolic dynamics, and chaos*. CRC:Boca Raton, Ann Arbor, London, Tokyo, 1995.

[109] A. M. Samouilenko and N. A. Perestyuk. *Impulsive differential equations*, volume 14 of *World Scientific Series on Nonlinear Science. Series A: Monographs and Treatises*. World Scientific Publishing Co. Inc., River Edge, NJ, 1995. With a preface by Yu. A. Mitropolcskiui and a supplement by S. I. Trofimchuk, Translated from the Russian by Y. Chapovsky.

[110] W. Schiehlen and R. Seifried. *Iutam Symposium on Dynamics and Control of Nonlinear Systems with Uncertainty: Proceedings of the IUTAM Symposium held in Nanjing, China, September 18-22, 2006*, chapter Impact Systems with Uncertainty, pages 33–44. Springer Netherlands, Dordrecht, 2007.

[111] S. Shaw and P. Holmes. A periodically forced piecewise linear oscillator. *Journal of Sound and Vibration*, 90(1):129 – 155, 1983.

[112] S. Sherman. A third order nonlinear system arising from a nuclear spin generator. *Control Differential Equations*, 2:197–227, 1963.

[113] P. S. Simeonov and D. D. Bainov. Orbital stability of the periodic solutions of autonomous systems with impulse effect. *RIMS, Kyoto Univ.*, 25:312–346, 1989.

[114] R. A. Smith. Orbital stability for ordinary differential equations. *Journal of Differential Equations*, 69(2):265 – 287, 1987.

[115] W. Stronge. *Impact mechanics*. Cambridge University Press, Cambridge, 2000.

[116] D. Tabor. A simple theory of static and dynamic hardness. *Proceedings of the Royal Society of London. Series A, Mathematical and Physical Sciences*, 192(1029):pp. 247–274, 1948.

[117] J. R. Taylor and S. N. Patek. Ritualized fighting and biological armor: the impact mechanics of the mantis shrimp's telson. *Ritualized fighting and biological armor: the impact mechanics of the mantis shrimp's telson*, 213:3496–3504., 2010.

[118] J. J. Thomsen and A. Fidlin. Near-elastic vibro-impact analysis by discontinuous transformations and averaging. *Journal of Sound and Vibration*, 311(1–2):386 – 407, 2008.

[119] W. T. Thomson. *Theory of Vibration with Applications*. EUA : Prentice-Hall, Englewood Cliffs, 1972.

[120] P. Tung and S. Shaw. The dynamics of an impact print hammer. *Journal of Vibration, Acoustics, Stress, and Reliability in Design*, 110:193–200, 1988.

[121] M. Urabe. Numerical study of periodic solutions of the van der pol equation. *International Symposium on Nonlinear Differential Equations and Nonlinear Mechanics, New York*, pages 184–192, 1963.

[122] F. Verhulst. *Methods and Applications of Singular Perturbations*. Springer-Verlag, New York, 2005.

[123] A. Visintin. Homogenization of the nonlinear kelvin–voigt model of viscoelasticity and of the prager model of plasticity. *Continuum Mechanics and Thermodynamics*, 18(3-4):223–252, 2006.

[124] S. Vogel and S. J. Linz. Regular and chaotic dynamics in bouncing ball models. *International Journal of Bifurcation and Chaos*, 21(03):869–884, 2011.

[125] D. J. Wagg and S. R. Bishop. Chatter, sticking and chaotic impacting motion in a two-degree of freedom impact oscillator. *International Journal of Bifurcation and Chaos*, 11(01):57–71, 2001.

[126] G. Whiston. Singularities in vibro-impact dynamics. *Journal of Sound and Vibration*, 152(3):427 – 460, 1992.

[127] C.-Y. Wu, L.-Y. Li, and C. Thornton. Energy dissipation during normal impact of elastic and elastic–plastic spheres. *International Journal of Impact Engineering*, 32(1–4):593 – 604, 2005. Fifth International Symposium on Impact Engineering.

[128] S. Zheltukhin and R. Lui. One-dimensional viscoelastic cell motility models. *Mathematical Biosciences*, 229(1):30 – 40, 2011.

CURRICULUM VITAE

PERSONAL INFORMATION

Surname, Name: Kıvılcım, Ayşegül
Nationality: Turkish (TC)
Date and Place of Birth: 22.10.1985, Kepsut
Marital Status: Single
Phone: +90 (505) 769 4368
E-mail: akivilcim@gmail.com

EDUCATION

Degree	Institution	Year of Graduation
B.S.	Middle East Technical University	2009
High School	Balıkesir Ticaret Odası Lisesi	2003

PROFESSIONAL EXPERIENCE

Year	Place	Enrollment
2009-2016	Middle East Technical University	Research Assistant

PUBLICATIONS

M. Akhmet, M. O. Fen ve A. Kıvılcım. Chaos by neural networks: the quasi-periodic route International Conference on Applied Informatics for Health and Life Sciences in conjunction with Turkish-German Workshop on Bioinformatics: Recent Developments from Health to Nanotechnology, Pages 119-123, 19-22 October 2014,

Kusadasi-TURKEY.

M. Akhmet and A. Kıvılcım The Models with Impact Deformations *Discontinuity, Nonlinearity, and Complexity* **4** , 2015, 49-78.

M. Akhmet, M. O. Fen and A. Kıvılcım, Li-Yorke chaos generation by SICNNs with chaotic/almost periodic postsynaptic currents, 173, Part 3, 15 January 2016, Pages 580-594.

M. Akhmet and A. Kıvılcım, Discontinuous dynamics with grazing points, *Communications in Nonlinear Science and Numerical Simulation*, 38, 2016, 218-242.

M. Akhmet and A. Kıvılcım, Vertical and Horizontal grazing, Dynamic Systems and Applications, Proceeding of International Conference on Pure and Applied Mathematics, ICPAM 2015, Van-Turkey (accepted)

M. Akhmet and A. Kıvılcım An impact oscillator with a grazing cycle *Discontinuity, Nonlinearity, and Complexity* (accepted).

M. Akhmet and A. Kıvılcım Stability in non-autonomous periodic systems with grazing stationary impacts *Carpathian Journal of Mathematics* (accepted).

International Conference Presentations

SICNNs with Chaotic/Almost Periodic Postsynaptic Currents, 5th International Conference on Nonlinear Science and Complexity August 4-9, 2014 Academic Exchange Center, Nan-Yang Hotel, Xi'an Jiaotong University, Xi'an, China (with Marat Akhmet and Mehmet Onur Fen).

Chaos by neural networks: the quasi-periodic route, 10th Colloquium of the Qualitative Theory of Differential Equations (10QTDE), July 1-4, 2015, Bolyai Institute, University of Szeged, Hungary (with Marat Akhmet and Mehmet Onur Fen).

Chaos by neural networks: the quasi-periodic route, International Conference on Applied Informatics for Health and Life Sciences in conjunction with Turkish-German Workshop on Bioinformatics: Recent Developments from Health to Nanotechnology, 19-22 October 2014, Kuşadası-Turkey (with Marat Akhmet and Mehmet Onur Fen).